Molecular and genetic analysis of a symbiosis-specific locus of the *Lotus japonicus* genome and its potential as a tool for dissecting the symbiotic signal transduction pathway.

Elaine Fiona Tuck

Institute of Biological Sciences
University of Wales,
Aberystwyth

April 2005

This thesis is submitted in fulfilment of the requirements for the degree of

Doctor of Philosophy of the University of Wales

Statement 1

The work presented in this thesis has been carried out at the Institute of Grassland and Environmental Research (IGER), Aberystwyth.

This thesis is the result of my own investigations, except where otherwise stated. Other sources are acknowledged through explicit references. A bibliography is appended.

_____

Elaine Fiona Tuck

Statement 2

I hereby give consent for my thesis, if accepted, to be available for photocopying and for inter-library loan, and for the title and summary to be made available to outside organisations.

_____

Elaine Fiona Tuck

Declaration

This thesis has not already been accepted in substance for any degree, and is not currently submitted in candidature for any degree.

_____

Elaine Fiona Tuck

Abstract

Nitrogen-fixing nodules on legume roots result from a symbiotic interaction with soil bacteria known as rhizobia. This relationship is important in sustainable agriculture and the genetic and molecular basis of root nodule formation and functioning is the subject of intense research.

A promoter-tagging programme using the model legume *Lotus japonicus* and a β-glucuronidase (*gus*) reporter identified one line, T90, which exhibited GUS expression only after inoculation with the plants' rhizobial symbiont *Mesorhizobium loti*, and its arbuscular mycorrhizal fungal symbiont *Glomus mosseae*. Molecular analysis showed that insertion of the reporter gene construct had occurred approximately 1.1 Kb upstream of an open reading frame encoding a putative calcium-binding protein, *LjCbp1*.

Calcium is a well-known second messenger and is involved in root nodule symbiosis. This thesis describes the *in silico* analysis of *LjCbp1* and putative regulatory elements upstream of the coding region. Altered protein mobility changes on polyacrylamide gels in the presence of calcium suggest that *Lj*Cbp1 indeed has calcium-binding properties. The spatiotemporal expression patterns of *LjCbp1* before and after inoculation with *M. loti* correlated with that of *gus* in T90. This suggests that reporter gene expression accurately reflects that of the endogenous gene. T90 *gus* expression was up-regulated by calcium treatment and modulated by pharmaceutical agents (for example the calcium channel blocker nifedipine) that modify calcium influx. Such data suggest that *LjCbp1* transcription is influenced by calcium.

Various lines of evidence, including the absence of a nodulation deficient phenotype in lines expressing reduced levels of *LjCbp1,* indicate that *LjCbp1* is not essential for symbiotic interactions but that this gene nevertheless plays a role in the early stages of association with rhizobia and arbuscular mycorrhizal fungi.

The specificity of *gus* expression was also analysed in detail. Nod factor purified from *M. loti*, as well as chitosan and various rhizobial strains also elicited GUS activity, thus confirming its specificity to both symbionts.

This specificity was exploited in a chemical mutagenesis programme to create a range of symbiotic phenotypes. Significant changes were observed in expression patterns of the *gus* reporter gene following inoculation with *M. loti* in three mutants. This emphasises the value of T90 as a powerful tool in dissecting the signalling events in the early stages of nodulation.

Acknowledgements

Thank You Lord for the things you have done.

Thank you Judith, Leif and Luis for your experience, patience, support and enthusiasm. Judith, I'm sure your support has gone way beyond the call of duty, thank you.

There are so many people at IGER who have made all the difference. Scooby, Rhys, Pete, Jen, Kerrie and loads of others who have been so good to me and who have given time, support, experience and encouragement. Thank you all so much.

Thank you also to Martin for the opportunity to work in your lab and with your very special team. Thank you also to those in Martin's lab for your welcome, acceptance and inclusion.

Special thanks to the pray-ers at IGER…..Andy B, Steve, Jon, John, Alison, Hazel. You've been a major support and blessing over the years and I am grateful for you all.

Mum and Dad thank you for all the things I know about and many more I don't which you have done for me. Rachel and John, you're fab.

Thank you to my church family for accepting and loving me so much. Thank you to all those (many) who have prayed, encouraged and supported me and drawn me closer to Jesus.

To so many other friends I am blessed with: John, Rachel, Kate, Lizbit, Nomi, Emily, Jackie, Jayne, Sarah, Claire, Jacqui, Andy, Ellie and many more. Thank you.

Richard, thank you for coming along now when I am ready for you :0). I love you. I look forward to a lifetime together.

In loving memory of Hilary

O Lord, you have searched me
and you know me.
You know when I sit and when I rise;
you perceive my thoughts from afar.
You discern my going out and my lying down;
you are familiar with all my ways.
Before a word is on my tongue
you know it completely, O Lord.

You hem me in – behind and before;
you have laid Your hand upon me.
Such knowledge is too wonderful for me,
too lofty for me to attain.

Where can I go from your Spirit?
Where can I flee from your Presence?
If I go up to the heavens, you are there;
if I make my bed in the depths, you are there.
If I rise on the wings of the dawn,
if I settle on the far side of the sea,
even there your hand will guide me,
your right hand will hold me fast.

For you created my inmost being;
You knit me together in my mother's womb.
I praise you because I am fearfully and wonderfully made;
your works are wonderful,
I know that full well.
My frame was not hidden from you
when I was made in the secret place.
When I was woven together in the depths of the earth,
your eyes saw my unformed body.
All the days ordained for me
were written in your book
before one of them came to be.

Search me, O God, and know my heart;
test me and know my anxious thoughts.
See if there is any offensive way in me,
and lead me in the way everlasting.

Table of Contents

List of Figures

Chapter 5

List of Tables

Abbreviations

2, 4-D	2, 4-dichlorophenoxy acetic acid
6-BAP	6-benzylamine purine
ABA	abscisic acid
ACC	aminocyclopropane-1 carboxylic acid
ADP	adenosine diphosphate
AM	arbuscular mycorrhiza
APS	ammonium persulfate
BLAST	basic local alignment search tool
BNF	biological nitrogen fixation
bp	base pairs
bv	biovar
$[Ca^{2+}]_{cyt}$	cytosolic calcium concentration
cDNA	complementary DNA
CaM	calmodulin
CER	controlled environment room
CIP	calf intestinal phosphatase
CSPD	disodium 3-(4-methoxyspiro(1,2-dioxetane-3,2'-(5'-chloro)tricyclo[3.3.1.1^{3,7}] decan-4-yl) phenyl phosphate)
cv	cultivar
DEPC	diethyl pyrocarbonate
DHZ	dihydrozeatin
DMF	N,N-Dimethyl-formamide
DNA	deoxyribonucleic acid
DNase	deoxyribonuclease
dNTP	deoxynucleoside triphosphate
dpi	days post inoculation
DTT	dithiothrietol
EDTA	ethylenediaminotetra-acetic acid, disodium salt
EMS	ethyl methane sulphonate
ENOD	early nodulin
EST(s)	expressed sequence tag(s)
Fix^-	non-fixing
gDNA	genomic DNA
GFP	green fluorescent protein
GUS	β-glucuronidase
hpi	hours post inoculation
IAA	indole-acetic acid
IGER	Institute of Grassland and Environmental Research
IP3	(1,4,5)-trisphosphate
IPTG	isopropyl-beta-D-thiogalactopyranoside
Kb	kilobases
KDa	kilo daltons
LA	Luria agar
LB	Luria broth
LTR(s)	long terminal repeat(s)
Mb	megabases
M_MLV	Moloney Murine leukaemia virus

MOPS	10x 3-[N-Morpholino]propanesulfonic acid
mRNA	messenger RNA
myc	mycorrhiza
myc^-	mycorrhization deficient
N	nitrogen
N_2	dinitrogen
NAA	1-naphthylacetic acid
NaOAc	sodium acetate
Nod	nodulation
Nod^-	non-nodulating
Nod^+	nodulating
Nos	nopaline synthase
Npt II	neomycin phosphotransferase
ORF(s)	open reading frame(s)
PAGE	polyacrylamide gel electrophoresis
PCR	polymerase chain reaction
POD	peroxidase
Poly-A	poly-adenosine
RACE	rapid amplification of cDNA ends
RMM	relative molecular mass
RNA	ribonucleic acid
RNase	ribonuclease
ROS	reactive oxygen species
RT	reverse transcriptase
RT-PCR	reverse transcriptase-polymerase chain reaction
SDS	sodium dodecyl sulphate
SDW	sterile distilled water
sec	seconds
SNP	sodium nitroprusside
SSC	20x sodium-sodium citrate
STW	sterile tap water
TAC	transformation-competent artificial chromosome
TAE	Tris, acetic acid, EDTA buffer
Taq	*Thermus aquaticus*
TAP	tobacco acid phosphatase
TBE	Tris, boric acid, EDTA
TBS	Tris-buffered saline
TEMED	C, N, N, N, N'-tetra-methyl-ethylenediamine
$T_{10}E_1$	TrisCl-EDTA buffer
Tn	transposon
TY	tryptone/yeast extract agar
v/v	volume for volume
X-Gal	5-bromo-3-indoyl-b-d-galactopyranoside
X-Gluc	5-bromo-4-chloro-3-indolyl glucuronide
YM	yeast mannitol

Chapter 1

1.0 General Introduction

Dinitrogen (N_2) contributes around 78% of the air we breathe, making it the most abundant element in the earth's atmosphere. Eukaryotes cannot convert this very stable gas into a biologically useful form. Since nitrogen is a vital component of proteins and nucleic acids, and is thus an essential nutrient, a source is required that is accessible to eukaryotic organisms.

Plants generally rely on the availability of mineralised nitrogen in the soil. This takes the form of nitrates or ammonia and is accessible either through the direct application of nitrogen fertiliser or by the action of certain prokaryotes that are able to reduce N_2 to ammonia (Postgate, 1982). Indeed, the only organisms that can fix atmospheric N_2 into a compound that can be metabolised are members of the prokaryote kingdom. This process is known as biological nitrogen fixation. Humans and animals rely on the nitrogen already obtained by plants. The system of nitrogen cycling is outlined more comprehensively in Figure 1.0.

The application of nitrogen fertiliser is one way of making nitrogen available to plants. The Haber-Bosch process, used in its manufacture, is an efficient process, although it requires high pressure and temperature and thereby also a high energy input. There are also certain environmental, ethical and economical issues regarding the use of nitrogen fertiliser. Firstly, it requires high input of a non-renewable fossil fuel (Galloway *et al*., 1995). Secondly, nitrogen fertiliser is not available to farming communities in some developing countries because of its cost or because of difficulties in transportation. This puts such farmers and their communities at a disadvantage. There is therefore a shortage of protein in the world not met through fertiliser application. In addition, unless managed effectively, the application of fertiliser may exceed that which is necessary, subsequent rainfall can then lead to run off and nitrate leaching. These leachates pollute water sources and can lead to eutrophication.

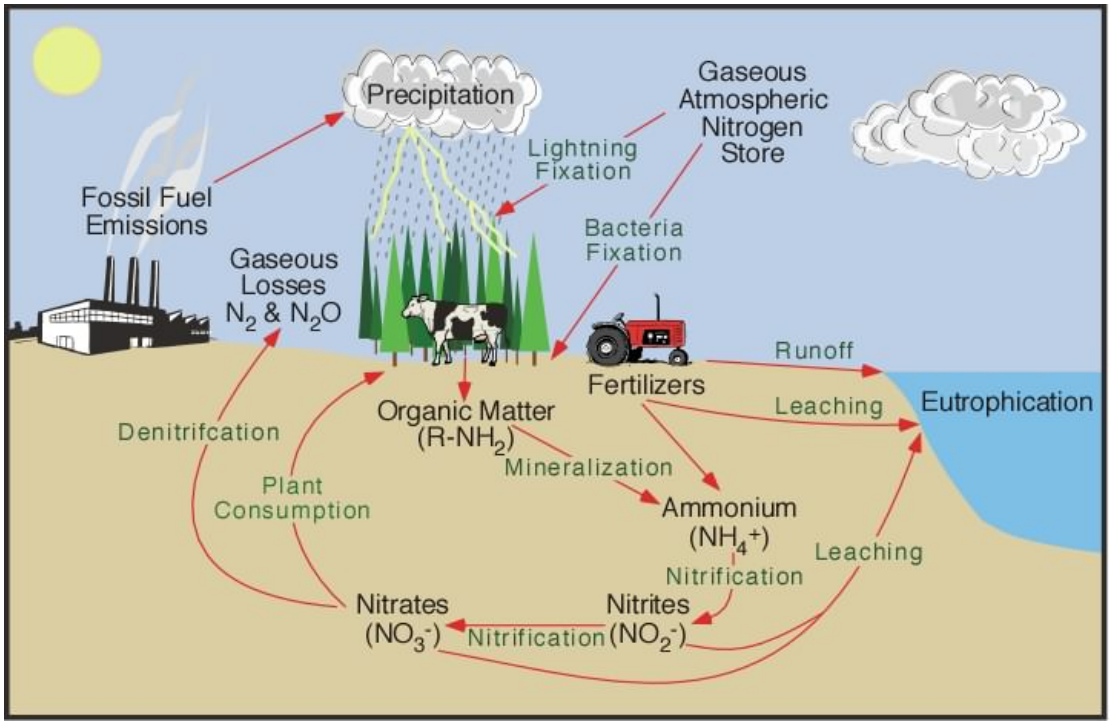

Figure 1.0. The nitrogen cycle. Atmospheric dinitrogen is made available to most plants via the uptake of nitrates in the soil through the application of fertilizer or through the decomposition of organic matter. Decomposers chemically modify the nitrogen found in organic matter from ammonia (NH_3) to ammonium salts (NH_4^+). This process is known as mineralization and is carried out by a variety of bacteria, actinomycetes and fungi. Ammonium is often chemically altered by a specific type of autotrophic bacteria into nitrite (NO_2^-). Further modification by another type of bacteria converts the nitrite to nitrate (NO_3^-). Both processes involve chemical oxidation and are known as nitrification. Nitrate is very soluble and can be lost from the soil system by leaching, sometimes causing eutrophication, or it can be returned to the atmosphere by denitrification. Denitrification also occurs in anaerobic soils and is carried out by heterotrophic bacteria. Denitrification involves the reduction of nitrate into nitrogen (N_2) or nitrous oxide (N_2O) gas. Both gases then diffuse into the atmosphere. Significant amounts of dinitrogen also enter the soil in rainfall or through the effects of lightning. The majority is biochemically **fixed** within the soil by specialized micro-organisms like **bacteria**, **actinomycetes** and **cyanobacteria**. This process is called biological nitrogen fixation. The activities of humans have severely altered the nitrogen cycle. Eutrophication can occur through the excess application of nitrogen fertilizer to crops, the release of large amounts of ammonia from livestock wastes and leakage from septic tanks and sewage works. Increased deposition of nitrogen from atmospheric sources occurs because of fossil fuel combustion and forest burning. Image and text adapted from Pidwerny, 2005.

The ability of some organisms to make nitrogen available to plants means that there is a sustainable alternative to nitrogen fertiliser application. It has been estimated that globally, biologically fixed N_2 ranges between 100 and 290 million tons of nitrogen per year, of which only 40-48 million tons of nitrogen per year are estimated to be biologically fixed in agricultural crops and fields (Cleveland *et al*., 1999). In comparison, approximately 83 million tons per year are fixed industrially for the production of fertiliser (Jenkinson, 2001). Biological nitrogen fixation (BNF) is therefore a vital component of sustainable agriculture but is not exploited to its full potential.

1.1 Biological nitrogen fixation

The ability to incorporate atmospheric N_2 into the organic compounds usable by plants is limited to a group of prokaryotes known as the diazotrophs. Diazotrophs are found in diverse habitats and environments including both alkaline and acid soils, fresh and salt water, intestines and rumens. They are also widely distributed amongst the prokaryotic bacteria, occurring in at least 20 families (Sprent and Sprent, 1990). These families include the Chromatiaceae, anaerobic, phototrophic purple sulphur bacteria amongst which N_2-fixation is rare (Postgate, 1982; Sprent and Sprent, 1990) and the Enterobacteriaceae, which were originally isolated from intestinal flora but have since been reported from habitats such as leaf, nodule and bark surfaces. The Enterobacteriaceae are facultative anaerobes, only a few strains actively fix N_2 (Postgate, 1982; Sprent and Sprent, 1990). The Methanomonadaceae are aerobic bacteria that utilise methane, they can be found in soil and water and are generally N_2-fixers (Sprent and Sprent, 1990). There is also a range of cyanobacteria within which N_2-fixation is widely distributed, for example in the genus *Anabaena* (Postgate, 1982).

Diazotrophs fix N_2 using energy from photosynthetic or chemical sources to produce ammonia ($N_2 + 3H_2 \Rightarrow 2NH_3$). This naturally occurring process provides some advantages over the use of artificially produced nitrogen fertiliser. BNF occurs at ambient temperature and atmospheric pressure, in contrast with the

Haber-Bosch process, which requires high temperature and pressure. BNF also occurs 'on site', meaning that there are no distribution costs.

Some microorganisms can only fix N_2 in symbiosis with higher plants. Within this group are the root-nodulating bacteria, the most important in agronomic terms. These organisms are able to exist as free-living, soil-dwelling aerobes, or in close relationship with certain plants. In such associations, the bacteria become diazotrophic and provide nitrogen in a form usable to the plant, in exchange for carbon compounds produced by the plant during photosynthesis (Fisher and Long, 1992). Root-nodulating bacteria of agricultural significance are collectively known as rhizobia and are from the family Rhizobiaceae (Table 1.1). They are gram negative bacteria which fix nitrogen micro-aerophilically whilst in symbiosis with certain members of the Leguminoseae, or legume, plant family.

Table 1.1. Selected phylogenetic classifications within the Rhizobiaceae.

Genus	Species
Rhizobium	*meliloti, trifolii, leguminosarum, phaseoli*
Mesorhizobium	*Loti*
Bradyrhizobium	*japonicum, lupinus, vigna, elkanii*

Rhizobia can also be divided into fast- and slow-growing strains. The fast-growing strains form acid from mannitol, the slow-growing ones do not (Postgate, 1992). Generally the *Bradyrhizobium* species are slow-growing.

There is one notable exception to the rule that nodules only form within a legume/rhizobia relationship. Within the group of rhizobia that form nodules on cowpea is a strain that also colonizes the non-legume *Parasponia*, a tropical plant belonging to the family Ulmaceae (Postgate, 1982).

1.2 The Leguminoseae

The Leguminoseae are the third largest family of Angiosperms. Doyle and Lucknow (2003) describe them as "diverse in every way imaginable, defying generalisation about almost any attribute". This is unsurprising considering the family comprises some 700 genera and around 20000 species. Fruit can form tiny, single seeds or meter-long woody pods. Ecologically, legumes can be found in rain forests and deserts, lowland and alpine environments and can even include aquatic species (Doyle and Lucknow, 2003).

The agronomic significance of legumes is that they represent an important component of the human diet either directly, consumed principally as grains such as soybeans, peas and beans, or indirectly in the form of forage eaten by sheep and cattle. Legumes are important components of any sustainable system. In addition to their more familiar uses, they are exploited in alley cropping, as cover crops and in agro-forestry. Giant forest trees are prominent sources of lumber and expensive woods, for example Brazilian rosewood (*Balbergia nigra*), whilst at the opposite end of the scale there are shrubs of all sizes and tiny annual herbs (Doyle and Lucknow, 2003). The introduction of legumes into farmed land can reduce soil erosion, weed problems and incidents of fungal root disease (Giller and Wilson, 1991). Smartt (1990) has commented that in vast areas of Africa agriculture would have been impossible were it not for the restorative capacities of legumes.

The contribution of legumes globally to agriculture is not as high as cereals and potatoes, but they are cultivated either as major or minor crops in all the agricultural regions of the world (Borget, 1992).

Legumes divide into three sub-families: the Mimosoideae, the Cesalpinoideae, and the Papilionoideae. The largest sub-family are the Papilionoideae, with 476 genera and around 14000 species. The Cesalpinoideae and Mimosoideae each have around 3000 species but in the former these are spread amongst 162 genera, whilst the Mimosoideae consists of only 77 genera. It is species within the Papilionoideae that are valued for their high protein pulses and pods which provide

food, rich oils and forage, as well as simple cover crops and green manures. Species within the Mimosoideae and Cesalpinoideae are known more for their timber, dyes, tannins, resins, gums, insecticides, medicines and fibres (Allen and Allen, 1981).

In addition to the occurrence of root nodules in many legume/rhizobia relationships and also in the non-legume *Parasponia*, they can also occur between non-legumes and actinorrhizal bacteria. In all there are nine families outside the legumes where nodulation symbiosis is found. However, all of these plant families belong to a phylogenetic grouping known as Eurosid I, which also contains legumes (Doyle and Lucknow, 2003). This may suggest that some factor(s) arose within the Eurosid I group enabling, but not committing, plants to form nitrogen-fixing symbioses (Soltis, *et al.* 1995).

There is no evidence for nodulation at the start of the existence of legumes. It is not until the Papilionoideae group diverge away from the remaining lineages that enormous diversity in nodule morphology, anatomy and chemistry is seen (Sprent, 2001). However, phylogenies of legume genera and species have not resolved how many times nodulation evolved. Indeed the pattern of nodulation amongst legumes is complex and has so far defied any simple explanation for its origin or origins (Doyle and Lucknow, 2003).

1.3 Legume models

The importance of legumes in global agriculture, the push for sustainability and the increased demands on food production combined with a growing population provide great impetus to legume research, particularly that relating to nodulation. Traditionally, legume research has centred on the agriculturally important crop species such as pea, beans, soybean and clover. However, because large genomes and multiple sets of chromosomes (polyploidy) complicate genetic studies, legume research has been substantially influenced in recent years in the same ways as many other biological disciplines, by the introduction of model species. Many of the traditionally important legume crop species are physically large and so occupy

expensive and extensive glasshouse space. However, large-scale mutagenesis programmes to identify relevant phenotypes and associated genes require small plants with small genomes. A model species must offer genetic and physiological characteristics that make them amenable to manipulation, crossing and molecular analyses.

Arabidopsis thaliana (thale cress) is the best-known plant model and has become the subject of intensive research across almost every area of plant science. An incredible range of data has been acquired through genetic and molecular investigations conducted on *Arabidopsis*. However, as a member of the Brassicaceae, belonging to the Eurosid II group of plants, *Arabidopsis* is unable to develop symbioses with root-nodulating bacteria. Neither is it able to accommodate another important form of symbiosis with arbuscular mycorrhizal (AM) fungi.

A model species must be amenable to techniques such as chemical mutagenesis and genetic transformation, have a relatively small genome, produce plenty of seed and be self-fertile, thus aiding the production of homozygous mutants. The organisation of the genome must also permit the quickest possible route to the detection of the genes responsible for mutant phenotypes.

In the last two decades, two principal model legume species emerged that meet the specifications mentioned above. These are *Medicago truncatula* (Barker *et al.*, 1990) and *Lotus japonicus* (Handberg and Stougaard, 1992). It should be noted, however, that many researchers still prefer more traditional legume species and consider these their models. Legumes such as *Glycine max, Phaseolus vulgaris* and *Pisum sativum* are all agriculturally important and still provide valuable and relevant physiological, biochemical and genetic data. These data frequently complement, or are complemented by, work carried out on the newer model legumes.

Both *M. truncatula* and *L. japonicus* (Figure 1.1) permit studies into plant interactions with mycorrhizal fungi and root-nodulating bacteria. In addition,

Figure 1.1. Model legumes *Medicago truncatula* (A) and *Lotus japonicus* (B). *M. truncatula* image courtesy http://www.ccrc.uga.edu/web/personnel/hahn/cotetest.html.

these legumes are susceptible to transformation by *Agrobacterium tumefaciens* and *A. rhizogenes*, bacterial species now used routinely to insert foreign DNA into a species under investigation. Both plant models have genomes roughly one tenth of the size of that of Mendel's pea (Table 1.2).

In addition to the above, the complete genome of the nitrogen-fixing symbionts of *M. truncatula* and *L. japonicus*: *Sinorhizobium meliloti* and *Mesorhizobium loti*, respectively, have been determined (Galibert, *et al*., 2001; Kaneko *et al*., 2000).

Enormous resources are being poured into both legume models, often through international collaborations. These resources include sequencing efforts (Sato *et al*., 2001), gene-tagging programmes (Scholte *et al*., 2002; Webb *et al*., 2000), metabolomics (Sumner *et al*., 2003), proteomics (Watson *et al*., 2003) and reverse genetics (Perry *et al*., 2003), not to mention the ever-increasing bioinformatics packages already developed and being developed to support these initiatives (Sumner *et al*., 2003). One of the challenges facing researchers is in which model to invest resources. As mentioned, both models provide systems for studying two types of plant-microbe interactions. These will be described in more detail in Section 1.4. *Lotus japonicus* was the legume model chosen for this thesis because it had been successfully used in a genetic transformation programme (Webb *et al*., 2000) and several lines were available for further investigation.

Table 1.2. Legume genome sizes (diploid) in selected species within the Papilionoideae.

Latin name	Genome size	Source
Lablab niger (relative of hyacinth bean)	368 Mb	Doyle and Lucknow, 2003
Phaseolus macvaughii	441 Mb	Doyle and Lucknow, 2003
Lotus japonicus	450 Mb	Nakamura and Tabata, 2001
Medicago truncatula	500 Mb	Cook *et al*., 1997
Vigna radiata	515 Mb	Bennet and Leitch, 2004
Phaseolus vulgaris	588 Mb	Doyle and Lucknow, 2003
Trifolium repens	956 Mb	Bennet and Leitch, 2004
Arachis hypogaea	1740 Mb	Bennet and Leitch, 2004
Pisum sativum	4337 Mb	Bennet and Leitch, 2004
Vicia faba	26852 Mb	Bennet and Leitch, 2004

1.3.1 The *Lotus* taxon

The *Lotus* genus has been defined and redefined since the 1700's. Most recently, Polhill (1981; cited in Kirkbride, 1999) circumscribed *Lotus* as consisting of 173 species. These species are found worldwide with the exception of some arctic regions and the low land tropical areas of S. E. Asia and S. and C. America (Kirkbride, 1999). They are found in Finland and through the Baltic countries into Europe, in Africa, Asia and N. America. The *Lotus* genus is particularly species rich in Mediterranean climates: there are 29 species in N. W. Mexico and 31 species located in California, out of a total of only 39 in the whole of the U.S.A. *Lotus* species are also common and widespread in N. W. Europe, but here there are fewer species (Kirkbride, 1999). Seven species only are found in Eastern Asia (in Mongolia, Korea, Tibet and Japan). Six of these are wide ranging species at the edge of their distribution. The seventh has also been reported in Taiwan, the Ryuku Islands and in Australia. Another, endemic species is also found in Australia (Kirkbride, 1999).

Lotus species constitute complexes of closely related groups with similar vegetative characteristics, making them difficult to distinguish (Arambarri, 1999). Heyn (1970; cited in Kirkbride, 1999) has even noted seasonal polymorphisms. However, genetic variability for many useful characteristics occurs both within and between *Lotus* species (Papadopoulos and Kelman, 1999). Three perennial forage species of *Lotus*, namely *L. corniculatus* (birdsfoot trefoil), *L. glaber* and *L. pedunculatus* are cultivated in the major forage production centres throughout the world (Papadopoulos, 1999). Of these, *L. corniculatus* is the most variable and widely distributed (Kirkbride, 1999).

Despite the greater agricultural significance of *L. corniculatus*, *L. japonicus* has received preference as a legume model because it fits more closely the criteria of model species, such as being diploid, perennial and autogamous. *L. corniculatus* is tetraploid and allogamous and is therefore not useful for mutant isolation and segregation studies.

1.4 Plant-microbe interactions

1.4.1 Plant-mycorrhiza relationship

Many species of legumes, as well as non-legumes, interact with arbuscular mycorrhizal (AM) fungi of the order *Glomales*. This symbiosis involves penetration of fungal hyphae within the plant root (Figure 1.2) and facilitates water uptake and nutrient transfer (Smith and Read, 1997). The infection process involves the development of an appressorium at the infection site when the hyphal tip comes into contact with the root surface. Penetration is accompanied by thickening of the cell walls (Gianinazzi-Pearson, 1996), the hyphal tip narrows and penetrates root cells where it invades the root cortex (Smith and Read, 1997). Invasion of the cortex is accompanied by the formation of intracellular arbsuscules which are thought to act as sites of nutrient transfer (Ewaza *et al*., 2002). AM fungi associations have received increased attention over recent decades largely because of the realisation that the effective use of symbiotic microorganisms is likely to be essential in sustainable agriculture (Kapulnik and Douds, 2000). Mycorrhizal symbionts assist host plants in phosphate uptake and contribute to increased disease resistance (Smith and Read, 1997). Schweiger and Jakobsen (1999) showed that routine phosphate influx into hyphae was two orders of magnitude greater than the maximum influx into roots. In some cases the improved disease resistance may simply be a consequence of improved plant nutrition and greater biomass. However, competition for infection sites, which would favour the already established AM fungi (Cordier *et al*., 1996), and AM fungi-induced changes in root exudation that alter the physiology and micro-flora of the rhizosphere may also improve plant disease resistance.

Mycorrhizal fungal associations occur in about 80% of land plants so far examined, including some members of most families of angiosperms and gymnosperms, as well as ferns, lycopods and bryophytes (Smith and Read, 1997). In recent years researchers have identified a number of plant mutants that are impaired in their associations with mycorrhizal fungi. These mutant plants

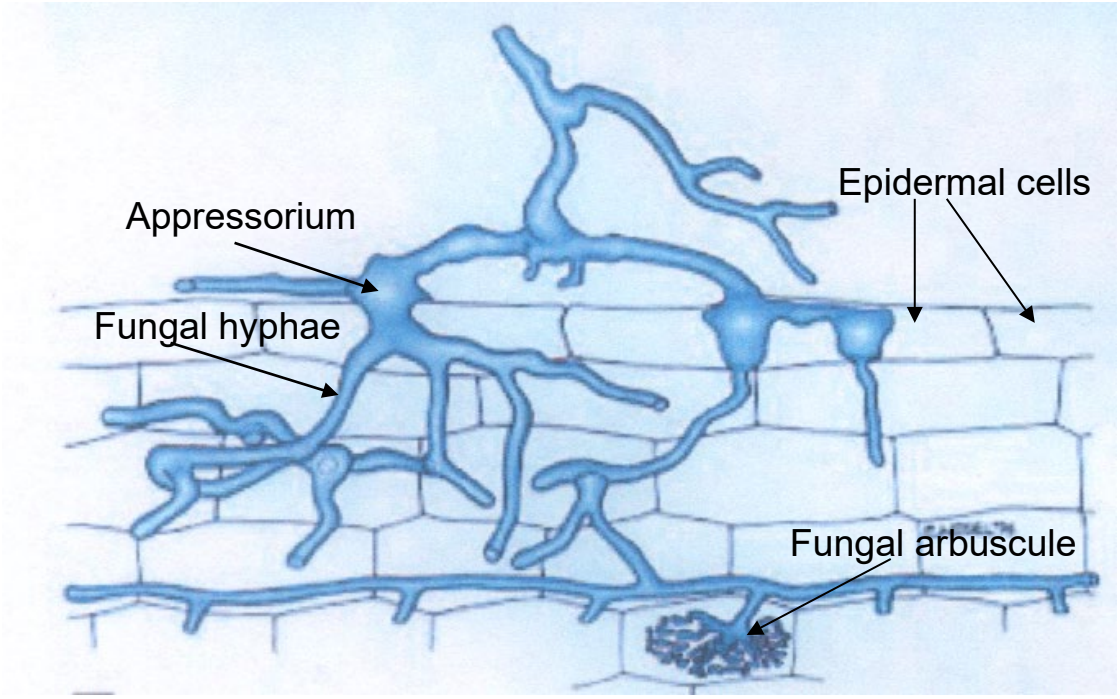

Figure 1.2. Semi-schematic drawing representing mycorrhizal colonisation of legume root. Once the hyphal tip comes into contact with the epidermal cells at the root surface an appressorium is formed. The hyphal tip then invades the root cortex. This is accompanied by the formation of intracellular arbsuscules (Gianinazzi-Pearson, 1996). Image based on Wegel *et al*. (1998).

are also affected in their ability to form root nodule symbioses, suggesting that at least a subset of genes is common to both interactions (Stougaard, 2001). Genes that may lie on a pathway common to both interactions will be mentioned in more detail later. Fossil evidence indicates that plant associations with mycorrhizal fungi are more ancient than those with rhizobia (Remy *et al*., 1994) and it has been suggested that root nodulation has evolved using a group of genes commandeered from the more ancient mycorrhizal interaction (Frühling *et al.,* 1997; La Rue and Weeden, 1994; van Rhijn *et al*., 1997). Research into rhizobial symbiosis is therefore increasingly associated with that of mycorrhizal symbiosis and often study of the two interactions are carried out side by side.

1.4.2 Legume-rhizobia relationship

The root nodule symbiosis is almost entirely restricted to the Leguminoseae, with the exceptions noted in Section 1.2. Within the legume family, nodulation exists in more than 90 per cent of the Papilionoideae, 83 per cent in the Mimosoideae and only around five per cent in the Cesalpinoideae (Allen and Allen, 1981; Doyle and Lucknow, 2003). The relationship between legumes and rhizobia exhibits a high, but often complex, degree of host-specificity. There are bacterial strains with a broad host range, such as *Rhizobium* sp. NGR234, which is able to nodulate more than 70 genera of legumes (Price *et al*., 1992). The majority of other rhizobia have a much more limited range of hosts and are classified accordingly. For example, rhizobia nodulating *Trifolium* species are *Rhizobium leguminosarum* biovar *trifolii*. A list of several species/strains and their legume hosts is shown in Table 1.3. The host-specificity is attributable to a number of factors. In keeping with its high level of promiscuity, the broad host range *Rhizobium* species NGR234 is also able to nodulate the non-legume *Parasponia* (Price *et al.,* 1992).

Considerably more is understood of the physiological, molecular and genetic bases of root nodulation, as compared with mycorrhizal interactions, and it is this interaction which forms the basis of this thesis.

Table 1.3. Examples of host-strain specificity in the legume-rhizobia relationship.

Rhizobial species/strain	Host plant
Rhizobium etli	*Phaseolus*
Rhizobium broad host range NGR234	Broad host range
R. leguminosarum bv *viciae*	*Pisum* (pea), *Vicia* (bean), *Lathyrus,*
bv *trifolii*	*Lens* (lentil)
bv *phaseoli*	*Trifolium* (clover)
	Phaseolus
Sinorhizobium meliloti	*Medicago truncatula* (barrel medic)
Mesorhizobium loti	*Lotus japonicus*
Bradyrhizobium japonicus	*Glycine max* (soybean)
B. vigna	*Arachis hypogaea* (peanut)
B. lupinus	*Lupin* species

1.5 The root nodule symbiosis

1.5.1 Root nodules: determinate and indeterminate

The culmination of the relationship between the legume and rhizobia is the root nodule, the site of N-fixation and nutrient exchange. Root nodules are generally classified into one of two groups, depending on the presence or absence of a persistent, active meristem. Those nodules with meristems that endure are elongated in shape, and often branched. Here, extensive, persistent ramifications of infection threads are required to infect newly formed cells. The term indeterminate is used because the meristem persists even in mature nodules (Sprent, 2001). Examples of species forming indeterminate nodules are pea (*Pisum sativum*), clover (*Trifolium* spp.) and alfalfa/lucerne (*Medicago sativa*). Nodules without a persistent meristem or extensive infection threads are found in such species as soybean (*Glycine max*), bean (*Phaseolus* spp.) and *Lotus*. These are called determinate nodules and are more or less spherical in shape with a closed vascular system. Here the bacteria spread through divisions of pre-infected cells. Schematic illustrations of the determinate and indeterminate nodules are presented in Figure 1.3.

One of the major differences between *L. japonicus* and *M. truncatula* is that the former develops nodules of the determinate variety, whilst *M. truncatula* forms indeterminate nodules. This characteristic may be a decisive factor in selecting the model most appropriate for study.

The root nodule itself appears as an outgrowth from the plant root and is the site of nitrogen fixation. The nodule is also the site of the exchange between plant-manufactured carbon compounds from photosynthesis and bacteria-derived ammonia from N_2-fixation.

N_2-fixation is made possible by the enzyme complex nitrogenase-nitrogenase reductase (frequently abbreviated to nitrogenase). This enzyme consists of two components each serving different functions. Nitrogenase reductase is the

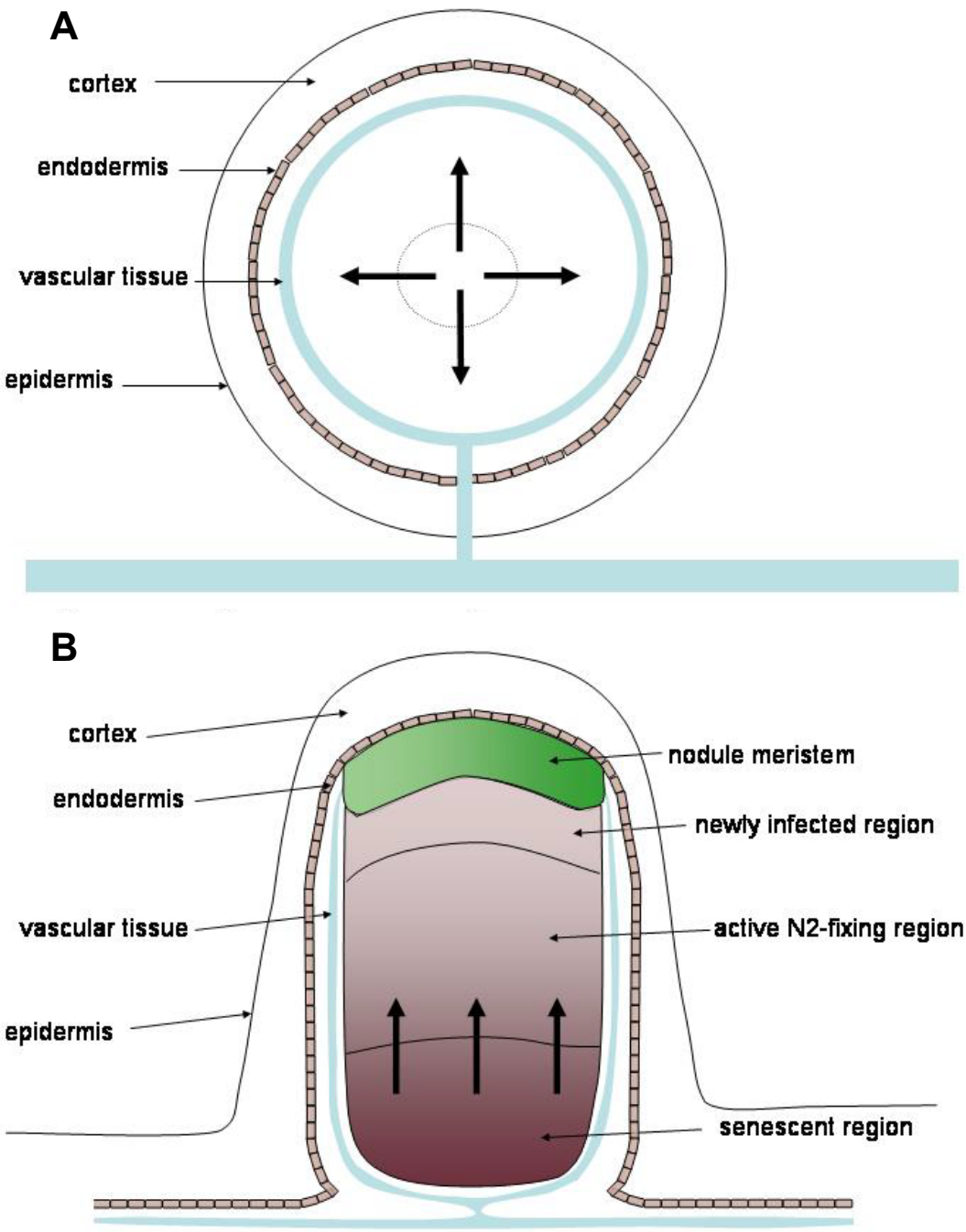

Figure 1.3. Illustration of longitudinal section through determinate (A) and indeterminate (B) root nodules. Thick black arrow indicates direction of increase of senescent tissue (adapted from Puppo *et al*., 2005).

constituent that collects reducing power and energy. The other factor, nitrogenase, collects and reduces the substrate, $N_2 \Rightarrow NH_3$. As the high fossil type input used in the industrial Haber-Bosch process indicates, this reduction requires a lot of energy. Six cycles of nitrogenase reductase activity are required for every molecule that is reduced, requiring 15 molecules of the chemical energy source adenosine triphosphate (ATP) for every molecule of NH_3 (Hughes, 1996). N_2-fixation in nodules is therefore a major feat: it requires energy, and is thus dependent on ATP, but ATP is usually generated during aerobic respiration. However, O_2 irreversibly inactivates the nitrogenase enzyme (Sprent and Sprent, 1990). How is this paradox resolved in the legume root nodule?

Many of the free-living organisms that fix N_2 only do so using substrate-level phosphorylation to generate ATP under anaerobic conditions. Symbiotic bacteria, however, control the supply of O_2 in direct collaboration with the plant by producing the protein product leghaemoglobin. This, combined with a variable diffusion resistance to O_2 within the nodule, provides a good system for tailoring O_2 demand to supply (Sprent and Sprent, 1990). The globin is produced by the plant, whilst the bacteria provide the haem cofactor (Hughes, 1996).

Leghaemoglobin is a rare molecule in the plant kingdom but is structurally very similar to animal haemoglobin. It can accumulate to very high levels within the nodule, accounting for 30% of the total protein content (Hughes, 1996) and it is this that leads to the characteristic pink coloration of a healthy, N_2-fixing root nodule (Allen and Allen, 1981).

1.5.2 Flavonoids initiate the early stages of nodulation

Nodulation begins under conditions of low nitrogen with the release of flavonoid and other compounds from the plant (Fisher and Long, 1992). These secondary metabolites derive from the phenylpropanoid pathway and vary between species, thus accounting for some of the host-specificity of the symbiosis. Although many of the chemical structures of these phenolic compounds and metabolic pathways have been determined there is still a lack of information regarding the types of

molecules that are active in eliciting a rhizobial response. Flavonoids serve both as chemoattractants of rhizobia and inducers (sometimes inhibitors) of specific nodulation genes within the rhizobial strains (Gagnon and Ibrahim, 1998). Flavonoids also serve several other functions including the promotion of rhizobial growth (Hartwig *et* al., 1991). The structures of some flavonoids are illustrated in Figure 1.4. In addition to flavonoids, other classes of secondary metabolites are also involved in nodulation gene induction. These include some aldonic acids and betaines (Gagnon and Ibrahim, 1998).

1.5.3 Nodulation factors are released by the bacteria in response to flavonoids

The bacterial genes expressed at this stage of the symbiosis are the nodulation (*nod*) genes and the products they encode are nodulation (Nod) factors. Although the NodD protein is constitutively expressed, it is the first bacterial protein to respond to the right flavonoid signals. NodD is a transcriptional activator to which the plant flavonoid compounds bind. This binding initiates a conformational change in NodD, enabling it to bind to the promoter regions of *nod* gene operons (Fisher and Long, 1992). This elicits the expression of a series of *nod* genes that encode the major determinants of host-specificity: N-acylated oligomers of ß1-4-linked *N*-acetyl-D-glucosamine (Lerouge *et al*., 1990; Roche *et al*., 1991). The 'common' *nod* genes are *nodABC*, encoding enzymes responsible for building the oligosaccharidic backbone of the *N*-acetyl-D-glucosamine residues. Other, host-specific, *nod* genes are also initiated at this point, including those responsible for the acyl chain attached to the terminal glucosamine (Fisher and Long, 1992; Peters *et al* 1986; Schlaman *et al*., 1992). The chemical structure of a Nod factor molecule and its associated genetic determinants is shown in Figure 1.5. Nod factors resemble chitin in structure and are therefore frequently referred to as lipo-chitin oligosaccharides (López-Lara *et al*., 1995).

Mutations in the *nodABC* genes result in complete abolishment of the nodulation process. The host-specific genes determine chemical decorations to the reducing

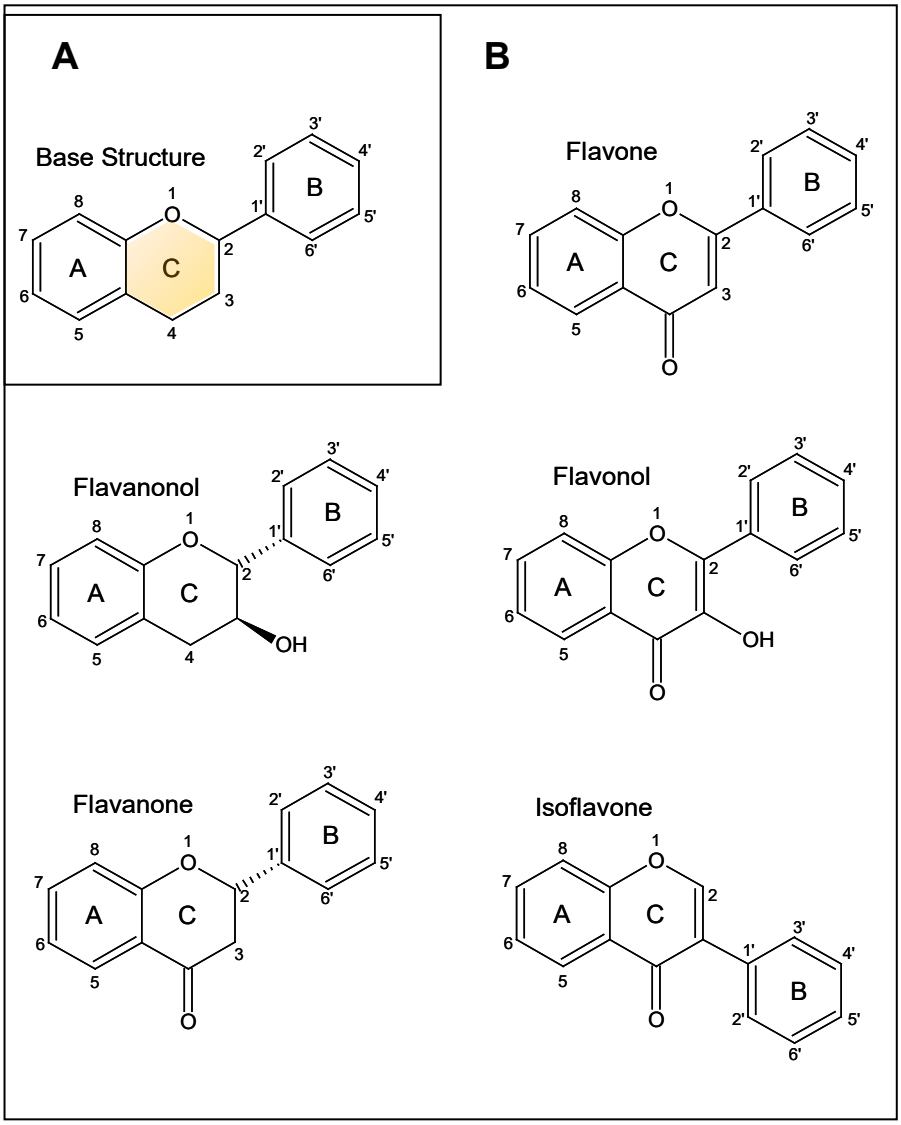

Figure 1.4. Structure of legume flavonoids. **A**, general structure of flavonoid compounds. The different classes of flavonoids are defined by the structure of the C-ring (shaded orange) and function carried by the C-3 and C-4. **B**, chemical structure of selected sub-classes and biologically active flavonoids. Adapted from Aoki *et al*., 2000.

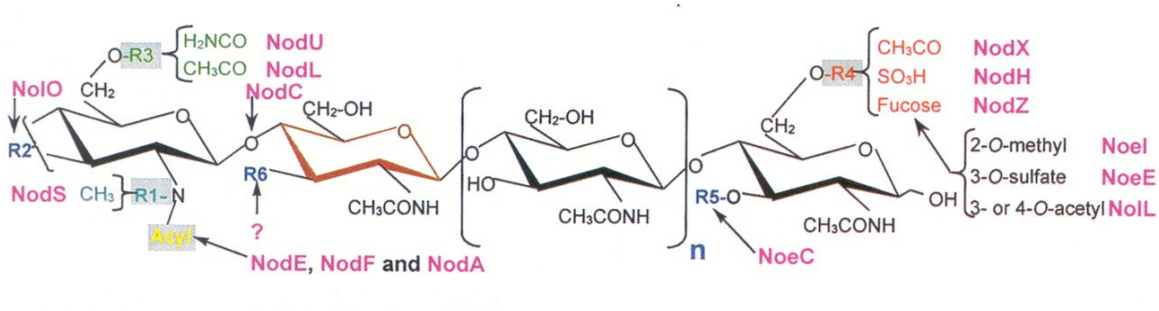

Figure 1.5. Chemical decorations, and their genetic determinants, of N-acylated oligomers of *N*-acetyl-D-glucosamine (Nod factors). Adapted from Perret *et al*. (2000) and Spaink *et al*. (1993).

and non-reducing end of the chitin oligomer backbone, as well as the length and degree of saturation of the fatty acyl chain (Dénarié *et al*., 1996; Fisher and Long, 1992). Nod factor structural modifications, and in many cases their corresponding genes, have now been determined for more than 20 rhizobial strains (Perret *et al*., 2000). Other bacterial genes involved in the symbiosis have been designated *nif* and *fix*. These have roles in N_2-fixation. *Rhizobium* with mutations in the *nif* or *fix* genes are able to induce nodule formation on their legume host but these nodules do not fix N_2 (Hughes, 1996). Many of the rhizobial genes required for nodulation are situated on large plasmids of about 200 Kb, whilst those in the slow-growing *Bradyrhizobium* are located on symbiosis 'islands' on the bacterial chromosome (Finan, 2002; Hughes, 1996).

The elicitation of Nod factors from the bacteria and subsequent perception by the plant initiates various physicochemical responses in the plant. These changes include membrane depolarisations as well as deformations in root hair morphology such as swelling, branching and curling (referred to as shepherds' crooks) and the induction of divisions in cortical cells (Dénarié *et al*., 1996; Fisher and Long, 1992). The cortical cell divisions indicate the initiation of nodule primordia. The bacterial cells will eventually arrive here and begin fixing N_2. Bacteria enter root hair cells through the invagination of the plasma membrane and subsequent formation of a tubular structure known as the infection thread. Within the infection thread bacteria grow and divide and make their way to the developing nodule primordia. Figure 1.6 outlines the process of nodulation as described here, showing the curling of root hairs following rhizobial attachment (Figure 1.6a), development of the infection thread (Figure 1.6b), division of cortical cells and branching of the infection thread (Figure 1.6c) followed by the release of bacteria into nodule primordial cells (Figure 1.6d). All of the above takes place in response to the presence of rhizobia and perception of rhizobial Nod factors. In fact, Nod factors in picomolar concentrations are able to elicit many of the above responses in the absence of rhizobia (Lerouge et al., 1990; Spaink et al., 1991; Truchet *et al*., 1991), but the mechanisms whereby the plant perceives such low concentrations of this molecule are currently unknown.

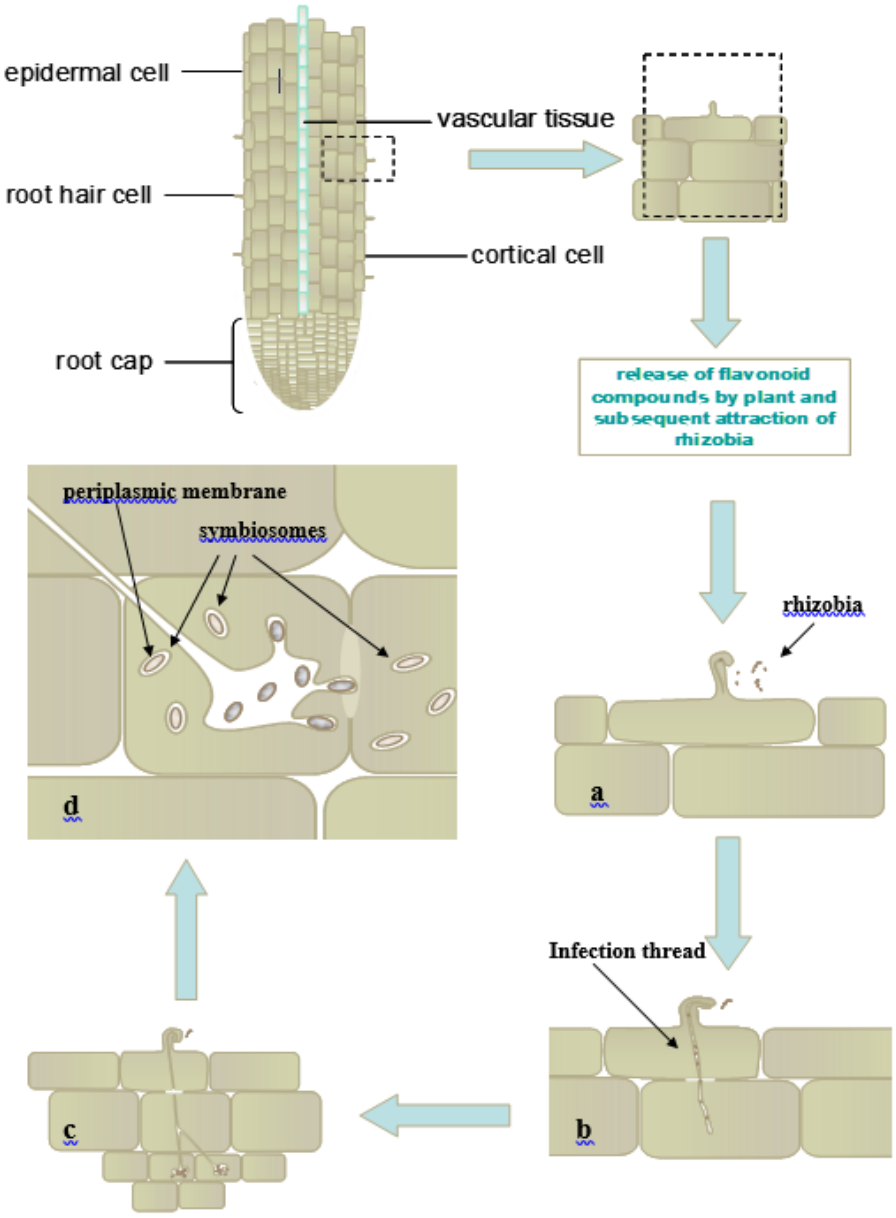

Figure 1.6. Early stages in the nodulation signalling pathway. The attachment of rhizobia elicits root hair deformations including curling (a). Infection thread formation permits rhizobial entry through outer cortical cells (b) and into developing nodule primordia (c) where bacteria are eventually released via exocytosis (d).

1.5.4 The nodulation zone and Nod factor perception

Perception of Nod factor by the legume root is restricted to a small part of the root system. Heidstra *et al*. (1994) describe a zonation, where zone I corresponds to young, growing hairs that do not deform in response to Nod factor inoculation, zone II contains root hairs that respond to Nod factor with root hair deformation and zone III comprises fully grown root hairs. An illustration of these areas is shown in Figure 1.7.

The means by which bacteria adhere to root hair cells and elicit the very earliest host responses has been a much studied and sometimes controversial subject. Lectins produced by the plant may be involved in physical binding of rhizobia to the host but the requisite high degree of binding between lectins and rhizobia has not been consistently identified (Sprent, 1979). Perhaps of greater interest for many researchers is the mechanism by which the plant first perceives the Nod factor signal. The existence of an actual Nod factor receptor has long been speculated, particularly since, as mentioned above, purified Nod factors in pico molar concentrations can elicit a range of host responses in legumes (Lerouge et al., 1990; Spaink et al., 1991; Truchet *et al*., 1991). Recently, the map-based cloning of two genes, *Nfr1* and *Nfr5* from *L. japonicus*, has been reported (Madsen *et al*., 2003; Radutoiu *et al*., 2003). Plants mutated in either locus do not exhibit root hair deformation and are either altered (*nfr1*) or blocked (*nfr5*) in Nod factor-induced depolarisation of the root hair plasma-membrane. *Nfr1* and *Nfr5* both encode receptor kinases with extracellular LysM-type domains. Other LysM kinases have also been reported to be involved in symbiosis. In *M. truncatula* a reverse genetics approach has revealed the involvement of two LysM domain–containing receptor-like kinases (*Lyk3/4* and *Nfp*) in infection thread formation (Limpens *et al.*, 2003). This, and the involvement of the LysM-type domains in peptidoglycan- and chitin-binding proteins, strongly suggests that they are Nod factor entry receptors. Therefore, the LysM kinases identified in *L. japonicus* and *M. truncatula* are likely candidates for Nod factor receptors. This exciting discovery opens up new opportunities for binding studies as well as

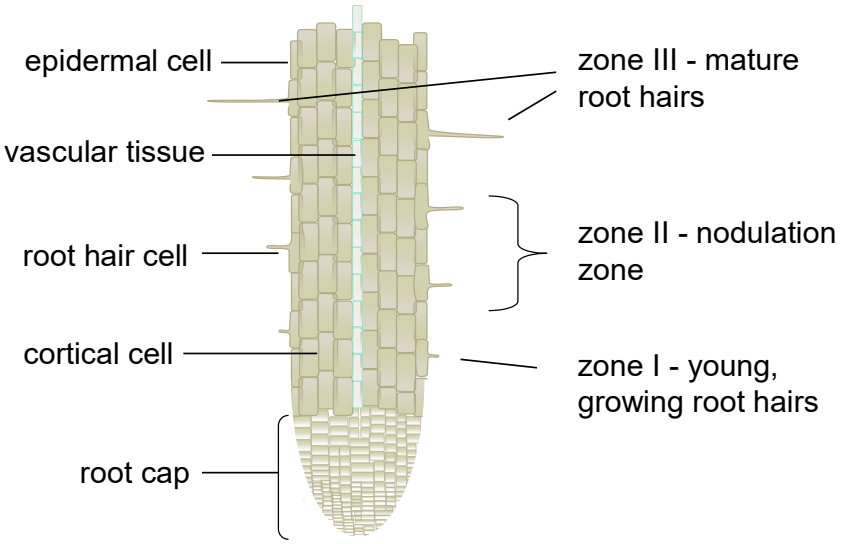

Figure 1.7. Schematic diagram illustrating the nodulation zone of a legume root. Zone I contains young, growing root hairs that do not deform in response to Nod factor, zone II root hairs respond to Nod factor with root hair deformation and zone III comprises fully grown root hairs (Heidstra *et al*., 1994).

investigations into the possible operation of multimeric receptor complexes in Nod factor perception and signalling.

1.5.5 Calcium responses and G-protein-mediated signalling during root nodulation

As mentioned above, the responses elicited in the plant by purified Nod factor include root hair deformations (Lerouge *et al*., 1990; Spaink *et al.,* 1991), activation of cell cycle machinery leading to cortical cell divisions (Spaink *et al*., 1991; Truchet *et al*., 1991) and membrane depolarisations (Felle *et al*., 1995). The first of these responses appear to be those observed by Felle *et al*. (1995). Membrane depolarisations take the form of calcium influx, followed by efflux of chloride and potassium ions and have been shown to occur at the tip of the root hair cell within minutes of the application of purified Nod factor (Felle *et al*., 1995).

In addition to the increase of the calcium gradient at the root hair tip, a second phase of ionic change occurs in the form of oscillations in the concentration of cytoplasmic calcium ($[Ca^{2+}]_{cyt}$ in the root hair cell (Oldroyd, 2001). Such oscillations, known as Ca^{2+}-spiking, occur after about ten minutes of the application of Nod factor or rhizobia (Oldroyd, 2001). The role and effects of Ca^{2+} in signalling has been studied more widely in animal systems than in plants. In animals, it is known to be involved in the control of a wide range of cellular functions, including cell development and differentiation and gene transcription (Berridge, *et al*., 1998; Sanders *et al*., 2002). The role of Ca^{2+} in the nodulation process will be discussed further in Chapter 3.

In efforts to further dissect the Ca^{2+}-spiking response, Pingret *et al*. (1998) designed experiments using pharmacological techniques. These experiments suggested the involvement of G-proteins during early nodulation. G proteins are membrane-associated proteins, molecular switches that use GDP to control their signalling cycle. When GDP is bound the G protein is inactive. Activation occurs when GDP is replaced with GTP, then the G protein will deliver its signal (Figure

1.8c) (Goodsell, 2005). G proteins vary in shape and size. Most are used for cell signalling, but some have other roles, such as powering protein synthesis. Heterotrimeric G proteins are composed of three different chains, alpha, beta and gamma. A loop on the surface of the alpha subunit is important in transmitting the signal (Goodsell, 2005). Pingret *et al*. (1998) determined that the G-protein activator mastoporan was able to induce expression of a reporter gene fused to the promoter region of a plant gene, *ENOD12*, which is induced in the early stages of the legume-rhizobium relationship. In support of these results, the G-protein antagonist pertussis toxin was found to inhibit Nod factor and mastoporan induced expression of the reporter gene (Pingret *et al*., 1998). In the same study, the involvement of phospholipase C was also investigated. A common feature of signal transduction in plants is the cleavage of phosphatidylinositol (4,5)-bisphosphate (PIP_2) to yield (1,4,5)-trisphosphate (IP_3) and diacylglycerol (DAG), a reaction that is frequently catalysed by G protein-mediated activation of specific phospholipase C (PLC) (Figure 1.8c) (Pingret *et al*., 1998). Neomycin, a widely used antagonist of phospholipase C, was found to totally inhibit expression of the *ENOD12* promoter-reporter gene fusion. Based on these and other experimental evidence Pingret *et al*. (1998) argued that Nod factor sequentially acts through a G protein, then phospholipase C and is followed by Ca^{2+} influx. Figure 1.8 illustrates what is known of the sequence of events and some of the elements likely to be involved in the early nodulation signalling pathway.

Interestingly, G-proteins have also been implicated in the signalling between an ecto-mycorrhiza and spruce (Hebe *et al.,* 1999). No such reports have yet been made regarding the involvement of G-proteins in the arbuscular mycorrhizal signalling pathway but it seems likely that several signalling mechanisms may overlap in the development of rhizobial and mycorrhizal interactions.

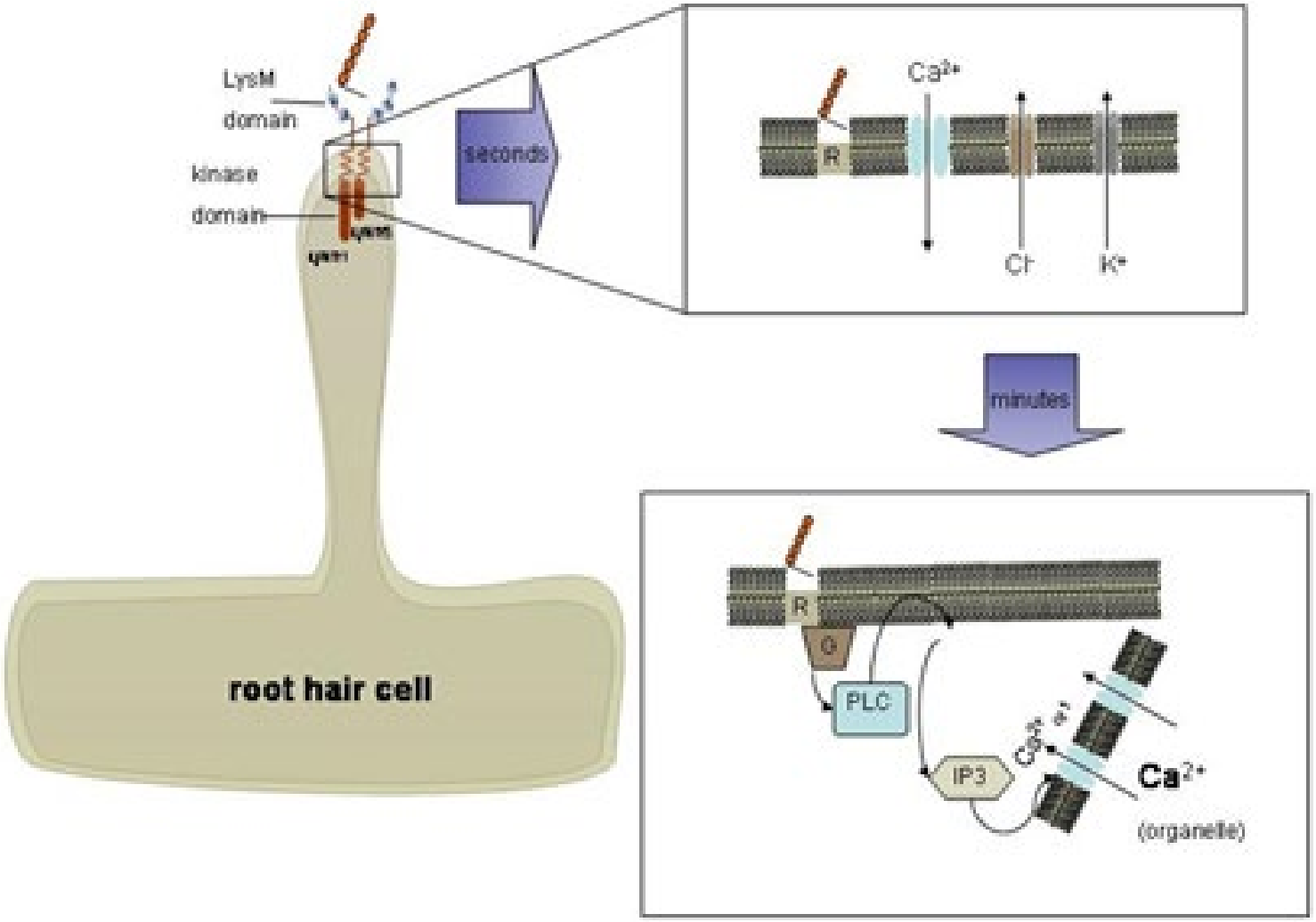
LysM
domain
kinase
domain
seconds
root hair cell
R
Ca^{2+}
Cl^-
K^+
minutes
R
G
PLC
IP3
Ca^{2+}
Ca^{2+}
(organelle)

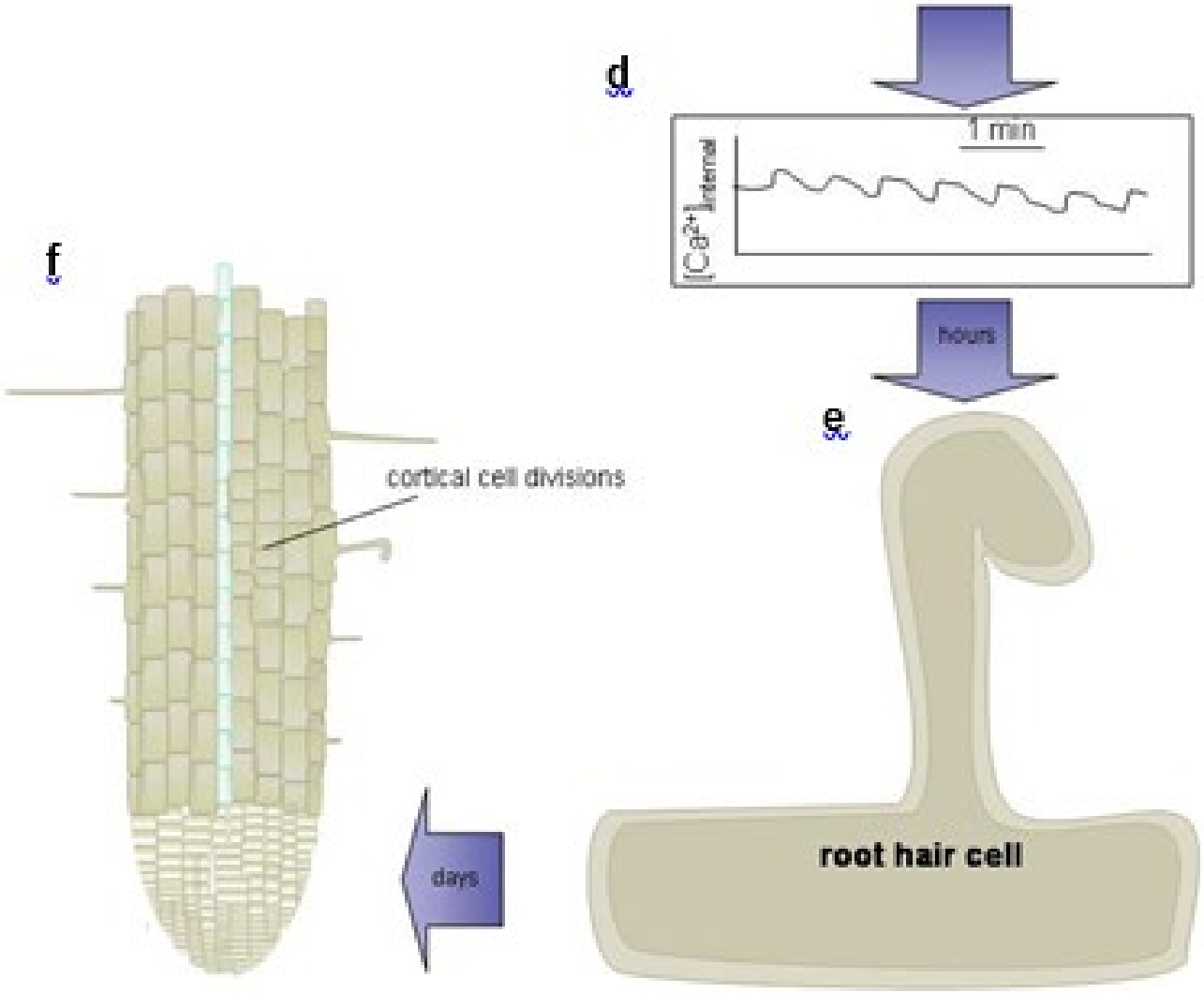
d
1 min
[Ca2+]internal
hours
e
root hair cell
f
cortical cell divisions
days

1.5.6 Infection thread development and bacterial entry into the nodule

The binding of a rhizobium to a root hair cell creates a refractile spot (hyaline) that indicates changes in root hair structure. Such changes signal the beginnings of the infection thread, a tubular structure formed by invagination of the plasma membrane as it encloses the invading bacterium (Figure 1.4a). The infection thread precedes the bacteria all the way to the nodule primordia. Interestingly, Esseling *et al*., (2004) observed that *M. truncatula nork* mutants are unable to form three-dimensional, multi-faceted root hair curls. They also determined that such curls are necessary for the entrapment of the colonising bacterium and subsequent formation of infection threads, perhaps because the bacterium continues to grow against increasing pressure at the root hair cell wall.

Within the infection thread the bacteria grow, divide and eventually differentiate into their N_2-fixing form, the bacteroid. It is not clear whether multiple rhizobia enter the infection thread or whether the bacteria that colonise the nodule primordia originate from one cell that has multiplied. However, Stuurman *et al.* (2000) observed two strains of auto-fluorescently labelled bacteria colonising the same nodule of siratro (*Macroptilium atropurpureum*), a member of the *Pisum* family, indicating that multiple entry can occur.

On entering the nodule primordia in the inner root cortex, the plant takes the bacteria from an unwalled infection droplet into nodule cells (Figure 1.4d). This is achieved through exocytosis. The intracytoplasmic bacteria, now differentiated into their bacteroid form, are then enclosed with a periplasmic membrane of plant origin and together these form the symbiosome (shown in Figure 1.6d).

1.5.7 Hormonal involvement during nodulation

In addition to the role of flavonoids, Nod factors, Ca^{2+} and G-proteins, there are considerable data suggesting the involvement of plant hormones in the root nodulation process. Hormones such as auxin are known to be associated with cell wall loosening and growth and these have been strongly implicated in the infection process (Sprent, 1979). The induction of cell division in the root cortex during nodulation also infers a role for plant hormones. Furthermore, plant hormones appear to affect the regulation of some plant genes activated during the onset of symbiosis, for example, *ENOD2*. Hirsch *et al.* (1989) demonstrated that auxin transport inhibitors were able to induce the formation of nodule-like structures on *M. sativa*. In addition to the formation of these "pseudo" nodules, transcripts of the *ENOD2* gene were identified from pseudo nodule tissues (but not from root tissue) indicating that the same auxin perturbation events had resulted in the induction of certain plant genes known to be involved during nodulation (Hirsch *et al*., 1989). *ENOD2* transcripts were also identified in the spontaneously induced nodules described by Truchet *et al.,* (1989). Finally, flavonoid compounds, such as those described in Section 1.5.2, are now known to play a part in this negative regulation of auxin transport (Mathesius *et al*., 1998; Mathesius *et al*., 2000). Bhatla *et al*. (2002) suggested that an auxin receptor, located at the plasma membrane, may lead to a phosphorylation of anion channels and a subsequent depolarisation of the plasma membrane, in turn stimulating the opening of Ca^{2+} channels, responses that bear resemblance to the early events in nodulation.

In addition to the probable role of auxin in nodule organogenesis a number of reports have also identified the potential involvement of gibberellin, cytokinin and abscisic acid (ABA) in nodulation (Hirsch and Fang, 1994; Nukui *et al*., 2000). Also, ethylene has been implicated in the regulation of events by limiting the number of infections (Penmetsa and Cook, 1997). Elevated levels of this hormone have been shown to dramatically reduce Ca^{2+}-spiking both in the initiation of the signal and its subsequent maintenance (Oldroyd *et al*., 2001). Further data suggested that ethylene may define both the plant's sensitivity to Nod factor and

the threshold concentration of Nod factor that is required for a response (Oldroyd *et al*., 2001).

1.5.8 Plant gene expression during early nodulation

The development of an entirely new organ, the root nodule, and the creation of an environment that is favourable for N_2-fixation requires complex exchanges of signals between plant and bacteria. Some of the signals involved in the exchange have been identified and have been discussed (Sections 1.5.2 to 1.5.6). This signal exchange controls the expression of both bacterial and plant genes. The bacterial genes are *nod*, *nif* and *fix* and these have been characterised over a number of years. The *nif* and *fix* genes are involved in nitrogen fixation, whilst *nod* genes are generally those involved in the earlier stages of infection. In plants, the proteins encoded by genes that are either specific to nodulation or are upregulated in response to nodulation, are termed nodulins. The globin part of leghaemoglobin (Section 1.5.1) is one such protein and is only made in root nodules.

Nodulins are divided into two categories: the early nodulins (ENOD) are induced within the first few days, or even hours, of application of rhizobia or Nod factor (Journet *et al*., 1994; Journet *et al*., 2001; Scheres *et al*., 1990). These include the genes *ENOD12* and *ENOD2* mentioned in Sections 1.5.5 and 1.5.7, respectively. The late nodulins are those plant genes induced at the onset of N_2-fixation and include leghaemoglobins, glutamine synthase, sucrose synthase, uricase and other household genes (Tajima *et al*., 2000).

The use of model legumes such as *L. japonicus* and *M. truncatula* has speeded up the identification of plant genes that are induced in either or both, rhizobial and mycorrhizal symbiosis. The identification of such genes has largely been mediated by the analysis of plant mutants impaired in one or both interactions and the development of 'libraries' comparing transcripts of both wild-type and mutant mycorrhized/nodulated and non-mycorrhized/non-nodulated plants. In both *L. japonicus* and *M. truncatula* these types of analyses have led to the characterisation and publication of three genes required for both rhizobial and mycorrhizal

symbioses (Ané, *et al*., 2004; Endre *et al*., 2002; Imaizumi-Anraku *et al*., 2004; Lévy *et al*., 2004; Mitra, *et al*., 2004; Stracke *et al*., 2002). In *L. japonicus* a further three genes have been characterised and published which are required for successful interaction with rhizobia (Madsen *et al*., 2003; Radutoiu *et al*., 2003; Schauser *et al*., 1999). Orthologues of two of these genes have also been identified in *M. truncatula* (Limpens *et al*., 2003).

The identification of such genes and detailed characterisation of the associated mutant phenotypes in the plant permits hypotheses regarding the signalling pathways involved in establishing both symbioses. In Section 1.5.4 two genes from *L. japonicus* (*Nfr1* and *Nfr5*) and two from *M. truncatula* (*Lyk3*/*4* and *Nfp*) were described, which are somehow involved in the perception of bacterial Nod factor. These genes are strong candidates for Nod factor receptors. However, plants mutated in these loci are not impaired in mycorrhizal symbiosis. Conversely the genes *SymRK* (for symbiosis receptor-kinase), in *L. japonicus*, and *Dmi2* (does not make infections), in *M. truncatula*, are required for successful interaction with both symbionts and therefore represent common symbiotic (sym) genes (Stracke *et al*., 2002; Endre *et al*., 2002). *SymRK* and *Dmi2*, together with *Nork* in *M. sativa*, are orthologues of a receptor-kinase gene and since they are required for both symbioses can be placed downstream of the putative Nod factor receptors, on a common pathway. Two other genes in *L. japonicus*, *Castor* and *Pollux*, have recently been published (Imaizumi-Anraku *et al*., 2004). These are highly homologous genes and encode proteins that may be involved in the mediation of ion fluxes between plastids and the cytosol. Both genes are required for rhizobial and mycorrhizal symbioses and mutant phenotypes demonstrate that they function downstream of *SymRK*. *M. truncatula* mutant *dmi1* shows a strongly similar phenotype to *pollux* mutants as well as high sequence identity (Ané, *et al*., 2004). *Pollux* and *Dmi1* are therefore considered orthologous. Details of the *Dmi3* gene have also recently been published. This gene encodes a putative Ca^{2+}- and calmodulin-dependant protein kinase also required for both symbioses (Mitra *et al*., 2004). The *dmi3* mutant is capable of responding to Nod factor with a Ca^{2+}-spiking response that is not observed in plants mutated in the other genes described above, *Dmi3* therefore functions further downstream (Mitra *et al*., 2004).

Several other plant mutants have been identified with phenotypes which place them either up or downstream of those described. These include *L. japonicus sym24, 3, 15* and *30* (Parniske *et al*., 2000; Parniske, 2004; Schauser *et al*., 1998; Szczyglowski *et al*., 1998). Using these data, a scheme such as the one shown in Figure 1.9 can be used to visualise the genetic development of the symbiotic pathway. The *Nin* gene is included in Figure 1.9, as it is known to be involved during nodule inception (Schauser *et al*., 1999) and its protein functions downstream of all others detailed above. Several *P. sativum* genes are also shown on Figure 1.9 which, for the sake of brevity, will not be discussed here, but illustrate the way data from parallel studies can be used together to further our understanding of this signalling pathway. Although the pathway depicted is linearised it must be remembered that most aspects of plant growth and physiology are regulated by networks of signalling mechanisms, rather than linear pathways.

Despite the characterisation of the above *ENOD* genes and those later nodulins also described, micro array data has identified that more than 750 genes are differentially expressed during root nodulation in *M. truncatula* (El Yahyaoui *et* al., 2004). This represents an enormous challenge to root symbiosis researchers and contrasts starkly with the extensive data already held regarding the bacterial genes involved in the root nodule symbiosis. A major challenge for plant researchers, therefore, is to restore some balance to this ratio.

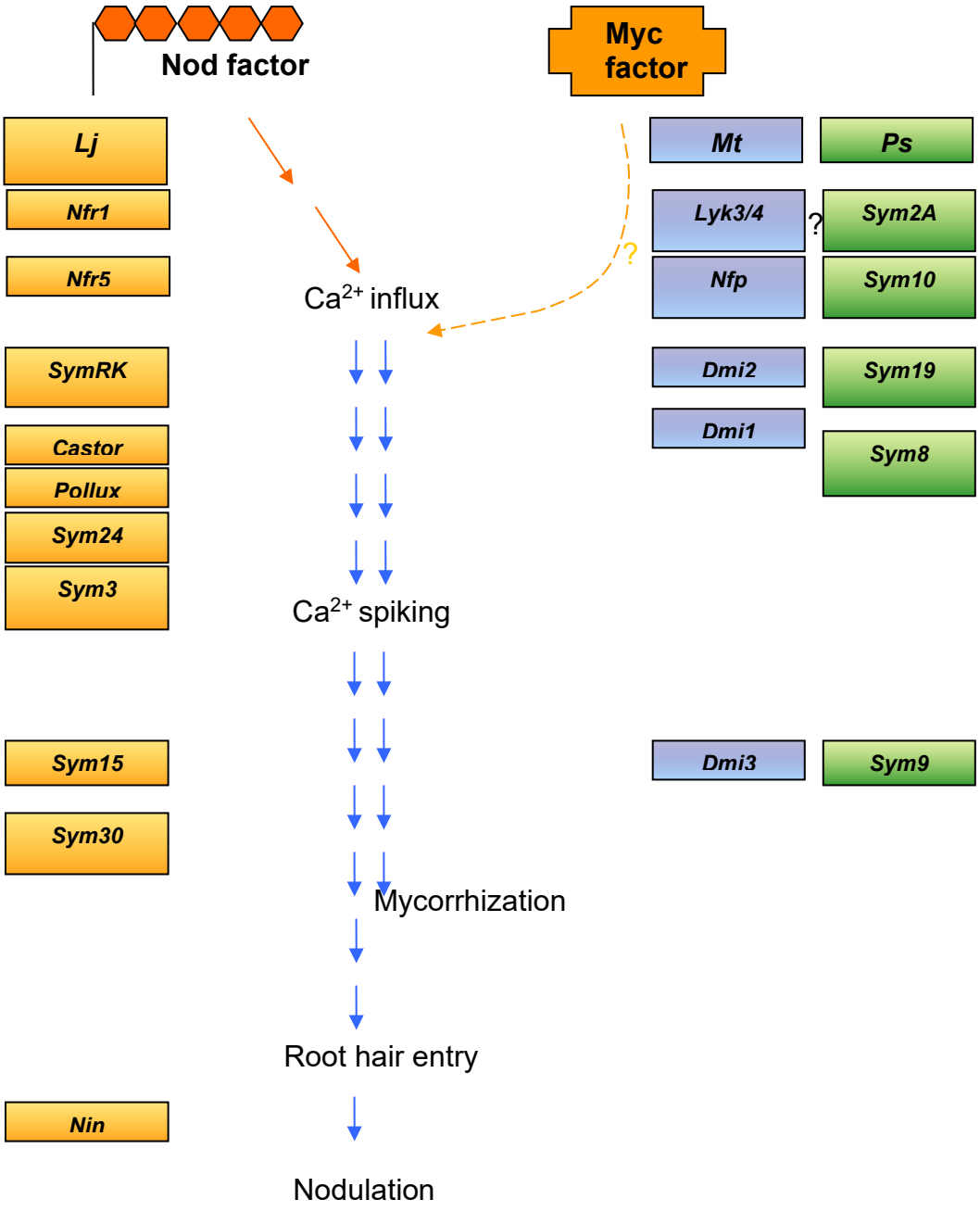

Figure 1.9. Proposed simplified signalling pathway of early symbiosis genes. The image depicts orthologous genes in three legume species, *Lj* (orange) =*Lotus japonicus*; *Mt* (blue) =*Medicago truncatula*; *Ps* (green) =*Pisum sativum*. Genes that are aligned horizontally show true orthology, based on sequence comparisons, or are putative orthologues (marked '?'), based on phenotypic similarities and relative map locations. *L. japonicus* genes known to be common to both symbioses are positioned relative to Ca^{2+}-spiking as tested in the *Lotus* mutant or an orthologue. Therefore, for instance, *Nfr5*, *Nfp* and *Sym10* (in *P. sativum*) are orthologous and mutations in the proteins they encode block Ca^{2+} influx and all downstream nodulation responses. This scheme does not incorporate the findings of Esseling *et al*., (2004), which suggest that the *Dmi* genes are on a branch of the pathway not required for root hair deformation responses. In addition to the above, three further genes from *M. truncatula* and one from *P. sativum* could be placed on the above diagram, downstream of *Dmi3* and *Sym9,* respectively. Adapted from Oldroyd and Downie (2004) and Parniske (2004).

Major collaborative investigations are underway to determine precisely which plant genes are involved in nodulation, how the plant/rhizobia regulate them and what the function of the encoded gene products are.

1.6 Gene-trapping in *L. japonicus*

In an effort to identify plant genes involved during the early stages of symbiosis with root-nodulating bacteria, Webb *et al*. (2000) established a programme to 'tag' genes involved in the early stages of the rhizobium symbiosis using the model legume *L. japonicus*. The technique adopted by Webb *et al*. (2000) is known as gene-trapping and uses the insertion of foreign DNA, in this case a gene encoding an easily assayed enzyme, into the model species to act as a marker, or tag, to report expression of native plant genes. Webb *et al*. (2000) generated a number of plant lines that showed promise for investigations into the legume/rhizobia symbiosis. One line, T90, was particularly interesting as a research tool. Experimental data suggested that the inserted DNA tag was reporting expression of a gene in *L. japonicus* that encoded a Ca^{2+}-binding protein (Webb *et al*., 2000).

1.7 Early characterisation of transgenic line, T90

Following initial screening, Webb *et al*. (2000) identified four transgenic lines that exhibited expression of the inserted reporter gene in roots and nodules only after inoculation with the rhizobial symbiont of *L. japonicus*, *Mesorhizobium loti*. T90 was characterised further by Webb *et al*. (2000) because of the expression pattern observed in response to inoculation with *M. loti*. Furthermore, the primary transformant contained only one copy of the T–DNA insertion, thus simplifying the subsequent isolation of plant DNA adjacent to the insertion.

In T90 plants a distinct pattern of enzyme activity was observed in root tissue, initiating in hairs and epidermal tissue within three days following inoculation; expression then became focussed in developing nodules before disappearing as nodules senesced (Webb *et al*., 2000) (Figure 1.10).

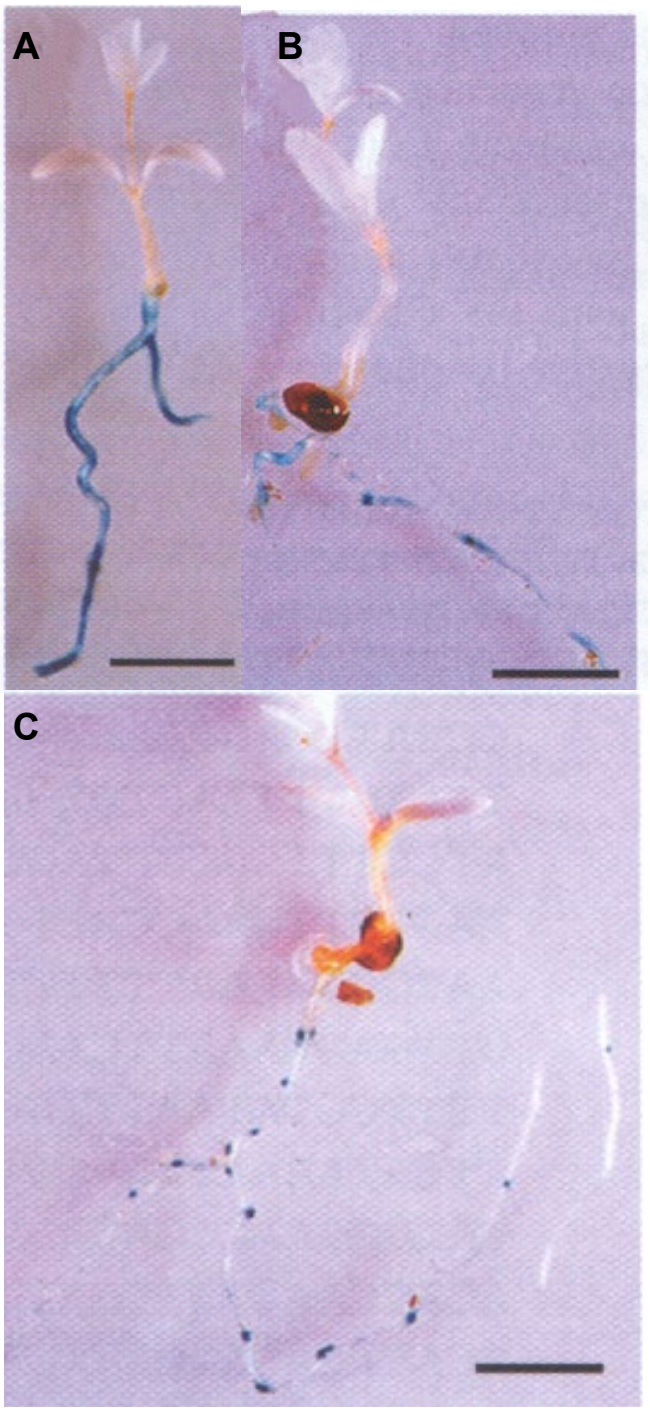

Figure 1.10. Enzymic activity showing expression of inserted reporter gene in T90 transformant. A, B and C, 3, 7 and 21 days after inoculation with *M. loti*. Bar = 0.5cm. Image courtesy of Webb *et al*. (2000).

Restriction digestion of T90 genomic DNA with the restriction enzyme *Hin*dIII and subsequent hybridisation with a probe designed from the inserted reporter gene produced a 3.8 Kb fragment, approximately 1 Kb of which was likely to be *L. japonicus* DNA upstream of the inserted DNA (Webb *et al*., 2000). Inverse polymerase chain reaction (PCR) (Lindsey *et al*., 1993), using primers from the reporter gene sequence, was used to clone this plant DNA. The clone was then used as a probe in a Southern hybridisation experiment to investigate nine randomly chosen T_2 progeny of T90. Two of these progeny were found to be homozygous for the inserted DNA, two heterozygous and five identical to the untransformed wild-type parent (Webb *et al*., 2000).

Subsequent analysis of this same cloned fragment failed to detect the presence of any likely coding sequence. The use of the clone in Northern hybridisation with root, nodule and shoot tissue from *L. japonicus* failed to produce a signal. Webb *et al*., (2000) therefore speculated that the reporter gene might have inserted in the promoter region of a native plant gene. Uneven PCR (Chen and Wu, 1997) was therefore used to clone downstream of the reporter gene. A 1.7 Kb fragment found to contain an open reading frame (ORF) was identified. This sequence, however, contained only the 5' end, the first 50 amino acids, of a peptide showing strong homology to Ca^{2+}-binding proteins, including calmodulins, from a range of plant and animal species. A further 750 bp was isolated using reverse transcriptase (RT)-PCR with RNA from root tissue and a gene specific primer designed from the 5' end of the predicted sequence. In total, a polypeptide of 150 amino acids with a molecular mass of 17 KDa was deduced from the nucleotide sequence (Webb *et al*., 2000). Four EF-hand motifs, typical of many classes of Ca^{2+}-binding proteins (Section 3.1.1.), were identified by Webb *et al.* (2000); the gene was therefore named *LjCbp1* for *Lotus japonicus* calcium binding protein.

Northern blot hybridisation failed to detect any hybridisation in shoot tissue, with or without inoculation with *M. loti*, whilst the strongest signal was detected in *M. loti*-inoculated roots; substantially lower expression was detected in roots inoculated with a NodC mutant (Webb *et al*., 2000), which fails to induce nodulation (Section 1.5.3). Levels of expression were found to decrease in nodulated tissues with the age of the nodule.

Southern hybridisation using *L. japonicus* genomic DNA with a probe from the region upstream of the inserted DNA suggested the presence of a unique sequence, whilst a probe derived from cloned *LjCbp1* cDNA suggested that a family of closely related genes encoding Ca^{2+}-binding proteins may be present (Webb *et al*., 2000).

1.8 Objectives

The transgenic line T90 provides an excellent basis as a tool for the characterisation and dissection of early signalling events in the legume/rhizobium interaction. The line has been shown to contain only one copy of the inserted transgene and to exhibit expression of this gene only following inoculation with *L. japonicus's* rhizobial symbiont *M. loti* (Webb *et al*., 2000). In addition, the reporter gene may be used to characterise expression of a putative Ca^{2+}-binding protein downstream of the T-DNA insertion (Webb *et al*., 2000). Ca^{2+} is a well-known second messenger (Berridge *et al*., 1998) and is also involved in nodulation signalling (Section 1.5.5).

The work presented in this thesis further investigates the gene (*LjCbp1*) identified by Webb *et al*. (2000) by characterising its role in symbiosis. The hypothesis that *LjCbp1* encodes a Ca^{2+}-binding protein was tested using a calcium mobility shift assay. In order to identify the extent to which reporter gene expression reflected that of *LjCbp1*, the correlation of the two genes was explored. These data provided a basis on which to investigate *LjCbp1* involvement in Ca^{2+} signalling. The effects of a range of signalling molecules, known to be involved in Ca^{2+} signalling, were tested against reporter gene activity in T90. Other potential signalling molecules were assessed to determine whether any factors other than *M. loti* and Ca^{2+}-signalling molecules could elicit transgene expression. In order to substantiate the role of *LjCbp1* in symbiosis, upstream regions of *LjCbp1* were compared with promoters of other symbiosis-related genes.

In addition to the above, the potential use of T90 as a tool in further mutagenesis experiments was assessed. A screening programme of mutagenised T90 plants was initited with the objective of identifying genes impaired in the very early stages of nodulation, using reporter gene expression in the transgenic line as a marker.

Chapter 2

2. General Materials and Methods

2.1 Preparation of solutions

Unless otherwise stated, chemicals and antibiotics were obtained from Sigma Chemical Co. (Poole, U.K.), BDH Laboratory Supplies (Poole, U.K.) and Fisher Scientific U.K. Ltd (Loughborough, U.K.) and glassware and plasticware were obtained from Fisher Scientific U.K. Ltd. Yeast extract, tryptone and agar for bacterial media were Difco products obtained from Beckton Dickinson (Oxford, U.K.). Unless otherwise stated all solutions and media were made up with ultra pure water obtained from a Maxima system (Elga Ltd, High Wycombe, U.K.) and pH corrections were made using 1M NaOH and 1M HCl, as relevant.

2.2 Sterilisation procedures

Where volumes exceeded 500ml filter-sterilisation was carried out using Gelman Laboratory AcroCap™ (Ann Arbor, U.S.A..) filter units with a 0.2µm Supor® Membrane and for volumes of 500ml or less Sartorius Minisart-plus 0.2µm CA-membrane + GF-prefilter (Göttingen, Germany) were used.

Glassware and plasticware required for DNA manipulation and media, solutions and filter paper, were sterilised by autoclaving at 121ºC (15 p.s.i.) for 15 minutes. Items used in RNA manipulation were autoclaved at 121ºC (15 p.s.i.) for 45 minutes. Vermiculite and Biosorb® were autoclaved at 121ºC (15 p.s.i.) for 40 minutes. All genetically manipulated material (including growing media) was autoclaved at 121ºC (15 p.s.i.) for 40 minutes before disposal.

All sterile operations were performed in a laminar flow hood (Centronic Europe Ltd), and all bacterial work in a Class II Biological Safety Cabinet (Microflow/Astecair).

2.3 Stock solutions

All stock solutions were filter-sterilised and kept at -20ºC unless otherwise stated.
Antibiotics: ampicillin was made up to 25mg/ml.
5-bromo-3-indolyl-β-D-galactopyranoside (X-gal) (Melford Laboratories, Ipswich, U.K.) was made up to 20mg/ml in N, N-dimethyl-formamide (DMF). This was added to hand-hot agar.
Isopropyl-beta-D-thiogalactopyranoside (IPTG) was made up to 2.4mg/ml.
5-bromo-4-chloro-3-indolyl-β-D-glucuronide (X-gluc) (Melford Laboratories, Ipswich, U.K.) contained 100mg X-gluc powder, 2ml N, N-dimethyl-formamide (DMF) and 5µl TRITON-X-100 made up to 200ml with phosphate buffer pH 7.0 ($Na_2HPO_4.2H_2O$ 5.13g/l and $NaH_2PO_4.1H_2O$ 2.92g/l). This was kept at 4ºC.
Ethidium bromide was made up to 10mg/ml. This was not filter-sterilised and was kept at room temperature.

2.4 Routine maintenance of plants and seedlings

2.4.1 Source of material

Wild-type *Lotus japonicus* cv. Gifu selfed (S_9) seeds were originally supplied by Dr Jens Stougaard, University of Aarhus, Denmark. *L. japonicus* T90 line was generated in a T-DNA insertional mutagenesis programme and provided by Drs Leif Skøt and Judith Webb, IGER, Aberystwyth, U.K.

2.4.2 Substrate for seedlings and plants

Filter paper: Whatman (Whatman International Ltd, Maidstone, U.K.) 9cm Grade 1 filter papers were autoclaved in foil pouches.

Vermiculite: medium grade vermiculite (Vermiperl®, William Sinclair Horticulture Ltd, Lincoln, U.K.) was washed in running water for 24 hours before autoclaving.

Compost: John Innes No3 (Richardson Moss Litter Co Ltd, Gretna, U.K.) with added wetting agent and Intercept™ (Scotts Co. Ltd, Ipswich, U.K.).

2.4.3 Plant nutrient solutions

a) Plant nutrient solution without nitrogen: $MnSO_4.4H_2O$ 2.025mg/l, $CuSO_4.5H_20$ 80µg/l, $ZnSO_4.7H_2O$ 220µg/l, H_3BO_3 2.85mg/l, $Na_2MoO_4.2H_2O$ 100µg/l, $CoSO_4.7H_2O$ 57.5µg/l, NaCl 5µg/l, $NiSO_4.6H_2O$ 44.5µg/l, $MgSO_4.7H_20$ 138mg/l, EDTA 40mg/l, K_2SO_4 62.5mg/l, K_2HPO_4 100mg/l, $CaSO_4.2H_2O$ 359mg/l (Ryle *et al*., 1978). This solution was made using reverse osmosis water and was not autoclaved.

b) Fåhraeus medium (Fåhraeus, 1957): $CaCl_2$ 100mg/l; $MgSO_4$ 120mg/l; KH_2PO_4 90mg/l; Na_2HPO_4 150mg/l; $C_6H_8O_7$ 5mg/l; Gibson's trace elements: H_3BO_3 2.86µg/l; $MnSO_4$ 2.03µg/l; $ZnSO_4$ 0.22µg/l; $CuSO_4$ 0.08µg/l; H_2MoO_4 0.08µg/l. The final solution was adjusted to pH 6.3-6.7 before adding 0.5% w/v Phytagel® and autoclaving.

2.4.4 Pest and disease control

Biological control: red spider mite (*Tetranychus urticae*) was controlled using Spidex (Koppert U.K. Ltd, Wadhurst, U.K.), which contains the biological control agent *Phytoseiulus persimilis*.

Chemical spraying: plants with serious infestations of red spider mite were treated as follows: 2ml/l Hallmark pyrethroid insecticide MAFF registered number 10480 (ICI Agrochemicals, supplied by Syngenta Crop Protection U.K. Limited, Whittlesford, U.K.). Western flower thrips (*Frankliniella occidentalis*) were controlled using 3.25ml/l Murphy's systemic insecticide containing heptenophos and permethrin (Fisher Scientific U.K. Ltd, Loughborough, U.K.).

2.4.5 Preparation, germination and growing conditions of seedling and plant material

Routine growth of seedlings: unless otherwise stated *L. japonicus* T90 and wild-type seeds were scarified by rubbing with medium grade sandpaper, placed in a sterile universal container and surface-sterilised in a 50:50 sodium hypochlorite solution (with 6.5% available chlorine): sterile tap water solution containing 0.01% Tween® 20. Seeds were shaken on a flatbed stirrer at 150 rpm in this solution for 20 minutes and then rinsed seven times in sterile tap water and left to imbibe at room temperature for approximately three hours. Seeds were sown into one of the following:

a) Approximately 350ml sterile vermiculite in PhytatrayII™ (Sigma, Poole, U.K.) containers, with 10ml filter-sterilised plant nutrient solution (Section 2.4.3a). Seeds were placed just below the surface of the medium.
b) Approximately 250ml sterile vermiculite in Magenta containers (Sigma, Chemical Co., Poole, U.K.), with 5ml filter-sterilised plant nutrient solution (Section 2.4.3a).
c) Sterile filter paper (x 3) in 90mm Petri dishes with 2ml filter-sterilised plant nutrient solution (Section 2.4.3a).
d) Fåhraeus medium (Fåhraeus, 1957) (Section 2.4.3b) in 90mm Petri dishes. The Petri dishes were placed at a 30^{o} angle and half-filled with approximately 15ml medium. Ten seeds per dish were placed along the top of the set medium. Petri dishes were placed flat and kept dark (covered with black plastic) until more than 70% had germinated. They were then uncovered and placed at an angle of approximately 130^{o}.

Growth in a controlled environment: the containers were sealed with Nescofilm® and placed in a controlled environment room at 20^{o}C with a light intensity of 40μmol/m^{2}/sec and a 16 hour photoperiod. Lighting was provided by Sylvania (Sylvania U.K. Ltd, London, U.K.) 70W white fluorescent tubes.

Routine growth of plants in glasshouse: minimum temperature 10^{o}C, daylight was supplemented with artificial light to provide a minimum photoperiod of 16 hours. Lighting was provided by Philips (Philips U.K., Ltd, Guildford, U.K.) Son-

T Agro 400W high pressure sodium lamps. Plants were watered daily with tap water.

2.5 Treatment of seedlings

2.5.1 Microbiology

Solutions

Luria Broth (LB) contained yeast extract 5g/l, tryptone (Difco, Detroit, U.S.A.) 10g/l, NaCl 5g/l and was adjusted to pH 7.0-7.2.
Luria Agar (LA) was as LB with 1.5% w/v Difco bacto-agar added.
LA/LB with X-gal, IPTG and ampicillin were as LA/LB with 40µg/ml X-gal, 48µg/ml IPTG and 25µg/ml ampicillin (Section 2.3).
LA with ampicillin was as LA/LB with 25µg/ml ampicillin (Section 2.3).
SOC contained tryptone 20g/l, yeast extract 5g/l, NaCl 584mg/l, KCl 186mg/l and was adjusted to pH 7.0. The mixture was autoclaved and supplemented with MgCl.6H2O 2.03g/l, $MgSO_4$.7H2O 2.46g/l and glucose 3.6g/l, made up to 100ml and filter-sterilised.
Tryptone/Yeast Extract Agar (TY) contained tryptone 5g/l, yeast extract 3g/l, $CaCl_2.6H_2O$ 1.33g/l, Difco-bacto agar 1.5% w/v and was adjusted to pH 6.8-7.0.
Yeast Mannitol (YM) Agar contained K_2HPO_4 50g/l, $MgSO_4$ $7H_2O$ 20g/l, NaCl 10g/l, mannitol 10g/l, yeast extract 4mg/l, Difco bacto-agar 1.5% w/v and was adjusted to pH 7.0-7.2.

All rhizobia were supplied as agar stabs or slopes except *Rhizobium* species NGR234, which was supplied in a freeze-dried form. This was resuspended by injecting sterile reverse osmosis water into the ampoule; it was then subcultured onto TY plates. *M. loti* NZP2235 were initially maintained on YM slopes. Later, TY plates were used routinely, as for all other rhizobia. After subculturing, plates were incubated at 28ºC for four days, then kept at 2ºC.

Microorganisms

Table 2.0. *Rhizobium* and sources.

Species	Source
Mesorhizobium loti strain NZP2235	Dr. Scott, Institute of Molecular Biosciences, Massey University, Palmerston North, New Zealand.
Bradyrhizobium lupinus USDA 3211	IGER, Aberystwyth, U.K.
B. japonicum USDA 3407	IGER, Aberystwyth, U.K.
B. elkanii USDA 61	USDA, Beltsville, U.S.A.
B. vigna USDA 3824	IGER, Aberystwyth, U.K.
S. fredii USDA 257	USDA, Beltsville, U.S.A.
Rhizobium leguminosarum bv *viciae* USDA 1001	IGER, Aberystwyth, U.K.
Rhizobium broad host range sp. NGR234 USDA 4146	USDA, Beltsville, U.S.A.
Rhizobium etli USDA 9032	USDA, Beltsville, U.S.A.

Inoculation of seedlings with rhizobia bacteria *in vitro*: two procedures for the inoculation of seedlings with rhizobia were routinely used.

Method 1: a loopful of rhizobia was taken from YM agar media slopes and subcultured into liquid YM in a 250ml flask. The flask was closed with a foam bung and foil and shaken on a horizontal shaker at 30 rpm in the dark at 28ºC for three to four days, prior to inoculation. Seedlings were inoculated with 5ml of this culture per 100 seedlings. Control seedlings remained uninoculated.

Method 2: a fresh subculture of rhizobia was made onto TY agar media on Petri dishes and grown at 28ºC for three to four days before inoculation. On the day of inoculation one to two loops of the subculture were dispersed into sterile reverse osmosis water. The concentration was adjusted to an optical density of 0.1 at 600nm (Philips PU 8720 UV/VIS scanning spectrophotometer, Philips Electronics U.K. Ltd, Croydon, U.K.). Approximately 5ml of the inoculum was used for each Phytatray II™, or 50µl per root was applied directly to the nodulation zones of seedlings in Petri dishes. Control seedlings were inoculated with sterile reverse osmosis water.

Contamination check for uninoculated seedlings: where stated, one 1ml sample of liquid was taken from each Phytatray II™, using a sterile plastic Pasteur pipette. The liquid was spread onto individual TY plates and incubated for 5 days at 28ºC.

2.5.2 Nod factor

Crude extract of Nod factor, derived from *M. loti* R7A, was provided by Herman Spaink, University of Leiden, The Netherlands (Bras, 2003). Nod factor was applied by pipette (0.4µl per root) directly onto the nodulation zone and was carried out under sterile conditions.

2.5.3 Chitosan

Using a pipette, 2µl 5mg/ml Chitosan (Sigma Chemical Co., Poole, U.K.) was applied to the nodulation zone (Section 1.5.4) of each seedling. This was carried out under sterile conditions.

2.5.4 Calcium, agonists and antagonists

T90 seedlings were prepared as in Section 2.4.5d and placed under controlled environment conditions (Section 2.4.5) for seven days. All procedures were carried out under sterile conditions.

All $CaCl_2$ concentrations were at a pH of 7.0. Seedlings were incubated in treatments for 24 hours in a controlled environment (Section 2.4.5).

Treatments for the Ca^{2+} channel blocking experiments were either: 0, 0.5, 1.0 or 5µM ruthenium red, or 0, 0.5, 1.0 or 5mM nifedipine (Calbiochem-Novabiochem, Nottingham, U.K.), or 0, 1.25, 2.5 or 5µM verapamil. The same procedure was used as for the Ca^{2+} treatments above, including the inoculation of *M. loti*. Three seedlings in each of three wells were used for each treatment.

2.5.5 Plant hormones

Table 2.1. Hormone groups and experimental concentrations.

Hormone group	Concentration used	Stock solutions dissolved in
Auxins		
indole acetic acid (IAA)	50µM	10% methanol
naphthalene acetic acid (NAA)	50µM	"
2, 4-dichlorophenoxy acetic acid (2, 4-D)	50µM	"
ethylene precursor		
aminocyclopropane-1 carboxylic acid (ACC)	0.1, 0.5 or 1.0mM	de-ionised water
abscisic acid (ABA)	50 or 100µM	de-ionised water
cytokinins		
6-benzylamine purine (6-BAP)	50µM	10% ethanol
6-furfurylamino purine (kinetin)	50µM	"
dihydrozeatin (DHZ)	50µM	"

2.6 Histochemical staining

Two or three seedlings were placed in 1ml X-gluc (Section 2.3) in 1.5ml flip-top microcentrifuge tubes and incubated at 37°C for 16 hours. Samples were washed three times in sterile water and cleared in glacial acetic acid and absolute ethanol (3:1, v/v) for 16 hours, before being fixed in lactic acid: water: glycerol (1:1:1, v/v/v).

2.7 Screening of mutagenised *L. japonicus* T90 line

Production of ethyl methane sulphonate (EMS)-treated seed was done at the Sainsbury Laboratory (Norwich, U.K.) and initial screening of the M_1 and M_2 generations was carried out in collaboration with Dr Martin Parniske at the Sainsbury Laboratory. Screening was continued at IGER (Aberystwyth, U.K.), thus conditions for seedling and plant growth differed.

2.7.1 Source of material

Dr Scott Coomber (Sainsbury Laboratory) treated *L. japonicus* T90 seeds from IGER with ethyl-methane sulphonate (EMS) (0.4% for 16 hours) (Webb, *et al*., in press). M_2 generation seeds from this treatment were used for the mutant screen.

A single spore descent line of the arbuscular mycorrhiza, *Glomus intraradices*, was provided by Dirk Redecker (University of California, Berkeley, California, U.S.A.). The strain was deposited at the International European Bank for the Glomeromycota (BEG) within the University of Kent, Canterbury, U.K. and given the accession number 195.

Culture of *M. loti* NZP2235 was as described in Section 2.5.1, Table 2.0.

Chive seeds (*Allium schoenoprasum*) were bought locally from a commercial source.

2.7.2 Substrate for seedlings and plants

Biosorb®: medium grade Biosorb® was obtained from Agrobiochemicals Ltd, Essex, U.K..

Compost: John Innes compost No. 3 (L & P Peat Ltd, Carlisle, U.K.) with 280g/m^3 Intercept™ (Scotts Co. Ltd, Ipswich, U.K.), containing 5% (w/v) imidacloprid was used in 7cm diameter pots.

2.7.3 Plant nutrient solution

Low phosphate (3.11mg/l) nutrient solution for chive nurse plants: plants were watered daily with tap water and once a week with the following: KNO_3 323.52mg/l; $MgSO_4$ x $7H_2O$ 493mg/l; KH_2PO_4 2.31mg/l; K_2HPO_4 14.46mg/l; $CaCl_2$ x $2H_2O$ 370.44mg/l; H_3BO_3 1.43mg/l; $MnSO_4$ x $4H_2O$ 1.11mg/l; $ZnSO_4$ x $7H_2O$ 230µg/l; $CuSO_4$ x $5H_2O$ 75µg/l; Na_2MoO_4 x $4H_2O$ 56µg/l; $CoCl_2$ x $4H_2O$ 101 µg/l; EDTA was used in concentrations described by Randall and Bouma (1973).

2.7.4 Pest and disease control

Plants were sprayed every six weeks with Eradicoat® (Defenders Ltd, Ashford, Kent, U.K.) to treat for Western Thrips. Intercept™-containing compost (Scotts Co. Ltd, Ipswich, U.K.) was used to reduce infection by Sciarid fly (*Sciaridae*).

2.7.5 Maintenance of microorganisms

M. loti strain NZP2235 (Section 2.5.1) was cultured on TY medium at 28ºC for three days and then stored at 8ºC. Fresh lawn cultures were taken every two weeks and streaked to produce single colonies to check for contamination.

G. intraradices was maintained using chive nurse plants in Biosorb® (Wegel *et al.*, 1998). Approximately 50 chive seeds (Section 2.7.1) were sown into a 7cm diameter pot already containing a *G. intraradices*-infected chive plant in Biosorb®. About four weeks after germination the roots of the young seedlings became infected by the fungus. The seedlings were then separated and re-planted into new 7cm diameter pots containing Biosorb®, one plant per pot. After six weeks these chive plants were used to infect *L. japonicus*. Nurse pots were grown in a glasshouse, with supplemented light, under a 16 hour photoperiod at 22ºC and watered once a week with ½ strength Hoagland's solution (Hoagland and Arnon, 1938).

2.7.6 Preparation, germination and growing conditions of seedling and plant material

Routine growth of seedlings: approximately 30 seeds per line of EMS-treated M_2 seeds of transgenic line T90 were scarified by immersion in 98% v/v sulphuric acid for 20 minutes in a fume hood. They were subsequently washed three times with excess sterile water before being left to imbibe in fresh sterile water for at least three hours. Following imbibition, seeds were transferred under sterile conditions to 90mm Petri dishes containing Fåhraeus growth medium (Section 2.4.5d), using 0.5% Gelrite® instead of Phytagel®. Thirty seeds were sown per line. Sticky tape was used to hold together the batch of three Petri dishes for each line. Ten seeds of T90 control were used each sowing.

Growth in a controlled environment: Petri dishes were placed flat and covered with black plastic until at least 70% seedlings had germinated at which time they were uncovered and placed at an angle of approximately 80°. Seedlings were grown under a 16 hour photoperiod, with a light intensity of 200µmol/m^2/sec at day/night 21°C/16°C. After inoculation with *M. loti*, plants were transferred, for 16 hours, to a controlled environment with a 16 hour photoperiod at day/night 20°C/15°C, with a light intensity of 200µmol/m^2/sec.

Routine growth of plants in glasshouse: After transfer into *G. intraradices*-colonised pots (Section 2.7.5), plants were placed in a glasshouse under a minimum 16 hour photoperiod, minimum day/night 20°C/18°C, with supplementary lighting.

2.7.7 Inoculation of M_2 generation seedlings with *M. loti* NZP2235

Plant lines were selected for inoculation when at least 70% of the seedlings within that line had reached a root length of 1.5cm or more. The number of individuals that had germinated in each line was recorded. Any altered morphologies were also noted. Two loopfuls of *M. loti*, taken from lawn cultures (Section 2.7.5) were placed in sterile water in universal tubes and adjusted to an optical density of 0.1

at 600nm. Rhizobia were dispensed via pipette, approximately 50µl suspension per root.

2.7.8 Harvesting and staining of seedling root tips in M_2 generation

Root tips were harvested approximately 16 hours post inoculation (hpi). Approximately 2mm root tip was taken and transferred to a 96-well PCR plate containing 20µl X-gluc (Section 2.3). Harvesting was carried out under sterile conditions in a laminar flow cabinet. Root tips were cut with a scalpel and transferred using forceps. Sealed PCR plates were transferred to a 37°C incubator for five hours, after which root tips were scored for staining. Root tips were subsequently returned to the incubator for a further 12-15 hours and then re-scored, they were then examined for absence of, or unusual GUS expression using a Leica (Solms, Germany) DMLS bench-top binocular microscope.

2.7.9 Infection of seedlings with *G. intraradices*

After harvest and scoring, all seedlings from each plant line were transferred into a single 7cm diameter pot containing *Glomus intraradices*-colonised Biosorb® with chive nurse plants (Section 2.7.6). Individual seedlings that showed absence of GUS or abnormally staining root tips were marked by the presence of a toothpick.

2.7.10 Screening of plants in M_2 generation

Approximately three weeks after seedling transfer into Biosorb® roots were examined for nodule abnormalities. Plants with abnormal phenotypes, and those previously identified as having absent or abnormal GUS expression were transferred to compost (Section 2.7.2) and maintained in the same glasshouse.

Dr Scott Coomber initially screened roots of the putative mutants for mycorrhiza colonisation by:

1 Visualising GUS after challenge with *G. intraradices*.
2 Immersing in potassium hydroxide and using trypan blue stain, in accordance with Phillips and Hayman (1970).

The roots were examined using light microscopy at 200x magnification (Zeiss Axiophot, Zeiss, Jena, Germany). The presence and appearance of surface hyphae, penetration point, internal hyphae, vesicles and arbuscules were noted.

Plants that showed altered leaf morphologies but were neither nodulation/GUS, nor mycorrhiza putative mutants were given to Dr Julie Hofer (John Innes Institute, Norwich) for further analysis. Plant lines showing a potential mutant mycorrhiza phenotype were kept at the Sainsbury Laboratory, Norwich and analysed further by Dr Thilo Winzer (Sainsbury Laboratory, Norwich). All nodulation/GUS putative mutants were transferred to IGER, Aberystwyth for screening of the M_3 generation. M_1 plants that had not yet produced sufficient seeds and 268 M_2 plants were also transferred to IGER, Aberystwyth. M_2 and M_3 plants were harvested for seed as pods matured.

2.7.11 Screening of seedlings in M_3 generation

Putative mutants were sown and inoculated as Section 2.4.5d and 2.5 Method 2. Whole seedlings were harvested 15 hpi into X-gluc (Section 2.6). Putative mutant lines (as well as those formerly categorised as nod^-, fix^- or hypernodulator) were maintained in the glasshouse (Section 2.4.5) awaiting the collection of adequate numbers of M_3 seed. Three putative mutants were examined further. These were sown and inoculated as described in Sections 2.4.5 and 2.5.1. Each seedling was then transferred into compost (Section 2.4.2) in 7cm pots and placed in a controlled environment (Section 2.4.5). Forty days later plants were examined for altered phenotypes. Subsequently, 5cm root sections from each plant were harvested into X-gluc (Section 2.6) and examined under both binocular and high power light

microscope and images were captured (Section 2.9). Individual plants were labelled with the T90 EMS line number from the parent M_2 plant followed by a, b, c, etc., and maintained under a controlled environment (Section 2.4.5) as previously, awaiting collection of M_4 seed. Seed were harvested as pods matured and approximately 100 seeds were collected from each plant.

2.8 Molecular biology

Unless otherwise stated the following precautions were routinely used to minimise the possibility of degradative RNases and DNases: all glassware and plasticware used in nucleic acid extraction and manipulation were autoclaved (Section 2.2) and gloves were used in the handling of all materials, equipment and reagents.

Unless otherwise stated all solutions were autoclaved (Section 2.2).

Harvested plant material was separated into roots and shoots and placed immediately into foil packets, flash-frozen in liquid nitrogen and stored at –80ºC.

Escherichia coli competent cells JM109 were obtained from Promega, Southampton, U.K. *E. coli* cells were maintained on LA containing ampicillin (Section 2.5.1).

2.8.1 Standard solutions

50x Tris acetic acid and ethylenediaminotetra-acetic acid (EDTA) (TAE) buffer contained Tris base 242g/l, glacial acetic acid 57.1ml/l, 0.5M EDTA (pH 8.0) 100ml/l .

1 Kb DNA size marker (Invitrogen Life Technologies, Paisley, Scotland) was made up to 50µl/ml, with 5M NaCl 292.2µg/ml and was not autoclaved. This was stored at 4ºC.

Agarose loading dye contained sucrose 4g, sterile reverse osmosis water 8ml, Bromophenol blue 25mg (added when sucrose had dissolved in water) and was

made up to 10ml. This was filter-sterilised, was not autoclaved and was kept at 4ºC.

Diethyl pyrocarbonate (DEPC) of 1ml/l was added to ultra pure water.

RNA gel loading dye contained Bromophenol blue 40mg, Xylene Cyanol 40mg and 2.5g Ficoll 400. Ficoll 400 was dissolved in 8ml sterile reverse osmosis water, the two dyes were added and the volume was made up to 10ml. This was stored at room temperature.

Sodium dodecyl sulphate (SDS) stock contained SDS 10g/ml and was made up in a sterile container and not autoclaved.

DNA Extraction buffer contained 1M TrisCl pH 8.0 10% v/v, 0.5M EDTA pH 8.0 2.0% v/v, 10% SDS 12.5% v/v, 0.0625% beta-mercaptoethanol and sterile reverse osmosis water 75% v/v.

10x 3-[N-Morpholino]propanesulfonic acid (MOPS) buffer contained 0.2M MOPS pH 7.0, 0.05M sodium acetate (NaOAc) pH 7.0 and 0.01M EDTA. This was dissolved in DEPC-H_20 and adjusted to pH 7.0 and filter-sterilised. MOPS buffer was made fresh for each gel.

TrisCl-EDTA buffer ($T_{10}E_1$) contained TrisCl 10mM pH 8.0 and EDTA 1mM.

Denaturation buffer contained NaCl 1.5M and NaOH 0.5M. This was not autoclaved.

Neutralisation buffer contained NaCl 3M and TrisCl 0.5M and was adjusted to pH 7.0.

20x Sodium-sodium citrate (SSC) contained NaCl 3M and Na citrate 0.3M and was adjusted to pH 7.5.

10x SSC contained v/v 20x SSC and DEPC-H_2O.

2x SSC contained 1:10 v/v 20x SSC and DEPC-H_2O.

1x SSC contained 1:20 v/v 20x SSC and DEPC-H_2O.

Maleic acid buffer contained maleic acid 0.1M and NaCl 0.2M and was adjusted to pH 7.5 using solid NaOH.

Wash buffer contained maleic acid buffer and Tween 20™. This was not autoclaved.

Blocking buffer stock solution contained blocking buffer reagent (Roche Diagnostics Ltd, Lewes, U.K.) 10% w/v in maleic acid buffer. This was stored at 4ºC.

Blocking buffer contained blocking buffer stock solution 1:10 in maleic acid buffer and was not autoclaved.
Detection buffer contained TrisCl 100mM and NaCl 100mM and was adjusted to pH 9.5. This was stored in the dark.
Disodium 3-(4-methoxyspiro{1,2-dioxetane-3,2'-(5'-chloro)tricyclo[3.3.1.1^{3,7}] decan-4-yl) phenyl phosphate) (CSPD) (25mM) (Roche Diagnostics Ltd, Lewes, U.K.) **working solution** was made up to 1% (v/v) in the detection buffer.

2.8.2 Primer design and sequence information

Primers for the *gus* gene were designed from the *pΔgusBin19* sequence, Genbank Accession number U12638, using the Prime software on GCG® version 10.0 (Accelrys Ltd, Cambridge, U.K.). Primers were obtained from Sigma, Genosys (Cambridge, U.K.).

Primers for *LjCbp1* gene were designed as described in Webb *et al*., (2000) and using the Prime software on GCG® version 10.0 (Accelrys Ltd, Cambridge, U.K.).

The actin primers were a gift from Dr. G. Allison, IGER, Aberystwyth.

Table 2.2. Primer sequences, annealing temperatures and expected fragment sizes.

Primer name	Forward 5' to 3'	Reverse 5' to 3'	Melting temperature °C	Amplified fragment size (bp)
gus	ACCTCGCATTACCCTTAC		56.5	270
		GTGGTGATGTGGAGTATTG	56.0	
LjCbp1	AATACCAAAAATGGACCCCAC		63.3	470
		GCTAAAGCCACCACCTTTC	61.2	
Actin	TGGGATGACATGGAAAAGATCTGGCA		76.0	348[1] 271
		AGATTGGCACAGTGTGACTCACACCATC	74.0	
GeneRacer™ 5'	CGACTGGAGCACGAGGACACTGA		74	810
Racer 1	ACCATCTCCATCAACATCCACCTTC		69.8	
GeneRacer™ nested 5'	GGACACTGACATGGACTGAAGGAGTA		78	501
Racer 2 Nested	ACCCATCTCCGTTCACATCAATC		70.7	
GeneRacer™ 3'	GCTGTCAACGATATACGCTACGTAACG		76	720
GeneRacer™ nested 3'	CGCTACGTAACGGCATGACAGTG		72	705
SP6	CTATTTAGGTGACACTATAG		45.2	Not applicable
T7	GTAATACGACTCACTATAGGGC		56	Not applicable

[1] the actin gene contains an intron of 77 bp and thus gives a larger fragment in genomic DNA compared with complementary DNA prepared from RNA.

2.8.3 Total DNA extraction

DNA extraction buffer (10ml) was pipetted into each of two 30ml centrifuge tubes (Nalgene Ltd, Hereford, U.K.) and placed in a 65ºC water bath. Plant material (1g young leaf tissue from a mature plant) was ground to fine powder with pre-cooled pestle and mortar in liquid nitrogen. Whilst some liquid nitrogen remained, fully ground material was poured into a centrifuge tube containing 10ml extraction buffer and incubated at 65ºC for a minimum of 10 minutes. To each tube, 2.5ml 5M potassium acetate was added, samples were then incubated on ice for 20 minutes before being centrifuged for 20 minutes at 4ºC at 11300 x*g*. The supernatant was then transferred to clean tubes and an equal volume of isopropanol was added to each. The solutions were mixed and left for 16 hours at –20ºC. Samples were centrifuged for 20 minutes at 4ºC and 11300 x*g*, the supernatant was then discarded, the tubes were inverted and the pellets left to air dry for approximately 10 minutes. The pellets were re-suspended in 7ml of $T_{10}E_1$ (Section 2.8.1) before adding 2.5ml Aquaphenol™ (Appligene, Uxbridge, U.K.) and 2.5ml chloroform to each tube. The tubes were vortexed briefly and spun for five minutes at 4ºC and 11300 x*g*. The aqueous phase was removed from each tube to two clean tubes and 700µl 3M sodium acetate (pH 4.8) and 5ml isopropanol was added. The tubes were left on ice for 20 minutes and then spun at 4ºC and 11300 x*g* for 20 minutes. The supernatant was discarded and each pellet resuspended in 10ml cold 80% ethanol and spun for a further 10 minutes at 11300 x*g* and 4ºC. The supernatant was discarded and the pellet allowed to air dry for approximately 30 minutes. After drying each pellet was suspended in 800µl $T_{10}E_1$ and transferred to a 1.5ml microcentrifuge tube. To each sample 2µl 10mg/ml RNase A (Invitrogen Ltd, Paisley, U.K.), 20µl 5M NaCl, and 1ml 100% ethanol was added. Samples were incubated for 30 minutes at –70ºC and then spun for 10 minutes at 14800 x*g* in a microcentrifuge. The supernatant was discarded and the pellets suspended in 200µl $T_{10}E_1$ before quantification with a spectrophotometer. DNA was quantified by absorbance (A) at 260nm and calculations of purity were made at 230 and 280nm with a PU 8720 UV/VIS scanning spectrophotometer (Philips PU 8720 UV/VIS scanning spectrophotometer, Philips Electronics U.K. Ltd,

Croydon, U.K.), using 5µl sample in 95µl sterile reverse osmosis water. Samples were stored at -20ºC.

2.8.4 Total RNA extraction

Total plant RNA was extracted using TRIzol™ Reagent (Invitrogen Ltd, Paisley, U.K.). Roots were ground to powder using a clean, pre-chilled pestle and mortar for each harvest. Approximately 8mg polyvinyl pyrrolidone was added to each 100mg of powdered material. Material was kept frozen using liquid nitrogen, transferred to 2ml microcentrifuge tubes and weighed. To each tube 1ml TRIzol™ Reagent (Invitrogen™, Paisley, U.K.) was added. The tubes were then vortexed for 30 seconds, left to incubate at room temperature for five minutes and subsequently spun in a microcentrifuge at 14800 x*g* and 4ºC for 10 minutes. The supernatant was transferred to a clean 2ml tube. Chloroform (0.3ml) was added to each sample and the tubes were vortexed for 10 seconds, left to incubate at room temperature for 10 minutes and then centrifuged for 15 minutes at 14800 x*g* and 4ºC to separate the different phases. The aqueous phase was collected using cut filter pipette tips, to avoid disturbing the solid phase, and transferred to a clean 1.5ml centrifuge tube to which 0.5ml isopropyl alcohol was added. The tubes were mixed gently, left to incubate at room temperature for 10 minutes and then centrifuged for 10 minutes at 14800 x*g* and 4ºC to pellet the RNA. The supernatant was then removed from each tube and the pellets were washed in 0.5ml 80% ethanol in DEPC-H_20 by flicking the tube and then centrifuging for five minutes at 5800 x*g* and 4ºC. The wash was repeated and the tubes inverted to allow the pellets to air dry for approximately five minutes. After drying the pellets were suspended in 50µl DEPC-H_2O. RNA was quantified as in Section 2.8.3 using 5µl sample in 95µl DEPC-H_2O and stored at –80ºC.

Where sample sizes were 50mg or less, half the volume of TRIzol™, chloroform and isopropanol was used.

2.8.4.1 DNase treatment

Samples were thawed and 5.7µl 10x reaction buffer and 1.0µl of DNase I (10 units/µl) (MessageClean™, BioGene, Kimbolton, U.K.) was added to each. Samples were incubated for 30 minutes in a 37°C water bath before 30µl RNase-free phenol and 10µl chloroform was added. Samples were then vortexed for 30 seconds and left on ice for 10 minutes before being spun at 17400 x*g* and 4°C for five minutes. The upper phase of each sample was transferred to a clean microfuge tube and re-precipitated with 5µl 3M sodium acetate and 200µl 100% ethanol at –70°C for 16 hours. Samples were centrifuged for 10 minutes at 17400 x*g* and 4°C to re-pellet the RNA which was then washed in 80% ethanol in DEPC-H_2O for five minutes at 5800 x*g* and 4°C. The supernatant was then discarded and the tubes inverted to allow the pellets to air dry before being re-suspended in 50µl DEPC-H_2O. Material was stored at -70°C.

2.8.4.2 RNA clean-up for single strand complementary (c)DNA synthesis

Samples were made up to a 50µl volume using DEPC-H_2O. To each were added 5µl 10x buffer and 1µl RNase-free DNase (Ambion Europe Ltd, Huntingdon, U.K.). The samples were mixed gently and incubated at 37°C for one hour. A 0.1 volume of DNase inactivation slurry (Ambion Europe Ltd, Huntingdon, U.K.) was added to each sample. After mixing, samples were incubated at room temperature for two minutes and then centrifuged for 10 minutes at 17400 x*g* and 4°C. The supernatant was transferred to a clean tube and kept on ice ready for cDNA synthesis.

2.8.4.3 Single strand cDNA synthesis

Complementary DNA was generated using the Moloney Murine Leukaemia Virus (M_MLV) RT enzyme and buffer from Ambion Europe Ltd (Huntingdon, U.K.) and other reagents from Roche Diagnostics Ltd (Lewes, U.K.). The reaction was

set up to give the final concentrations/volumes: M_MLV reaction buffer 1x, $MgCl_2$ 5mM, deoxynucleotide mix 1mM, random primer p(dN)6 3.2µg, RNase inhibitor 50 units (U), M_MLV RT 80 U, RNA template 1µg. The samples were placed in a 25°C water bath for 10 minutes followed by one hour at 42°C. Samples were then boiled for five minutes and cooled on ice for at least five minutes before polymerase chain reaction. Samples were stored at -20°C.

2.8.4.4 Reverse transcription polymerase chain reaction (RT-PCR)

The Titan® One Tube RT-PCR system supplied by Boehringer Mannheim, (now Roche Diagnostics, Lewes, U.K.) was used according to the manufacturer's recommended instructions. This system permits the synthesis of cDNA and subsequent amplification of the synthesised cDNA in one addition of reagents so that both reverse transcription and polymerase chain reaction amplification can take place in one uninterrupted thermocycler programme. Reactions were performed in 0.2ml thin-walled tubes from ABGene (Epsom, U.K.) on a Perkin Elmer (Cambridge, U.K.) GeneAmp PCR System 2400.

2.8.5 Polymerase chain reaction (PCR)

PCR reactions were performed in 0.2ml thin-walled tubes on a Perkin Elmer GeneAmp PCR System 2400. Taq polymerase 10x concentration buffer containing 100mM Tris-HCl, 15mM $MgCl_2$ and 500mM KCl at pH 8.3 and deoxynucleoside-triphosphate molecules (dNTPs) were all obtained from Roche Diagnostics (Lewes, U.K.). PCR reactions were made up to achieve final concentrations/volumes of the following: 10x buffer 10% v/v, dNTPs 0.2mM, forward and reverse primer 0.2µM each, Taq polymerase 1.5 U. Template DNA/RNA was added to give a final concentration of around 0.5µg and autoclaved ultra pure water used to make up any required volume. Thermocycler programmes were as shown in Table 2.3.

Table 2.3. Thermocycler programmes.

Primer/Reaction[1]	Programme details
gus	95ºC 1 minute; 35 x (94ºC 30 seconds; 58ºC 30 seconds; 68ºC 45 seconds); 68ºC 7 minutes; 4ºC hold
LjCbp1	95ºC 1 minute; 35 x (94ºC 30 seconds; 58ºC 30 seconds; 68ºC 45 seconds); 68ºC 7 minutes; 4ºC hold
Actin	94ºC 2 minutes; 35 x (94ºC 30 seconds; 58ºC 30 seconds; 72ºC 1 minute); 72ºC 5 minutes; 4ºC hold
Racer 1	94ºC 2 minutes, 5x (94ºC 30 seconds, 72ºC 1 minute), 5x (94ºC 30 seconds, 68ºC 1 minute), 25x (94ºC 30 seconds, 61ºC 30 seconds, 72ºC 1 minute), 72ºC 10 minutes, 4ºC hold
Racer 2	94ºC 2 minutes, 30x (94ºC 30 seconds, 61ºC 30 seconds, 72ºC 1 minute), 72ºC 7 minutes, 4ºC hold

[1]Refer to Table 2.2 for details of primers.

2.8.6 Electrophoresis gels

Electrophoresis gels were made up using 1% agarose (High Gel strength, Melford Laboratories, Ipswich, U.K.) in 1x TAE buffer (Section 2.8.1). Ethidium bromide was added to hand-hot agarose to a final concentration of 0.5mg/ml. Loading dye of 2µl per 10µl sample, or per 10µl 1 Kb size marker was used. Gels were run on a 300 power pac (Bio-Rad Laboratories Ltd, Hemel Hempstead, U.K.) at 60V for 30-60 minutes until the desired separation was achieved and analysed and photographed using an AlphaImager™ 1200 gel analysis system (Alpha Innotech Corporation, San Leandro, U.S.A.).

2.8.7 Northern blot analysis

Details of all solutions are found in Section 2.8.1. Samples were made up to 90µl with DEPC-H_2O and re-precipitated by adding 10µl 3M NaOAc and 250µl absolute ethanol and left for 16 hours at –20°C. RNA was then centrifuged at 14800 x*g* at 4°C for 20 minutes and then re-suspended in 5µl (0.5mg/ml) ethidium bromide, 5.5µl formaldehyde, 15µl formamide, 1.5µl 10x MOPS, and 3.0µl DEPC-H_2O. Samples were then placed in a water bath at 55°C for 15 minutes to relax any secondary structure and subsequently cooled on ice prior to loading.

The gel tank and comb were pre-soaked for 16 hours in 1M NaOH to eliminate RNase activity and subsequently rinsed in excess DEPC-H_2O. The gel was prepared using 1.87g agarose and 85ml DEPC-H_2O melted in a microwave oven. In a fume hood 12ml pre-warmed 10x MOPS and 7ml formaldehyde were added to the cooled agarose mixture and the gel was poured with the comb in place. After setting, running buffer of 675ml DEPC-H_2O and 75ml 10x MOPS was poured into the gel tank sufficient to reach the gel surface without running into the wells. In the fume hood 3µl 10x loading buffer was added to each sample and this mixture was then loaded into the appropriate well. A small amount of running buffer was used to rinse the pipette tip into the well after the sample had been dispensed. The gel was run at 100V for 10 minutes to allow the samples to move into the gel and then buffer was added to the tank to cover the agarose completely. The gel was

then run at 60V for approximately two hours and then photographed *in situ* with a ruler using an AlphaImager™ 1200 gel analysis system (Alpha Innotech Corporation, San Leandro, U.S.A.). Formaldehyde was removed from the gel by washing gently in DEPC-H_2O on a rotating platform for 15 minutes and then by rinsing twice in 10x SSC.

Northern blot analysis was carried out using 10x15cm nylon membrane (Hybond™-N, Amersham Life Sciences, Little Chalfont, U.K.), 6x (10x15cm filter paper) and a 28 x 16cm filter paper wick. A glass tray was filled with 10x SSC and a glass plate, previously cleared with ethanol, was placed over the top of this, with the wick running across the plate so that the ends drew liquid up onto the surface of the plate. The RNA gel was placed face down onto the wick and surrounded by Nescofilm® (Bando Chemical Ind. Ltd, Kobe, Japan) to prevent movement of liquid away from the blot. The membrane was then placed carefully on top of the gel. Three of the filter paper blots were soaked in 10x SSC and placed on top of the blot, and the remaining three placed, dry, on top. Absorbent sheets (paper towels) were cut to size and placed on top of the filter paper, with a weight held in place to draw the nucleic acids onto the blot. The equipment was disassembled the following day and positions of the wells were marked in pencil on the blot which was then rinsed in 2x SSC, air dried, and placed in Saran wrap™ and exposed for 90 seconds to UV light to cross link the nucleic acids to the membrane. The membrane was then probed with radio-labelled cDNA corresponding to the *LjCbp1* gene and subsequently washed twice in 2x SSC, 0.1% SDS at 30ºC for 20 minutes and once in 0.2x SSC, 0.1% SDS at 65ºC for 20 minutes before being exposed to X-ray film for three days. The filter was stripped by immersing it in boiling 0.1x SSC, 1% SDS. It was then exposed to a radio-labelled ubiquitin gene cDNA and washed and exposed to autoradiography film (Hyperfilm™, Amersham, Little Chalfont, U.K.). Autoradiography films were examined and photographed using an AlphaImager™ 1200 gel analysis system (Alpha Innotech Corporation, San Leandro, U.S.A.). All radioisotope work was carried out by Dr Leif Skøt.

2.8.8 Identification of transcription start site

Approximately 3µg total RNA was used in the procedure, which was performed according to the manufacturer's instructions (GeneRacer™ Kit, Invitrogen™, Paisley, U.K.). A summary of the protocol is presented.

RNA was first treated with calf intestinal phosphatase (CIP) to catalyze the hydrolysis of 5′-phosphate groups and thereby remove the 5' phosphate group from truncated mRNA and non-mRNA in the sample. RNA was re-extracted using phenol and chloroform and re-precipitated using mussel glycogen, sodium acetate and ethanol. Following precipitation, the sample was treated with tobacco acid pyrophosphatase (TAP). TAP was used to cleave the pyrophosphate bond of the 5'-terminal methylated guanine nucleotide 'cap' of the intact, full length mRNA in the sample. The complete hydrolysis of pyrophosphate removes β and γ phosphates, leaving only the α phosphate attached. After extraction and precipitation of RNA (as above) the 5'-monophosphorylated terminus resulting from the use of TAP was ligated to a 3'-hydroxylated terminus, the GeneRacer™ RNA Oligo, using T4 RNA ligase. The mRNA was again extracted and precipitated as above. It was then ready for RT and PCR. Reverse transcription was carried out with Superscript™II RT (Roche diagnostics, Lewes, U.K.) and using the GeneRacer™ Oligo dT primer to anchor the RT enzyme and provide full length transcripts of all the mRNA. The resulting single strand cDNA was then amplified using PCR (Section 2.8.5) and either GeneRacer™ 5' primer plus a reverse gene specific primer for amplification of 5' ends, or GeneRacer™ 3' primer plus forward gene specific primer for amplification of 3' cDNA ends (Table 2.3). Reactions included negative 5' and 3' controls that consisted of all components except template cDNA, as well as additional controls that included template cDNA but excluded either the gene specific primer or the GeneRacer™ primer. The reverse gene specific primer for amplification of the 5' end was Racer 1 (Table 2.2) and the forward gene specific primer for amplification of the 3' end was the *LjCbp*1 forward primer (Table 2.2). PCR cycling parameters were as in Table 2.3, "RACE 1". The PCR products from these reactions were visualised on an agarose gel (Section 2.8.6) and 1µl of the product utilised in a second PCR

substituting the GeneRacer™ 5'and 3' primers with GeneRacer™ 5' and 3' nested primers (Table 2.2). The nested reverse gene specific primer for amplification of the 5' end was Racer 2 (Table 2.2). The reaction for the amplification of the 3' end was only nested at the 3' end, therefore the *LjCbp1* primer was again used as the 5' primer (Table 2.2). For negative control reactions the template cDNA was omitted. PCR cycling parameters for the second PCR were as in Table 2.3, "RACE 2".

The PCR products were purified using QIAGEN PCR purification kit and then ligated into a pGEM T-easy plasmid (Promega) according to the manufacturer's instructions. From the ligated sample, 2µl was mixed with 50µl *E. coli* competent cells (Section 2.8) in a 1.5ml microcentrifuge tube and left on ice for 20 minutes. The bacterial cells were then heat shocked at 42°C for 45 seconds, to allow the plasmid to be taken up by the cells, and then immediately cooled on ice for two minutes. The cells were transferred to universal containers with 950µl SOC medium (Section 2.5.1) and incubated at 37°C for 90 minutes at 225 rpm. After incubation the contents were transferred to a 1.5ml microcentrifuge tube and spun for 10 minutes at 400 x*g*. The supernatant was removed and the pellet suspended in 200µl SOC (Section 2.5.1). The tube was flicked gently to mix the cells in the SOC (Section 2.5.1) and 100µl was spread onto LB containing X-gal, IPTG and ampicillin (Section 2.5.1) and incubated at 37°C for 16 hours. Single white colonies, indicating the presence of the pGEM T-easy plasmid with an insert (i.e. the insertional inactivation of the *lacZ* gene leading to the inability to digest X-gal), were placed in 5ml LB with 20µl ampicillin (Section 2.5.1) and incubated at 37°C for 16 hours at 225 rpm.

The following day plasmid DNA was isolated using Wizard® *plus* SV Mini-preps (Promega, Southampton, U.K.) according to the manufacturer's instructions and 5µl of the eluted plasmid was digested with 20 units of the *Not1* restriction enzyme, plus 2µl buffer (Promega, Southampton, U.K.) and 11µl sterile reverse osmosis water. The digest was incubated at 37°C for approximately five hours to excise the inserted fragment and permit visualisation of the plasmid and inserted sequence on an agarose gel. The plasmid DNA (4µl) was then prepared for sequencing by mixing with 3.2µl either 1µM SP6 or T7 primer (Section 2.8.2) and 4.8µl sterile

reverse osmosis water. Six replicate sequences using each primer were sequenced. Primers SP6 and T7 are located at the left and right borders, respectively, of the plasmid's multiple cloning site. The sequencing was carried out as described in Section 2.11.

2.8.9 SDS polyacrylamide gel electrophoresis (PAGE)

Electrophoresis was carried out in a polyacrylamide gel under denaturing conditions that should minimise aggregation and ensure dissociation of the proteins into their individual polypeptide subunits. Samples were suspended in a buffer containing SDS and boiled to denature the proteins.

Acrylamide/Bis solution (29:1) with 3.3% cross-linking, C, N, N, N, N'-tetra-methyl-ethylenediamine (TEMED), ammonium persulfate (APS), and prestained SDS-PAGE low range standard were all obtained from Bio-Rad Laboratories Ltd, Hemel Hempstead, U.K. SDS-PAGE gel volumes listed below were sufficient to provide two gels of 0.75mm thick.

E. coli cells harbouring an epitope tagged vector, pHB6™ (Roche Diagnostics Ltd, Lewes, U.K.), ligated to a partial cDNA of *LjCbp1* containing the four EF-hand motifs, were supplied by Leif Skøt (unpublished data). The epitope tag is a hemagglutanin sequence. The pHB6™ vector harbours resistance to ampicillin. A control vector, pHB*lac*Z6, was also supplied as part of the pHB6™ kit (Roche Diagnostics Ltd, Lewes, U.K.).

SDS-PAGE gels were set up on Mini 2-D Cell apparatus and western blots were run on Mini Trans Blot equipment, both provided by Bio-Rad Laboratories Ltd (Hemel Hempstead, U.K.). Procedures were according to manufacturer's instructions. Hybond™-C nitrocellulose 0.45µm (Amersham, Little Chalfont, U.K.) membrane was used for western blotting.

Solutions

Lysis buffer contained Tris 20mM, pH 8.0, NaCl 100mM and 1 complete protease inhibitor tablet (with EDTA)/50ml (Roche Diagnostics Ltd, Lewes, U.K.).

10 x gel loading buffer was made up to give 1 x final concentration Tris 10mM, pH 8.0, EDTA 1mM, SDS 2.5% (w/v), DTT 100mM and bromophenol blue 0.01% (w/v).

Running gel buffer contained Tris 181.5g/l and SDS 4ml stock/l and was adjusted to pH 8.9.

Stacking gel buffer contained Tris 72.6g/l and SDS 1ml stock/l and was adjusted to pH 6.7.

Electrode buffer contained Tris 3g/l, SDS 10ml stock/l and glycine 14.4g/l.

12.5% SDS-PAGE running gel was made up using sterile reverse osmosis water 3.5ml, 40% acrylamide/bis solution 2.5ml, running gel buffer 2ml, TEMED 8µl and 10% APS 80µl.

5% Stacking gel was made up using sterile reverse osmosis water 2.5ml, acrylamide/bis solution 0.5ml, stacking gel buffer 1ml, TEMED 5µl and APS 40µl.

Coomassie stain contained Coomassie blue 1g, methanol 90ml, sterile reverse osmosis water 90ml and acetic acid 20ml.

De-stain solution contained methanol 500ml, water 1360ml and acetic acid 140ml.

Tris-buffered saline (TBS) contained Tris 1.21g/l, NaCl 8.18g/l and was adjusted to pH 7.4.

Transfer buffer contained Tris 2.42g/l, glycine 11.55g/l and methanol 400ml. The glycine and Tris were dissolved in water before methanol was added. The solution was stored at 4^{o}C.

Blocking solution contained 1% blocking reagent 10% stock (Roche Diagnostics Ltd, Lewes, U.K.) in TBS.

Antibody solution contained 0.5% blocking reagent 10% stock in TBS, anti-HA antibody (Roche Diagnostics Ltd, Lewes, U.K.) 10µl.

Wash solution contained Tween® 20 0.1% in TBS.

Peroxidase (POD) staining solution contained TrisCl pH 8.0 100mM, 50mM $MgCl_2$, NaCl 100mM, pH 8.0 made up to 10ml with sterile reverse osmosis water, BM Teton substrate (50µl) (50mg/ml) (Roche Diagnostics Ltd, Lewes, U.K.) and 6µl H_2O_2.

One colony each of epitope tagged cells and pHB*lac*Z6 control cells were transferred to universals containing 5 ml LB (Section 2.5.1) with 20µl ampicillin and placed in an orbital environ-shaker (Jencons Scientific Ltd, Leighton Buzzard, U.K.) at 37ºC and 225 rpm for 16 hours. The following day 200µl from each for 16 hours culture was transferred into fresh universals containing 10ml LB and 40µl ampicillin (Section 2.5.1). These samples were returned to incubate at 37ºC and 225 rpm.

At mid-log phase (optical density of 0.6 at 600nm), 1ml from each sample was transferred into a microfuge tube and spun at 15700 x*g* for 30 seconds to pellet the cells. The supernatant was removed and the samples were stored at –20ºC. To the remaining 9ml of each culture 90µl of the inducer, IPTG (Section 2.3), was added and samples returned to incubate as before. Samples of 1ml were taken at hourly intervals until six hours after the addition of IPTG and treated like the non-IPTG sample.

Pellets were re-suspended in 100µl lysis buffer, to which 100µl gel loading buffer was added. Tubes were boiled for five minutes, centrifuged briefly and placed on ice. A 12.5% SDS-PAGE gel was used to run 10µl of each sample, plus 3µl prestained standard at 150V on a 300 Power Pac (Bio-Rad Laboratories Ltd, Hemel Hempstead, U.K.) for approximately one hour, until the loading dye had reached the base of the gel.

Gels were stained in Coomassie blue for 15 minutes on a flatbed stirrer and cleared with several washings of 15 minutes each with a de-staining solution.

A fresh colony of the *LjCbp1* cells was taken and treated as above. Two 100µl samples were taken from the 16 hour (overnight) culture and at early log phase 100µl IPTG was added to one sample, the other was retained as a control. Samples were returned to the same incubation conditions for four hours.

After four hours 1ml aliquots were taken from the IPTG treated sample for each of six treatments, and one 1ml aliquot was taken from the non-IPTG control. All samples were spun as before and dissolved in 100µl of one of six treatments below:

1. lysis buffer only (EDTA-free tablet)
2. lysis buffer + 10mM $CaCl_2$ + 2mM EGTA
3. lysis buffer + 10mM $MgCl_2$ + 2mM EGTA
4. lysis buffer + 10mM EGTA
5. lysis buffer + 10mM $CaCl_2$, plus 100µl gel loading buffer.

The control sample without IPTG was dissolved in lysis buffer + 10mM$CaCl_2$. A SDS-PAGE, using replicate gels, was run using 10µl of each sample and 3µl prestained standard. One gel was stained and cleared as previously, the other was placed in transfer buffer in preparation for western blotting.

2.8.10 Western blotting

Western blotting was carried out at 100V for one hour at 4°C to allow electrophoretic transfer of polypeptides on the gel to a nitro-cellulose membrane. After transfer had taken place the membrane was washed twice for 30 seconds in TBS buffer to remove the methanol from the buffer system. The membrane was then submerged in 20ml blocking solution in a disposable square Petri dish (100x100mm) and incubated for one hour at 4°C to block non-specific binding of the antibody.

The blocking solution was drained from the container and the membrane was covered with 10ml antibody solution and incubated at room temperature on a gently rotating platform for one hour.

The antibody solution was then drained off and the membrane was washed four times for 10 minutes in wash solution on a rotating platform. During the last wash the peroxidase (POD) staining solution was prepared. After the last wash the membrane was drained and rinsed twice with TBS and then covered with POD staining solution and incubated at room temperature for approximately 20 minutes until bands appeared. The membrane was then rinsed several times in ultra pure water (Section 2.1) and dried. It was then wrapped in Saran wrap (Dow Chemical

Co., Midland, U.K.) and photographed using an AlphaImager™ 1200 (Alpha Innotech Corporation, San Leandro, U.S.A.).

2.9 Microscopy and photography

Seedlings were examined using either an Olympus BH2 light microscope (Tokyo, Japan) or an Olympus LSG binocular microscope (Tokyo, Japan).

Whole seedlings were photographed on a Jencons (Scientific) Ltd (Leighton Buzzard, U.K.) light table and photographed using a FujiFilm (Fuji, Tokyo, Japan) FinePix S1 Pro digital camera with a Nikon 60mm lens.

Microscopic images were captured using a MagnaFire® SP Digital Imaging System (Optronics™, California, U.S.A.).

2.10 Statistics

Data were analysed using Genstat for Windows Version 6.1 (Payne, 2000). Evaluation of data was achieved through binomial regression using the logit link function.

2.11 Sequence analysis

Sequencing was carried out on a central sequencing facility (ABI-3100 Genetic Analyser, Applera U.K., Warrington, U.K.) based at IGER, Aberystwyth, according to the manufacturer's instructions. Analysis of raw sequence data was carried out using the Unix-based GCG package (Accelrys Ltd, Cambridge, U.K.). For the pGEMT-easy based sequencing the vector-specific primers T7 and SP6 (Table 2.2) were used. Vector sequences were edited from the data using Chromas version 1.45 (Technelysium Pty Ltd, Helensvale, Australia) and GCG® version 10.0 (Accelrys Ltd, Cambridge, U.K.) software was used to align the replicates and determine a consensus sequence.

The Kazusa search engine, located on http://www.kazusa.or.jp/en/database.html, the BLAST and FASTA (basic/ local alignment search tool) facility of the GCG® version 10.0 software and NCBI (Altschul, 1997), respectively, were used to search genomic, expressed sequence tag (EST) and protein databases for matches to the *LjCbp1* gene in other species. These sequences were translated into their predicted polypeptides and aligned using GCG® version 10.0 software GeneDoc (Free Software Foundation, Inc., Boston, U.S.A.) was used to present sequence data. The peptide plot facility of GCG® version 10.0 was used to determine the isoelectric point and predicted molecular weight of the protein LjCbp1. The phylogenetic tree was generated using the PROTPARS programme in the Phylip Inference Package (Felsenstein, 1993). Pairwise comparisons were generated using the bestfit option in GCG ® version 10.0.

Analysis of the TAC sequence (LjT15I02), provided by Dr Shusei Sato (Kazusa Institute, Japan), was also carried out using GCG (Accelrys Ltd, Cambridge, U.K.).

Web-based sequence analysis tools were used to characterise the translation start site of *LjCbp1*. These were Place signal scan and homology search at http://www.dna.affrc.go.jp/htdocs/PLACE (Higo *et al*., 1999), PlantCARE at http://oberon.rug.ac.be:8080/PlantCARE/index.html (Lescot *et al*., 2002) and PlantProm http://www.softberry.com/berry.phtml?topic=plantprom (Shahmuradov *et al*., 2003).

Promoter sequences from various published ENOD genes were also analysed against the untranslated 5' sequence of *LjCbp1* using GCG (Accelrys Ltd, Cambridge, U.K.).

The peptide sequence, LjCbp1, was analysed for potential hydrophobic domains to identify putative membrane spanning domains and signal peptides. The peptide sequence was loaded into both CBP SignalP V1.1 World Wide Web Prediction Server at http://www.cbs.dtu.dk (Nielsen *et al*., 1997) and the "DAS"

transmembrane prediction server of the Stockholm Bioinformatics Centre at http://www.sbc.su.se/ (Cserzo *et al*., 1997).

Chapter 3

3 Characterisation of *LjCbp1* locus

3.1 Introduction

A wide range of cellular functions in both animals and plants has been shown to be under the control of divalent calcium, a ubiquitous intra- and intercellular second messenger (Rottingen and Iversen, 2000). Variations in the parameters of amplitude, duration and location afford the calcium ion a versatility in functioning as a 'tool kit' for different cellular requirements and thus encrypt a diverse array of signals (Berridge *et al*., 1998).

Organisms are able to perceive changes in Ca^{2+} by maintaining nanomolar (30-200nM) concentrations in the cytosol and millimolar (1-10mM) concentrations in the cell wall and organelles (Piñeros and Tester, 1997; Reddy, 2001). Changes in $[Ca^{2+}]_{cyt}$ can be mediated by influx/efflux across the plasma membrane and release/uptake into intracellular stores (Sanders, *et al*., 1999). Intracellular organelles act as stores for Ca^{2+}, which may be released through the opening of specific channels in organellar membranes to increase $[Ca^{2+}]_{cyt}$ (Piñeros and Tester, 1997). Once the elevated $[Ca^{2+}]_{cyt}$ signal has been perceived and acted upon, low concentrations are restored to the cytosol through Ca^{2+} efflux to the cellular exterior or sequestering into organelles, requiring the active pumping of Ca^{2+} against a concentration gradient (Reddy, 2001).

An array of signals, such as light, hormones, gravity, touch, wind, cold, drought, oxidative stress and microbial elicitation have been shown to elicit an increase in $[Ca^{2+}]_{cyt}$ (Reddy, 2001). Ca^{2+} is therefore involved in the control of a wide range of cellular functions in eukaryotes including, amongst others, cell development and differentiation (Legue *et al*., 1997), gene transcription (Berridge *et al*., 1998), gravitropism (Gehring *et al*., 1990), stomatal closure (Allen *et al*., 1999) and root hair growth (Sanders *et al*., 2002); it has also been shown to be involved in the nodulation process (Ehrhardt *et al*., 1996).

Ca^{2+}-permeable channels have been detected in all plant membranes, although some speculation exists regarding the genes encoding them (White and Broadley, 2003). In plants, inositol 1, 4, 5-trisphosphate (IP_3), cyclic adenine dinucleotide phosphate (ADP) ribose and Ca^{2+} channels are currently believed to be involved in elevating $[Ca^{2+}]_{cyt}$. IP_3 has been shown to stimulate the release of Ca^{2+} from the vacuole (not the endoplasmic reticulum, as in animals) and IP_3- and cyclic ADP-ribose-gated channels have been found in vacuolar and endoplasmic reticulum membranes in plants (Reddy, 2001). The recent finding that nicotinic acid ADP releases Ca^{2+} exclusively from the plant endoplasmic reticulum suggests that multiple Ca^{2+} mobilisation pathways exist in plants, and that these are regulated by different agents. Thus, different signals may use distinct Ca^{2+} stores to increase $[Ca^{2+}]_{cyt}$ (Reddy, 2001).

The dynamic effects of Ca^{2+} in the cell require mediation by a specialised group of cellular Ca^{2+}-binding proteins, or 'sensors', able to perform a number of tasks including the transduction of the Ca^{2+} signal, the integration of its effect with those of other signalling pathways and the maintenance of a homeostatic-effect balance of Ca^{2+} signals. It is these sensor proteins that are the principle target of Ca^{2+} signals in eukaryotes (Roberts and Harmon, 1992; Zielinski, 1998).

3.1.1 Ca^{2+} sensors

A large number of Ca^{2+} sensors have been described in plants and can be grouped into four main classes: calmodulin (CaM); CaM-like proteins and other EF-hand containing Ca^{2+}-binding proteins; Ca^{2+}-regulated protein kinases and other Ca^{2+}-binding proteins without EF-hand motifs (Reddy, 2001).

The EF-hand motif is the distinguishing feature of many Ca^{2+}-sensing proteins. Its nomenclature derives from a description of the C-terminal E-helix-loop-F-helix Ca^{2+}-binding site in parvalbumin, the first EF-hand Ca^{2+}-binding protein to be purified (Henrotte *et al*., 1955; cited in Celio *et al*., 1996), sequenced (Pechére *et al*., 1971; cited in Celio *et al*., 1996) and crystallized (Kretsinger *et al*., 1971; cited

in Celio *et al*., 1996). The typical canonical EF-hand binding site comprises 29 residues, consisting of two helices flanking a "loop" of 12 contiguous residues, within which the oxygen ligands for binding Ca^{2+} are derived (Strynadka and James, 1989). The three-dimensional structure of the EF-hand site can be simulated by the right hand, with the extended thumb and index finger representing the α-helices and the bent middle finger indicating the Ca^{2+}-binding loop (Figure 3.0).

Each EF-hand is responsible for binding a single Ca^{2+} ion which causes the protein to undergo a conformational change rendering it active for diverse and numerous downstream proteins. High-resolution crystal structure analyses demonstrate that the majority of Ca^{2+}-binding sites usually contribute seven oxygen ligands to the metal ion. Most of these ligands come directly from the 12 residue EF-hand loop (Strynadka and James, 1989). The remaining residues of the loop contribute hydrogen bonding via main-chain NH groups to stabilise the geometry of the loop for Ca^{2+}-binding.

One of the best characterised of the EF-hand proteins is CaM, the prototype of which is a highly conserved acidic protein of around 16.7 KDa and consisting of 148 amino acids. CaMs, with one exception, have two pairs of intimately linked EF-hands numbered I-IV from the amino terminus (Snedden and Fromm, 1998; Strynadka and James, 1989; Zielinski, 1998). EF-hands I and II form the first globular domain of the protein and III and IV form the second, so that the overall structure resembles a dumbbell (Roberts and Harmon, 1992).

CaM has no enzymatic properties of its own but modulates other proteins in the Ca^{2+}-dependant manner indicated above (Roberts and Harmon, 1992). Upon binding Ca^{2+}, hydrophobic clefts are exposed within each globular domain, these clefts may be involved in binding amphipathic sequences in CaM-target proteins (Roberts and Harmon, 1992). This binding of Ca^{2+} results in a conformational

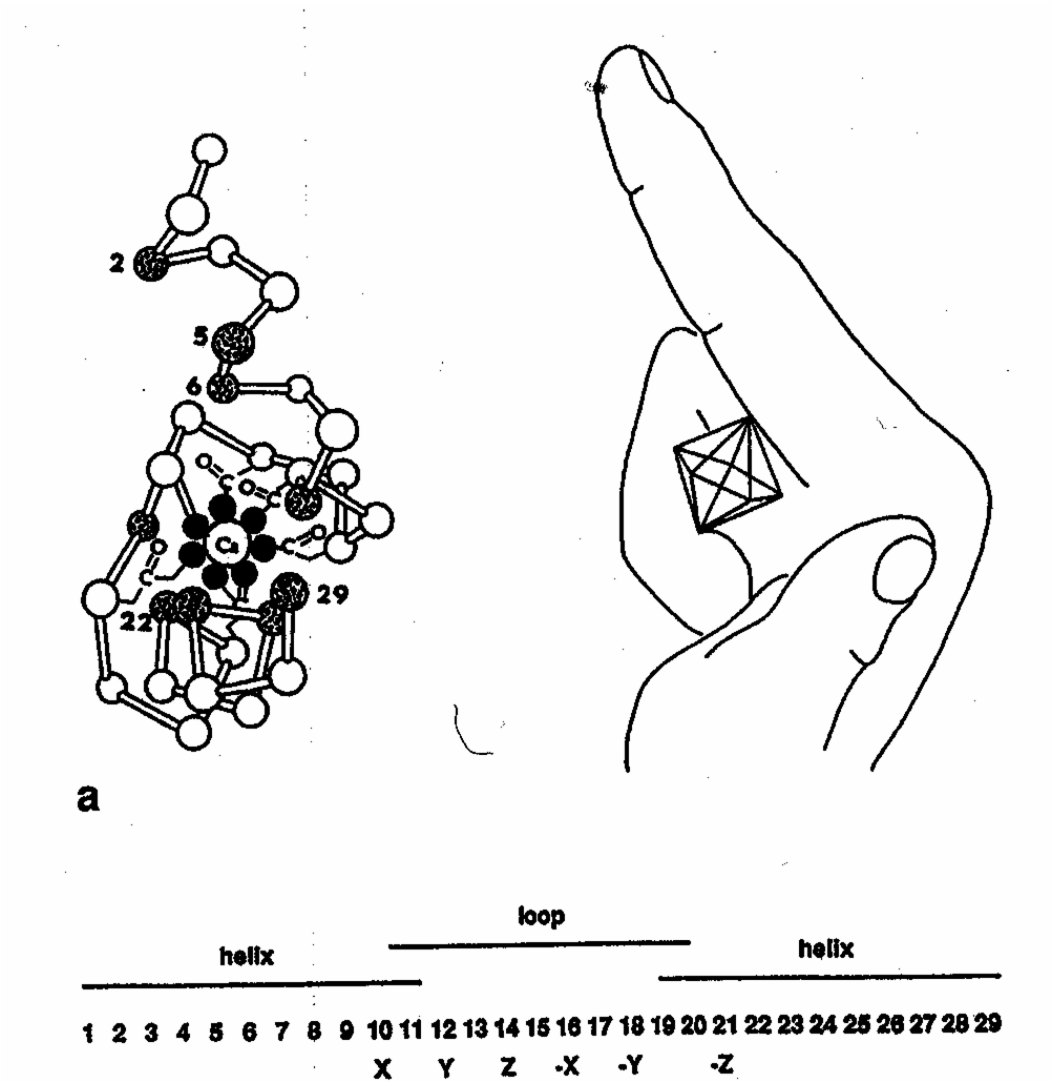

Figure 3.0. The EF-hand Ca^{2+}-binding motif. There are 29 residues in all, incorporating two α-helices, oriented at approximately 90^0 with respect to one another. The helices flank a "loop" of 12 contiguous residues, within which are five amino acid residues at positions X, Y, Z, -X and –Y, which provide one oxygen ligand, and the residue at position –Z, which provides two. The three-dimensional structure of the EF-hand site can be simulated by the right hand, with the extended thumb and index finger representing the α-helices and the bent middle finger indicating the Ca^{2+}-binding loop. Modified from Celio *et al*., 1996.

change, leading to modulation of activity (Reddy, 2001). CaM is a ubiquitous Ca^{2+} receptor in plants (Reddy, 2001).

Unlike mammalian systems, where CaM appears to be encoded by small gene families producing a single polypeptide, multiple isoforms of CaM have been found in *Arabidopsis* (Liao *et al*., 1996; Zielinski, 1998) and soybean (Lee and Harmon, 1995) and have been inferred in *Phaseolus* (Camas *et al*., 2002). One implication of this is that different isoforms may act to extend the range of downstream elements with which CaM may interact, so providing an even greater level of Ca^{2+}-based signal transduction to that afforded in mammalian systems (Liao *et al*., 1996). Therefore, small changes in amino acid composition may lead to the differential interaction of each isoform with target proteins, permitting fine-tuning of signalling mechanisms (Reddy, 2001).

In order to dissect the Ca^{2+} signalling pathway in plants, efforts have been made to identify and characterise CaM-binding proteins. Biochemical assays and protein-protein interaction-based screening of expression libraries with labelled CaM have determined over 20 proteins that interact with CaM in a Ca^{2+}-dependent manner. These proteins have a range of functions and include a transcription factor, heat shock inducible proteins, an auxin-induced gene and NAD kinase (Reddy, 2001). Ca^{2+}-independent CaM-binding proteins have also been identified. These are the myosins and are better characterised in animals although two myosins have recently been purified from plants. Yokota *et al*., (1999) demonstrated that CaM associates with the purified myosin and regulates its actin-based motor activity. Ca^{2+} has been shown to inhibit this activity (Yokota *et al*., 1999). Such proteins may be involved in cytoplasmic streaming in plant cells (Reddy, 2001).

In addition to the CaMs there are CaM-like proteins, having between one and six EF-hands (Reddy, 2001; Snedden and Fromm, 2001; Zielinski, 2002; White and Broadley, 2003). CaM-like proteins include NADPH oxidases (Torres *et al*., 1998), Ca^{2+}-binding protein phosphatases (Leung *et al*., 1997) and the *Arabidopsis* touch-induced *Tch2* and *Tch3*. *Tch3* contains six EF-hands and is 324 amino acids long (Braam *et al*., 1997).

Jakobek *et al*. (1999) identified a cDNA encoding a small putative Ca^{2+}-binding protein of 161 amino acids and containing four EF-hand motifs. The gene, *Pvra32*, is highly expressed during the hypersensitive response (HR) in bean tissue challenged with *Pseudomonas syringae*, thus supporting data regarding the involvement of Ca^{2+} in plant defence responses. Other plant proteins implicated in defence are centrins. These proteins are between 167 and 177 amino acids long and contain four EF-hands. Centrin genes are induced upon inoculation of the plant with HR-eliciting strains of bacteria (Reddy, 2001).

A new family of Ca^{2+}-binding proteins have recently been suggested by White and Broadley (2003) as a separate group, although previously included by Reddy (2001) in the CaM-like group. These are the calcineurin B-like proteins. These possess three EF-hands and in *Arabidopsis* there are at least ten such proteins, one of which is induced by drought, cold and wound stress signals (White and Broadley, 2003).

Ca^{2+}-regulated protein kinases have been implicated in a number of responses, including host-pathogen interactions, cold stress, gravitropism, light-regulated gene expression and hypo-osmotic shock (Reddy, 2001). These findings are all based on the manipulation of intracellular Ca^{2+} levels with pharmacological agents. Four or five types of Ca^{2+}-regulated protein kinases can be described (Reddy, 2001; White and Broadley, 2003), the most abundant and ubiquitous of which are the Ca^{2+}-dependent and CaM-independent protein kinases (CDPKs). Here, Ca^{2+} binds directly to the protein and stimulates kinase activity. At least 34 genes encoding CDPKs exist in the *Arabidopsis* genome with similar numbers in other species (White and Broadley, 2003). These proteins generally have four EF-hands at their C-terminus that bind to Ca^{2+} to activate their serine-threonine kinase activity. Other Ca^{2+}-regulated protein kinases are less well described but include CaM-dependent protein kinases, whose kinase activity is triggered by CaM-dependent autophosphorylation (White and Broadley, 2003).

Several proteins have also been identified in plants which bind Ca^{2+} but do not contain EF-hands (Reddy, 2001). Within this group are phospholipase D, the

annexins and those proteins which sequester Ca^{2+} in the endoplasmic reticulum, such as calreticulin, calsequestrin and calnexin (White and Broadley, 2003). Phospholipase D cleaves membrane phospholipids and is regulated by $[Ca^{2+}]_{cyt}$. It is implicated in cellular responses to ethylene and ABA, α-amylase synthesis in aleurone cells, pathogen responses, stomatal closure, leaf senescence and drought tolerance (White and Broadley, 2003). Annexins generally contain four repeats of a motif consisting of around 70 amino acids. The exact function of this group of proteins is not known. Most annexin-encoding genes are found ubiquitously in plants but some are highly expressed in secretory cell types (Reddy, 2001; White and Broadley, 2003). The Ca^{2+} sequestering proteins are implicated in Ca^{2+} homeostasis, protein folding and post-translational modifications (White and Broadley, 2003).

Most categories of Ca^{2+} sensors appear to contain a diverse range of proteins implicated in a wide variety of processes.

3.1.2 Ca^{2+} signalling in the root nodule symbiosis

As outlined in Section 1.5.5, the addition of Nod factors to legume roots induces two phases of ionic changes. The first is a rapid influx of Ca^{2+}, which triggers the activation of anion channels through plasma membrane depolarisation and extracellular alkalinization (Felle *et al*., 1998, 1999). The second phase is Ca^{2+}-spiking within the cytosol (Ehrhardt *et al*., 1996).

Evidence supporting the role of Ca^{2+} as a second messenger in root nodulation has come from a variety of sources. Felle *et al*. (1998) demonstrated the ability of the Ca^{2+} ionophore A23187 to mimic some of the effects of Nod factor in *M. sativa*. Felle *et al*. (1998) also demonstrated the inhibition of Nod factor-induced elevation of $[Ca^{2+}]_{cyt}$ in the presence of the Ca^{2+} channel antagonist nifedipine. Ehrhardt *et al*. (1996) describe nodulation-defective *M. sativa* mutants where Ca^{2+}-spiking is not exhibited. Pingret *et al*. (1998) reported the interference of a variety of pharmacological antagonists with Nod factor-induced increases in $[Ca^{2+}]_{cyt}$ that

prevented the subsequent expression of downstream genes normally associated with Nod factor application.

Ca^{2+} influx appears to be the fastest physiological response to Nod factors (Felle *et al*., 1998, 1999). The addition of 0.1μM Nod factor, purified from *R. meliloti*, to root hair cells of *M. sativa* resulted in an increase in $[Ca^{2+}]_{cyt}$ within two minutes (Felle *et al*. 1999). This was followed, seconds later, by an efflux of chloride ions, alkalinization and a delayed efflux of potassium ions. The efflux of potassium ions is presumed to bring a charge balance and repolarization initiated through the activity of the proton pump (Felle *et al*., 1998). In fact, one experimental set up used by Felle *et al*. (1998) measured the decline of Ca^{2+} in the medium surrounding the root hair. In this instance, $[Ca^{2+}]$ levels fell within seconds of the addition of Nod factor. If elevated $[Ca^{2+}]_{cyt}$ is the result of influx from external stores, as these experimental data indicate, the increase may actually prove to be within seconds of Nod factor application (Cárdenas *et al*., 2000). Felle *et al*. (1999) also demonstrated that the influx of Ca^{2+} into root hair cells is likely to come from external stores and that the elevation of $[Ca^{2+}]_{cyt}$ is indispensable for the activation of downstream events, such as the activation of anion channels.

M. truncatula dmi mutants have provided evidence that the flux response in wild-type plants is biphasic and can be separated into an initial rapid increase in $[Ca^{2+}]_{cyt}$, observed in all three *dmi* mutants, and a second, plateau-like increase that is found only in the *dmi3* mutant and lasts for around five minutes (Shaw and Long, 2003). Since the *dmi1* and *dmi2* mutants exhibit only root hair swelling, the latest data from Shaw and Long (2003) indicate that the initial phase of Ca^{2+} may function in regulating root-hair growth, which is consistent with other findings that Ca^{2+} functions in co-ordinating root-hair tip growth (Sanders et al., 2002).

Ehrhardt *et al*., (1996) demonstrated that purified Nod factors induced transient oscillations in $[Ca^{2+}]_{cyt}$ in root hair cells of *Medicago* species within approximately ten minutes of their application. This phenomenon, known as Ca^{2+}-spiking, avoids the danger of prolonged increases in $[Ca^{2+}]_{cyt}$ that can be lethal to a cell (Berridge *et al*., 1998). Ca^{2+}-spiking is also a common response to many different environmental stresses (Knight and Knight, 2001). The spikes are predominantly

restricted to the area surrounding the nucleus and are likely to result from the opening of Ca^{2+} channels from intracellular stores (Ehrhardt *et al*., 1996; Pingret *et al*., 1998; Walker *et al*., 2000).

Shaw and Long (2003) and Walker *et al*. (2000) have demonstrated that the two Ca^{2+} responses (i.e. Ca^{2+} influx and Ca^{2+}-spiking) can be uncoupled, under different experimental conditions. For instance, modified Nod factors can activate Ca^{2+}-spiking in *P. sativum* without activating a flux and some *M. truncatula* mutants can activate the flux without inducing spiking. Shaw and Long (2003) also noted that higher concentrations of Nod factor were required to induce the flux response, compared with the spiking response, in *M. truncatula*.

Recently, Harris *et al*. (2003) confirmed the occurrence of Ca^{2+}-spiking in *L. japonicus*, illustrating its importance in both determinate and indeterminate nodulation pathways in legumes. In *L. japonicus* Ca^{2+}-spiking was observed within 20 minutes of the addition of Nod factor, or *M. loti* bacteria in which *nod* gene induction had already commenced (Harris *et al*., 2003).

3.1.3 Ca^{2+}-binding proteins in the root nodule symbiosis

So far, only a few genes encoding Ca^{2+}-binding proteins have been implicated in the legume symbiosis with rhizobia. They include *MtAnn1*, an annexin (Section 3.1.1) homologue from *M. truncatula* expressed in infected roots and nodules and CaM homologues *PvCaM-1*, *-2*, and *–3* isolated from a *Phaseolus vulgaris* nodule cDNA library (Camas *et al*., 2002; de Carvalho-Niebel *et al*., 2002; Niebel *et al*., 1998).

The annexin *MtAnn1* was isolated following a differential display approach to identify new plant genes induced in the early stages of symbiosis (de Carvalho-Niebel *et al*., 2002). *MtAnn1* is upregulated from a basal level of expression within 48 hours of the addition of Nod factors purified from *R. meliloti*. The function of the gene is not yet known, but its regulation bears some resemblance to that of the *ENOD11* and *12* genes and it may be involved in the preparation of cells for

infection or nodule organogenesis, perhaps in relation to changes in the cellular cytoskeleton (de Carvalho-Niebel *et al*., 2002).

PvCaM-1, *-2*, and *-3* (*-2*, and *-3* may be alleles) are expressed early in nodule development. Transcripts increase between the stages of nodule primordia and the nodule-like structures induced with Nod factor, whereas expression in roots is lowered after Nod factor application. A polar auxin transport inhibitor was also found to inhibit expression of *PvCaM-1* suggesting that the regulation of this gene is mediated by auxins (Camas *et al*., 2002).

3.1.4 A T-DNA-tagged putative Ca^{2+}-binding protein in *L. japonicus*

T-DNA-tagged line, T90, was identified by Webb *et al*. (2000) during a gene-tagging programme in *L. japonicus*. The T-DNA-tag harboured a reporter gene which, in T90, appeared to be reporting expression of a downstream gene encoding a putative calcium-binding protein, therefore named *LjCbp1*. The *LjCbp1* locus was sequenced using a combination of uneven- and RT-PCR to deduce a polypeptide of 150 amino acids with a molecular mass of 17 KDa (Webb *et al*., 2000). Data mining showed that *LjCbp1* showed the strongest similarity (73.9% identity) to a Ca^{2+}-binding protein predicted from a genomic sequence of *A. thaliana*. Four EF-hand structural motifs were also identified in the *LjCbp1* cDNA sequence providing further evidence that this gene may encode a Ca^{2+}-binding protein (Webb *et al*., 2000). According to Webb *et al*. (2000), the coding sequence for the putative Ca^{2+}-binding protein was situated approximately 1.3 Kb downstream of the T-DNA insertion.

No obvious nodulation or nitrogen-fixation phenotype was observed in the T90 line, suggesting that the T-DNA insertion did not interrupt the *LjCbp1* coding sequence and permitted sufficient residual expression and synthesis to generate a normal nodulation phenotype. Alternatively, the *LjCbp1* gene may not be essential for nodulation, or a close homologue may have made it functionally redundant (Webb *et al*., 2000).

The gene identified by Webb *et al*. (2000) shared identity with several plant and animal CaMs. Both the coding and the non-coding sequence were used to probe the *L. japonicus* genomic sequence during Southern blot analysis and these results suggested that the non-coding sequence is likely to be unique, whereas the putative Ca^{2+}-binding sequence may be one of several closely related genes in a family (Webb *et al*., 2000). This supports the findings that several isoforms of such genes exist in some plant species.

Key resources available to aid computational, or *in silico*, sequence analyses are the vast databases currently being generated and developed. There are presently sequencing projects underway for several important crop species such as soybean, rice and alfalfa, whilst sequencing of the model species *Arabidopsis* has been completed (Arabidopsis Genome Initiative, 2000). In 2000 the Kazusa DNA Research Institute in Japan began sequencing the genome of *L. japonicus* accession MG-20 using transformation-competent artificial chromosome (TAC) vectors as a host for the genomic libraries. In this database over 32 000 EST entries have been made available to the public, while a further 74 317 ESTs reside in the in-house database; the length of the gene-rich regions determined so far is 18.7 Mb, covered by 183 TAC clones (Asaimizu *et al*., 2003). Details of progress and databases of ESTs can be found at: http://www.kazusa.or.jp/lotus/. This resource will therefore be exploited in the hope that sequences similar to that of *LjCbp1* will provide evidence as to the presence of a CaM or CaM-like gene family in *L. japonicus* as identified in other plant species.

The possibility that *gus* expression in the T90 line may be reporting the expression of a gene encoding a Ca^{2+}-binding protein involved specifically in symbiotic interactions suggests that this line could be used to investigate Ca^{2+} signalling in plant-rhizobium interactions. For this reason it is important to determine whether *LjCbp1* encodes a protein that binds Ca^{2+} that is involved in root-nodulating symbiosis and also whether expression of the *gus* and *LjCbp1* genes correlate. This chapter therefore aims to assess the Ca^{2+}-binding ability of the protein product of *LjCbp1* as well as the level of correlation in the expression of the two genes.

The binding of Ca^{2+} by Ca^{2+}-binding proteins has been shown to result in an electrophoretic mobility shift (Strynadka and James, 1989). Jang *et al.* (1998) demonstrated the Ca^{2+}-dependent electrophoretic mobility shift of a novel Ca^{2+}-binding protein in *A. thaliana*. They used an epitope-tagged cDNA of their protein ligated into an expression vector for subsequent Ca^{2+}-binding assays, an approach that will be adopted with *LjCbp1*. A mobility shift assay was performed using an epitope-tagged clone of the *LjCbp1* gene generated by Leif Skøt (unpublished work). Epitope-tagging attaches the DNA of a short peptide (epitope tag) sequence in frame with the DNA sequence of the target protein. The construct is then transferred into a suitable organism, in this case *E. coli*, where the protein is expressed. Protein extracted from the host organism can then be run out on a denaturing gel, blotted onto a membrane and then exposed to the epitope-specific antibody, thus identifying the protein of interest.

In sequencing parts of the *L. japonicus* genome, the Kazusa institute have also made available sequences from their TAC libraries, each containing around 100 Kb of genomic sequence. The sequence from the TAC library containing the *LjCbp1* locus was used to analyse extensive regions up- and downstream.

In T90, the T-DNA insertion itself consists of 5346 bp and therefore has potential to disrupt the expression of downstream genes. A number of websites exist to facilitate the identification of putative regulatory *cis*-elements around regions of ORFs. Several of the databases available online, as well as the in-house GCG software (Accelrys Ltd, Cambridge, U.K.) were employed to analyse the 2.7 Kb sequence upstream of the ATG start site of *LjCbp1*.

Investigations were also made into the presence of any potential membrane spanning regions of the protein that could indicate the existence of a signal peptide.

In order to gain a fuller understanding of the possible regulation of *LjCbp1* and to characterise more fully this locus the complete mRNA sequence, thereby containing the transcription start site, was cloned using rapid amplification of cDNA ends (RACE) technology. RACE exploits the phenomenon of 'capping', using a methyl group, of the 5' ends of eukaryotic mRNA. Transcription of mRNA

usually starts with a purine (A or G) but after transcription a guanine residue is added enzymatically by a 5'-5' trisphosphate linkage. This residue usually also carries methylated groups. Consequently, mature, full length mRNA do not have a terminal 5' phosphate group, while partial mRNA's do. A method of amplifying only full-length 5' ends of cDNA is thus possible through the elimination of truncated messages from the amplification process. The first step in the procedure involves the enzymatic removal of the 5' phosphate group from truncated mRNA and non-mRNA molecules. The sample is then treated with another enzyme that specifically cleaves the pyrophosphate bond of the 5'-5' terminal guanine cap of intact full length mRNA, exposing the α-phosphate attached to the 5'-end. This 5'-end is then ready for ligation of an RNA oligo, enabling subsequent PCR amplification of the cDNA strand using gene specific primers to identify the transcription start site. The region where transcription starts, in other words where RNA polymerase binds, is usually known as a TATA box. This has a consensus sequence TATAAA, although considerable variation is found in such elements. Some promoters may lack the TATA box and in this case produce mRNAs with different, staggered 5'-ends (Blackburn and Gait, 1990). Various software programs exist to facilitate the identification of TATA box elements; these were exploited to identify potential TATA sequences in the *LjCbp1* locus.

In addition to the *in silico* analysis of *LjCbp1* this chapter also covers the molecular analyses of *LjCbp1* and *gus* gene expression in response to rhizobial inoculation.

Investigations into the expression of *LjCbp1*, using Northern hybridisation and RT-PCR analyses, showed that mRNA transcripts for this gene were absent in shoot tissue, but present in roots of both Gifu and T90 plants inoculated with wild-type *M. loti* (Webb *et al*., 2000). These transcripts, to some extent, mirrored GUS expression. RT-PCR results revealed further similarities between GUS activity and expression of *LjCbp1*, since *LjCbp1* transcript and GUS activity diminished with nodule age. However, transcripts of *LjCbp1* were also found in roots inoculated with the *nodC* mutant where no corresponding GUS activity was observed, suggesting that the *gus* reporter gene and the *LjCbp1* gene were not subject to identical regulatory mechanisms (Webb *et al*., 2000).

Initial histochemical analyses had revealed extensive elicitation of GUS in roots of T90 72 hpi but an absence of expression in uninoculated roots (Webb *et al*., 2000). It was therefore expected that GUS activity was the result of *de novo* expression of this gene. RT-PCR analysis was initially used to investigate this hypothesis. It was expected that GUS expression would be accompanied by upregulation of the *Cbp1* gene. This was investigated using Northern blot analysis and variations of RT-PCR.

Northern blot analysis provides a number of advantages for gene expression studies. The levels of message present for a gene of interest can be quantified through reference to the intensity of RNA on the gel from which the blot was taken and also to the hybridisation of a 'normalising' standard such as the constitutively expressed ubiquitin or actin. There are certain drawbacks to Northern analysis, however, particularly in the study of certain organisms. Sufficient quality and quantity of RNA must be available to permit the optimisation of RNA levels for individual time-point assays and in *Lotus japonicus* endogenous polysaccharides can contaminate RNA samples, interefering with downstream processes. Other, more sensitive techniques were therefore employed in an effort to find a more accurate quantitative or semi-quantitative analysis.

Single strand cDNA synthesis permits the generation of a greater quantity of new cDNA template from messenger RNA, thus giving greater flexibility to ensure samples are of equal concentration. The use of both wild-type and T90 material, grown and inoculated in the same conditions, provides an opportunity for a direct comparison of expression of *LjCbp1* in the different lines and may provide additional information pertaining to the regulation of this gene. A direct correlation with expression of the *gus* transgene can also be made.

The purpose of this chapter, therefore, was to investigate further the *LjCbp1* locus, including the region containing the T-DNA insert, using *in silico* and molecular techniques. These investigations aim to classify the protein product amongst the range of Ca^{2+}-modulated proteins now known, determine the Ca^{2+}-binding ability of the protein product and identify regions that may be important in the regulation of this gene. Gene expression studies will also be carried out in response to

inoculation of *L. japonicus* with *M. loti* and to correlate the expression of *gus* and *LjCbp1*.

3.2 Results

3.2.1 *In silico* analysis of Ca^{2+}-binding proteins

Sequence analysis was as described in Section 2.11. Genomic, EST and protein databases were used to find *LjCbp1* matches. The region encoding the unusual repeat of serine residues was also used to try and identify similar sequences in other species.

Searches of EST databases using the nucleotide sequence of *LjCbp1* revealed an EST which showed extremely high similarity to the *LjCbp1* sequence but which contained an extended 5' region. This information led to doubt over the correct sequence of *LjCbp1*. Repeat analysis of this region was therefore carried out by Leif Skøt. This revealed that some errors were present in the initial published sequence. The correct coding sequence of *LjCbp1* is shown in Figure 3.1. The revised predicted protein is 230 amino acids long with a predicted molecular weight of 26 KDa, as opposed to 150 amino acids and 17 KDa.

The search of public domain ESTs using the new *LjCbp1* sequence (Aj251808) revealed matches with only moderate identity, around 40% at the amino acid level (Figure 3.1) and 60% at the nucleotide level (data not shown). A search for additional homologues of *LjCbp1* in Kazusa's in-house database also failed to identify any candidates in either genomic sequences or ESTs (Shusei Sato, personal communication). All the ESTs with a significant match were identical to the *LjCbp1* sequence on TAC LjT15I02.

An alignment of 22 sequences, including the peptide product of *LjCbp1*, is presented in Figure 3.2 and includes the sequences most closely matching LjCbp1, or its peptide product. The sequences were identified using the packages described in Section 2.11.

A phylogenetic tree derived from the above alignment is presented in Figure 3.3 and shows the sequences most closely resembling *LjCbp1* are those from *Populus tremuloides*, *Malus domesticus* and both from *G. max*. Pairwise

Figure 3.1. Multiple Sequence Alignment of *LjCbp*1 and other *L. japonicus* ESTs. Blue boxes show EF-hand regions, green boxes show primer sites used for RT-PCR.

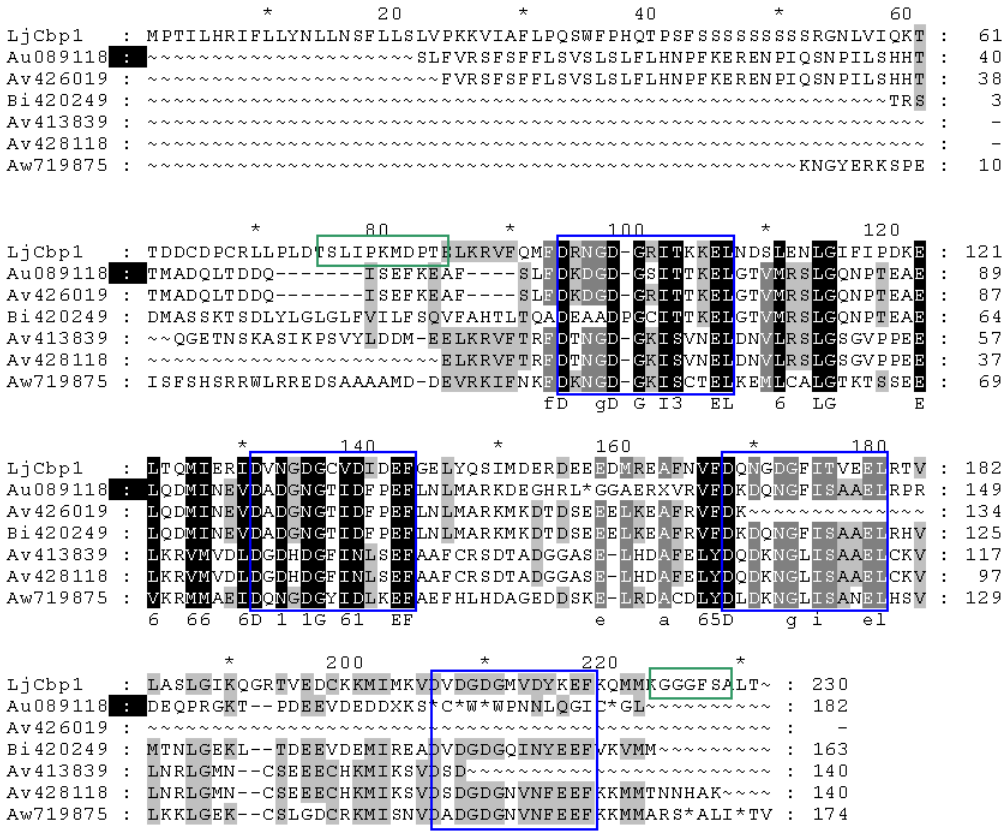

Figure 3.2. Multiple sequence alignment of the peptide encoded by *LjCbp1* and sequences in other species. *Lotus japonicus* (Aj251808); *Populus tremuloides* (ca928020); *Malus domesticus* (co898441); *Glycine max* (bg047423) and (bg790636); *Citrus* (ck932634); *Medicago truncatula* (bf634668); *Arabidopsis thaliana* (q9srr7); *Brassica oleracea* (bz053525); *A. thaliana* (q9lne7); *A. thaliana* (af332466); *G. max*

(bq740933); *Musa acuminate* (ay484589); *Solanum tuberosum* (cv497072); *A. thaliana* (o22845); *Gossypium arboretum* (bg440355); *G. max* (bm732150); *A. thaliana* (q9fyk2); *Loligo pealeii* (p14533); *Bos taurus* (mcbo); *Homo sapiens* (aah47523); *Castanea sativa* (af334833). Blue boxes depict regions of EF-Hands.

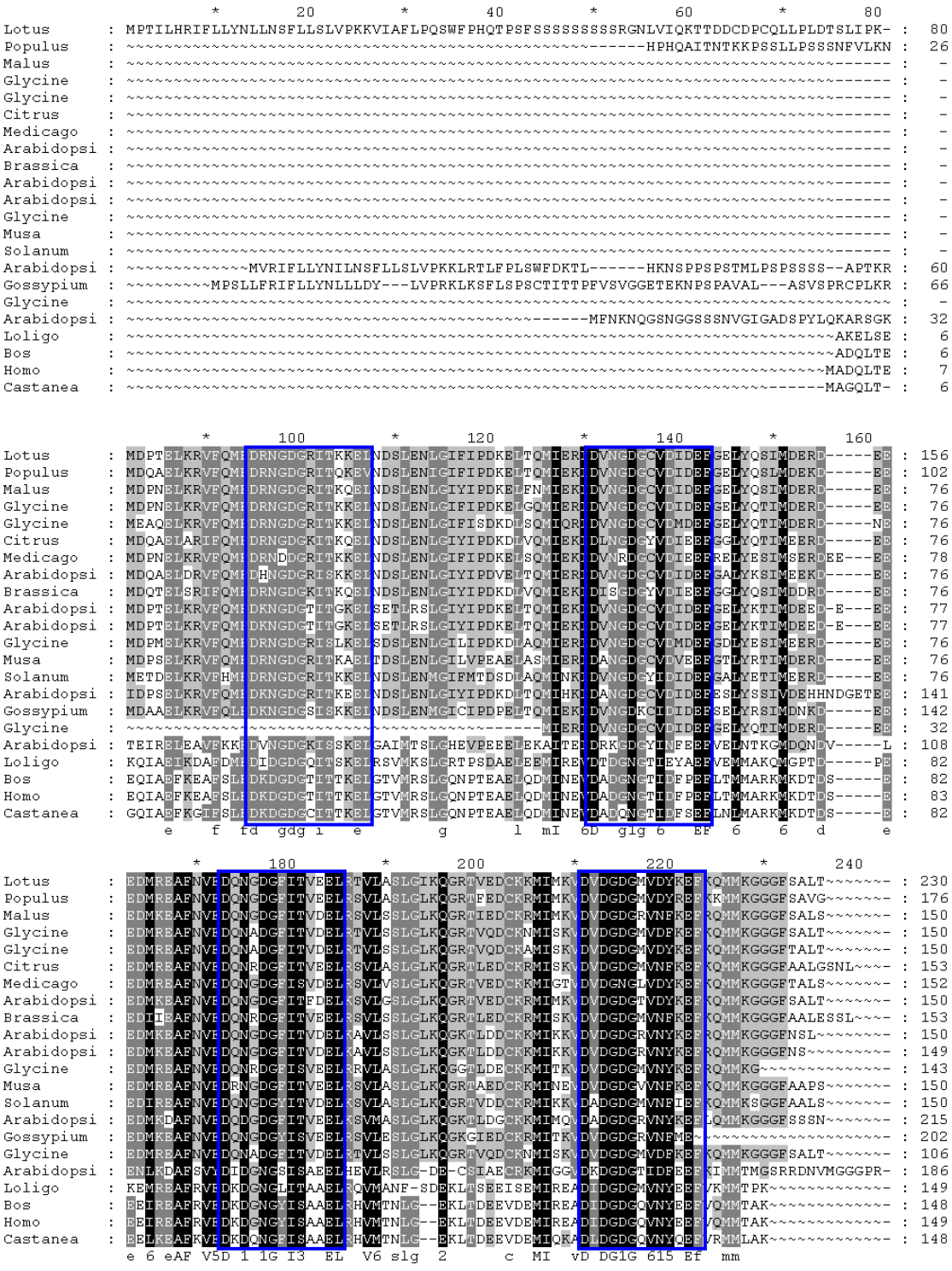

Figure 3.3. Phylogenetic tree of *LjCbp1*-like sequences based on peptide alignment from Figure 3.2.

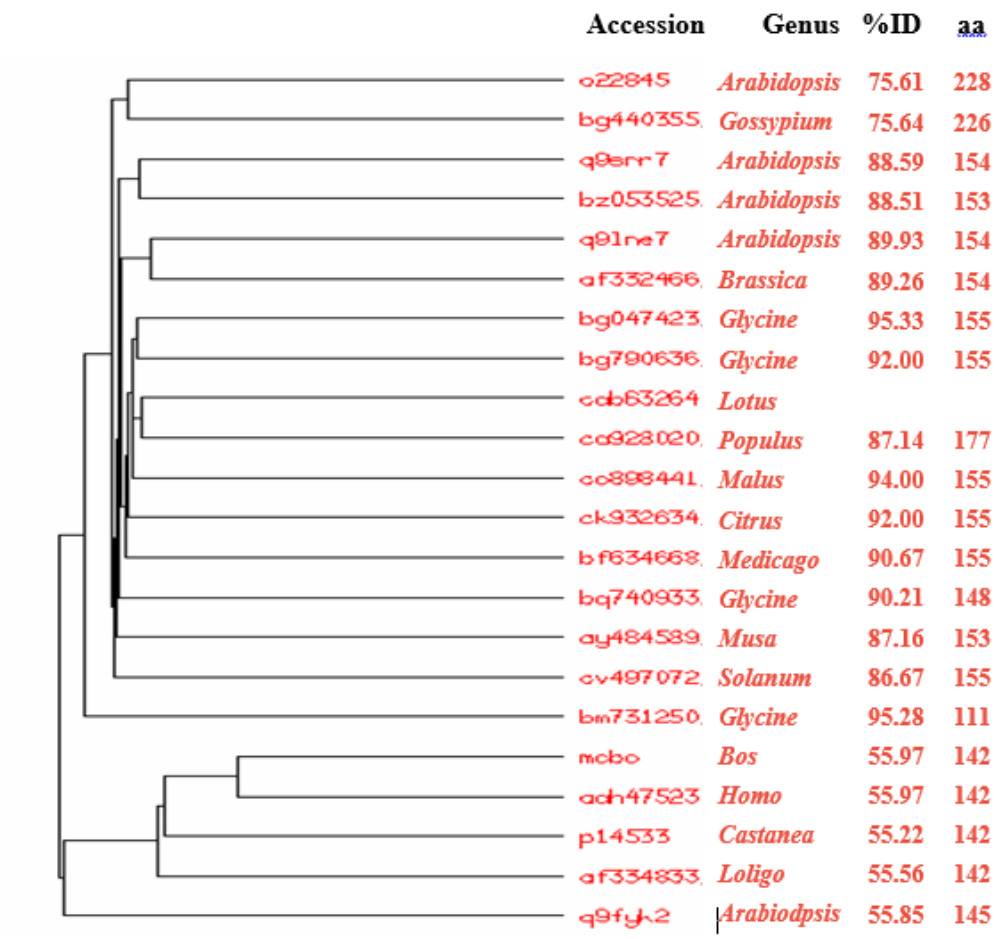

comparisons (Section 2.11) are shown for all of the peptide sequences against the LjCbp1 putative protein. Figure 3.3 shows the percentage identity and the number of amino acids over which this comparison was made.

Figure 3.4 shows an alignment of nucleotide sequences sharing some identity with the unusual serine repeat motif found towards the 5' end of *LjCbp1*. These sequences are from mouse and human clones. These predicted proteins have had no function assigned to them as yet but provide an indication that this repeat motif may not be unique.

Figure 3.4. Alignment of amino acid sequences bearing identity to short region of serine repeats in *LjCbp1*. Aj251808=*LjCbp1,* ac079043 and al806520=complete sequences from *Mus musculus* clones, ac023150, ac022903 and al683870= complete sequences from *Homo sapiens* clones.

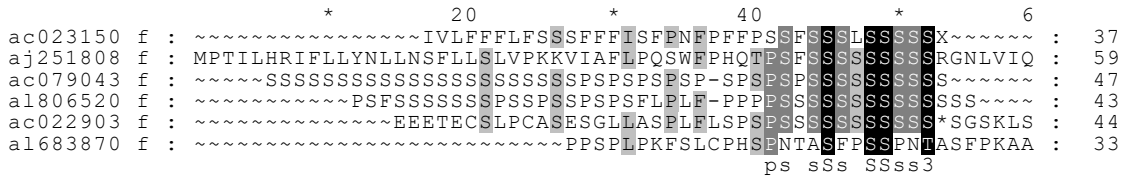

3.2.2 Calcium binding assay

In order to provide a complete account of the Ca^{2+} binding assay, a brief description of unpublished work carried out by Dr. Leif Skøt, at IGER, prior to the onset of this PhD project is given below.

A partial cDNA of LjCbp1, starting 76 amino acids into the peptide sequence, but containing the 4 EF-hand motifs, was cloned into pGEM®T-easy (Promega, Southampton, U.K.). The LjCbp1 cDNA was excised from pGEM®T-easy as a *Not*1 fragment and ligated into the *Not*1 site of the epitope tag vector pHB6, which harbours resistance to ampicillin (Roche Diagnostics Ltd, Lewes, U.K.). The coding sequence of the LjCbp1 gene is thus in frame with an N-terminal 9 amino acid hemagglutanin sequence, providing the epitope tag. The fusion was then sequenced in order to confirm the position of the tag at the N-terminus of the LjCbp1 sequence and the size of the protein product (27.4 KDa) (Skøt, unpublished data). Part of the sequence is shown in Figure 3.5.

Figure 3.5. Partial sequence of epitope-tag plasmid containing *LjCbp1* fragment. Red letters = LjCbp1 polypeptide; green letters = vector sequence; bold letters = epitope tag sequence of the vector; blue letters = *Not*1 site into which the *Cbp1* fragment was cloned.

```
CCGATTCATTAATGCAGCTGGCACGACAGGTTTCCCGACTGGAAAGCGGGCAGTGAGCGC
AACGCAATTAATGTAAGTTAGCGCGAATTGATCTGGTTTGACAGCTTATCATCGACTGCA
CGGTGCACCAATGCTTCTGGCGTCAGGCAGCCATCGGAAGCTGTGGTATGGCTGTGCAGG
TCGTAAATCACTGCATAATTCGTGTCGCTCAAGGCGCACTCCCGTTCTGGATAATGTTTT
TTGCGCCGACATCATAACGGTTCTGGCAAATATTCTGAAATGAGCTGTTGACAATTAATC
ATCCGGCTCGTATAATGTGTGGAATTGTGAGCGGATAACAATTTCACACAGGAAACAGCG
CCGCTGAGAAAAAGCGAAGCGGCACTGCTCTTTAACAATTTATCAGACAATCTGTGTGGG
CACTCGACCGGAATTATCGATTAACTTTATTATTAAAAATTAAAGAGGTATATATTAATG
TATCGATTAAATAAGGAGGAATAAACCATGGGTTACCCATACGACGTCCCAGACTACGCT
                          M  G  Y  P  Y  D  V  P  D  Y  A
GGAAGCTTGGGTACCTCCGCGGAGAATTCGCGGCCGCGGGAATTCGATTCGTCCCTAATA
G  S  L  G  T  S  A  E  N  S  R  P  R  E  F  D  S  S  L  I
CCAAAAATGGACCCCACCGAGCTCAAGCGTGTTTTCCAAATGTTTGATAGAAACGGGGAT
P  K  M  D  P  T  E  L  K  R  V  F  Q  M  F  D  R  N  G  D
GGCCGGATCACG
G  R  I  T
```

A control vector, pHB*lacZ6*, was supplied with the pHB6™ kit. The 3.2 Kb pHB6*lacZ* sequence contains the β-glycosidase gene cloned in frame with the N-terminal tag. This means that expression of the β-glycosidase gene can be observed in protein extracts alongside extracts from the cells transformed with the protein of interest. The

pHB6*lacZ* vector was used in a time-course assay to determine the optimal time for maximum expression of the *LjCbp1* gene in *E. coli.*

Coomassie-staining of the gel containing proteins extracted from *E. coli* cells containing the epitope tagged *LjCbp1* gene revealed that expression of a protein of around 24 KDa could be determined against the pHB6lacZ control at an early stage (i.e. within 2 hours; Figure 3.6 lane 6). The quantity of protein produced four hours after addition of the inducer IPTG was sufficient to indicate that LjCbp1 was strongly expressed at this stage (Figure 3.6 lane 10). This time-point was therefore chosen for subsequent experiments.

The Coomassie-stained gel of the protein extracts lysed in different buffers revealed distinct mobilities. Proteins lysed in the buffer containing 10mM $MgCl_2$ + 2mM EGTA or 10mM EGTA were visible at the 24 KDa molecular marker (Figure 3.7 lanes 4 and 5, arrow), as those from the time-course optimisation experiment (Figure 3.6). However, proteins lysed in buffers containing an excess of Ca^{2+} demonstrated the apparent mobility of a protein of around 21.5 KDa (Figure 3.7 lanes 1, 2, 3 and 6, arrowhead). The results indicate that, although proteins prepared in lysis buffer only did not contain added Ca^{2+}, traces of Ca^{2+} may have been present in the medium.

Antibody binding to a duplicate of the above SDS-PAGE gel revealed stained bands corresponding to those anticipated for the tagged protein (predicted to be around 20 KDa) (Figure 3.8). A high level of background staining was present in this blot. Such non-specific staining may be due to the use of a low affinity tag.

The SDS-PAGE and western blot were repeated three times and produced the same results. The antibody binding was not reproduced due to various technical difficulties. The SDS-PAGE and western blot were also carried out in a 'native' state, where SDS was omitted from all reagents. No difference was discerned in mobility between this and the denaturing gel (data not shown).

Figure 3.6. Coomassie-stained SDS-PAGE showing time-course of expression of LjCbp1 and pHBlacZ6 control expressed in *E. coli*. Lanes 1, 3, 5, 7, 9, 11, 13, pHBlacZ6 control 0, 1, 2, 3, 4, 5, 6 hours after addition of IPTG inducer; lanes 2, 4, 6, 8, 10, 12, 14; LjCbp1 0, 1, 2, 3, 4, 5, 6 h after addition of IPTG. Arrow indicates band, appearing after approximately 2 hours.

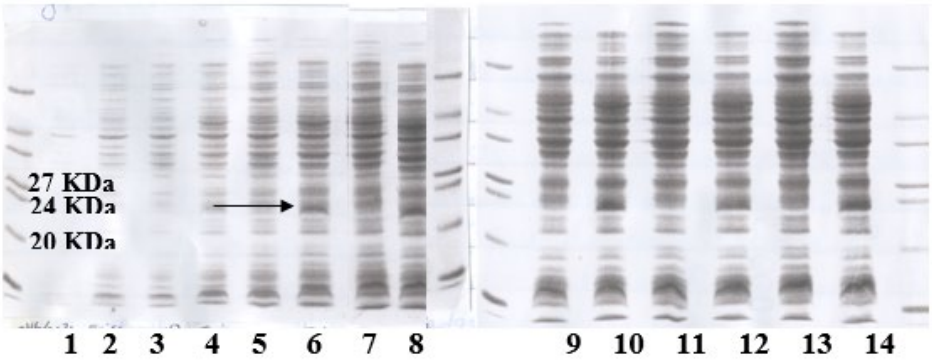

Figure 3.7. Coomassie-stained SDS-PAGE of protein extracts from *E. coli* cells expressing epitope-tagged LjCbp1 lysed in Ca^{2+} and non-Ca^{2+} containing buffers. Arrow indicates protein in non-Ca^{2+} bound conformation, arrowhead is Ca^{2+}-bound form with apparent molecular weight indicated in blue. Lane 1, control (no IPTG inducer) lysed in 10mM $CaCl_2$; lane 2, lysis buffer only; lane 3, 10mM $CaCl_2$ + 2mM EGTA; lane 4, 10mM $MgCl_2$ + 2mM EGTA; lane 5, 10mM EGTA; lane 6, 10mM $CaCl_2$.

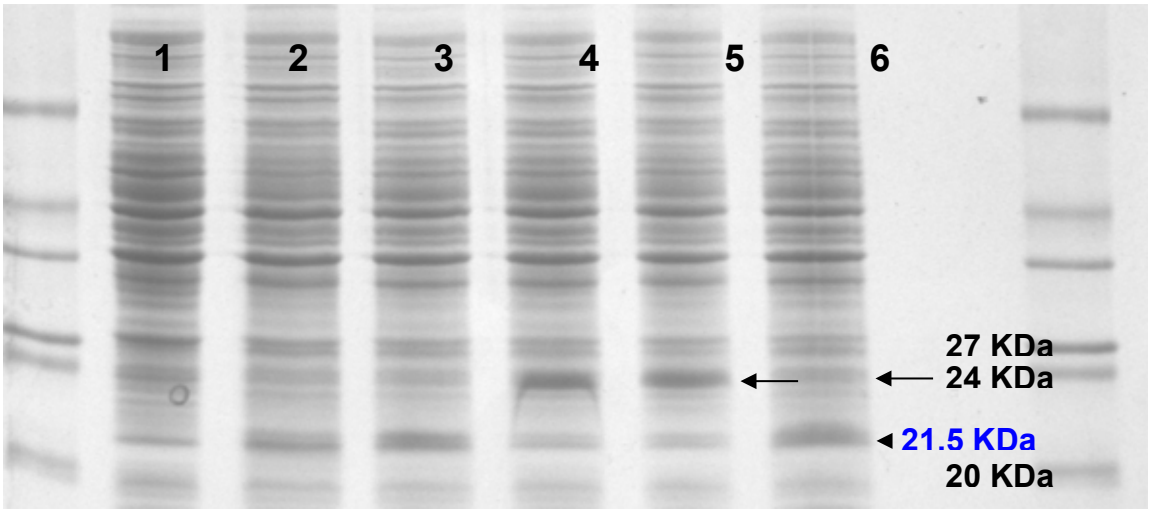

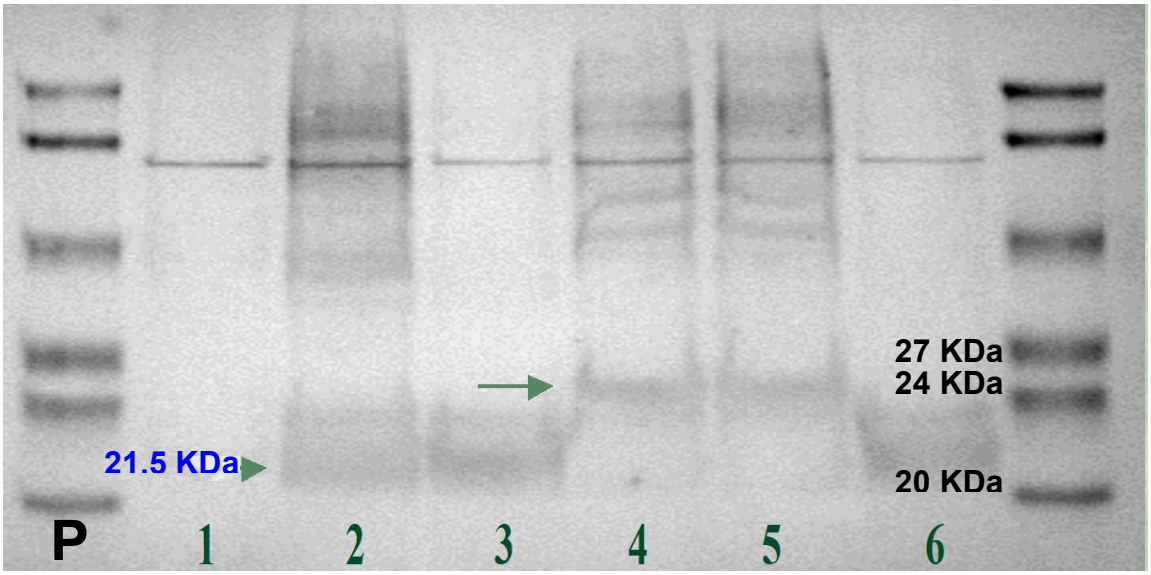

Figure 3.8. Western blot of protein extracts from *E. coli* cells expressing epitope-tagged LjCbp1 lysed in Ca^{2+} and non- Ca^{2+} containing buffers. Arrow indicates protein in non-Ca^{2+} bound conformation, arrowhead is Ca^{2+}-bound form with apparent molecular weight indicated in blue. P=pre-stained molecular marker; lane 1, control (no IPTG inducer) lysed in 10mM $CaCl_2$; lane 2, lysis buffer only; lane 3, 10mM $CaCl_2$ + 2mM EGTA; lane 4, 10mM $MgCl_2$ + 2mM EGTA; lane 5, 10mM EGTA; lane 6, 10mM $CaCl_2$.

3.2.3 *In silico* investigation of transcriptional regulatory elements

The sequence of the TAC containing the *LjCbp1* locus (TAC LjT15I02) was obtained from Dr Shusei Sato at the Kazusa Institute, Japan, and analysed for the presence of any other genes that could be potentially reported by the *gus* gene. Analysis of the TAC sequence revealed that the *LjCbp1* locus was the only likely gene candidate for which *gus* could be reporting transcriptional gene regulation (data not shown). It also revealed the presence of a retrotransposon of about 10 Kb, of the Ty3/gypsy type (Langdon *et al*., 2000). The long terminal repeat sequences (LTRs) that border the retrotransposon show little variation from each other indicating that this insertion may be quite recent (data not shown).

The region was also analysed by Dr Tim Langdon, University of Wales, Aberystwyth, for the presence of any further retroelements. The retrotransposon 5' LTR is 137 bp downstream of the *LjCbp1* stop codon but still within the message transcript. Further repeats exist within the retrotransposon LTRs which may represent further insertions. Retrotransposons can become carriers of other mobile elements (Tim Langdon, personal communication).

The 2.7 Kb sequence upstream of the translation start site of *LjCbp1* was submitted to the websites detailed in Section 2.11. Several matches of greater than 70% identity were recognised in newly generated TAC libraries from *L. japonicus*. The greatest identity was a region of around 180 bases approximately 1 Kb upstream of the T-DNA insertion site. A multiple alignment of this region with matches from several *L. japonicus* TAC sequences is shown in Figure 3.9. No other strong identities for this region were identified outside of *L. japonicus*.

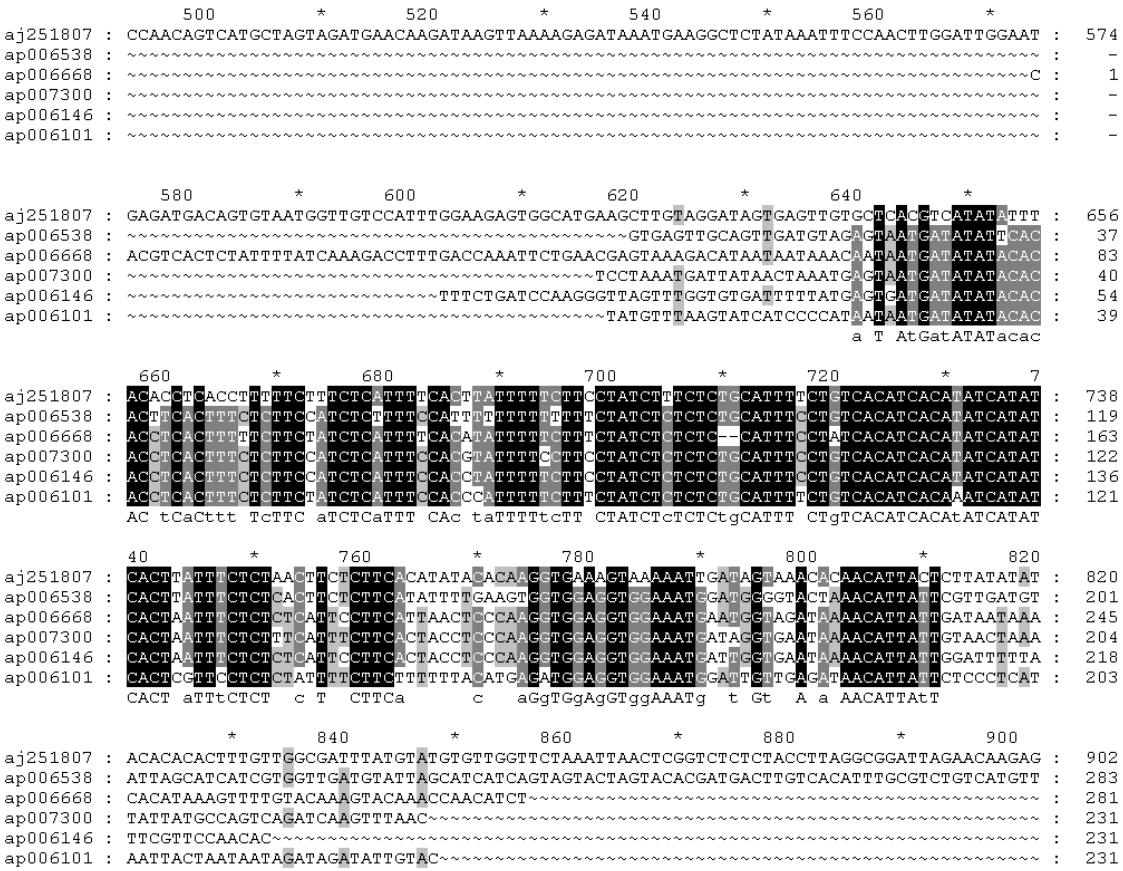

Figure 3.9. Alignment of six nucleotide sequences from *L. japonicus*. Matches are against Aj251807 in the region upstream of the T-DNA insertion in T90.

Sequences of approximately 4 Kb upstream of these regions that showed similarity to the promoter of *LjCbp1* were submitted to the NCBI ORF finder (Section 2.11). However, no ORFs were identified that were candidates for regulation by this region.

In addition to the database searches, promoter sequences from various published ENOD genes were analysed against the same upstream region of *LjCbp1*. In total, seven sequences were compared to *LjCbp1* to identify common sequences which could indicate regulatory regions. One sequence, a 200 bp region of the *PsENOD12* promoter was aligned to *LjCbp1* using the best fit options in the pairwise comparison tool of GCG (Section 2.11). The 2.7 Kb sequence upstream of the *LjCbp1* coding sequence is shown in Figure 3.10; the coding sequence is also included to facilitate orientation. Highlighted sequences, representing a proportion of those identified as putative *cis*-acting elements, are shown. Some of the putative elements were common to the regions both up and downstream of the T-DNA insertion, whilst others were found in one or other of the two regions. In addition to the regions highlighted in Figure 3.10, several motifs were identified that were common to other *ENOD* promoters. However, none of these were motifs that have so far shown symbiosis-specific regulation.

Analysis of promoter regions of various *ENOD* genes highlighted sequences that were common to all, including the *LjCbp1* locus, but these sequences did not contain characterised symbiosis-specific motifs. A pair-wise comparison of the upstream sequence of *LjCbp1* and a 200 bp region of the *PsENOD12* promoter, found to be sufficient for symbiosis specific expression in transgenic plants harbouring this promoter fused to GUS (Vijn *et al*., 1995), shared 63 % identity over a 135 bp region (Figure 3.11). However, it should be borne in mind that the predominant matches are A's and T's, which are naturally rich in promoter sequences. Furthermore, a 500 bp region of *L. japonicus*, containing this sequence, did not confer symbiosis-specific expression when fused to GUS in transgenic plants (Leif Skøt, unpublished data).

Finally, the peptide sequence was analysed for potential hydrophobic domains that could identify putative membrane spanning regions and signal peptides. The

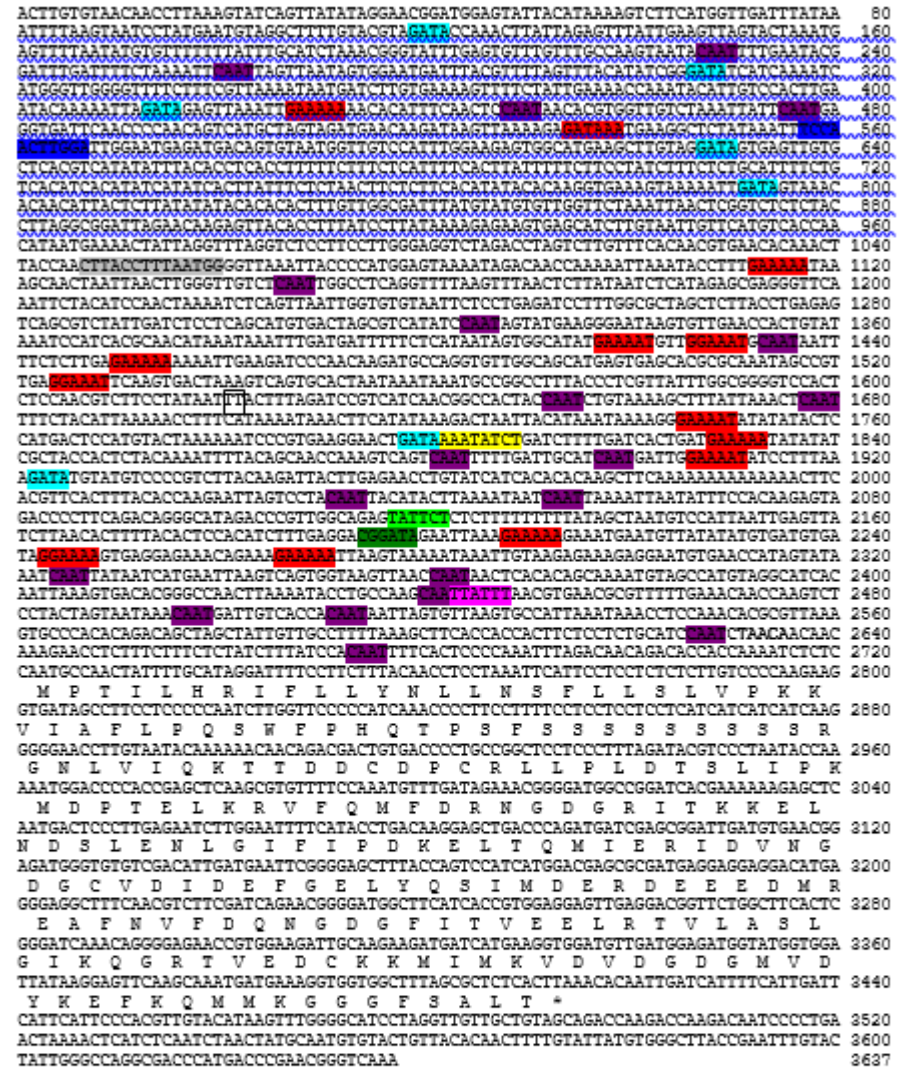

Nucleotide and predicted 230 amino acid polypeptide sequence of *LjCbp1* locus. Black box indicates site of T-DNA insertion in T90 line. Bold letters indicate transcription start site reflected by 5' RACE (Chapter 4). "Evening element" required for circadian control of gene expression. "-10 promoter element" involved in the expression of a plastid gene which encodes a photosystem II reaction centre chlorophyll-binding protein that is activated by blue, white or UV-A light. "CArG2" found in *Arabidopsis*, mediates discrete regulatory effects during floral development. Sequence required for tissue-specific promoter activation of pea legumin gene. Required for phytochrome regulation. "GATA box" required for high level, light regulated and tissue specific expression. Consensus GT-1 binding site in many light-regulated genes. Transcriptional activator regulating cell elongation by controlling gibberellin levels. "TATA box" found in the 5' upstream region of pea (*Pisum sativum*) glutamine synthetase gene. The transcription start site is 1013 bp downstream from the T-DNA insertion.

Figure 3.10. Putative *cis*-acting regulatory elements in the *LjCbp1* locus.

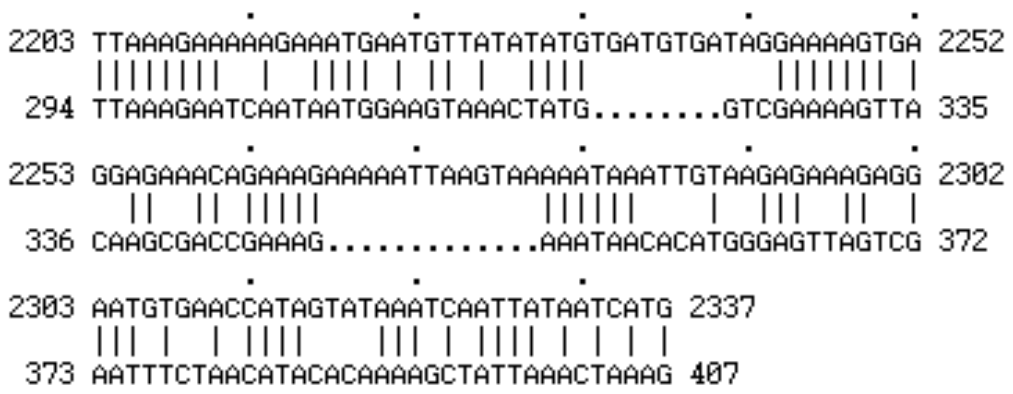

Figure 3.11. Pair-wise alignment of upstream sequence of *LjCbp1* and symbiosis-specific region in *PsENOD12* promoter. The uppermost sequence is *LjCbp1*.

SignalP World Wide Web server predicts the presence and location of signal peptide cleavage sites in amino acid sequences from different organisms. The method incorporates a prediction of cleavage sites and a signal peptide/non-signal peptide prediction based on a combination of several artificial neural networks. The output from the neural network model trained on eukaryotes is shown in Figure 3.12 and indicates that a putative signal peptide is present at the N-terminus of LjCbp1. The cleavage point predicted by both the neural network and hidden Markov model (data not shown) is between the amino acids alanine and phenylalanine at positions 29 and 30 of the sequence. The length of signal peptide is in general agreement with the average for eukaryotic signal peptides of 22.6 amino acids (Nielsen *et al*., 1997). The "DAS" prediction server of the Stockholm Bioinformatics Centre identified a putative hydrophobic domain of 13 amino acids near the N-terminus of LjCbp1 within the predicted 29 amino acid signal peptide (data not shown).

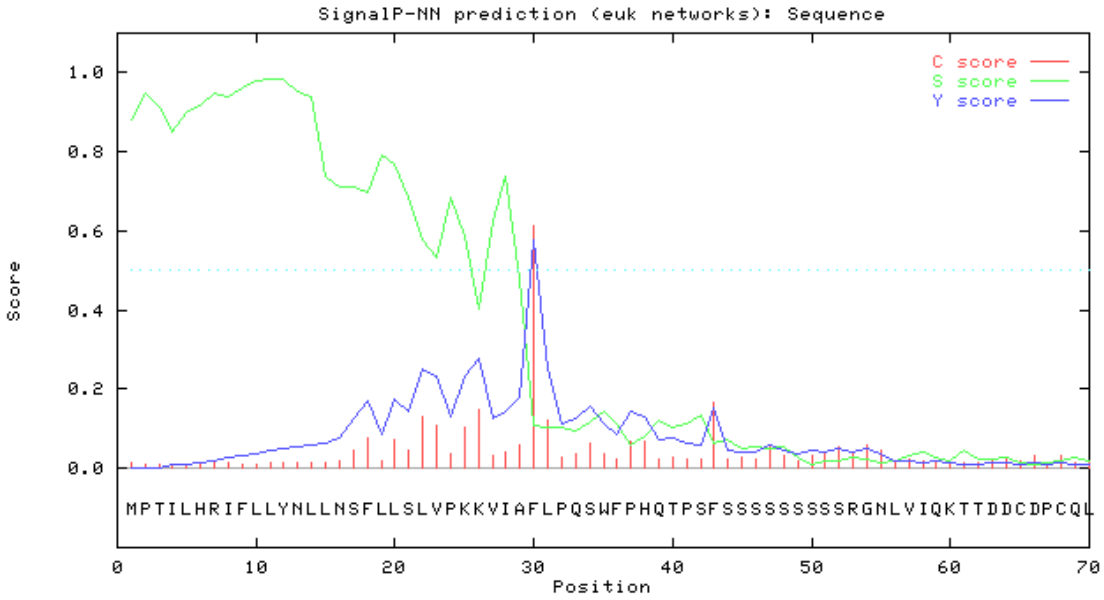

Figure 3.12. SignalP neural network model prediction of signal peptide and cleavage site in LjCbp1. C score (raw cleavage site score) = output score from networks trained to recognize cleavage sites *vs*. other sequence positions. Trained to be: high at position +1 (immediately after cleavage site) and low at all other positions. S-score (signal peptide score) = output score from networks trained to recognize signal peptide vs. non-signal-peptide positions. Trained to be: high at all positions before the cleavage site and low at 30 positions after the cleavage site and in the N-terminus of non-secretory proteins. Y-score (combined cleavage site score) = The prediction of cleavage site location is optimized by observing where the C-score is high and the S-score changes from a high to a low value. The Y-score formalizes this by combining the height of the C-score with the slope of the S-score. All three scores are averages of five networks trained on different partitions of the data (Nielsen *et al*., 1997).

3.2.4 Determination of the transcription start site and complete mRNA sequence of *LjCbp1*

Total RNA from wild-type seedlings 5 dpi was obtained using the protocols described in sections 2.4.5b and 2.5.3 Method 1. Determination of the 5' and 3' ends of the *LjCbp1* gene was achieved using the RACE protocol described in Section 2.8.8.

The consensus from the experiments here and those of Dr Leif Skøt (IGER) were used to produce the complete messenger RNA sequence of *LjCbp*. This sequence was submitted to Genembl under accession number Aj251808 and is presented in Figure 3.13. RACE products from both experiments were used to identify the transcriptional start site approximately 95 bases upstream from the translation start site.

```
GAAAAACAACAACAAAGAACCTCTTTCTTTCTCTATCTTTATCCACAATTTTCACTCCCC
AAATTTAGATAACAGACACCACCAAAATCTCTCCAATGCCAACTATTTTGCATAGGATTT
                                    M  P  T  I  L  H  R  I  F
TCCTTCTTTACAACCTCCTAAATTCATTCCTCCTCTCTCTTGTCCCCAAGAAGGTGATAG
  L  L  Y  N  L  L  N  S  F  L  L  S  L  V  P  K  K  V  I  A
CCTTCCTCCCCCAATCTTGGTTCCCCCATCAAACCCCCTCCTTTTCCTCCTCCTCCTCAT
  F  L  P  Q  S  W  F  P  H  Q  T  P  S  F  S  S  S  S  S  S
CATCATCATCAAGGGGGAACCTTGTAATACAAAAAACAACAGACGACTGTGACCCCTGCC
  S  S  S  R  G  N  L  V  I  Q  K  T  T  D  D  C  D  P  C  Q
AGCTCCTCCCTTTAGATACGTCCCTAATACCAAAAATGGACCCCACCGAGCTCAAGCGTG
  L  L  P  L  D  T  S  L  I  P  K  M  D  P  T  E  L  K  R  V
TTTTCCAAATGTTTGATAGAAACGGGGATGGCCGGATCACGAAAAAAGAGCTCAATGACT
  F  Q  M  F  D  R  N  G  D  G  R  I  T  K  K  E  L  N  D  S
CCCTTGAGAATCTTGGAATTTTCATACCTGACAAGGAGCTGACCCAGATGATCGAGCGGA
  L  E  N  L  G  I  F  I  P  D  K  E  L  T  Q  M  I  E  R  I
TTGATGTGAACGGAGATGGGTGTGTCGACATTGATGAATTCGGGGAGCTTTACCAGTCCA
  D  V  N  G  D  G  C  V  D  I  D  E  F  G  E  L  Y  Q  S  I
TCATGGACGAGCGTGATGAGGAGGAGGACATGAGGGAGGCTTTCAACGTCTTCGATCAGA
  M  D  E  R  D  E  E  E  D  M  R  E  A  F  N  V  F  D  Q  N
ACGGGGATGGCTTCATCACCGTGGAGGAGTTGAGGACGGTTCTGGCTTCACTCGGGATCA
  G  D  G  F  I  T  V  E  E  L  R  T  V  L  A  S  L  G  I  K
AACAGGGGAGAACCGTGGAAGATTGCAAGAAGATGATCATGAAGGTGGATGTTGATGGAG
  Q  G  R  T  V  E  D  C  K  K  M  I  M  K  V  D  V  D  G  D
ATGGTATGGTGGATTATAAGGAGTTCAAGCAAATGATGAAAGGTGGTGGCTTTAGCGCTC
  G  M  V  D  Y  K  E  F  K  Q  M  M  K  G  G  G  F  S  A  L
TCACTTAAACACAATTGATCATTTTCATTGATTCATTCATTCCCACGTTGTACATAAGTT
  T
TGGGGCATCCTAGGTTGTTGCTGTAGCAGACCAAGACCAAGACAATCCCCTGAACTAAAA
CTCATCTCAATCTAACTATGCAATGTGTACTGTTAAAAAAAAAAAAAAAAAA
```

Figure 3.13. Consensus of complete mRNA sequence of *LjCbp1* submitted to Genembl under accession number Aj251808.

3.2.5 Characterisation of *gus* and *LjCbp1* expression using RT-PCR, single strand cDNA synthesis and northern blot analysis

The following experiments set out to determine the degree of correlation between the expression of the *gus* and *LjCbp1* genes and start with an investigation into the levels of *gus* transcripts pre- and post-inoculation.

3.2.5.1 Expression of *gus* 0-4 hpi using RT-PCR

Since GUS activity seemed to be entirely absent in uninoculated tissue (Webb *et al*., 2000) it was hypothesised that the *gus* gene product may be synthesised *de novo* in T90 root epidermal and cortical tissue within hours of inoculation with *M. loti*. RT-PCR analysis was initially chosen in a preliminary experiment to determine levels of expression at 4 hpi with *M. loti*.

Seeds were sown and grown as in Section 2.4.5a under the CER conditions described in Section 2.5.4. Fourteen days after sowing, 16 seedlings were harvested (Section 2.8) from the uninoculated Phytatray™ as a control. The remaining seedlings were inoculated with *M. loti* strain NZP2235 (Section 2.5.1 Method 1) and harvested (Section 2.8) 4 hpi. Total plant RNA was extracted and DNase-treated as in Section 2.8.4 and 2.8.4.1, respectively. DNA was quantified according to Section 2.8.3.

RT-PCR was carried out according to the procedure outlined in Section 2.8.4.4. Starting concentrations of RNA were around 30pg and 80pg for 0 hpi and 4 hpi, respectively. Dilutions of 10x and 100x of both samples were included in the procedure in order to optimise concentrations for gene amplification. Control DNA samples were also included in the experiment, one positive for the *gus* transgene, the other negative. These samples were obtained using the DNA extraction procedure in Section 2.8.3.

Although the absence of any observable GUS expression in uninoculated T90 seedlings (Webb *et al*., 2000) indicated that the activity of the GUS enzyme post inoculation was the result of *de novo* synthesis, RT-PCR analysis of the *gus* gene indicated that transcription was present at a basal level in uninoculated tissue (Figure 3.14).

Electrophoresis gels showed the presence of a single band that corresponded to the expected size of the *gus* fragment. The band was present in the undiluted material of both inoculated and uninoculated roots. It was also in the positive control DNA sample and the 10x dilution of the inoculated root (Figure 3.14). This experiment was not repeated, but a later time-course was chosen in an effort to identify greater transcript abundance. The presence of genomic DNA contamination could not be entirely ruled out because, although samples were treated with DNase, a minus RT control was not included. Further experiments therefore included such controls. Furthermore, the presence of rhizobial contamination in uninoculated plants was also possible as seedlings were not grown long enough to inspect for the presence of nodules. Problems had also been encountered sterilising vermiculite. This may have permitted the survival of contaminating rhizobia. Later experiments therefore included checks for the presence of contaminating rhizobia.

3.2.5.2 Expression of *gus* 0 and 5 dpi using single strand cDNA synthesis

RT-PCR analysis to confirm the expression profile of the *gus* gene was hampered by the technical difficulties described at the end of Section 3.2.5.1. In addition, it was also difficult to extract sufficient, good quality RNA to permit not only the optimisation of RT-PCR conditions but also the repetition of analysis. A different approach was therefore chosen: the creation of single strand cDNA, using a RT enzyme, followed by PCR. This permitted the generation of larger quantities of template that reflects the mRNA population of the samples of interest.

Fluctuations in the transcript level of the *gus* gene may be more evident over longer time periods post inoculation. Since the time-point at 4 hpi did not appear to show any upregulation of *gus,* a later time point was chosen which could allow a greater build up of the transcript. This section refers to the use of single strand cDNA and subsequent PCR from T90 material at 5 dpi.

T90 samples were obtained from homozygous plant material grown according to Section 2.4.5a. The possibility of rhizobial contamination was excluded following checks carried out according to Section 2.5.1. Seedlings were inoculated as described in Section 2.5.1 Method 2 and root tissue was harvested as detailed above. Total plant RNA was extracted from 100mg fresh weight from both inoculated and uninoculated root tissue according to the method in Section 2.6. To remove the potential of polysaccharide contamination ¼ volume isopropyl alcohol was used and supplemented with 250µl 0.8M sodium citrate and 1.2M NaCl. The RNA was dissolved in 40µl DEPC-H_2O and placed in a 55ºC water bath for 10 minutes to relax any secondary structure. RNA was DNase-treated and converted into cDNA using the procedures in 2.8.4.1 and 2.8.4.3, respectively.

PCR reactions were set up according to the standard procedure outlined in Section 2.8.5 but using 50µl final volume. Reactions to amplify the actin gene were also included as an internal standard. Forward and reverse primer details for the *gus* and actin gene were as in Table 2.2. The thermocycler temperature profile was according to Table 2.3.

To provide semi-quantitative PCR, 10µl was removed from the actin samples after 32 cycles.

A band corresponding to the *gus* gene at 0 hpi confirmed the presence of GUS activity in uninoculated tissue (Figure 3.15 B). However, loading of cDNA was uneven. The intensity of the band corresponding to the actin gene was diminished at 5 dpi in comparison to that at 0 hpi and was just visible in the shoot sample (Figure 3.15 A). It is difficult to tell, therefore, whether there is an increased abundance of the *gus* transcript at 5 dpi. No contamination was detected in the master mix but it was possible that either the shoot material or the well on the gel had become contaminated in some way with cDNA from root tissue. Further efforts to clarify *gus* regulation were subsequently conducted in parallel with investigations into the transcript abundance of *LjCbp1* in order to correlate the expression of the two genes.

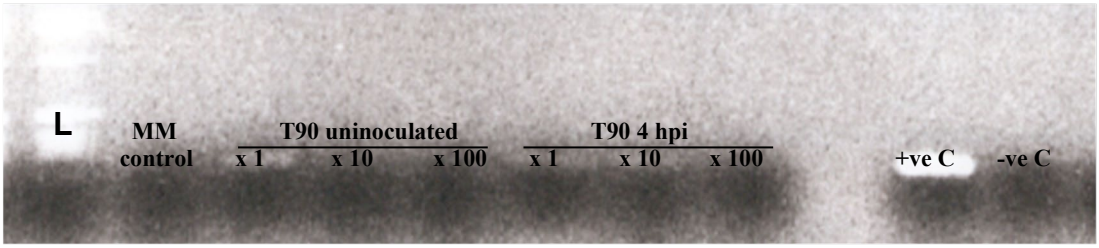

Figure 3.14. Agarose gel RT-PCR products of *gus* in *L. japonicus* T90 line, 0 and 4 hpi. L, 1 Kb ladder, MM, Master mix control; +ve C, DNA positive control; -ve C, wild-type negative control DNA. Arrows indicate bands corresponding to expected fragment for *gus* gene, 270 bp.

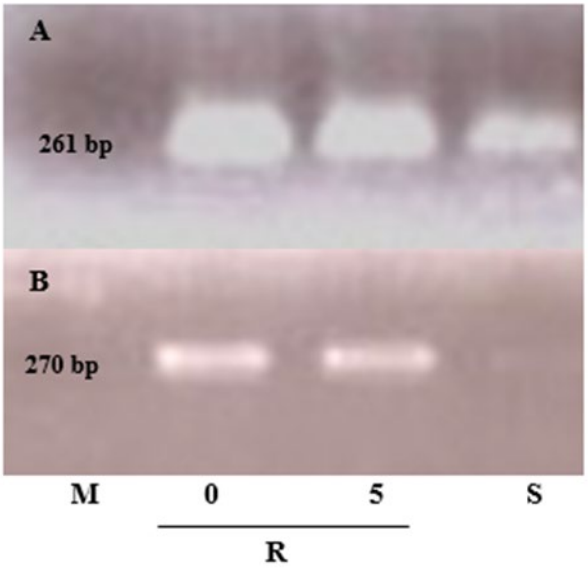

Figure 3.15. Electrophoresis gel showing actin and *gus* gene expression in T90. A, actin; B, *gus*; M, master mix; R, root, S, shoot; 0, uninoculated; 5 & S, 5 dpi root and shoot, respectively.

3.2.5.3 Correlation of *gus* and *LjCbp1* expression 0 and 16 hpi using single strand cDNA synthesis

In order to investigate any correlation in the expression of *gus* and *LjCbp1* an experiment was set up in wild-type and T90 material to determine the levels of expression of both genes before and after inoculation.

Wild-type and T90 homozygous plant material was generated according to Section 2.4.5a. In order to verify that rhizobial contamination was not present in any material, samples of liquid from each Phytatray II™ were taken prior to inoculation and transferred to individual TY plates and incubated for 5 days. Plant root tissue was harvested 16 hpi. At the point of harvesting, approximately 10 seedlings from T90 inoculated and uninoculated samples were placed immediately in X-gluc in accordance with Section 2.6 to confirm the presence or absence of GUS expression at the time of *LjCbp1* analysis.

Total plant RNA was extracted in accordance with Section 2.8.4 with the following modifications: sample sizes were smaller, therefore half the volume of TRIzol™ and chloroform was used and ¼ volume isopropyl alcohol was used and supplemented with 250µl 0.8M sodium citrate, 1.2M NaCl to remove unwanted polysaccharides. The RNA was dissolved in 40µl DEPC-H_2O and placed in a 55^oC water bath for 10 minutes to relax any secondary structure. Samples were DNase treated and cDNA was synthesised using the procedures in Section 2.8.4.1 to 2.8.4.3. After 32 PCR cycles, a 10µl aliquot of each actin sample was taken to compare with that of 35 cycles in order to determine whether saturation had been reached during amplification to 35 cycles.

PCR reactions were set up according to the standard procedure outlined in Section 2.8.5 and Table 2.3. Primer details for the actin and *LjCbp1* genes are detailed in Section 2.8 and Table 2.2.

In both wild-type and T90 material, further evidence of the expression of both genes in uninoculated tissue was observed (Figures 3.16 B and C), suggesting that

basal levels of transcript are present. In T90 material a band corresponding to the expected *gus* fragment was of greater intensity at 16 hpi than that at 0 hpi (Figure 3.16 B lanes 3 and 2, respectively), implying upregulation of this gene post inoculation. No corresponding increase in intensity was seen in *LjCbp1* expression in T90 material (Figure 3.16 C lanes 3 and 4). However, an increase in *LjCbp1* expression was seen at 16 hpi in wild-type material (Figure 3.16 C). This is in agreement with Webb *et al*. (2000) where a lower level of expression of *LjCbp1* was observed in T90 roots compared to wild-type. Experimental data also indicates the presence of both transcripts in very low levels in shoot material (Figure 3.16 C). The low intensities of these bands perhaps explains why expression was not previously observed (Webb *et al*., 2000).

The increased abundance of the transcript of the *gus* gene in T90 material (Figure 3.16 B) and *LjCbp1* in wild-type material (Figure 3.16 C) at 16 hpi indicates that the expression of the two genes is correlated and that the observed upregulation of *gus* results in the GUS activity observed by Webb *et al*. (2000) in inoculated material. The data also suggest that T-DNA insertion in T90 has interfered with expression of *LjCbp1* in this line.

GUS activity was strong and evenly distributed in inoculated, but absent in uninoculated T90 roots following histochemical staining (data not shown). Absence of contaminating DNA in cDNA samples was confirmed with the gDNA control (Figure 3.16 A). The use of the actin gene as an internal control in these experiments permitted the detection of any gDNA contamination through the design of primers spanning an 87 bp intron of this gene. In Figure 3.16 A the 348 bp actin fragment of the gDNA sample (C) can clearly be seen in comparison to the smaller, intron-less fragment of the cDNA samples. The fragments amplified from the *gus* gene therefore represent only cDNA reverse transcribed from the original mRNA.

Slight variations in the intensities of bands corresponding to the actin gene indicate that, even after 35 cycles, saturation had not been reached (Figure 3.16

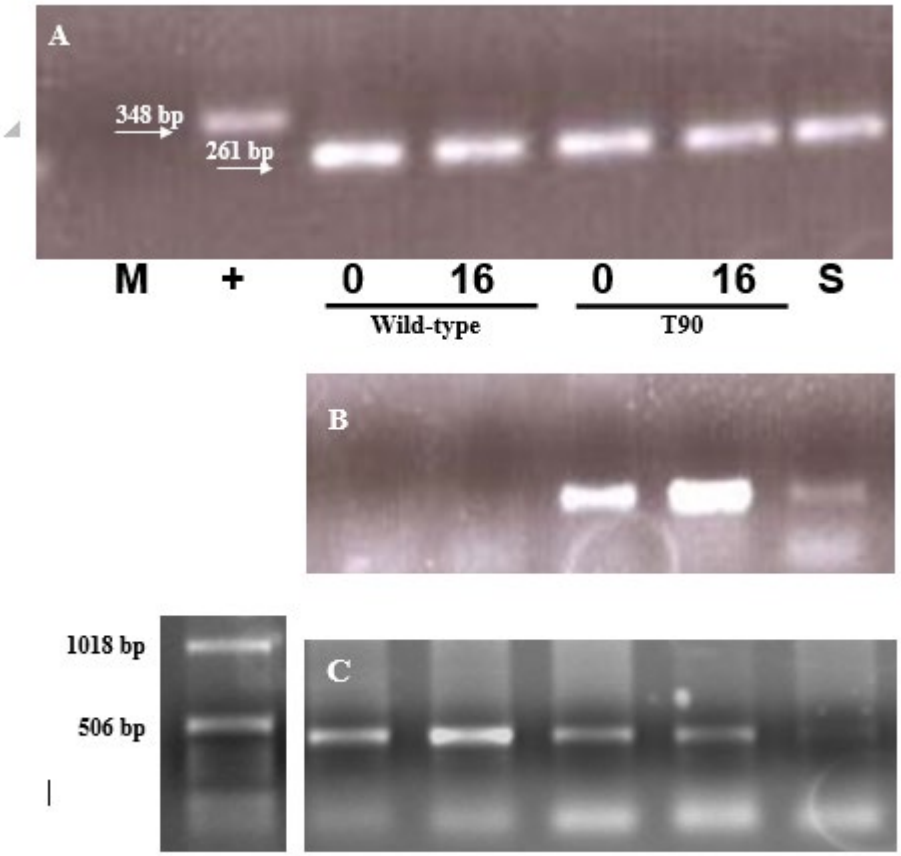

Figure 3.16. Electrophoresis gels of actin, *gus* and *LjCbp1* gene expression in roots of wild-type and T90 *Lotus japonicus* roots 0 and 16 hpi. A, Actin; B, *gus*; C, *LjCbp1*; M, Master mix control; +, gDNA +ve control; S, shoot. Left of figure C is a 1 Kb marker. The actin primers give a 348 bp fragment in the gDNA, the intron is 87 bp. *LjCbp1* primers give a 470 bp fragment.

A). The actin band representing T90 root material 0 hpi appears slightly more intense than the equivalent at 16 hpi (Figure 3.16 A). This supports the suggestion that the band of increased intensity relating to T90 root material 16 hpi (Figure 3.16 B) is genuinely upregulated and not the result of a greater level of starter template.

Neither master mix controls were contaminated (only that for actin is shown). The wild-type material also serves as a negative control for the *gus* gene (Figure 3.16 B). Several attempts were made to repeat this time-course and similar time-courses. However, these were all excluded due to various experimental errors, which included contamination with genomic DNA, concern that saturation had been reached during PCR amplification and too much variation in actin levels to permit meaningful analysis.

3.2.5.4 *Cbp1* expression in T90 heterozygous material 0-72 hpi and wild-type material 0-6 hpi using northern blot analysis

Approximately 600 *L. japonicus* T90 seeds, heterozygous for the T-DNA insertion, were sown in 7x Phytatrays II™ and placed in a CER (Section 2.4.5a). After 12 days 2x Phytatrays II™ were inoculated with *M. loti* (2.5.1 Method 1) and returned to the CER. After 16 hours one inoculated and one uninoculated control tray were removed and 100mg tissue was harvested (Section 2.8). The remaining trays were inoculated as previously described and harvested 6, 11, 23, 45 and 72 hpi.

Approximately 600 *L. japonicus* wild-type seeds were sown in Phytatrays II™ (approx. 80 seeds per tray) according to Section 2.4.5a. Seedlings were inoculated on day 14 with *M. loti* strain NZP2235 (Section 2.5.1 Method 1). The control tray was harvested at 6 hours; this had been left untouched since sowing. The remaining samples were harvested 1, 2 ½, 3, 3 ½, 4, 5, 5 ½, and 6 hpi. Approximately 150mg tissue was obtained for each time point. Shoot tissue was also harvested from the 6 hpi material as an additional control for RNA extraction.

Total RNA extraction, DNase treatment and northern blot analysis were carried out for both experiments in accordance with Sections 2.8.4 and 2.8.4.1. The RNA concentration of each sample was determined (Section 2.8.4). These readings were used to calculate the quantity of sample required for 10µg RNA.

Experiments with both T90 and wild-type material indicated upregulation of *LjCbp1* within six hours of inoculation. Figures 3.18 and 3.20 summarise the results of densitometrical analyses used to optimise the data from these experiments.

Analysis of the RNA gels (Figure 3.17 A and 3.19 A) shows some retention of nucleic acid in the loading wells. This may be due to the presence of polyphenolic or carbohydrate compounds. The gels also evidence uneven

Figure 3.17. RNA gel and Northern blot of T90 shoot and root material 0-72 hpi. Northern hybridisations were carried out using cDNA probe from *LjCbp1* (B) and ubiquitin (C). A, RNA gel; B and C, Northern blots for *LjCbp1* (B) and ubiquitin (C); s, shoot; r, root.

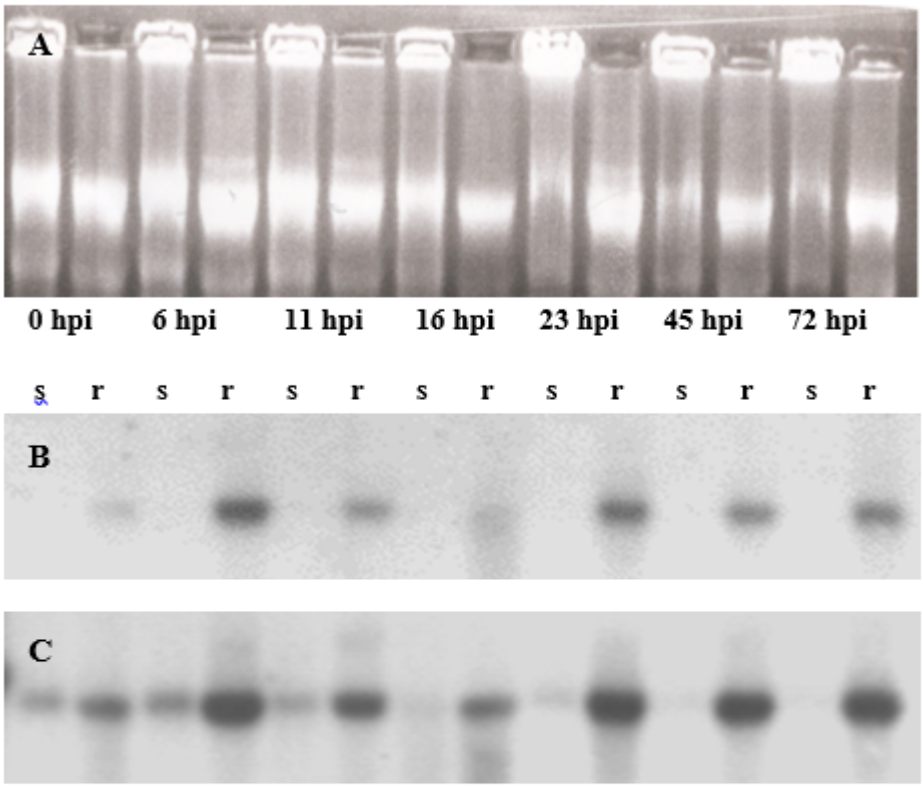

Figure 3.18. Line graph of densitometry analysis of *LjCbp1* and ubiquitin probe hybridisation signals to Northern blot of *L. japonicus* T90 root RNA 0-72 hpi.

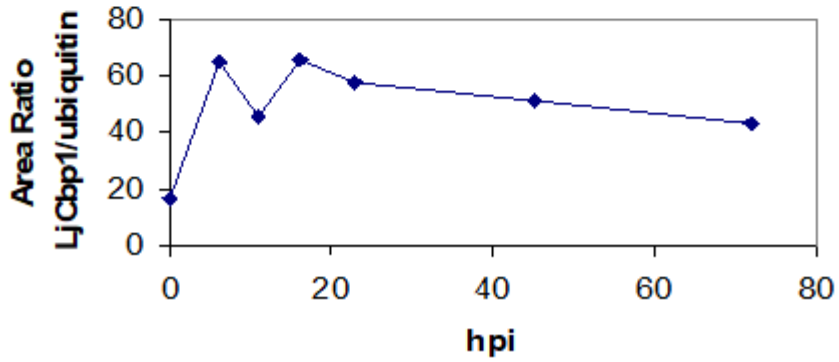

Figure 3.19. Expression analysis of *LjCbp1* in wild-type (untransformed) *L. japonicus* 0-6 hpi. A, RNA gel; B and C, Northern hybridisation with radio-labelled (B) *LjCbp*1 and (C) ubiquitin. Lanes 1-8, root 1, 2 ½, 3, 3 ½, 4, 5, 5 ½, 6 hpi, respectively, with *M. loti*; lane 9, shoot 6 hpi with *M. loti*; lane 10, root 6 hpi with water (control).

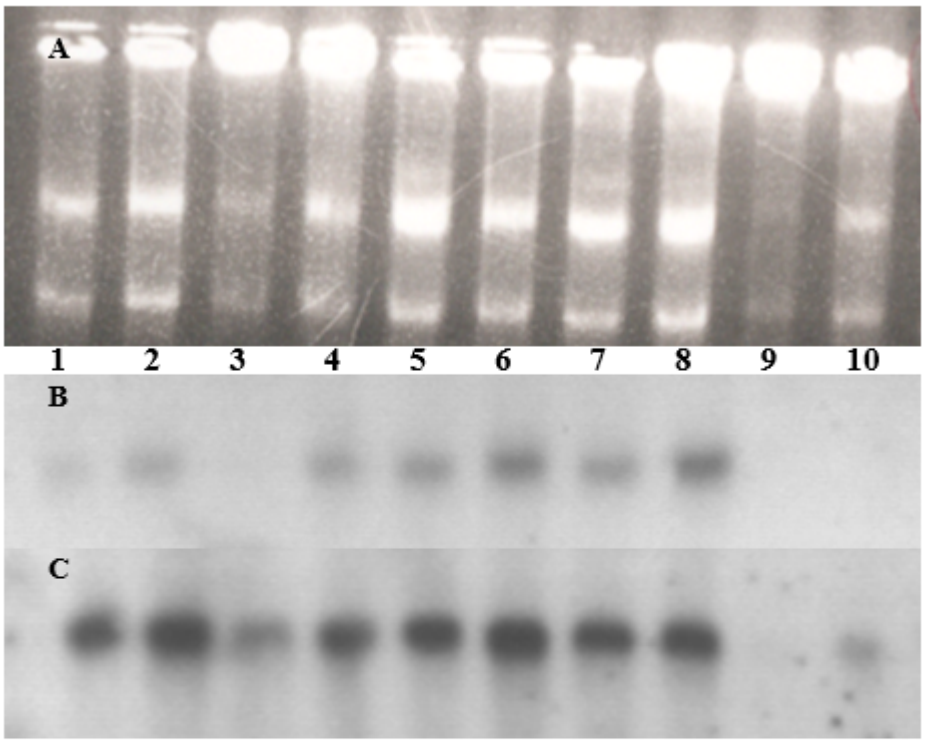

Figure 3.20. Line graph of densitometry analysis of *LjCbp1* and ubiquitin probe hybridisation signals to Northern blot of *L. japonicus* wild-type root RNA 0-6 hpi.

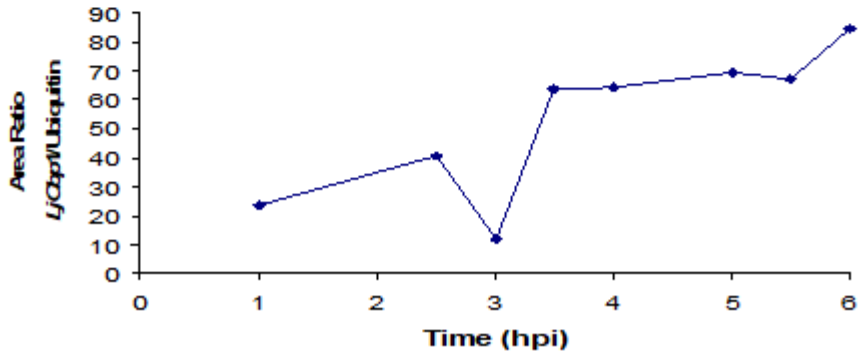

loading and variable integrity of RNA. RNA measurements using spectrophotometer readings (Section 2.8.4) at A260 and 280 indicated the poor integrity of some of the samples, in particular those from shoot tissue (Table 3.0).

The absence of any visible hybridisation between T90 shoot samples at 45 and 72 hpi and the wild-type shoot sample and the ubiquitin probe (Figures 3.17 and 3.19 C, respectively) may be due to the poor quality RNA.

The variability in RNA loading made it difficult to determine whether any upregulation of *LjCbp1* had occurred post inoculation. The x-ray films of the northern blot probed with both *LjCbp1* and ubiquitin cDNA were therefore examined using the densitometry tool of the AlphalMager Imaging System™. This permitted the measurement of band density for each hybridisation spot. The results summarised in Figure 3.18 and 3.19 show the area ratio of *LjCbp1* to ubiquitin and indicate that an increase in *LjCbp1* expression occurred in both cases by six hpi. One problem with this analysis, however, is that any saturation of the x-ray film results in a poor dynamic range. Polysaccharide contamination may be present in the samples, as indicated by the retention of nucleic acids in the wells. Efforts to prevent this in further experiments were taken, using polyvinyl pyrollidone (Salzman *et al*., 1999). However, problems of low quantities of RNA hampered additional northern blot experiments.

Table 3.0. Spectrophotometer readings at A260 and A280 for RNA root and shoot samples.

Sample	A260/A280
Time-course 0-72 hpi	
0 hpi shoot	1.84
0 hpi root	1.52
6 hpi shoot	1.77
6 hpi root	1.54
11 hpi shoot	1.62
11 hpi root	1.91
16 hpi shoot	1.81
16 hpi root	1.78
23 hpi shoot	1.51
23 hpi root	1.87
45 hpi shoot	1.74
45 hpi root	1.95
72 hpi shoot	1.80
72 hpi root	1.92
Time-course 0-6 hpi	
1 hpi root	1.96
2 ½ hpi root	1.79
3 hpi root	1.83
3 ½ hpi root	1.97
4 hpi root	2.07
5 hpi root	2.40
5 ½ hpi root	1.90
6 hpi root	2.06
shoot	1.91
control	1.75

3.3 Discussion

At present there appears to be little evidence to support the presence of a family of *LjCbp1*-like genes in *L. japonicus*. The search of *L. japonicus* ESTs indicates that the gene may be present as a single copy with no closely related family members, although several ESTs were identified with EF-hand domains (Figure 3.1). Conversely, a large number of sequences of high identity were found in several non-*Lotus* species, including some non-legumes (Figure 3.2), illustrating that conservation of *LjCbp1*-like sequences is not restricted to legumes. In some cases the presence of gene families is inferred. The multiple sequence alignment of peptides in Figure 3.2 shows three sequences in both soybean and *A. thaliana* with at least 88% identity to LjCbp1. In fact, many additional soybean and *M. truncatula* sequences with a high degree of similarity to *LjCbp1* were found in database searches (data not shown for soybean). It seems surprising, therefore, that homologous ESTs with higher identity were not identified in *L. japonicus*. However, this may simply be due to the larger numbers of sequences available for *A. thaliana* and *G. max*. According to the NCBI website the numbers of ESTs available for soybean and *A. thaliana* exceed *L. japonicus* by factors of around three.

The alignment also illustrates that protein sequences from animal species still show relatively high homology. A human and bovine calmodulin (accessions aah47523 and mcbo, respectively) and a Ca^{2+}-binding protein from a squidulin optic lobe (accession p14533) show over 50% identity at the amino acid level in pairwise comparisons (Figure 3.3).

Apart from the calmodulin and Ca^{2+}-binding sequences mentioned already, none of the other proteins, or predicted proteins, have yet been assigned functions. However, the predicted protein isolated from *Castanea sativa* (European chestnut) is wound inducible (Schafleitner and Wilhelm, 2002) and that in *M. truncatula* is induced by drought and in roots infected with the arbuscular mycorrhiza *G. versiforme* (NCBI, PubMed).

Greater identity was found at the peptide, rather than the nucleotide level (data not shown). This may reflect the different usage of the third base of codons by diverse taxa.

The western blot data showed an apparent mobility shift in LjCbp1 upon binding Ca^{2+}, which appeared to induce a conformational change that permitted the Ca^{2+}-bound protein greater mobility. The tagged and bound protein indicates a size of around 22 KDa and the unbound protein around 24 KDa against an expected 24 KDa. It is noteworthy that after denaturing, the Cbp1 protein retained sufficient secondary structure to bind Ca^{2+}. Other papers have reported similar findings for a number of Ca^{2+}-binding proteins, including the increased migration of the protein in the Ca^{2+}-bound form (Yang *et al*., 1999; Camas *et al*., 2002). One reason could be that the conditions used to dissociate proteins, achieved through heating and a subsequent combination of reducing agent and SDS in the polyacrylamide gel, may be insufficient to achieve complete dissociation of the secondary structure of the polypeptide. Alternatively, the affinity of the residues involved in binding Ca^{2+} in the EF-hand sites may be so high that they are able to retain the bound Ca^{2+} even with the breakdown of tertiary structure.

The background staining observed in the western blot (Figure 3.12) may be due to the presence of contaminating carbohydrates, or simply because a low affinity tag was used and non-specific binding has occurred. A repeat experiment is recommended using purified LjCbp1 protein. Radio-labelling is a further option that may be used to confirm the shift in LjCbp1 mobility.

The other observation of this experiment is that the Ca^{2+}-bound protein migrates further in the gel, and therefore appears to have a lower molecular weight, than that without Ca^{2+}. In polyacrylamide gels, SDS is bound by the denatured protein. Since the amount of SDS bound is almost always proportional to the molecular weight of the polypeptide and is independent of its sequence, SDS-polypeptide complexes should migrate through such gels in accordance with the size of the polypeptide. It therefore appears that, despite the presence of SDS, samples dissolved in lysis buffers contaning Ca^{2+} retain sufficient integrity within their polypeptide units to give the appearance of a lower molecular weight protein. It

also follows that this could only be the case if the previous argument was true, that complete dissociation of the proteins had not taken place. In order to provide further evidence to support the data from the western blot, the protein could be purified and the procedure repeated, or antibodies could be raised specific to the LjCbp1 protein.

The location of the retrotransposon element within the 3' untranslated region of the locus means there is a possibility that the insertion may have altered the *LjCbp1* transcript stability in some way, although the orientation of the gene makes this less likely. The fact that the insertion seems to be recent means that this may be a useful polymorphism marker. Details of the *LjCbp1* locus were sent to Dr Niels Sandal of the University of Aarhus, Denmark, for mapping. Dr Sandal identified that *LjCbp1* is located on linkage group III. However, an inversion between *L. japonicus* ecotype Gifu and *L. filicaulis*, the two parents in the mapping family, has resulted in strong suppression of recombination. Fine mapping of this part of chromosome III has therefore not yet been possible (Niels Sandal, personal communication).

The search for *cis*-acting elements within the 3.7 Kb *LjCbp1* locus did not reveal any symbiosis-specific motifs, although little work has been done to characterise nodulin promoters. The data do, however, provide information that may prove valuable for later experiments to identify regions specific for regulation during symbiosis. Regions found to be required for symbiosis-specific or root-specific expression may be identified through *in silico* analysis in other *ENOD* promoters and subsequently confirmed experimentally. It might have been expected that the region in the *LjCbp1* putative promoter containing a sequence similar to the 200 bp regulatory region of *PsENOD12*, found to be sufficient for symbiosis-specific expression, would also elicit symbiosis-specific expression in the *LjCbp1* promoter/GUS fusion. However, this was found not to be the case (Leif Skøt, unpublished data). It is tempting to speculate that some physical requirements were not met in the arrangement of the construct, for instance that some *cis*-acting elements were not brought into physical contact because of a spatial conformation that was not in place. Some of the other regulatory elements identified and highlighted in Figure 3.6 may have an effect on the regulation of *LjCbp1*. The

investigation highlights the possibility that certain factors may be acting downstream of the T-DNA insertion, resulting in *LjCbp1* having a potentially different regulatory mechanism to that of *gus*.

Database searches did not reveal an obvious TATA box, although one suggested motif is highlighted (pink box) in Figure 3.6. There seems to be some uncertainty over the consensus position of TATA box elements in plant promoters. The Softberry website (http://www.softberry.com/berry.phtml) lists over 200 plant promoter sequences with TATA box elements all within 45 bp from the transcription start site. However, unpublished reports infer that more distant binding sites for RNA polymerase machinery may exist in plant promoters (Iain Donnison, IGER, personal communication). It is also possible that *LjCbp1* does not have a TATA box. According to one website, nearly half of all known promoters are TATA-less (Genomatix, 1998). The absence of a TATA element could suggest that *LjCbp1* yields RNAs with several different, staggered 5'-ends (Blackburn and Gait, 1990). Indeed, a recent report suggests that multiple transcription initiation sites are much more common than previously thought; numerous cases of alternative mRNA splicing have been reported (Haas, *et al*., 2002). However, it also seems likely that there exist many, as yet unidentified, sequences that may also act as binding sites for RNA polymerase. Since no obvious TATA box has been identified in the promoter region of *LjCbp1* further replicates of 5' RACE should be carried out in order to determine more clearly whether *LjCbp1* produces transcripts with staggered 5'-ends, as mentioned above.

Investigations into the structure of the LjCbp1 peptide revealed that a putative signal peptide may be present at the N-terminus, suggesting that this protein is delivered into an organelle or the cell wall. This finding was supported by the identification of a corresponding hydrophobic domain within this putative signal peptide sequence. LjCbp1 may therefore function in the endoplasmic reticulum or vacuole, two major sources of Ca^{2+} within the cell. It seems unlikely that the protein is targeted to the symbiosome since it is expressed in root tissue before the presence of any bacteroids. The search for LjCbp1-like proteins failed to reveal an obvious class of Ca^{2+}-binding proteins, such as CaM, within which LjCbp1 fits. Of note is the 5' region of the LjCbp1 coding sequence that contains the unusual

serine repeat and bears the least homology with other sequences. A second ATG triplet is located eighty amino acids downstream of the ATG start site. The ORF from this point bears much closer resemblance to CaMs and would most likely be classified as such. However, the identification of the transcriptional start site of *LjCbp1* and sequencing of the full transcript has confirmed that the first ATG is correct. One possibility is that some form of post-translational modification takes place that removes part of the 5' region from the peptide. The existence of a putative signal peptide supports this hypothesis, although the cleavage site indicated is upstream of the second ATG triplet.

GUS expression was not observed in uninoculated T90 roots by Webb *et al*. (2000). Therefore, following the observation of *gus* transcripts in uninoculated T90 material (Section 3.2.5.1) the possibility of experimental error was considered. The presence of genomic (g)DNA contamination could not be entirely ruled out. Samples were treated with DNase but a minus RT control was not included in the experiment. The prokaryotic origin of the *gus* gene means that it does not contain an intron so any fragment amplified from gDNA will be the same size as that amplified from cDNA. It was also possible that rhizobial contamination was present in the uninoculated control sample. Control plants were not grown long enough to detect the presence/confirm the absence of nodules and problems had been encountered in sterilising vermiculite that may have permitted the survival of rhizobial contamination.

However, subsequent experiments confirmed the presence of *gus* transcripts pre-inoculation, even though such expression had not previously been detected through histochemical means (Webb *et al*., 2000). Interestingly, a recent report discusses the asymmetric distribution of mRNAs achieved through *cis*-acting elements that govern their localisation. The mRNA can be silenced until an appropriate destination or point in time is reached, when silencing can then be de-repressed or translationally activated (Méndez and Wells, 2002). In such a way, transcripts of *gus* may be present at a low level, but remain untranslated until the point of inoculation. There is also the possibility that post-translational modification renders the GUS enzyme active, and therefore visible, in T90 (Kawaguchi, 2002).

Transcripts of *LjCbp1* were also identified in uninoculated T90 and wild-type material and show upregulation following inoculation with *M. loti* in wild-type material only (Figure 3.16 B). This upregulation correlated with that of the *gus* gene in T90 material, suggesting that expression of *LjCbp1* is reflected in GUS activity observed through histochemical means. The lack of apparent upregulation of *LjCbp1* in T90 suggests interference from the T-DNA insertion. This is supported by the observation that an increase in *LjCbp1* expression was observed in heterozygous T90 material (Section 3.2.5.4), where such interference would be reduced. A model may thus be hypothesised that places a mechanism of *LjCbp1* regulation upstream of the T-DNA insertion in T90. This mechanism may be Ca^{2+} (Figure 3.21).

The technique using single strand cDNA synthesis from the mRNA means that greater quantities of template cDNA can be generated for PCR providing flexibility for the optimisation of conditions. Figure 3.16 A shows that the cDNA template was relatively even for PCR analysis. This facilitates the interpretation of the results.

Further analysis of *LjCbp1* expression using northern blotting techniques produced inconclusive data, although densitometric analyses showed an increase in the level of *LjCbp1* expression compared with that of ubiquitin at six hpi (Figures 3.18 and 3.20). This expression appeared to fluctuate over the time period, diminishing 11 hpi, and increasing again 16-45 hpi and diminishing gradually until 72 hpi. It seems likely that the 11 hpi data were spurious and that a much steadier decrease in expression would be expected over 72 hours following the initial upregulation at six hours. Additional replicate samples are necessary for a more rigorous quantitative analysis. The peak obtained with wild-type material was higher than that with T90 material (Figures 3.20 and 3.18, respectively), as would be expected due to the lower levels of expression of *LjCbp1* in T90 seedlings.

Figure 3.21. Hypothetical model illustrating *LjCbp1* regulation. A, an upstream element (possibly triggered by Ca^{2+}) within the *LjCbp1* promoter is responsible for gene upregulation (blue arrow). B, Insertion of T-DNA abolishes upregulation (red arrow) leaving basal expression only. Blue box = potential Ca^{2+} responsive cis-acting element; green box = element responsible for constitutive expression of *LjCbp1*; orange box = *LjCbp1*.

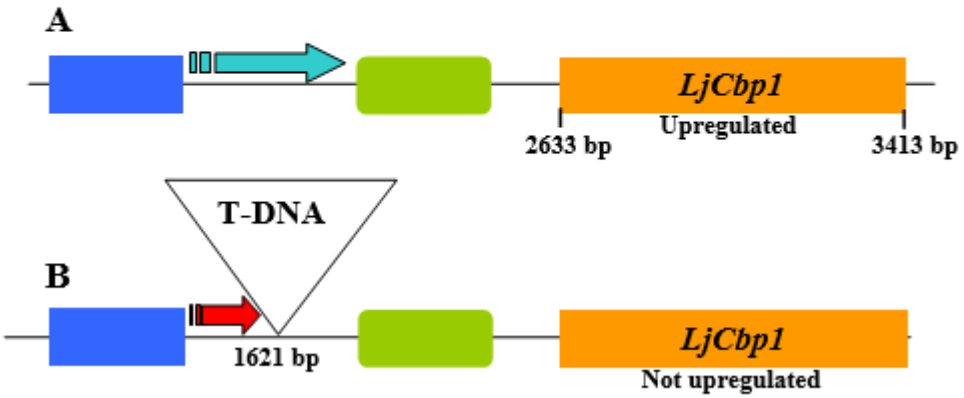

The timing of upregulation of *LjCbp1* following inoculation with *M. loti* suggests that this gene is not involved in the plant's initial perception of the interaction, but rather is part of a downstream signalling cascade. Results indicate that transcripts of *LjCbp1* increase in abundance after the onset of Ca^{2+}-spiking as reported by Ehrhardt *et al*. (1996) and Harris *et al*. (2003) and even Ca^{2+}-spiking is likely not to be the first response in legumes to rhizobial communication as it occurs some minutes after Nod factor application. It also seems unlikely that *LjCbp1* expression is directly linked with the first Ca^{2+}-spiking responses because it does not appear to be upregulated quickly enough after the onset of Ca^{2+}-spiking. However, it would be interesting to determine whether some of the pharmacological agents found recently to inhibit the Ca^{2+}-spiking in *Medicago* species (Engstrom *et al*., 2002) also inhibit GUS expression following rhizobial or Nod factor application to the T90 line.

Comparing nodulation gene expression events across different species and trying to identify the point at which *LjCbp1* is upregulated in this overall scheme is difficult as many genes, such as *ENOD*s *11* and *12*, have not yet been identified in *L. japonicus.* In addition, nodulation in *L. japonicus* proceeds more slowly than in *M. truncatula*, where young emerging nodules can be observed 4 dpi (Journet *et al*., 2001). This further complicates the applicability of results obtained with *M. truncatula* to *L. japonicus*. However, it is still interesting to review the data. Other genes similarly described as being expressed in these early stages of nodulation, but not related in function, include some of those mentioned previously, such as *ENOD11* and *12*. In *M. sativa ENOD11* and *12B* mRNA transcripts accumulate as early as 3 hpi with purified Nod factor but are maximally induced at around 4 dpi (Pichon *et al*., 1992; Journet *et al*., 1994; Gamas *et al*., 1996).

Of the genes that encode Ca^{2+}-modulated proteins so far identified as having a role in nodulation, *LjCbp1* appears to be the first in the signalling cascade: *MtAnn1* shows enhanced expression in root and nodule tissues in response to rhizobial inoculation 12-24 hours following Nod Factor addition (de Carvalho-Niebel *et al*., 2002). It is not clear at what stage in nodule development *PvCaM-1*, *-2, and -3* (Section 3.1.3) first become actively transcribed. *PvCaM-1* appears to be correlated with a later stage of nodule development that is maximal at 15 and 18

dpi, whilst *PvCaM-2* and *-3* appear to be expressed earlier in nodule development, in a similar pattern to that of *ENOD40*. Again, expression of these genes was also identified in non-symbiotic tissues: *PvCam1* was identified in young roots, root apex and cotyledons, whilst transcripts of *PvCaMs-2* and *-3* were found in cotyledons, young stems, leaves, roots, root apices and young nodules (Camas *et al*., 2002).

One possible hypothesis for the regulation of *LjCbp1* is that a basal level of expression of this gene, prior to inoculation, permits the presence of LjCbp1 proteins that can then act as sensors for increases in $[Ca^{2+}]_{cyt}$. In this way, un-bound conformations of LjCbp1 may act to repress further transcription, but upon binding Ca^{2+}, change their conformation in a way that eliminates repression, thus triggering upregulation of the gene. As mentioned previously, some Ca^{2+}-binding proteins are not necessarily involved in triggering effector molecules, but may simply be regulators of Ca^{2+} concentration in the cell (Strynadka and James, 1989). Ca^{2+}-spiking is also independent of *de novo* gene expression as its occurrence is too fast for that to be possible.

In summary, no family has yet been identified in *L. japonicus* to which *LjCbp1* belongs, although such families are indicated in other species. *LjCbp1* appears to encode a protein that binds Ca^{2+}, as demonstrated by the Ca^{2+} mobility shift assay. Transcripts of both the *gus* gene and *LjCbp1* are present at a basal level in shoot tissue and in uninoculated root material of *L. japonicus*, but show upregulation in roots following rhizobial inoculation. Expression of the two genes appears to be correlated. Insertion of the T-DNA region may interfere with regulation of *LjCbp1*.

Chapter 4

4.0 Characterisation of GUS Activity in the T90 Line

4.1 Introduction

4.1.1 Insertional mutagenesis using *Agrobacterium*

The technique of introducing foreign DNA into plant cells is now a widely exploited and powerful tool for plant gene investigation. Two *Agrobacterium* species that are capable of incorporating their own bacterial DNA into a host genome are now used routinely to act as vectors for the insertion of new coding/control sequences. Successful integration of the foreign DNA can also act to remove gene function, as the insertion may disrupt a gene both structurally and functionally and thus provide a mutant phenotype. The creation of enhancer/promoter-trapped lines exploits this mechanism of insertional mutagenesis.

A. tumefaciens and *A. rhizogenes* cause crown gall and hairy root diseases, respectively. The diseases result from the insertion of bacterial auxin and cytokinin genes that interfere with the plant's natural hormonal ratio. The inserted genes are flanked by specific regions, known as the left and right borders of the T-DNA (transfer DNA), located on the Ti (tumour-inducing) or Ri (hairy root-inducing) plasmids. The incorporated DNA also encodes genes used by the *Agrobacterium* to manipulate its host into producing unusual amino acids, called opines, for its own growth and multiplication. Genetic manipulation of these *Agrobacterium* species has permitted the development of strains adopted for use in transformation techniques, through the removal of the genes responsible for opine biosynthesis and catabolism and in the case of *A. tumefaciens*-mediated transformation the removal of the auxin and cytokinin genes.

4.1.2 Reporter genes: *gus* and *gfp*

Since T-DNA tends to insert into actively transcribed regions of the genome, i.e. genes (Koncz *et al*., 1989), one application of T-DNA-mediated insertional mutagenesis is for the insertion of so-called reporter genes. Reporter genes are dominant genes whose expression can be determined in the tissues where they are expressed, for instance, through histochemistry, fluorimetry or fluorescence. The *gus* reporter gene encodes the β-glucuronidase enzyme, derived from *E. coli*. This enzyme gives a blue colouration in the presence of the histochemical stain, 5-bromo-4-chloro-3-indolyl glucuronide (X-gluc) (Jefferson *et al*., 1987). The identification of GUS enzyme activity using histochemistry relies on the cleavage of X-gluc and the oxidisation of a colourless indoxyl intermediate which precipitates as a blue product. This reaction permits the identification of GUS-positive cells. The half-life of the GUS protein has been reported in green tobacco plants to be three to four days (Weinmann *et al*., 1994) and in tobacco protoplasts to be no more than 50 hours (Jefferson et al., 1987). The GUS enzyme can also be assayed fluorimetrically. GUS fluorimetry is a sensitive means of determining GUS activity (Webb *et al*., 1996; Cooke and Webb, 1997) and thus provides an additional approach. However, neither method can be used in *vivo* as both require the sacrifice of plant material.

An alternative to GUS, and sometimes used in conjunction with it, is the green fluorescent protein (GFP), obtained from the Pacific jellyfish (*Aequora victoria*). Agitation of *A. victoria* elicits a green bioluminescence. This phenomenon is produced by two closely associated proteins: a Ca^{2+} activated luciferase, known as aequorin, and GFP (Shimomura *et al*., 1962; cited in Haseloff and Amos, 1995). Activation of GFP within a cell permits its observation using near-ultraviolet light. Since expression of the protein appears to have no physiological effect on cell operation, living plant tissue can be sectioned optically using a laser-scanning confocal microscope to allow the analysis of cellular and subcellular detail (Haseloff and Amos, 1995). Drawbacks with this method exist however: some naturally fluorescing compounds, such as lignin, occur in plants making *bona fide*

GFP hard to detect (Haseloff and Amos, 1995). GFP signals can also be weak and difficult to detect without high expression.

Transgenic plants, harbouring reporter genes such as those described above, have been successfully generated and used to study a variety of physiological and developmental processes (Topping *et al*., 1991; Lindsey and Wei, 1993; Haseloff and Amos, 1995; Webb *et al*., 1996; Cooke and Webb, 1997; Koizumi *et al.*, 2004; Gonzalez-Ballester *et al*., 2005).

4.1.3 Promoter/enhancer trapping

Constructs harbouring reporter genes under the control of inactive, minimal or incomplete promoter sequences can be used to generate enhancer/promoter-trapped lines of plants. Here, expression of the reporter gene will only occur if insertion events permit native plant enhancers or promoters to drive its transcription. This facilitates the identification of genomic sequences expressed in defined developmental fashions or which are functionally redundant and would not, therefore, provide a mutant phenotype. It also provides a means of identifying genes that are expressed in very particular tissue types, or which are important in regulatory terms but may be expressed at very low levels, making them difficult or impossible to detect through differential cDNA techniques. Therefore, reporter genes can help to identify particular developmental stages within an organism and lead to the detection of enhancer or promoter elements necessary for gene expression at a particular place and time.

The construct design within which reporter genes may be incorporated can vary. Here, two examples are described. The enhancer trap construct contains a minimal promoter, which may contain a TATA box, for instance, but no major upstream elements to direct the level or location of expression. In this case, native enhancer regions may direct tissue specific expression of the reporter gene (Topping *et al*., 1991). Since enhancers can function over a relatively large distance, even thousands of base pairs away, activation of the reporter may not be dependent on insertion directly into a gene sequence (Lindsey and Topping, 1996).

Conversely, promoter-trap constructs function without a minimal promoter. In this case activation is expected to depend upon insertion within a gene and downstream of a native promoter, to generate a transcriptional fusion.

Some of the earliest approaches to promoter-trapping using the *gus* reporter gene led to the identification of a nematode-induced gene expressed in *Arabidopsis* roots (Goddijn *et al*., 1993) and a phloem-specific promoter, also in *Arabidopsis* (Kertbundit *et al*., 1991). More recently, again in *Arabidopsis*, the *EXO* gene was identified. This gene may encode a component of a negative regulatory system required during cell division (Farrar *et al*., 2003).

The approach adopted by Goddijn *et al*. (1993) demonstrated the value of promoter-trapping for the identification of genes inducible by specific physiological or environmental factors. Here, the tagged lines were screened for expression after infection with nematodes, thereby providing the opportunity to isolate genes specifically induced under such circumstances.

The use of GFP is still being developed and explored (Haseloff *et al*., 1997) and there are currently no examples of successful enhancer/promoter-trapping in the literature. However, GFP has been introduced into a variety of plant species including *L. japonicus* and the non-legume *Casuarina glauca*, which forms N_2-fixing nodules with actinomycetes. In both cases GFP was under the control of the 35S Cauliflower Mosaic virus promoter. These works aimed to asses the potential of GFP for promoter expression studies in nodules (Quaedvlieg *et al*., 1998; Santi *et al*., 2003). GFP has now been introduced into *C. glauca* under the regulation of the *Cg12* promoter. *Cg12* is an early symbiotic gene from *C. glauca* (Santi *et al*., 2003).

4.1.4 Generation of mutants and identification of a putative symbiosis-specific reporter gene in the T90 line

The *L. japonicus* T90 line was generated during an insertional mutagenesis programme initiated to identify plant genes activated specifically during interactions with symbiotic root-nodulating bacteria, an application similar to that adopted by Goddijn *et al*. (1993). *Agrobacterium tumefaciens* strain LBA 4404 (Topping *et al*., 1991) was used to mediate insertion of a binary vector containing a selectable marker and the promoter-less *gus* gene as a reporter.

The construct, *pΔgusBin19* (Lindsey and Topping, 1996) (Figure 4.1), used in the Webb *et al*. (2000) programme, contains the *nptII* gene conferring kanamycin resistance and the *gus* gene encoding the β-glucuronidase enzyme from *E. coli*, as described above. Expression of the *nptII* gene is controlled by the nopaline synthase promoter (*nos*) and permits identification of successfully transformed calli during the first stage of screening. Once rooted, transformants that survived in media supplemented with the antibiotic were tested for GUS expression in response to rhizobium (Webb *et al*., 2000).

In the *pΔgusBin19* construct the promoter-less gene is close to the left border of the T-DNA. Expression of the *gus* gene depends on the flanking host plant DNA having promoter activity allowing transcription of the *gus* gene to take place (Figure 4.2). The blue staining of tissues expressing *gus* permits the identification of genes that are developmentally regulated during specific processes, such as the initiation of symbioses. Since the inserted sequence is known, altered loci can be identified using the T-DNA as a marker in the interrupted sequence. This construct and approach had already proved successful for Goddijn *et al*. (1993) in their investigations of nematode-induced gene expression (Section 4.1.3).

T90 was found to express *gus* in what appeared to be a symbiosis-specific manner (Webb *et al*., 2000). GUS activity appeared to be absent from all tissues until inoculated with *Mesorhizobium loti* bacteria. After inoculation, expression was identified in roots, becoming localised in nodules as the interaction

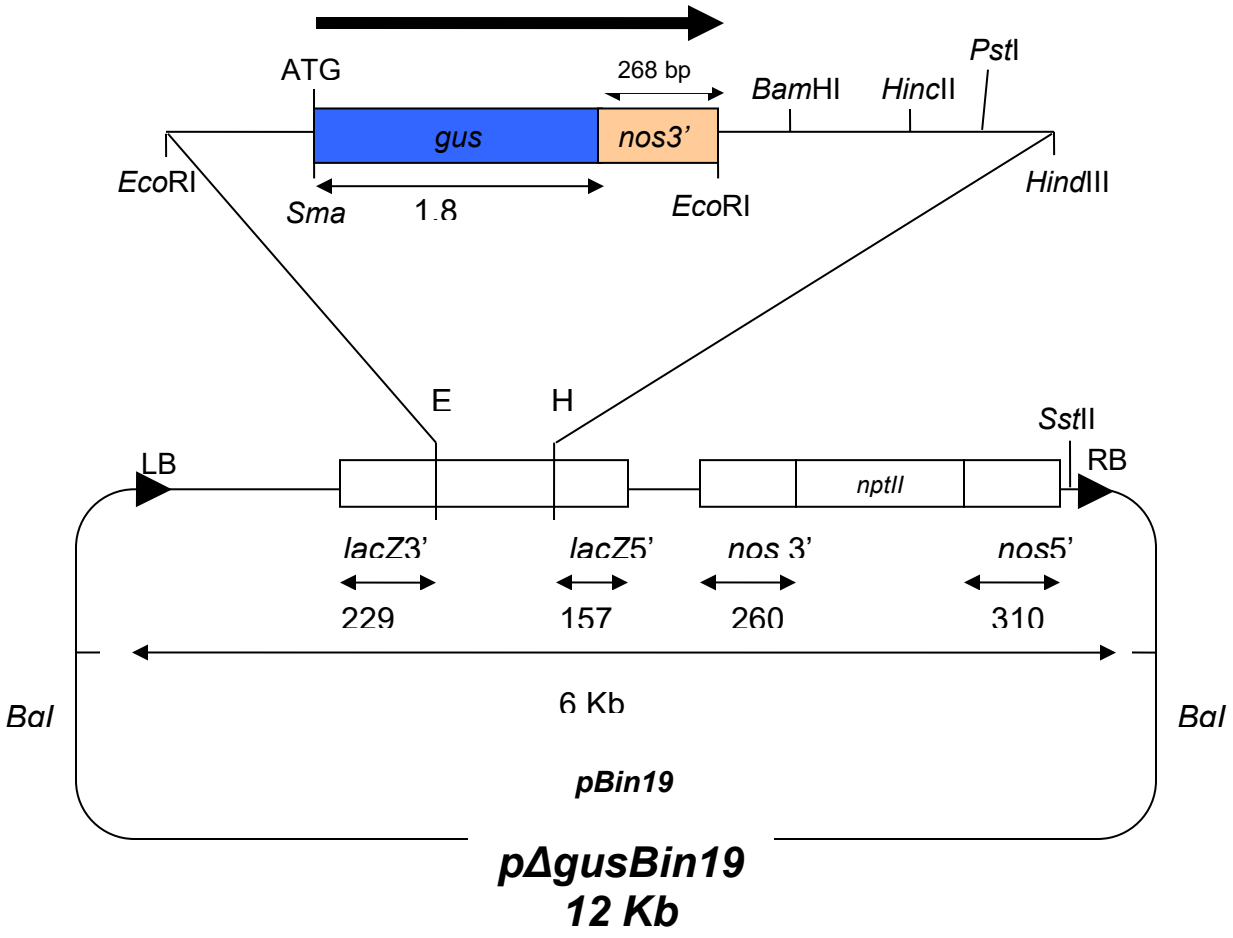

Figure 4.1. Promoter-trap vector *pΔgusBin19*. Adapted from Lindsey and Topping (1996).

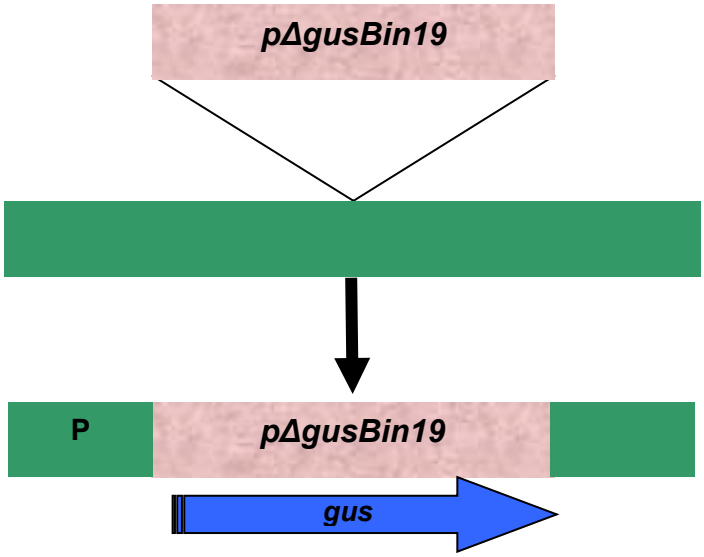

Figure 4.2. Schematic representation of the insertion of *pΔgusBin19* vector into the plant genome. Insertion of the vector (pink box) into the plant genome (green line) downstream of a native plant promoter (P) permits transcription of the reporter gene (blue arrow).

progressed (Figures 1.9 and 4.3). GUS activity was also observed in root tissue colonised by mycorrhiza fungi but here showed a different pattern of expression that was more dispersed, causing diffuse staining throughout the root, near vascular tissue and associated with AM hyphae (Parniske, personal communication) (Figure 4.4).

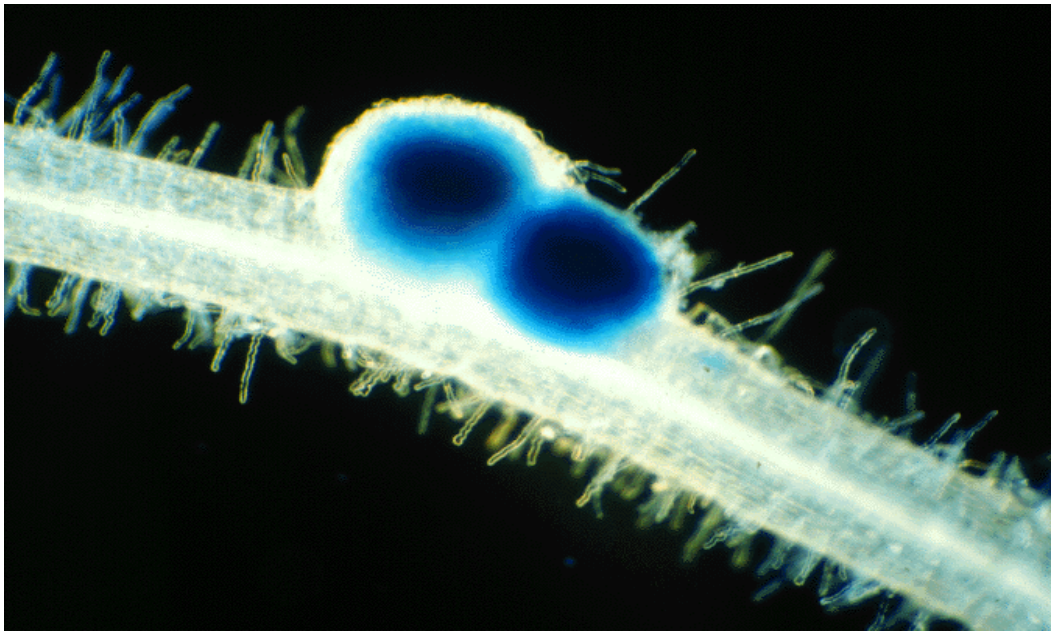

Figure 4.3. Localisation of GUS activity in *L. japonicus* T90 root nodules in response to *M. loti.* Magnification x20. Image courtesy of Maggie Nicholson.

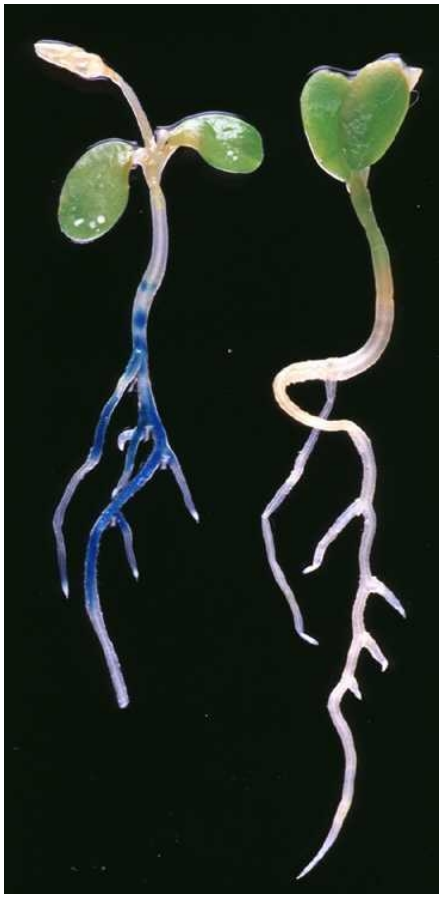

Figure 4.4. GUS activity in mycorrhizal infected *L. japonicus* T90 compared with uninoculated control. Magnification x4. Image courtesy of Martin Parniske.

4.1.5 Regulation of *gus* expression in T90

Sequencing of the region containing the T-DNA insert in T90 revealed that an open reading frame (ORF) encoding a putative Ca^{2+}-binding protein (*LjCbp1*) was located approximately 1 Kb downstream of the insertion (Figure 4.5). Ca^{2+} is a well-known second messenger (Sections 3.1) and changes in $[Ca^{2+}]_{cyt}$ occur soon after Nod factor perception by the plant (Section 3.1.2). If *gus* expression in the T90 line is reporting the expression of a gene encoding a Ca^{2+}-binding protein involved specifically in symbiotic interactions, it opens up the possibilities that this line could be used to investigate Ca^{2+} signalling in plant-rhizobium interactions. There is evidence for the regulation of Ca^{2+}-binding proteins by Ca^{2+}-sensitive transcriptional regulatory mechanisms in animal systems (Arnold and Heintz, 1997).

The *pΔgusBin19* construct (Lindsey and Topping, 1996) was designed to generate, primarily, transcriptional gene fusions. However, because the T-DNA insertion lies some distance upstream of the putative Ca^{2+}-binding protein it seems possible that the *gus* gene is reporting the activity of an enhancer element within the *LjCbp1* locus. In this case it would be the effects of transcriptional activators on such an enhancer region that are reported by the *gus* gene in T90. Although additional regulatory elements could act beyond the insertion and therefore mean that the transgene was not exclusively reporting expression of the downstream gene, the identification of factors affecting *gus* expression would still provide some information regarding the regulation of the putative promoter of *LjCbp1*. Furthermore, these data could highlight potential *cis*-acting regulatory elements affecting *gus* expression, as reported Chapter 3. This chapter will therefore characterise *gus* expression in T90 in response to various factors.

In the original paper, GUS activity was observed in root tissue only, in response to challenge by *M. loti* bacteria and within 3 days of inoculation; expression diminished in senescing nodules (Webb *et al*., 2000). In order to confirm these

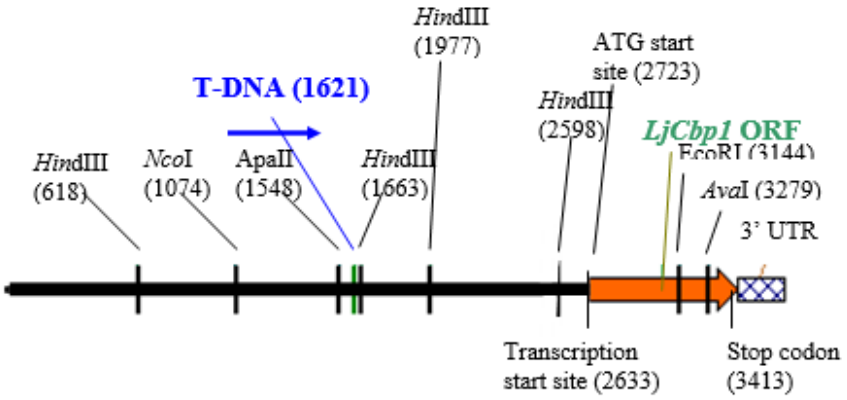

Figure 4.5. Restriction enzyme map of cloned *LjCbp1* locus showing position of T-DNA insert in relation to *Cbp1* open reading frame. Modified from Skøt (personal communication).

results and gain a clearer understanding of the temporal and developmental pattern of expression of *gus* in T90, as well as its specificity, a more detailed analysis was required. Hence, the timing of GUS activity in response to *M. loti* was investigated. This time course included the 3 dpi period already identified by Webb *et al.,* (2000) but also spanned the infection process before and after this time point in order to establish, precisely, the onset of enzymic activity.

The importance of Nod factors in early recognition and establishment of the symbiosis have been described in detail in Section 1.5.3. Analysis of the effects of these compounds on induction of GUS activity in T90 could give an increased indication of the specificity of the expression and whether the presence of the bacterium itself is also required for elicitation.

The N-acetylglucosamine residues that form the backbone of rhizobial Nod factors are similar in structure to chitin. Chitin is also a primary structural component of the walls of all true fungi. Since rhizobia and AM fungi are the only factors so far found to elicit *gus* expression in T90, chitin is an obvious common factor.

Chitosan, which is derived from crustacean shells, can be used as a crude preparation of chitin fragments. Here, chitosan was used to provide an indication whether chitin can act as a Nod factor without decorations. This may also have the potential to elucidate the importance of the structural modifications in Nod factors in eliciting GUS activity.

A range of different rhizobial strains was also used to gain further insight into GUS specificity in T90. These strains secrete a range of Nod factor molecules and other determinants of specificity.

The expression of the *gus* gene may correspond to that of the downstream gene encoding a putative Ca^{2+}-binding protein (*LjCbp1*). A number of pharmacological investigations will therefore be conducted to determine the effects of Ca^{2+} and inhibitors of Ca^{2+} on GUS activity. Factors such as calcium chloride ($CaCl_2$) and EGTA may either elicit or inhibit GUS activity if the reporter gene has inserted in a

gene which is part of a Ca^{2+}-mediated signalling pathway. EGTA is a chelator of metallic cations which, in comparison to EDTA, has a preference for Ca^{2+}. The ionophore A23187, a polyether antibiotic isolated from *Streptococcus chartreusensis* will also be exploited in GUS expression studies. A23187 binds and transports cations across membranes (Resendez *et al*., 1986).

Ca^{2+} enters cells through Ca^{2+}-permeable ion channels. In animal systems surface membrane Ca^{2+} channels include voltage-gated channels of types L, T, N, P, Q and R (Shattock, 2003). These channels generally share the same basic structure, the principle pore-forming unit of which is the α_1-subunit. This subunit differs between the various Ca^{2+} channel types and confers many of the key properties on the channel, thereby contributing to their biophysical, pharmacological and tissue distribution characteristics (Shattock, 2003). The pharmacological investigations will therefore include three types of Ca^{2+} channel blocker, each identified as an antagonist of a different type of Ca^{2+} channel.

The probable role of hormones in root nodulation by rhizobia has been identified in Section 1.5.7. Plant hormones, in contrast to Nod factors, are small molecules that diffuse readily across membranes making them ideal mediators of key developmental processes. The induction of cell division within the root cortex during nodulation strongly implicates a role for plant hormones (Truchet *et al*., 1989; Hirsch, 1992). The low concentration at which Nod factors are perceived indicates their perception must be through high-affinity Nod factor receptors, several candidates of which have been identified (Section 1.5.4).

The identification of certain genotypes of *M. sativa* which are able to form nodules spontaneously (Truchet *et al*., 1989) indicates that a different signal, one that is independent of Nod factor, transduces to internal cortical cells where it triggers cell division (Joshi *et al.,* cited in Hirsch, 1992). Plant hormones are therefore likely intermediaries in the signal transduction pathway initiated by Nod factors. Exogenous applications of a range of hormones was tested on T90 to determine their effects on GUS activity.

Reactive oxygen species (ROS) are free radicals, reactive molecules containing oxygen, or molecules containing oxygen that generate free radicals and are closely involved in regulating plant defence responses (Neill *et al*., 2002). ROS include nitric oxide, superoxide, peroxynitrite and hydroxyl radical. In addition to their roles in defence, ROS have also been shown to play a key part in establishing and maintaining the symbiosis between the plant and the rhizobia (Santos *et al.,* 2000; D'Haeze *et al.,* 2003; Shaw & Long, 2003). It has also been recently demonstrated that in mammalian cells levels of ROS are synchronously generated with the cell cycle indicating that ROS are closely connected with the cell cycle (Takashashi *et al*., 2004), a mechanism that is reactivated during nodulation (Section 1.5.3) (Spaink *et al*., 1991; Truchet *et al*., 1991).

Suppression of the ROS-generating system that sustains the prolonged oxidative burst associated with plant defence responses has been shown to involve Nod factor exposure (Shaw & Long, 2003). Evidence also exists that *Rhizobium* Nod factor is involved in the inhibition of the salicylic acid-mediated defence response in alfalfa roots (Martínez-Abarca *et al*., 1998).

In contrast, some events similar to those found in plant–pathogen interactions have been found in the plant interaction with AM fungi (García-Garrido and Ocampo, 2002). These events include signal perception, signal transduction and defence gene activation. The relationship between defence and symbiosis and common signalling elements suggest that factors involved in plant defence mechanisms may influence GUS expression in T90.

The molecular mechanism for nitric oxide synthesis or action is currently unknown, but its role in plant defence (Orozco-Cárdenas and Ryan, 2002) makes it a representative candidate in a preliminary investigation into the possible effects of ROS in eliciting GUS activity in T90. A donor of nitric oxide, sodium nitroprusside (SNP), will therefore also be assessed for its potential to elicit GUS expression in T90 plants.

The aim of this chapter was to investigate the timing and developmental expression of *gus* in more detail and to characterise this expression in response to a range of factors

that may be expected to elicit a response during the early stages of the symbiosis. These factors included those involved in the early recognition events, for instance Nod factor, different rhizobial strains and Ca^{2+}, as well as those likely to be involved in nodule establishment, such as hormones and ROS.

4.2 Results and discussion

4.2.1 Timing of GUS activity in response to *M. loti*

Webb *et al*. (2000) demonstrated that GUS staining was visible in T90 seedling roots three days post inoculation with the *M. loti* slow nodulating strain NZP2037. This strain was used as the (non-nodulating) Nod C mutant was also available in the same genetic background. In order to confirm the specificity and location of GUS activity in T90 seedlings, the present experiments were repeated using a faster nodulating strain (NZP2235) of *M. loti*. In addition, a time course was set up to establish the appearance of enzyme activity within the first five days following inoculation.

Approximately 100 *L. japonicus* T90 seeds were sown into 2 PhytatrayII™ containers, 50 seeds in each (Section 2.4.5a), and grown under the CER conditions described in Section 2.4.5. Seven days after sowing, one PhytatrayII™ was inoculated with *M. loti* strain NZP2235 (Section 2.5.1 Method 1) and returned to the CER. Seven seedlings were harvested at 8, 9, 10, 11 and 12 (hpi) and every 24 hours for 5 days. Seedlings from each treatment were histochemically stained (Section 2.6) and examined using a light microscope (Section 2.9). Five uninoculated control seedlings were harvested from the second PhytatrayII™ 5 dpi and treated as above.

In this present work microscopic analysis of *L. japonicus* seedling roots revealed that GUS activity first appeared in root hairs within the nodulation zone (Section 1.5.4) of T90 seedlings between 8 and 10 hpi with *M. loti* strain NZP2235 (Figure 4.6 A). Staining became progressively more widespread during the time-course, by 24 hpi it covered approximately 3mm of the root tip and was visible by eye (Figure 4.7 A and B). At 5 dpi most of the epidermal cells in the nodulation zone could be seen to be staining for GUS (Figure 4.7 C). The equivalent uninoculated roots showed no GUS activity (Figure 4.7 D).

By contrast, morphological changes in root hairs occurred over a longer time period, for example root hair deformations were observable from 3 dpi (Figure 4.6 B) and

shepherd's crook formations from 5 dpi (Figure 4.6 C and D). GUS activity was not observed elsewhere in the seedling.

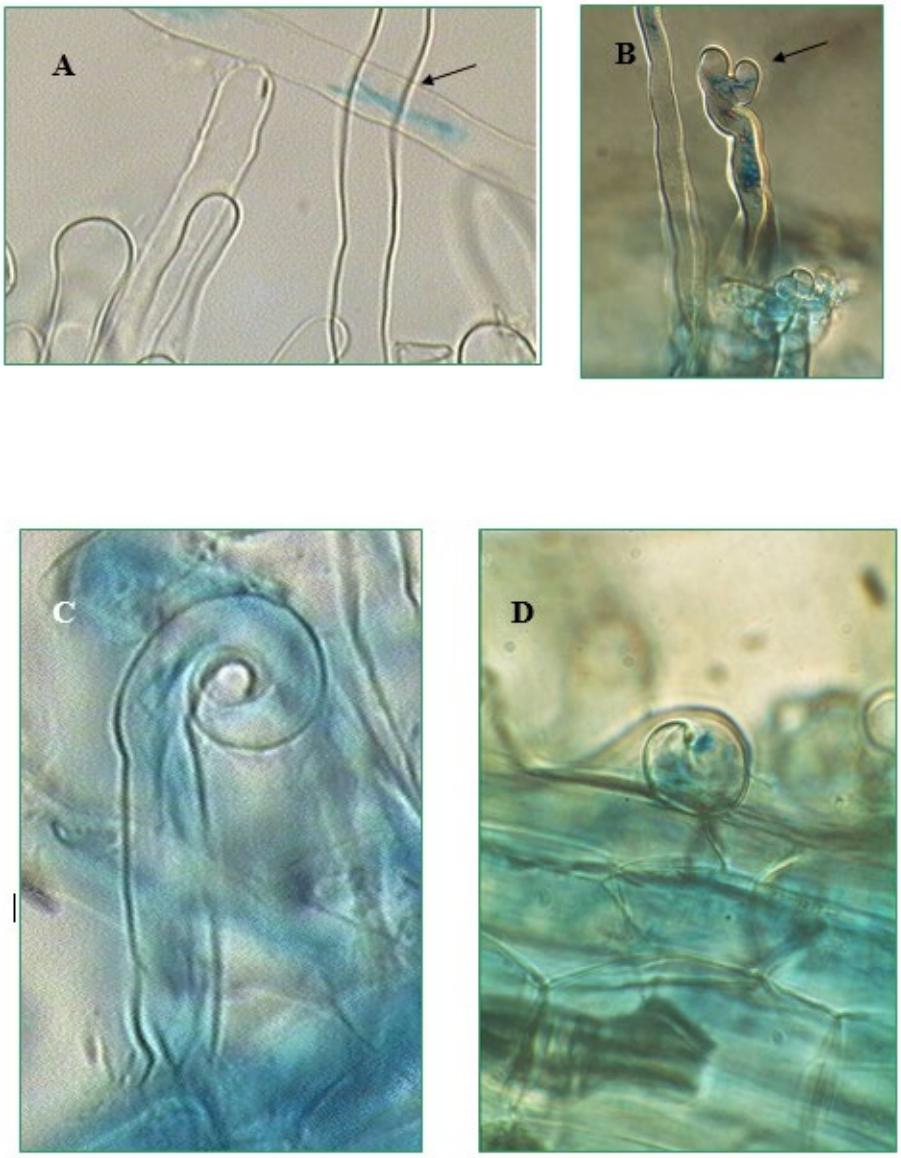

Figure 4.6. Histochemical localisation of GUS activity in root hairs of *L. japonicus* T90 line inoculated with *M. loti* strain NZP2235. A, First evidence of GUS activity at 8 hpi (arrow) (x60). B, root hair branching at 3 dpi (arrow) (x40); C (x100) and D (x50), shepherds crook and root hair curling at 4 and 5 dpi, respectively.

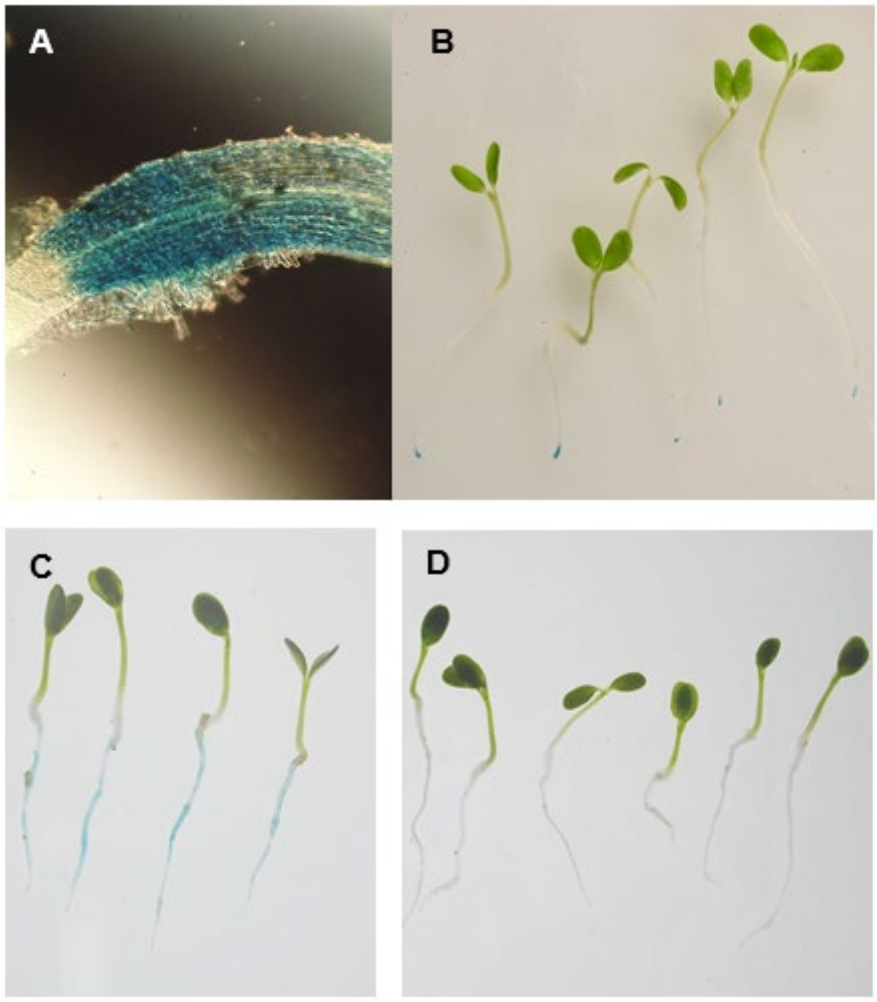

Figure 4.7. Histochemical localisation of GUS activity in seedlings of *Lotus japonicus* T90 inoculated with *M. loti* strain NZP2235. A, root tip 24 hpi (x40 magnification); B, 24 hpi; C, 5 dpi; D, uninoculated at 5 d (B, C and D x2 magnification).

4.2.2 GUS activity in response to Nod factor and chitosan

M. loti strain NZP2235 elicits GUS enzyme activity within eight hours of inoculation (Section 4.2.1). This raised a question over whether other substances could induce GUS activity, independent of bacterial proximity. The effect of purified Nod factors on host legumes in eliciting root hair deformations and nodulin gene activation has been well-documented (Section 1.5.3). An experiment was therefore set up to establish whether Nod factor could elicit GUS activity in T90. The timing of GUS response was monitored in order to assess any delay or acceleration in comparison with that elicited by *M. loti*. In parallel with this, T90 seedlings were also inoculated with chitosan. Since the backbone of Nod factor is the same structure as chitin and chitosan is a source of chitin, this experiment should provide further characterisation of the specificity of *gus* expression.

Approximately 70 T90 seeds were prepared as in Section 2.4.5d and placed under the CER conditions described in Section 2.4.5 for 2 weeks. Fifty seedlings were inoculated with Nod factor according to Section 2.5.2 and returned to the growth room for between 3 and 24 hours. Ten seedlings were inoculated with chitosan according to Section 2.5.3 and returned to growth room conditions for 24 hours. The remaining seedlings were inoculated with sterile tap water, as a control, and returned to the same growth room conditions. All seedlings were subsequently harvested into X-gluc (Section 2.6) and incubated for five hours. Seedlings were then examined for GUS staining and morphological responses using a binocular microscope (Section 2.9) and photographed (Section 2.9).

Nod factor was found to elicit localised responses of GUS within four hours of application and invoke root hair deformations within 16 hours (Figures 4.8 A and C). Activity was elicited in 80% seedlings. Where staining had occurred 24 hpi, it covered much of the nodulation zone (Figure 4.8 B).

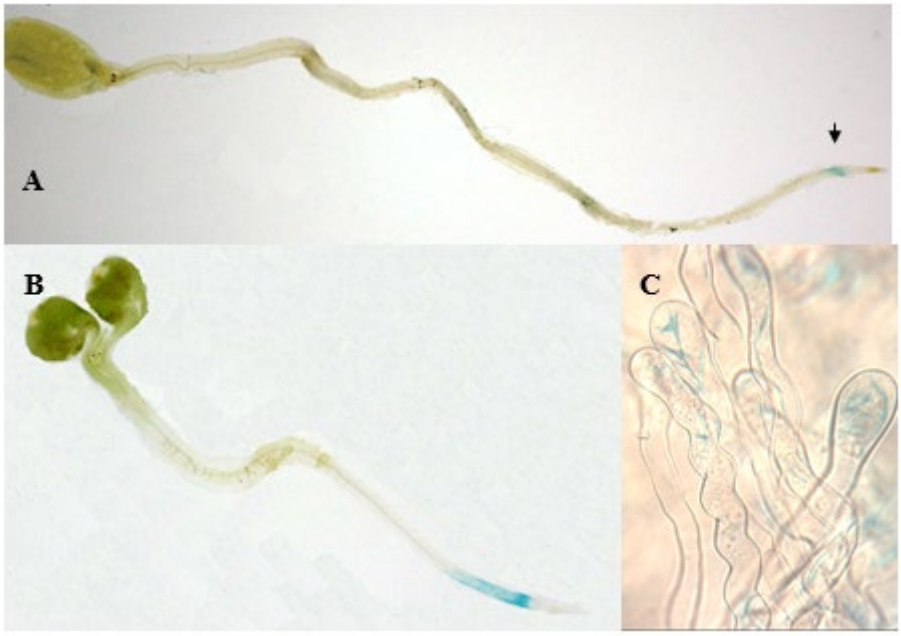

Figure 4.8. *L. japonicus* T90 seedlings inoculated with crude extract of Nod factor showing GUS activity in root tissue. A, 3 ½ hpi; B, 24 hpi; C, root hair deformations at 16 hpi. Magnification x5, x3 and x400, respectively. Arrow indicates point of inoculation of Nod factor 3 ½ hpi.

Chitosan (5mg/ml) also elicited GUS staining in half (n=10) seedling roots. Figure 4.9 shows expression identified on one such root. GUS could clearly be identified in epidermal tissue.

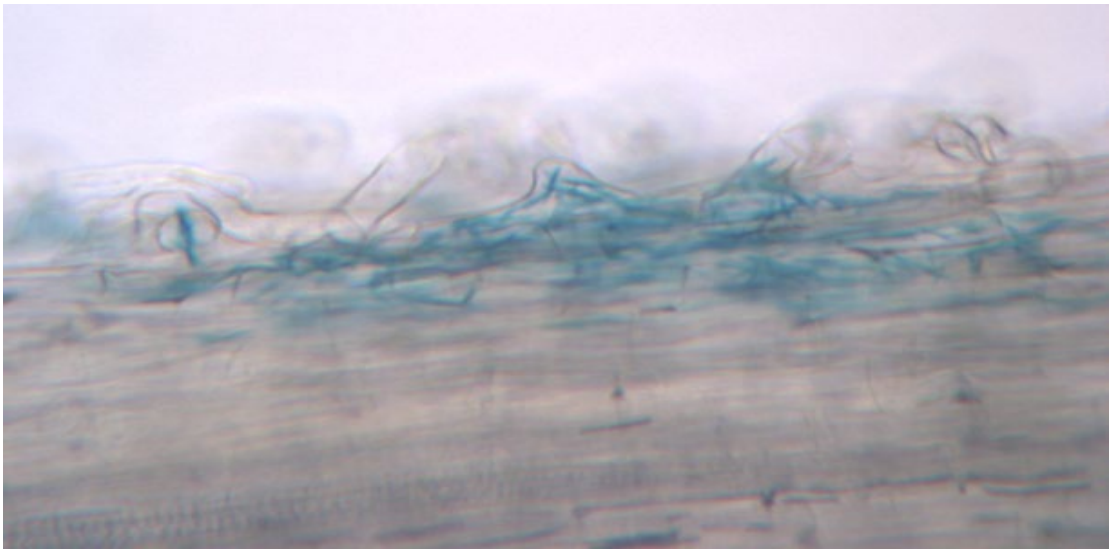

Figure 4.9. GUS activity in *L. japonicus* T90 roots in response to 5mg/ml chitosan. Magnification x90.

4.2.3 GUS activity and the development of nodulation in T90 in response to different rhizobial strains

The elicitation of GUS by crude Nod factor was demonstrated in Section 4.2.2. These Nod factor molecules were derived from *M. loti* and therefore carried the decorations specific for *L. japonicus.* Since chitosan was also shown to elicit GUS activity (Figure 4.9), a question was raised over the specificity of this expression in T90 in relation to different Nod factor decorations. To determine more precisely whether GUS staining was invoked by non *L. japonicus*-specific rhizobia, producing a range of Nod factors and other possible determinants of nodulation, T90 seedlings were inoculated with different rhizobial strains. Nine strains, representing a range of Nod factors with varying structural modifications, were selected from stocks at IGER and the United States Department of Agriculture (USDA), Beltsville, U.S.A., and used to compare and contrast the expression elicited by *M. loti.* The selection of strains was based on accumulated data on Nod factor structures, for example, strains that appeared to produce structures similar to those produced by *M. loti,* as well as those providing substantial variation. This work may also contribute to a better understanding of the role Nod factors play in determining host-specificity in nodulation. The timing of the appearance of GUS activity, root hair deformations, nodule primordia and nodules was also recorded to compare with results from Section 4.2.1. Data relating to Nod factor structure were used to compile Table 4.1.

Approximately 600 *Lotus japonicus* T90 seeds were prepared as in Section 2.4.5a. Approximately 60 seeds were sown into each of 10 Phytatrays II™. In order to verify that rhizobial contamination was not present prior to any of the inoculation treatments, a contamination check was carried out on day 5 (Section 2.5.1). Seedlings were inoculated (Section 2.5.1 Method 2) with one of the rhizobial species per tray, including the *M. loti* control rhizobium. Strains 3211 and 3824 had not grown sufficiently on the TY plates, therefore the inoculum was made straight from the agar slope.

Table 4.1. Rhizobial strains, their host plants (as recommended by the USDA) and details of the structural decorations of related Nod factors.

Rhizobial species/strain	Host plant	Nod factor Acyl chain	Specific decorations[1]
Mesorhizobium loti NZP2235	*Lotus japonicus*	C18:0 C18:1	R1, Me; R2, Cb; R3, H; R4, AcFuc; R5, H; R6, OH
Bradyrhizobium lupinus USDA 3211	*Lupin* spp.	-	-
Rhizobium leguminosarum bv *viciae* USDA 1001	Pea (*Pisum*) Vetch (*Vicia*)	C18:1 C18:4	R1, H; R2, OH; R3, Ac; R4, Ac;R5, H; R6, Fuc
Bradyrhizobium japonicum USDA 3442	Soybean (*Glycine max*) cv Hardee	C16:0 C16:1 C18:1	R1, H; R2, OH; R3H; R4, MeFuc; R5, H; R6, OH[2]
B. japonicum USDA 3407	Soybean (*Glycine max*)	C16:0 C16:1 C18:1	R1, H; R2, OH, AC, H; R3, H; R4, MeFuc; R5, H; R6, OH[2]
B. elkanii USDA 61	Soybean (*Glycine max*)	C18:1	R1, Me, H; R2, Cb, H; R3, Ac, H; R4, MeFuc; R5, H; R6, OH
S. fredii USDA 257	Soybean (*Glycine max*)	C18:1	R1, H; R2, OH; R3, H; R4, Fuc, MeFuc; R5, H; R6, OH
Bradyrhizobium vigna USDA 3824	Peanut (*Arachis hypogaea*)	-	-
Rhizobium broad host range sp. NGR234 USDA 4146	Broad host range	C16:1 C18:0 C18:1	R1, Me; R2 Cb, OH; R3, Cb, H; R4, MeFuc, AcMeFuc, SMeFuc; R5, H; R6, OH
Rhizobium etli USDA 9032	*Phaseolus* spp.	C18:1 C18:0	R1, Me; R2, Cb, OH; R3, H; R4, AcFuc; R5, H; R6, OH

[1]-For overall structure see Figure 1.3. Abbreviations: Ac, acetyl; Cb, carbamoyl; Fuc, fucosyl; H, hydrogen; Me, methyl; MeFuc, methylfucose; S, sulphate.

[2]Exact details of Nod factor structures are not available but are likely to be similar to *B. japonicum* USDA110, as indicated.

- Nod factor structure unknown.

Data extracted from Broughton and Perret, 1999 and Perret *et al*., 2000.

Four to five seedlings from each tray were stained in X-gluc (Section 2.6) at 7, 14, 21 and 38 dpi. Seedlings at 7, 14 and 21 dpi were mounted on slides, examined for staining, nodule primordia and nodule numbers using a light microscope (Section 2.9). Seedlings at 38 dpi were photographed (Section 2.9) and are shown in Figure 4.10 A-E and microscope images were captured (Section 2.9) at 3, 7, 14 and 21 dpi (Figures 4.11 to 4.13).

Table 4.2 provides a general summary of the key infection-associated events observed in this experiment. All strains elicited some GUS activity in T90 and all but one strain, *R. leguminosarum* bv *viciae*, induced root hair curling. This strain was, however, still able to elicit hair branching (Figure 4.12 C). Three out of the nine strains, *B. lupinus*, *Rhizobium* sp. NGR234 and *R. etli*, were able to form nodule structures (see Figures 4.10 B and D and Table 4.2). None of the nodules formed were tested for N-fixation but they were pink in colour which is usually a reliable indication of the presence of leghaemoglobin and, therefore, N-fixation (Judith Webb, personal communication).

Examination of the samples taken from each of the different rhizobial treatments revealed that in four cases contamination was present. These contaminants were not identified, but were later re-inoculated onto ten T90 seedlings (Section 2.5.1) and found not to elicit visible GUS activity. However, it should be borne in mind that although none of these contaminants alone elicited GUS, some accumulative effects in the presence of the rhizobial strains could have generated misleading GUS data.

Control seedlings inoculated with *M. loti* did not show an identical pattern of GUS activity to that observed by Webb *et al.* (2000), although growth conditions were not identical and a different strain of *M. loti* was used. Webb *et al*. (2000) used NZP2037, which carries an additional carbamoyl group on the non-reducing terminal residue (López-Lara *et al*., 1995) and may therefore induce a slightly different pattern of expression compared with NZP2235, certainly it is a slower nodulating strain.

Table 4.2. Summary of events in nodulation following inoculation of *L. japonicus* T90 line with different rhizobial strains.

Rhizobial species	Time			
	3 dpi	7 dpi	14 dpi	21 dpi
Mesorhizobium loti NZP2235	Abundant GUS, hair deformations and hair curling.	Nodule primordia, abundant hair deformations and curling.	1 young nodule, 2 more mature.	Several mature nodules, one with diminished GUS, still hair deformations and hair curling.
Bradyrhizobium lupinii USDA 3211	As above.	Possible nodule primordia and focalising of staining as above. Staining patchier than above.	Still abundant hair curling, several young nodules.	Some nodules of maturity, still abundant hair deformations and curling.
Rhizobium leguminosarum bv viciae USDA 1001	Rare and pale GUS, hardly noticeable and no obvious hair deformations, some root hair swelling.	More GUS (still pale) and more swelling. One hair curling.	Similar to 7 dpi, no hair curling noticed and very little GUS.	Where GUS is present it is stronger than previously, no hair curling.
B. japonicum cv Hardee USDA 3442	Patchy GUS and hair curling.	As 3 dpi.	Very little staining.	Quite dark GUS in places but patchy.
B. japonicum USDA 3407	Faint GUS, some hair swelling.	Patchy GUS, some hair curling in one patch.	Still patchy, more areas of hair curling.	As 14 dpi.
B. elkanii USDA 61	Generally patchy and pale GUS, one root hair swelling. Patch of stronger GUS with lots of hair curling.	Pretty strong GUS in places with abundant hair curling.	Dark patches of GUS, abundant hair curling.	Little patches look like nodule primordia. Other areas more like a 7/14 dpi dark stain. Abundant hair curling.
Sinorhizobium fredii USDA 257	Intermediate staining, some patches with hair deformations and hair curling.	Some quite dark areas that could be nodule primordia.	Paler than 7 dpi.	Plenty of nodule primordia, which seem smaller and closer to vasculature, but no nodules.
B. vigna USDA 3824	Very little and pale GUS, no hair curling seen.	More obvious, darker GUS, still patchy, some hair curling in those patches.	Not much GUS but on 1 root two stronger patches with nodule primordia.	Several nodule primordia.
Broad host range *Rhizobium* NGR234	General patchy staining, not much hair curling.	Much more staining abundant hair curling, some nodule primordia.	Lots of nodule primordia and young nodules, two with diminished GUS.	Still more young nodules and nodule primordia, only one mature nodule in four roots.
R. etli USDA 9032	Very faint GUS, some hair swelling and hair deformations.	Heavier but patchy staining, two areas with abundant hair curling, otherwise low numbers hair curling.	One fairly advanced nodule primordium.	Some nodule primordia and one nodule.

The pattern of GUS activity observed in seedlings inoculated with *M. loti* correlated to certain infection events observed by microscope. For instance, root hair deformation activity (3 dpi) was accompanied by generalised staining throughout epidermal cells, whilst the occurrence of cortical cell division (7 dpi) corresponded with generally patchier staining throughout the root, but intensifying at sites of cell division (Figures 4.10 A and 4.11). Roots with mature nodules (38 dpi) showed distinct, focal staining in the nodule area only (Figure 4.10 A).

A correlation of GUS expression patterns and associated infection events was also identified in seedlings inoculated with different rhizobial strains, as it was with seedlings inoculated with *M. loti*. The patterns described are typical of those seedlings examined and represent four to five seedlings. Those strains inducing only low to moderate hair deformation induced low to moderate GUS expression. For example, *R. leguminosarum* bv *viciae* (USDA 1001) elicited minimal GUS activity (Figure 4.10 C) and appeared to elicit only root hair swelling and branching (Figure 4.12 C); no root hair curling or subsequent stages indicative of the progression of nodulation were observed. In those strains inducing nodules, *B. lupinus*, *Rhizobium* sp. NGR234 and *R. etli* (Figure 4.10 B, D and E), much stronger GUS staining was elicited in the early stages and continued in a similar pattern to that induced with *M. loti* (Table 4.2). Figure 4.10 D shows an exceptionally high number of nodules on a seedling inoculated with *Rhizobium* strain NGR234 38 dpi, which was not typical of other seedlings inoculated with this or any other strain.

In addition to the three strains that could elicit nodules, three further strains were able to induce nodule primordia by 14 or 21 dpi, but failed to induce nodules even after 38 dpi. These strains were B. elkanii (USDA 61) (Figure 4.13 A and B), S. fredii (USDA 257) (Figure 4.13 C and D) and B. vigna (USDA 3824).

This and following two pages: Figure 4.10. GUS staining in *L. japonicus* T90 seedlings inoculated with different rhizobial strains. A, *Mesorhizobium loti* strain NZP2235; B, *Bradyrhizobium lupinus*; C, *Rhizobium leguminosarum* bv *viciae*; D, *Rhizobium* broad host range sp. NGR234; E, *Rhizobium etli*.

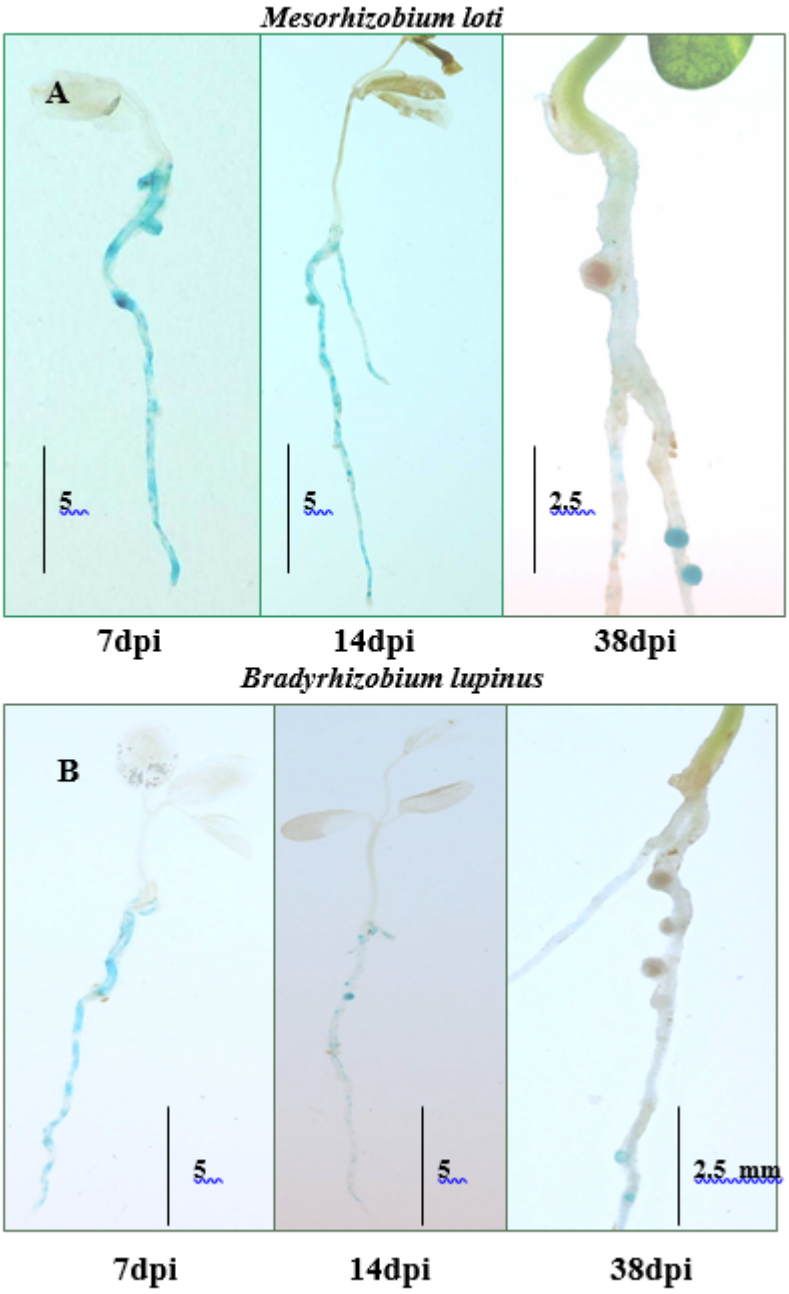

Rhizobium leguminosarum bv *viciae*

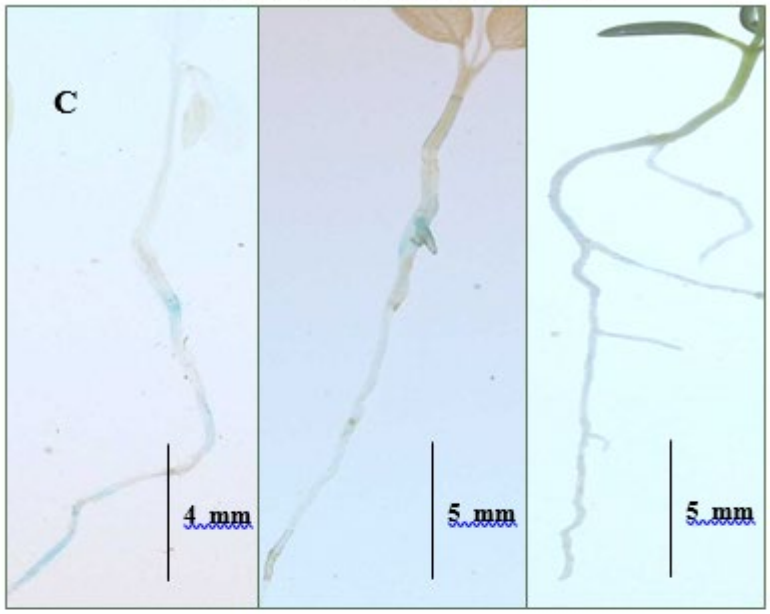

7dpi 14dpi 38dpi

Broad Host Range NGR234

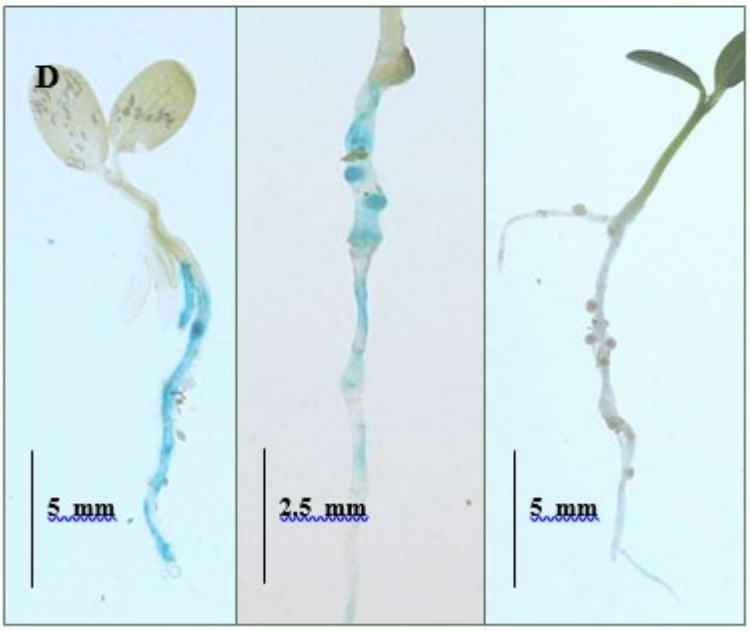

7dpi 14dpi 38dpi

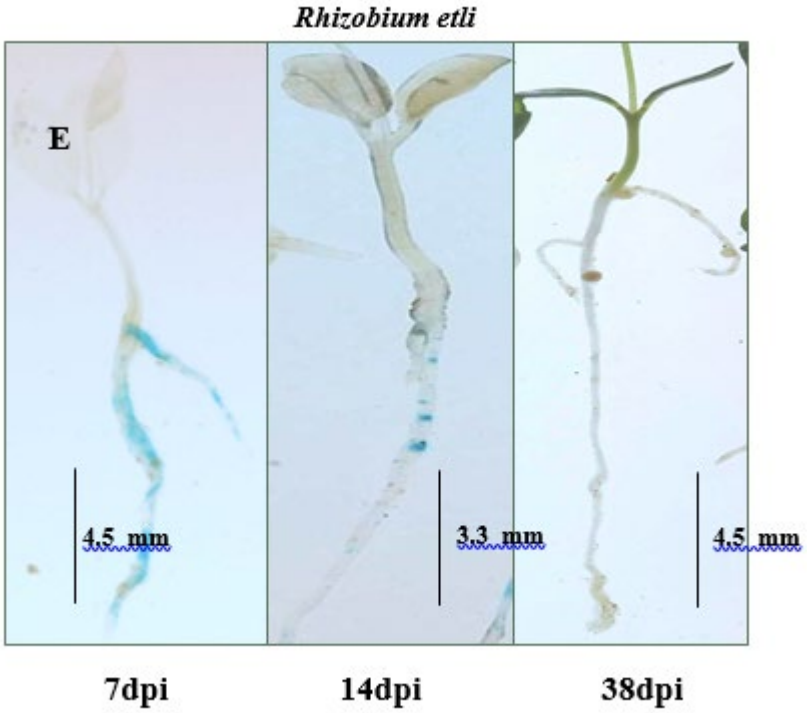
Rhizobium etli
E
4.5 mm
3.3 mm
4.5 mm
7dpi
14dpi
38dpi

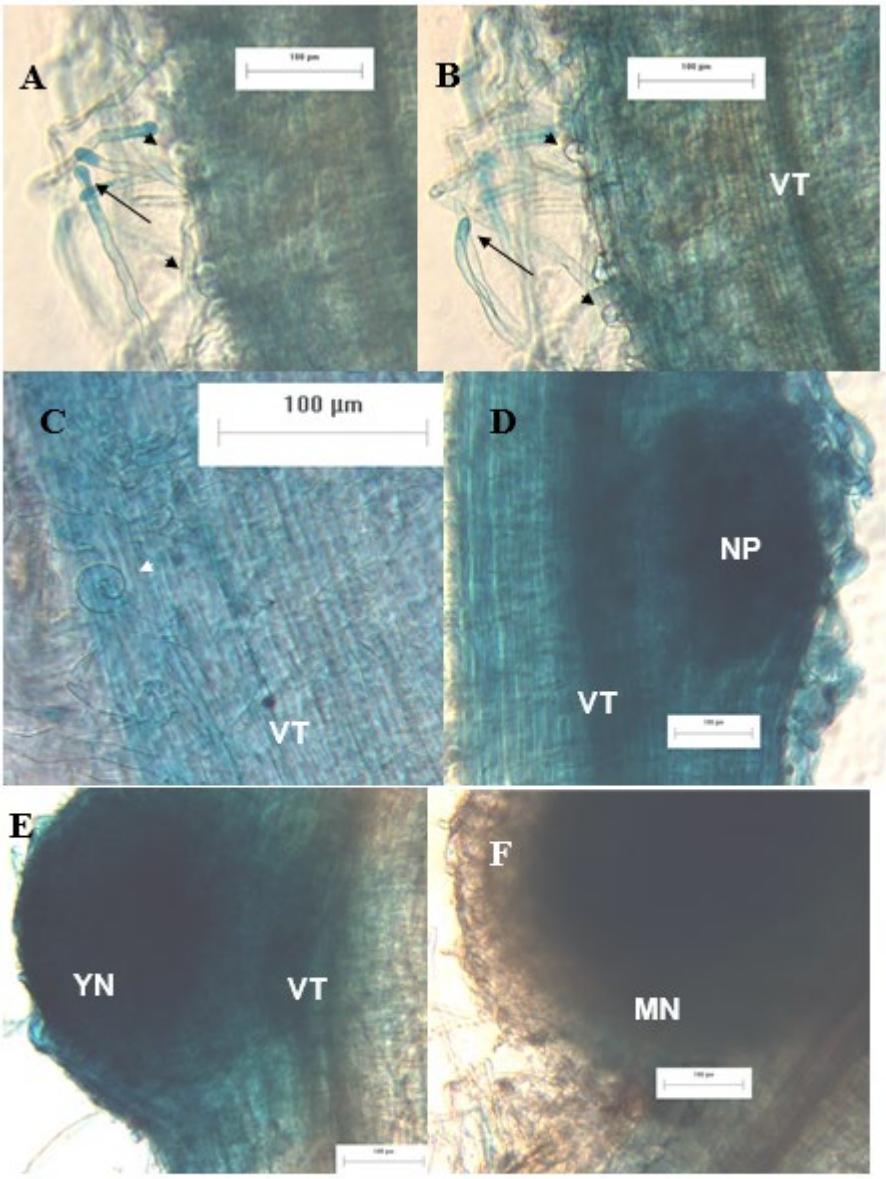

Figure 4.11. Pattern of GUS activity in *L. japonicus* T90 seedling roots inoculated with *M. loti* strain NZP2235 3, 7, 14 and 21 dpi. A and B, different focal plane of same frame 3 dpi showing root hair curling (arrowheads) and GUS crystals in root hairs (arrows) (x1300 magnification); C, (x180 magnification) shepherds crook 7 dpi; D-F (x17 magnification) D, nodule primordium 14 dpi; E, 21 dpi young nodule and F, mature nodule showing diminished GUS activity. (VT) vascular tissue, (YN) young nodule, (MN) mature nodule.

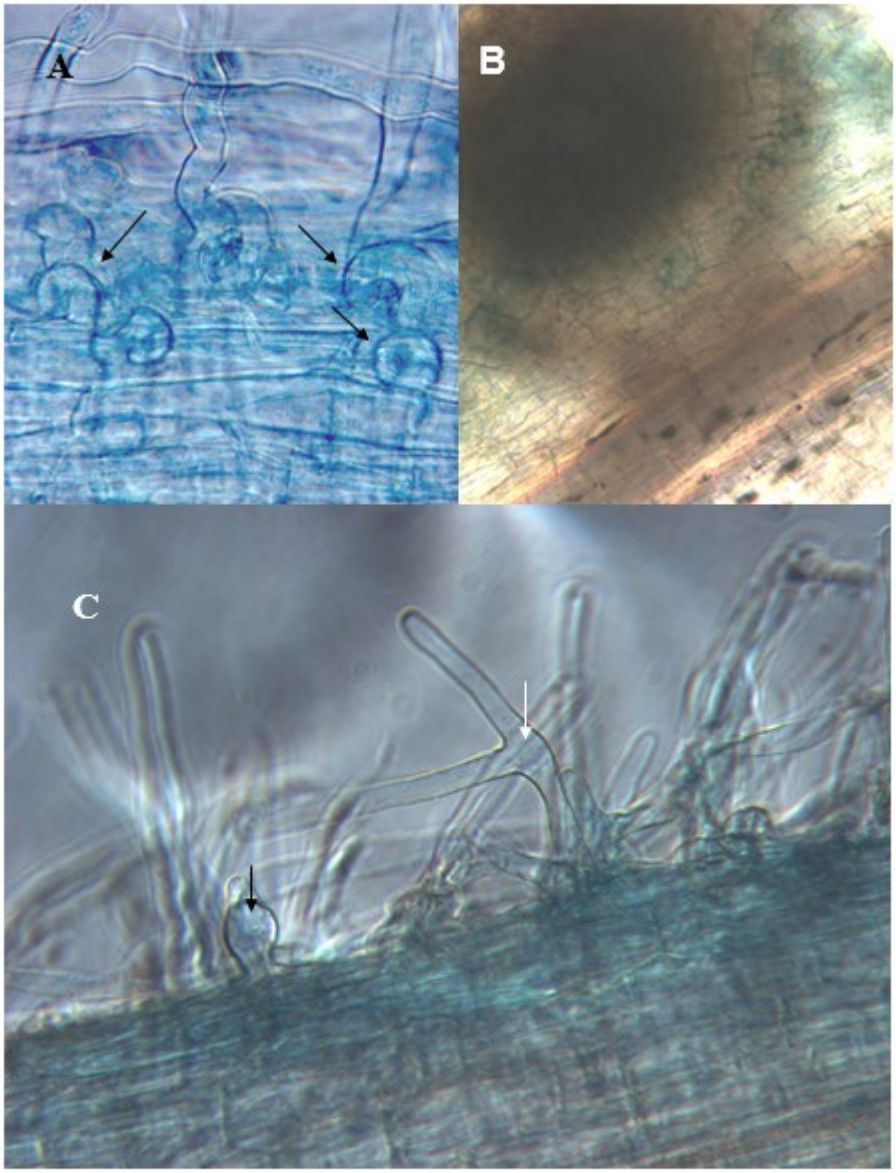

Figure 4.12. Microscopic analysis of GUS activity in *L. japonicus* T90 seedling roots inoculated with different rhizobial strains. A and B, *B. lupini* (USDA 3211) root hair curling (arrows) 3 dpi and mature/senescing nodule 21 dpi, respectively (x260 and x17 magnification, respectively); C, root hair swelling (black arrow) and branching (white arrow) (x260 magnification) in root inoculated with *R. leguminosarum* bv *viciae* (USDA 1001).

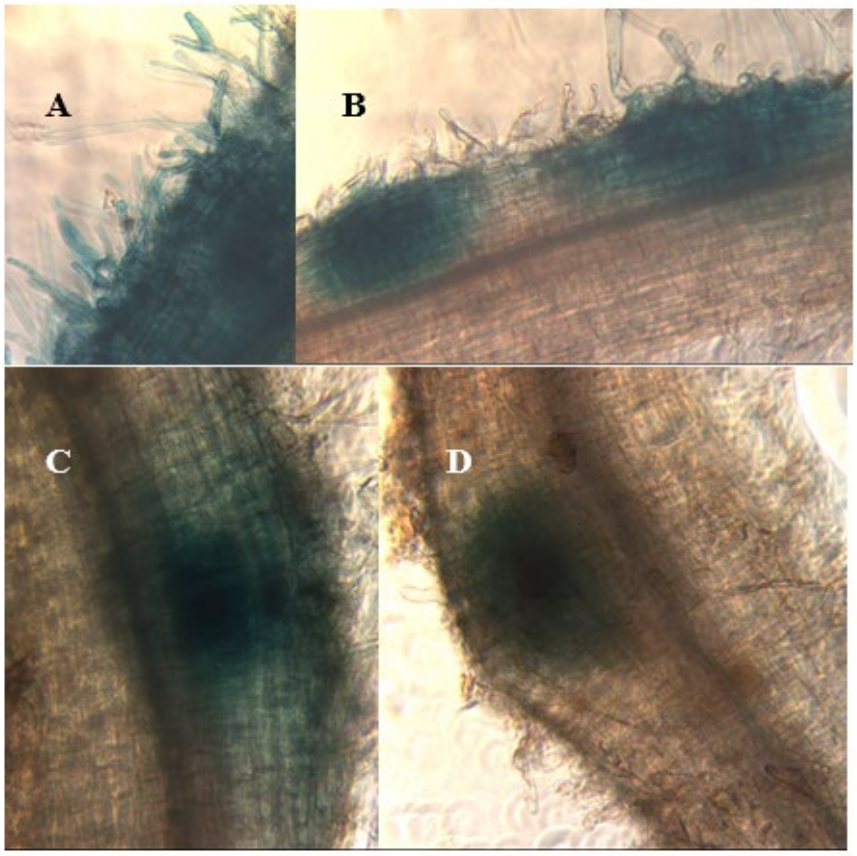

Figure 4.13. Pattern of GUS staining in *L. japonicus* T90 seedling roots inoculated with different rhizobial strains. A and B, moderate level GUS activity with *B. elkanii* (USDA 61) (A) hair deformations 3 dpi and (B) small nodule primordium 21 dpi . (A) and (B) are characteristic of the expression pattern 3 and 7 dpi with NZP2235. C and D, nodule primordium 21 dpi with *S. fredii* (USDA 257). The primordium shown in (B, C and D) are the most advanced stage of nodular development either of these strains appeared to reach in *L. japonicus*. All magnifications x100.

4.2.4 Effect and mechanism of Ca^{2+} on GUS activity

The effects of $CaCl_2$, EGTA and the ionophore A23187 were assessed. In addition, experiments to characterise the types of channels that may be employed in *L. japonicus* during its interaction with *M. loti* were also conducted.

Blockers of different types of Ca^{2+} channel (Section 4.1.5) provide an opportunity to study Ca^{2+} systems in *vivo*. Three such channel blockers are verapamil, ruthenium red and nifedipine. Each of these antagonists of Ca^{2+}-signalling has a different mode of action. Verapamil (a phenylalkylamine) and nifedipine (a 1,4-dihydropyridine) each have a unique binding site on the α_1-subunit of L-type Ca^{2+} channels. Verapamil binds to a site located deep within the pore of the Ca^{2+} channel and is therefore more effective when the channel opens regularly, whilst nifedipine binds better to depolarised cells (Ferrari *et al*., 1994; as cited in Piepho, 2003). Ruthenium red has an entirely different mode of action and appears to inhibit the release of Ca^{2+} from intracellular stores (Zucchi and Ronca-Testoni, 1997). Although it has not yet been demonstrated whether L-type channels exist in plant systems and most of the work involving Ca^{2+} channels has been carried out on animal systems, the above inhibitors of Ca^{2+} have been successfully used in plants (Pingret *et al*., 1998; Kenton *et al*., 1999).

T90 seedlings were treated according to Section 2.5.4 and were then transferred into 24-well microplates (Iwaki, Asahi Techno Glass, Japan), three seedlings per well, containing either 0, 0.1, 1.0 or 10mM $CaCl_2$, or one of the $CaCl_2$ treatments plus 0.5mM EGTA or 20µM A23187, or both. The same experiments were repeated using *M. loti*, prepared as in Section 2.5.1 Method 2. In total, four experiments (A-D) were conducted as shown below. An identical experiment to 'B' was set up as a control using wild-type 'Gifu' seedlings. Experiment A included 0, 0.1, 1.0 and 10mM $CaCl_2$, using three wells per treatment. Experiment B included 0 and 10mM $CaCl_2$ alone, or with 0.5mM EGTA and/or 20µM A23187, using two wells per treatment at 0mM $CaCl_2$ and four wells at 10mM $CaCl_2$. Experiment C included 0, 0.1, 1.0 and 10mM $CaCl_2$ alone, or with 0.5mM EGTA and/or 20µM A23187, using two wells per treatment. Experiment D was set up as Experiment C, but included *M. loti*. Originally, two wells per treatment were used

although these samples were pooled for ease of analysis. After treatment, each medium was removed using a sterile pipette and replaced with X-gluc (Section 2.6). Seedlings were then incubated for five hours and shoot and root tissue was subsequently examined for histochemical activity using a binocular microscope (Section 2.9). *M. loti* bacteria, sub-cultured as in Section 2.5.1 Method 2, were incubated in solutions of 0.5mM EGTA and 20µM A23187 and in the highest concentrations of each of the Ca^{2+} channel blockers at 28ºC in order to ascertain whether these chemicals had any adverse affect on bacterial growth. After 3 days spectrophotometer readings were taken on each sample at 600nm, using a Philips PU 8720 UV/VIS scanning spectrophotometer (Philips Electronics U.K. Ltd, Croydon, U.K.).

Neither EGTA, nor A23187 was found to have any adverse effect on the growth of rhizobia. Ruthenium red, however, was found to inhibit rhizobial growth (data not shown).

Statistical analyses (Section 2.10) relating to shoot tissues were based only on the presence or absence, not the extent, of GUS staining. The total number of seedlings and the number showing expression were recorded for each well. Binomial regression using the logit link function was used to evaluate the effect of the various treatment factors on the proportion of seedlings showing expression. Statistical analysis was carried out according to Section 2.10. Images were captured using a digital camera (Section 2.9).

The data are presented in two parts, the first relating to experiments using varying levels of $CaCl_2$, with and without EGTA and ionophore, and the second relating to the use of the Ca^{2+} channel blockers.

In each of the experiments A-D GUS activity was observed in isolated shoot tissue in a Ca^{2+}-dependant manner. Root-specific GUS activity was not observed in any of the Ca^{2+} treatments that did not include rhizobium (data not shown). However, the tissue-specific effect of Ca^{2+} in shoots versus uninoculated roots may simply reflect different penetration rates of the two tissues. Staining was also observed occasionally in the membranous tissue within the endosperm (data not shown).

In Experiment A the observed proportion of seedlings showing staining was 0, 11, 44 and 56 per cent for the 0, 0.1, 1.0 and 10mM levels, respectively. The number of seedlings staining for GUS increased ($P<0.05$) with increasing $CaCl_2$ concentration. Seedlings exposed to 0mM and 1mM $CaCl_2$ are shown in Figure 4.14 A and B, respectively, where GUS activity can clearly be identified in young shoot tissue treated with 1mM $CaCl_2$.

Based on fitted values, in the absence of EGTA, the presence of $CaCl_2$ increased activity from 8 to 46 percent ($P<0.10$) in Experiment B, while the presence of EGTA at 10mM $CaCl_2$ reduced expression from 55 to 12 % ($P<0.05$). Consistent with findings in experiment A, in the absence of EGTA the presence of $CaCl_2$ increased ($P<0.05$) activity. Similarly, the main effects of either $CaCl_2$ or EGTA were not statistically significant ($P>0.05$) but the interaction between $CaCl_2$ and EGTA was ($P<0.05$). In the first instance the data were analysed as a 2 x 2 x 2 factorial design (two concentrations of $CaCl_2$ x presence/absence EGTA x presence/absence A23187). There was no statistical evidence ($P>0.05$) to suggest that the ionophore A23187 increased the number of seedlings exhibiting GUS and in view of slight overdispersion in the data, the analysis was repeated excluding the effects of A23187 and its interactions with $CaCl_2$ and EGTA.

In Experiment C several treatment combinations showed either a complete absence of staining or 100 percent of seedlings showed GUS activity. Figure 4.15 illustrates the observed percentage of seedlings showing GUS staining under different concentrations of $CaCl_2$, EGTA and A23187. The data were analysed using a 4 x 2 x 2 factorial design (four concentrations of $CaCl_2$, presence/absence EGTA, presence/absence A23187). The statistical analysis suggested a) that there was no main effect of $CaCl_2$ ($P>0.05$), b) that the presence of ionophore A23187 increased the number of GUS exhibiting seedlings from

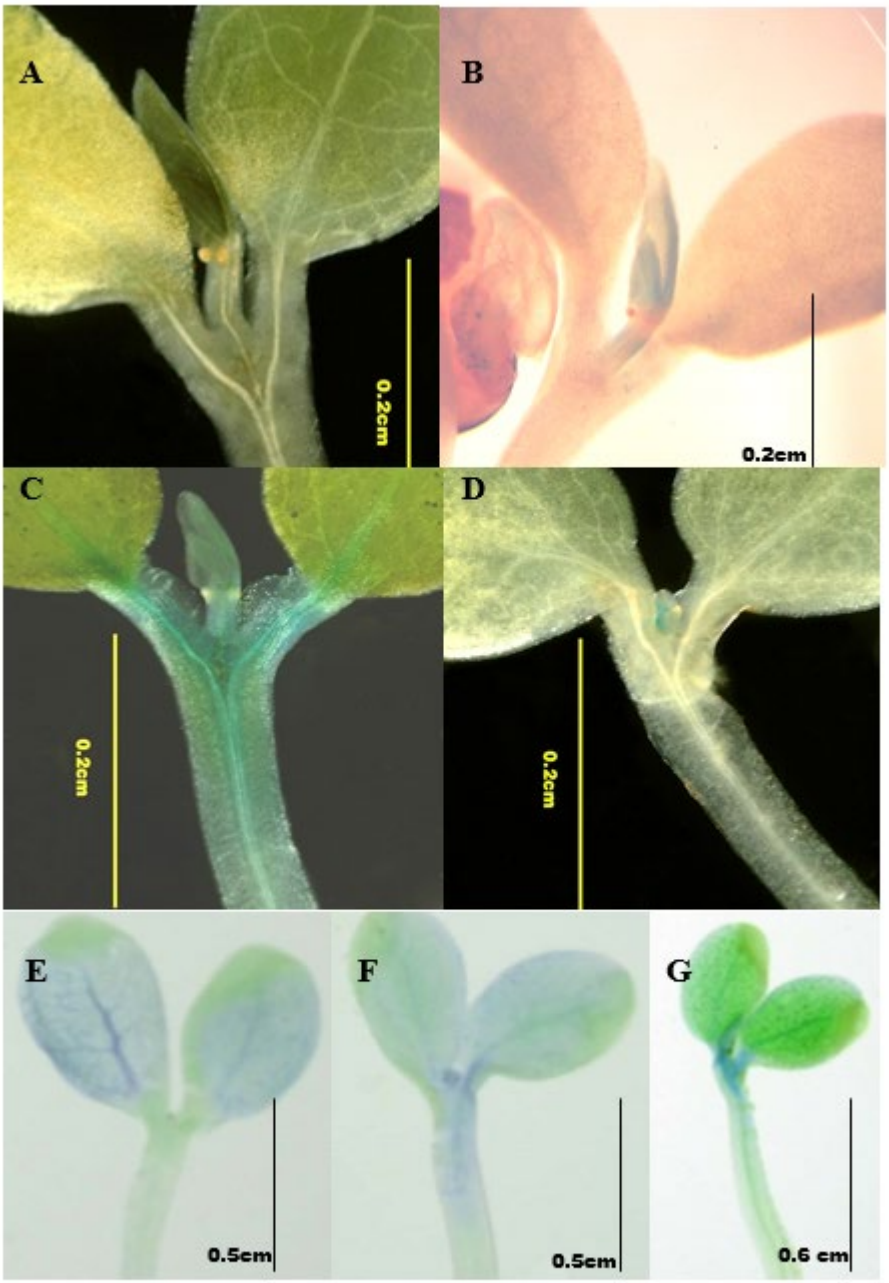

Figure 4.14. GUS activity in *L. japonicus* T90 shoot tissue following exposure to different levels of Ca^{2+}, EGTA and A23187. A, 0mM $CaCl_2$; B, 1.0 mM $CaCl_2$; C, 1.0mM $CaCl_2$ + 0.5mM EGTA; D, 10mM $CaCl_2$ + 20µM A23187; E and F, 1mM $CaCl_2$ + 0.5mM EGTA; G, 0mM $CaCl_2$ + 0.5mM EGTA.

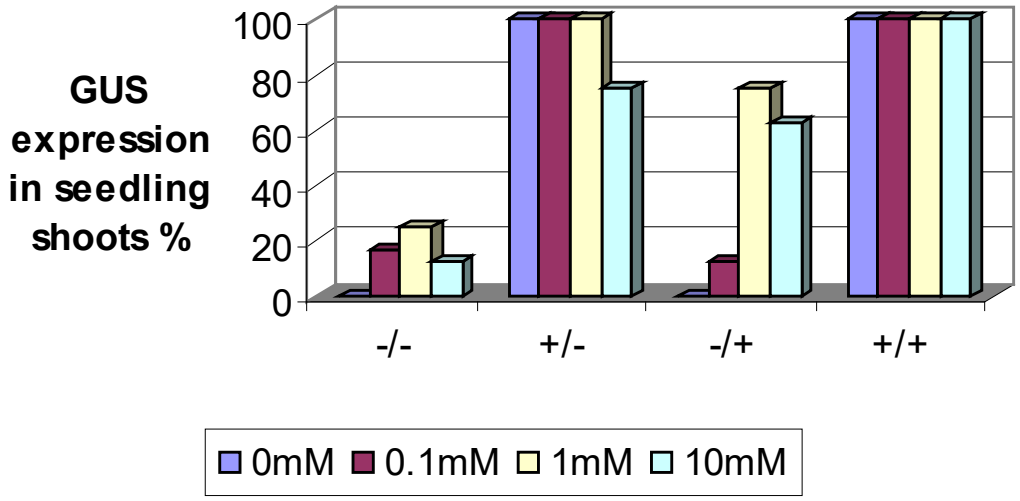

Figure 4.15. Observed effects of $CaCl_2$, EGTA and A23187 on GUS activity in *L. japonicus* T90 shoot tissue, Experiment C. -/-, no EGTA or A23187; +/-, EGTA without A23187; -/+ A23187 without EGTA; +/+, both EGTA and A23187. The data represent the mean of two replicates.

55.8 percent to 69.4 percent (data not shown) ($P<0.05$) and c) that there was a significant ($P<0.05$) interaction between $CaCl_2$ and EGTA. Low replicate numbers (n=2) were used in this experiment, although in this case n=number of wells, not seedlings (these were three per well). In addition, there was also low between-replicate variation. It therefore was not possible to make specific comparisons between treatments since these must be made on the logit scale. Figure 4.14 C illustrates the pattern of GUS activity typically observed in shoot tissue in the presence of 0.5mM EGTA and low (0.1mM) $CaCl_2$. Figure 4.14 D shows a smaller area of staining in shoot tissue exposed to 10mM $CaCl_2$ and the ionophore A23187. Based only on trends in the observed values, the presence of $CaCl_2$ elicited GUS, but the effect was not as pronounced as the higher concentrations compared with experiments A and B. Presence of EGTA increased the proportion of seedlings staining for GUS dramatically. With the exception of one replicate for the 10mM $CaCl_2$/EGTA combination, 100 percent of seedlings in all wells treated with EGTA showed GUS activity. Presence of the ionophore in the absence of EGTA increased activity only with $CaCl_2$ concentrations of 1 or 10mM. In error, data for the two replicates for each treatment combination were merged. This prevented full statistical analysis of the data.

Experimental design for D did not permit the use of any statistical analysis. However, many of the trends shown in Experiment C were also identified in Experiment D shoots (Figure 4.16). The observations were a) an increase in the number of GUS positive seedlings with 1mM and 10mM $CaCl_2$ in the absence of EGTA, b) a reduction in staining in the presence of EGTA in the highest concentration of $CaCl_2$ and c) an increase in staining in response to the ionophore. Examples of the expression observed in tissues treated with two different concentrations of $CaCl_2$ and 0.5mM EGTA can be seen in Figures 4.14 E to G and Figure 4.17 D.

GUS activity in root tissue in Experiment D, in the presence of *M. loti* bacteria, also appeared to increase with increasing Ca^{2+} concentration in the absence of EGTA and ionophore (Figure 4.17 A). In contrast to shoot tissue, the presence of EGTA appeared to abolish GUS activity, both in the low and high

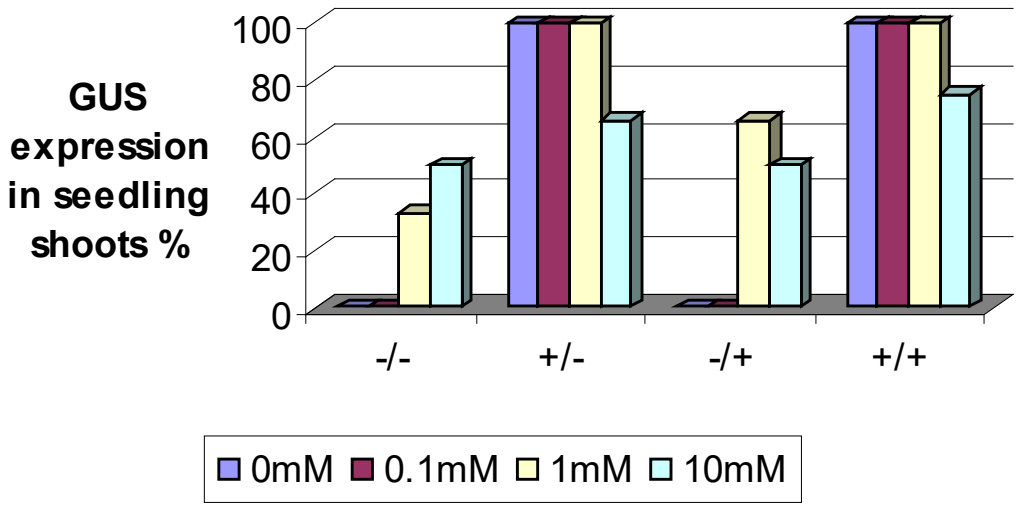

Figure 4.16. Observed effects of $CaCl_2$, EGTA and A23187 plus *M. loti* on GUS activity in *L. japonicus* T90 shoot tissue. Experiment D. -/-, no EGTA or A23187; +/-EGTA without A23187; -/+ A23187 without EGTA; +/+, both EGTA and A23187.

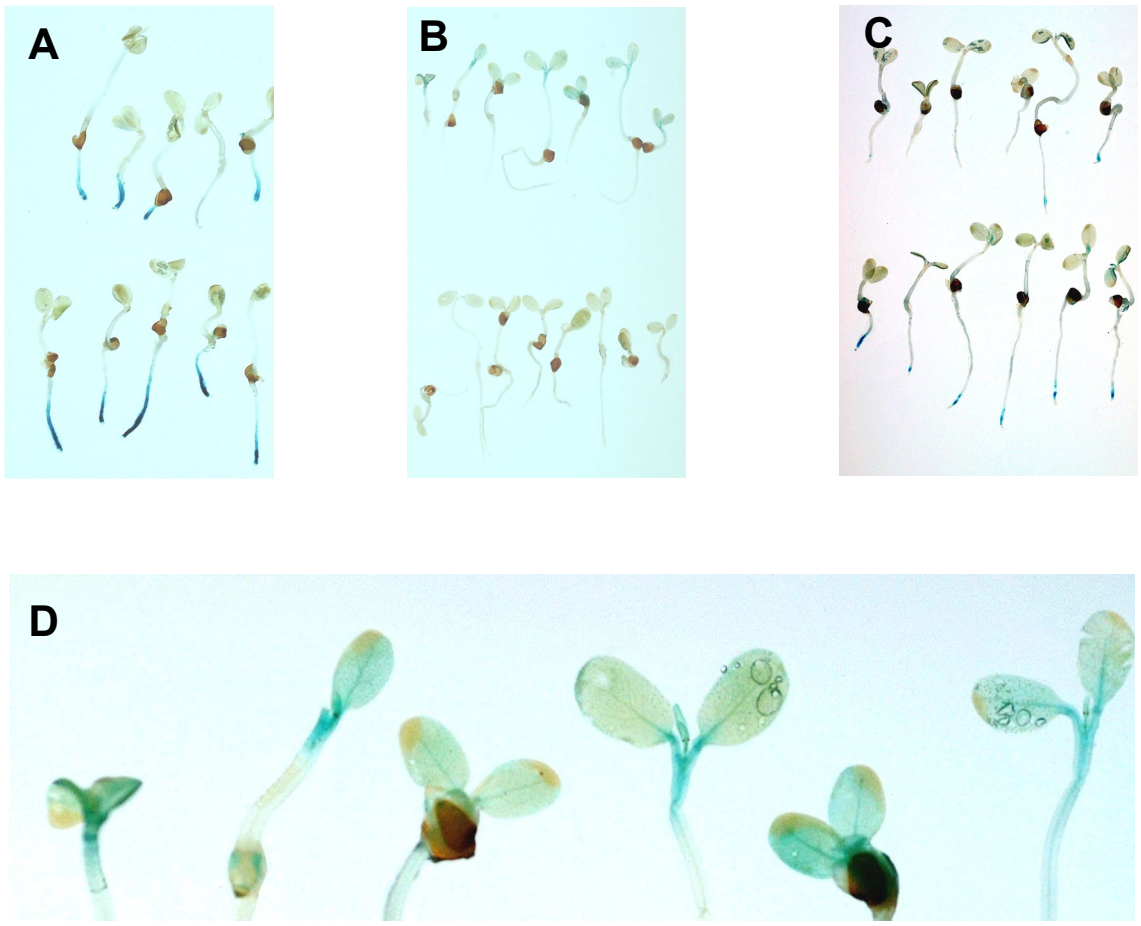

Figure 4.17. GUS activity in *L. japonicus* T90 roots and shoots following inoculation with *M. loti* and exposure to Ca^{2+}, EGTA and A23187. A, 0.mM (top) and 10mM (bottom) $CaCl_2$; B, 0.1mM (top) and 10mM (bottom) $CaCl_2$ + 0.5mM EGTA; C, 0mM (top) and 10mM (bottom) $CaCl_2$ + 20µM A23187; D, close-up of shoots from B (top) showing GUS staining in shoots. Magnifications: A-C x1.4; D x7.

levels of $CaCl_2$ (Figure 4.14 B). The presence of A23187 resulted in an increase in GUS staining in the higher concentrations of $CaCl_2$ (Figure 4.17 C). The increased activity of GUS in shoot tissue in response to elevated Ca^{2+} levels is consistent with the *gus* gene acting as a reporter for a downstream gene (*LjCbp1*) that is involved in Ca^{2+} signalling. These data are further supported by the increased activity observed in root tissues inoculated with *M. loti* in the presence of increased $CaCl_2$ (Figure 4.17 A). Statistical data suggest a role for the ionophore A23187 in enhancing GUS activity in shoot tissue in Experiment C and an increase in GUS is also shown in root tissue with A23187 at the higher level of $CaCl_2$ (Figure 4.17 C). These data were not consistent however, as statistical analysis revealed that the presence of A23187 did not significantly ($P>0.05$) affect GUS activity in Experiment B.

In summary, although GUS activity in shoot tissues is variable, both shoot and root activity appears to be influenced in a Ca^{2+}-dependent manner. This suggestion was substantiated by the added effects of EGTA. The limitations of the experiments in scoring the presence or absence, rather than the level of staining and low level of replicates, however, convey these data as preliminary investigations only.

Neither EGTA nor A23187 were found to be detrimental to rhizobial growth, nor was there any indication of toxicity to the plant. No staining was identified in any of treatments in the wild-type control seedlings.

Verapamil had no observable effect on GUS activity in T90 seedlings at any concentration; all seedlings stained for GUS to a similar level (data not shown). GUS staining in both nifedipine and ruthenium red was markedly affected by the two higher concentrations. GUS activity was not observable with either 1.0 or 5mM nifedipine and only slightly in the 1μM treatment of ruthenium red. However, growth of rhizobial cultures in the highest concentrations of ruthenium red, but not verapamil or nifedipine, were adversely affected (data not shown); conclusions regarding the effect of ruthenium red at this stage cannot therefore be drawn.

4.2.5 GUS activity in response to hormones and the nitric oxide donor, SNP.

The implied involvement of various signalling molecules in the early stages of the symbiosis has been described earlier (Section 1.5). In order to determine a potential role for such molecules in T90 *gus* expression a range were tested in exogenous application.

T90 seedlings were prepared as in Section 2.4.5d and placed in the CER (Section 2.4.5) for 7 days. Between six and nine seedlings were transferred into 24-well microplates (Iwaki, Asahi Techno Glass, Japan) containing one of the treatments detailed in Section 2.5.5. The treatments included synthetic hormones, these were: naphthalene acetic acid, 2,4-dichlorophenoxy acetic acid, aminocyclopropane-1 carboxylic acid, 6-benzylamine purine and 6-furfurylamino purine. Seedlings were returned to the same controlled environment conditions for 16 hours and then histochemically stained (Section 2.6).

None of the hormonal treatments, nor SNP, elicited any observable GUS activity under the concentrations and conditions used.

4.3 General discussion

This work has demonstrated that GUS activity in T90 responds within eight hours to inoculation with the *L. japonicus* rhizobial symbiont *M. loti*, but also to a number of other factors. These factors include Nod factor derived from *M. loti* strain R7A, to which the response was quicker than that elicited with *M. loti*, chitosan (a crude extract of chitin) and a range of rhizobial strains not specific for the nodulation of *L. japonicus*. In addition, preliminary investigations demonstrate that GUS activity in roots, in combination with rhizobial inoculation, and shoots was affected by different levels of Ca^{2+} in the external media. Finally, the Ca^{2+} channel blocker nifedipine was found to inhibit GUS in roots inoculated with *M. loti* bacteria.

GUS was not visible in histochemically-stained uninoculated seedling roots, although expression of the *gus* gene had previously been molecularly identified in uninoculated roots (Section 3.2.5). Since expression of the *gus* gene appeared to be subject to upregulation following inoculation with *M. loti*, it seems likely that the same upregulation is responsible for the appearance of GUS in histochemically-stained roots at 8 hpi.

Webb *et al.* (2000) reported the failure of the non-nodulating mutant, PN4047, of the *L. japonicus* root-nodulating symbiont, NZP2037, to elicit any visible signs of GUS activity. Strain PN4047 contains a Tn5 mutation in the *nodC* gene and is incapable of producing a Nod factor (Chua *et al*., 1985; Scott *et al*., 1996). This suggests that the GUS activity observed following the inoculation of *M. loti* and other strains of rhizobia is specifically in response to the Nod factor molecules. Furthermore, the elicitation of GUS in response to Nod factor, but not to strain PN4047, suggests that variations in GUS activity following inoculation with the range of rhizobial strains is largely in response to modifications in Nod factor structure. However, differences in bacterial extracellular and lipo-polysaccharides and bacterial/Nod factor affinity for putative binding sites/receptors, as well as the effects of plant chitinases and flavonoids are also likely to affect the passage of bacteria into the plant and therefore potentially result in alternative GUS staining patterns. Interestingly, the possible involvement of the *nolL* gene of *L. japonicus*

in the synthesis of other bacterial molecules, such as extracellular polysaccharides and lipopolysaccharides, was recently suggested (Bras, 2003). In this case the presence of this gene seems likely to be all the more important for both successful nodulation and prolonged GUS activity in T90.

The fact that GUS responds to Nod factor and that this response continues in the nodules provides some evidence that Nod factor production by rhizobium may continue in nodules even towards maturity and is supported by recent publications (Timmers *et al*., 2000; Tsyganov *et al*., 2003). The pattern of staining in response to Nod factor also demonstrates spatial and temporal similarity to that identified in studies in *Medicago* by Pichon *et al*. (1992) and Journet *et al*. (1994). In transgenic *Medicago*, GUS activity directed by either the *MtENOD11* or *MsENOD12* promoter was observed in a localised manner at the site of application of Nod factor within 3-6 hpi Pichon *et al*. (1992) and Journet *et al*. (1994). This implies that the mechanism activating GUS in these cases is non-systemic. *ENOD12* was first identified in *Pisum sativum* and encodes a putative proline-rich cell wall protein that is expressed in cortical cells traversed by infection threads and also in the invasion zone of the nodule (Scheres *et al*., 1990). Subsequent work identified both the *PsENOD12* homologue and a similar gene *ENOD11* in *M. sativa* and *M. truncatula*, respectively Pichon *et al*. (1992) and Journet *et al*. (2001).

The elicitation of GUS following chitosan application could indicate the presence of certain upstream elements responsive to plant chitinases during nodulation. In carrot, a somatic embryo mutant was shown to be rescued by chitinase (de Jong *et al*., 1992), indicating that these molecules may play a role in plant development; tissue-specific induction has also been observed during nodule development in soybean (Staehelin *et al*., 1992; Parniske *et al*., 1994). More recently Ovstyna *et al*. (2000) showed that pea chitinases have the capacity to discriminate between non-modified *R. leguminosarum* bv. *viciae* Nod factors and their derivatives carrying a reducing end substitution. These and other findings have led to speculations that a role exists for chitin derivatives in the signalling of higher plants (Spaink, 1992; Staehelin *et al*., 1994; Ovtsyna *et al*., 2000), perhaps even that they function in processing Nod factors. The analysis of GUS elicitation in

T90 in response to Nod factors bearing different chemical substitutions may add further support to this hypothesis.

Chitin oligomers have already been shown to induce Ca^{2+}-spiking in pea (Walker and Downie, 2000) and in *M. truncatula* (Oldroyd, 2001). Although the upregulation of the *gus* gene demonstrated in Section 3.2.5 is not early enough to be a Ca^{2+}-spiking response, the diversity of Ca^{2+} signalling and these present data imply that a further, downstream Ca^{2+} signalling event has occurred, which is also elicited by chitin. Walker *et al*. (2000) and Shaw and Long (2003) have demonstrated that the two Ca^{2+} responses induced very early in the nodulation process can be uncoupled (Section 3.1.2). Once again, the evidence for multiple signalling pathways is compelling. The putative Ca^{2+} demonstrated by GUS in T90 may indicate a further, downstream Ca^{2+}-spiking or other flux response. A complementary experiment with chitosan should be established using EGTA. If the effects of chitosan were abolished in the presence of EGTA it would provide strong evidence that chitin does elicit a Ca^{2+} response that is reflected in GUS activity. In addition to the elicitation of Ca^{2+}-spiking by chitin oligomers, cortical cell division has also been shown to result from the delivery of such molecules by ballistic microtargetting (Schlaman *et al*., 1997) and in soybean, non-specific chitin pentamers were able to induce *ENOD40* gene expression within 40 hours of inoculation (Minami *et al*., 1996).

The elicitation of GUS in response to chitosan implies that a derivative of chitin itself could be responsible for GUS activity. The means by which chitin elicits a response from the *gus* gene has not been tested. Certainly chitin is a common link between Nod factors and AM fungi. Recently, Kosuta *et al.* (2003) identified the existence of a diffusible factor from AM fungi capable of inducing *ENOD11* expression in *M. truncatula*. This finding supports the hypothesis that a 'Myc' (mycorrhizal) factor, analogous to the rhizobial Nod factor, exists in the mycorrhiza symbiosis. In the Kosuta *et al*. (2003) experiment, other fungal pathogens were found not to elicit *MtENOD11* expression. GUS activity in T90 was found not to be elicited in response to inoculation with powdery mildew (Judith Webb, personal communication). The factor(s) responsible for the

elicitation of both *MtENOD11* expression in Kosuta *et al.* (2003) and *gus* expression in T90 appears to have some symbiosis-specificity.

The fact that all rhizobial strains tested elicited some GUS staining in T90 perhaps suggests that the *gus* gene lies on a different pathway to that required for nodulation, since only four strains (including *M. loti*) were able to form nodules on *L. japonicus*.

B. lupinus normally nodulates lupin but in this study was able to form nodules on *L. japonicus* (Figure 4.10 B). The chemical structure of Nod factors secreted by *B. lupinus* has not yet been determined but sequence data available in Genbank shows the presence of *nodZ* and *nolL* genes implying that the Nod factor produced carries the 4-*O*-acetylated fucose residue also carried by *M. loti* Nod factors. It is therefore perhaps to be expected that this strain successfully nodulated *L. japonicus*. Interestingly, mutations in the *nodZ* and *nolL* genes in *B. lupinus* strain WM9 failed to produce any significant effect on nodulation of lupin plants (Tomasz Stêpkowski, personal communication), implying that these genes play no role in defining host-specificity in the lupin-*B. lupinus* relationship. However, they are known to be important in *M. loti* nodulation of *L. japonicus*. These genes may therefore be involved in deriving a key component in the initiation of signal transduction leading to sustained *gus* expression in T90.

Broad host range *Rhizobium* species NGR234 has been documented as eliciting nodules on *L. japonicus* in a study investigating the viability of bacteroids released from senescing nodules (Muller *et al*., 2001). Similarly, *R. etli* has also been documented as forming nodules on *L. japonicus*. Banba *et al.* (2001) examined nodulation of *L. japonicus* using *R. etli* strain CE3 and identified nodules comparable in timing and frequency to those elicited by *M. loti*. However, 21 days after inoculation these nodules were seen to enter into an early senescence, accompanied by a disintegration of membrane structures and a green coloration. In *L. japonicus* inoculated with *R. etli* strain USDA 9032 nodules were visible at the same time as those inoculated with *M. loti* (Table 4.2), but differed numerically by a factor of three. However, as only 5 seedlings were examined for each treatment and since only three nodules were identified in seedlings inoculated with

M. loti, even at 21 dpi, there are insufficient data to determine whether these results differ from those found by Banba *et al.* (2001). Comparisons of seedling sizes between the two different experiments indicate that seedling growth was more vigorous in the results of Banba *et al*. (2001). The early senescence observed in *L. japonicus* nodules elicited by *R. etli* strain CE3 was not observed in those nodules elicited by USDA strain 9032. However, the stage of nodulation may have been delayed in the latter study compared to that of Banba and co-workers (2001), and therefore too early to see the premature senescence effect.

To attempt to determine why strains elicited different degrees of nodulation and GUS staining patterns it is necessary to understand more of the structures of the Nod factors produced by the different rhizobial species and also their mode of action. The data in Table 4.1 provide details of the Nod factor structures of those strains for which this information is known. Broad host range *Rhizobium* NGR234 and *R. etli* both produce at least one Nod factor species that is identical in structure (in length, fatty acid structure and substituents) to that produced by *M. loti*. *B. lupinus* also appears to produce Nod factors of a similar species. There are no sequence data for rhizobial strains nodulating *Arachis hypogaea* (peanut) or details of Nod factor structures. Evidence from this experiment however, suggests that the *nodZ* and *nolL* genes may be present, because these genes seem prerequisite to nodulation (Bras, 2003). A wide range of genetic diversity has been found amongst rhizobial species nodulating *A. hypogaea* (Urtz and Elkan, 1996). All the strains, whose Nod factor structures are known, that progressed to a fairly advanced stage of nodulation of *L. japonicus* had a specific sugar attached to the reducing terminal residue.

B. elkanii USDA strain 61 and *S. fredii* USDA strain 257 produce Nod factor species that differ in several chemical substitutions from those produced by *M. loti*, including the acetyl fucosylation mentioned above. However, the acyl chains produced by these two strains are both C18's with one double bond. Since the Nod factors produced by *M. loti* include those acylated by both C18:1 and fully saturated C18 chains, the fatty acid requirements of *L. japonicus* were likely satisfied with Nod factors of *B. elkanii* and *S. fredii*. Similarly, although the precise Nod factor species produced by *B. japonicum* USDA strains 3442 and 3407

are not known, they are likely to be close variants of those indicated in Table 4.1 and include a C18:1 moiety.

Since the major differences in Nod factor structure between *M. loti* and the above strains are the chemical substitutions it seems reasonable to assume that these factors play a major role in determining not only the successful progression of nodulation in *L. japonicus,* but also of *gus* expression in T90. In the cases of the *B. japonicum* strains nodulation progressed only as far as patchy GUS staining and some root hair deformations (including curling), and in the cases of *B. elkanii* and *S. fredii* nodulation was able to progress as far as the initiation of nodule primordia (Figure 4.10 B, C and D) . Further attention to these infection events and a wider range of rhizobial strains could provide greater insight into the importance of specific decorations on the Nod factor molecules.

As a point of interest, a chalcone synthase-regulated *gus* transgene (CHS1:gusA) induced in cortical cells during spot inoculation with compatible rhizobia, was also induced by non-nodulating bacteria and foreign bacteria (Mathesius, 1999; as cited in Mathesius *et al*., 2000), just as GUS activity in T90 did not specifically correlate with effective nodulators of the plant.

The differences observed in *L. japonicus* seedlings inoculated with *R. leguminosarum* bv *viciae* were more pronounced than those elicited by other strains (Table 4.2 and compare Figures 4.10 A, B, D and E with C). Nod factors produced by this strain are *N*-acylated with α,β-unsaturated chains whose major moieties are C18:4, determined by *nodFE* (Spaink *et al*., 1991; 1993). Rhizobia producing such *N*-acyl substitutions are found in diverse bacterial genera but nodulate legumes belonging only to the tribes Galegeae, Trifolieae and Vicieae, now referred to as the galegoid group (Lerouge *et al*., 1990; Yang *et al*., 1999). In contrast, legumes such as *Lotus* and *Lupinus* species belong to the Loteae and Genisteae tribes, respectively. These legumes are nodulated by bacteria producing Nod factors in which the *N*-acyl chain consists of fatty acids of the general lipid metabolism, such as stearic and vaccenic acid (Legocki *et al*., 1997; López-Lara *et al*., 1995). This factor specifically could be the reason why the degree of hair curling observed with other strains was not observed with *R. leguminosarum* bv

viciae. The fatty acid chain may contain a major determinant of root hair curling. Indeed, Ardourel *et al*. (1994) have reported the reduced ability of *nodFE* and *nodL* mutants of *R. meliloti*, another strain producing α,β-unsaturated chains, to induce root hair curling on alfalfa. The faint GUS expression and minimal hair deformation elicited by *R. leguminosarum* bv *viciae* in T90 may be in response to the presence of the C18:1 Nod factor molecules secreted by this strain as a minor species, or perhaps an element of the Nod factor molecule that is in common with *M. loti*, maybe even simply the chitinous backbone of the molecule itself. It would be interesting to determine whether other bacteria nodulating plants within the galegoid group elicit a similar response, regardless of other structural decorations.

Interestingly, Catoira *et al*. (2000) recently characterised a *M. truncatula* mutant impaired in its ability to curl root hairs in response to rhizobial inoculation. It therefore seems that specific mechanisms controlling root hair curling exist in both the bacteria and host. It is likely that a similar case exists for the entire legume-rhizobia relationship, indeed, for any biological interaction: a continuous dialogue in signal perception, gene expression, signal transduction and subsequent downstream genetic responses. In the case of legumes and rhizobia this could be one indication why a single rhizobial strain produces different species of Nod factor: it could be a means of increasing the likelihood of successful nodulation where one genetic response/signal cascade is blocked. The prolonged elicitation of GUS in T90 in response to inoculation with compatible rhizobia may simply reflect perception of the continued presence of the bacteria, permitted through the on-going satisfaction of plant criteria. As a point of note, however, investigations using antagonists of PLC in *M. sativa* transformed with the *ENOD12* promoter-*gus* fusion suggested that short exposures to Nod factor, of around 15 minutes, were sufficient to elicit expression of the transgene downstream (Pingret *et al*., 1998).

The number and structure of mechanisms by which legumes perceive Nod factors has been something of an enigma, although the recent cloning of various members of the LysM family of receptor kinases in genes such as *Lyk3*, *Nfr1* and *Nfr5* has provided further insight (Limpens *et al*., 2003; Madsen *et al*., 2003; Radutoiu *et al.,* 2003) (as discussed in Section 1.5.4). The role of plant lectins, Nod factor

binding sites and entry receptors in the important early stages of nodulation signal perception is still a relatively controversial one however. Further information on these topics can be found in the following: Sharma *et al*., 1993; Perret *et al*., 2000; Cullimore *et al*., 2001; van der Holst *et al*., 2001 Gressent *et al*., 2002; Limpens *et al*., 2003; Madsen *et al*., 2003; Radutoiu *et al.,* 2003.

In addition to the role of Nod factors, lectins and binding sites in determining successful nodulation interaction, several other important factors may be responsible for the differences in elicitation of GUS in T90. Additional substances likely to affect successful nodulation include the various flavonoid compounds secreted by the plant before and during the infection process, plant chitinases, and extracellular polysaccharide and lipopolysaccharides molecules secreted by rhizobia.

Flavonoids act as transcriptional activators of the rhizobial *nod* genes during the initiation of nodulation. In this study some form of response to each of the different rhizobial strains was elicited in every case, implying that *L. japonicus* exudates effectively induced rhizobial *nod* genes in all of the species described. This is interesting as a recent study of *L. corniculatus*, also nodulated by *M. loti*, revealed that *R. etli* rhizobia were able to form root nodules on this plant only when a flavonoid-independent transcriptional activator of the *nodD* gene was present (Cárdenas *et al*., 1995). It seems therefore that the flavonoids secreted by *L. japonicus* are less specific in inducing *nodD* than those secreted by *L. corniculatus.* At present, the flavonoid compounds secreted by *L. japonicus* have not been characterised.

It is known that legumes continue to produce flavonoid compounds well into the infection process (Van Brussel *et al*., 1986). Since flavonoid compounds in this study have been shown to induce rhizobial *nod* genes from incompatible strains it seems feasible that these same compounds may have a subsequently negative effect on the rhizobial strains downstream of initial induction. Indeed, it is well known that some flavonoids inhibit the induction of certain *nod* genes (Firmin *et al*., 1986). Unpublished results show that endogenous flavonoids isolated in *L. japonicus* vary according to the strain of rhizobia used. In a study using a Nod

factor-producing and a non Nod factor-producing strain some compounds were found to be general and synthesised in common with both strains, whilst others were strain specific (Nicolas Rispail, IGER, personal communication). These data demonstrate not only the ability of the plant to detect differences in rhizobial strain, but also that the response to these differences is dynamic. Flavonoids are also known to perturb the auxin balance during nodule organogenesis (Mathesius *et al*., 1998; Murphy *et al*., 2000) and may therefore have additional roles in hormone-mediated signalling. Their effect is therefore diverse and probably far-reaching.

The action of certain chitinolytic enzymes may also be a factor in the recognition of Nod factors and subsequent successful interactions. Purified plant chitinases have been shown to have different affinities for different Nod factor structures, raising the question of whether Nod factor stability within the host could be one of the determinants of specificity (Staehelin *et al*., 1994). Elsewhere, however, it is suggested that the speed of action of these chitinases is too slow to function in this capacity (Perret *et al*., 2000). However, GUS elicitation in T90 could be related to the production of certain chitinase enzymes in a capacity that either facilitates or discourages the successful interaction of different rhizobial species.

Questions also remain regarding the involvement of the bacterial envelope in the legume-rhizobia interaction. Extracellular polysaccharides can be released by rhizobia in the form of a toxin, whilst lipopolysaccharides are distinct components of the outer membrane with the potential structural diversity to mediate specific adherence (van Workum *et al*., 1998).

Extracellular polysaccharide biosynthesis has been determined as a rhizobial requirement for the formation of nitrogen-fixing nodules on indeterminate type legumes (van Workum *et al*., 1998). Extracellular polysaccharide-deficient (*exo*) mutants have been reported to produce a number of responses, from the prevention of penetration more than superficially into the plant's cortical tissue (D'Haeze *et al*., 1998) to the complete failure of nodulation in pea (van Workum *et al*., 1998). Plant defence responses, resulting from the formation of pseudo-nodules by rhizobial mutants, have been observed. The absence of such a response in wild-

type relationships may indicate that one function of extracellular polysaccharide molecules is to act as suppressors of plant defence reactions (Niehaus *et al*., 1993).

Lipopolysaccharides have also been shown to play an essential role in the interaction of rhizobial symbionts with plant species. Experiments reported by Niehaus *et al*. (1998) detail rhizobial mutants carrying major modifications in the lipopolysaccharide molecule that were no longer able to establish normal, nitrogen fixing nodules. Lipopolysaccharide mutants of *R*. *leguminosarum* bvs. *trifolii* and *viciae* infected the root nodules, but rhizobial cells released from the infection thread failed to differentiate into normal, nitrogen-fixing bacteroids. Lipopolysaccharide mutants of *R. leguminosarum* bv. *phaseoli* and *B*. *japonicum* were blocked at an earlier stage. These mutants were arrested in the development of infection threads, leading to non-infected pseudo nodules. In contrast, *S. meliloti* lipopolysaccharide mutants formed N-fixing nodules on *M*. *sativa* (Clover *et al*., 1989). Again, one might speculate that GUS elicitation in T90 relates to the perception of differences in extracellular polysaccharides or lipopolysaccharide compounds released by the different bacterial strains and the subsequent suppression or facilitation of sustained interaction.

As well as the above, other biotic and abiotic factors such as salicylic acid, methyl jasmonate and the root knot nematode, *Meloidogyne hapla* have also been tested and found not to induce GUS activity (Judith Webb, personal communication). The response of T90 GUS activity in the light of such data suggests that its elicitation is neither stress- or defence-related. Table 4.3 summarises the effects of various factors tested on T90 both in this study and those conducted previously.

Table 4.3. Effects of biotic and abiotic factors on GUS activity in T90.

Factor	Location of GUS	Comments
Biotic elicitor		
Rhizobia (refer to Table 2.0)	root	this study
Glomus intraradices	root	Parniske, personal communication
***Meloidogyne hapla* (root-knot nematode)**	-	Webb, personal communication
***Blumeria loti* (powdery mildew)**	-	”
Abiotic elicitor		
Nod factor	root, site of application	this study
Chitosan	root, site of application	”
Hormones (Table 2.2)		
Auxins: IAA, NAA, 2, 4-D	-	”
Ethylene precursor: ACC	-	”
Abscisic acid	-	”
Cytokinins: 6-BAP, kinetin, DHZ	-	”
Sodium nitroprusside	-	this study
$CaCl_2$	shoot[1] root[2]	preliminary data, this study ”
A23187	shoot[3]	preliminary data, this study
Salicylic acid	-	Webb, personal communication
Methyl jasmonate	-	”
Abiotic inhibitor	**Inhibition of GUS**	
EGTA	variable[4]	preliminary data, this study
Nifedipine	yes[5]	”
Ruthenium red	IC	”
Verapamil	No	”

IC=inconclusive as blocker found to inhibit growth of *M. loti*; - = no GUS activity. [1] Effects were variable, increased activity in Experiment A; [2] activity identified in roots only in presence of *M. loti*, $CaCl_2$ increased GUS activity in absence of EGTA and ionophore; [3] effects were variable, increased activity in Experiments C and D; [4] reduced activity in roots inoculated with *M. loti* and increased activity in shoots to varying degrees; [5] inhibited activity in roots inoculated with *M. loti*.

Although unexpected in this study, the observation of GUS staining in shoot tissues of *L. japonicus* is consistent with that of many early nodulin genes that have been identified not only in non-symbiotic tissues but also in non-legumes. For example, transcripts of *ENOD*s *11*, *12* and *40* have all been found in aerial parts of the plant (Scheres *et al*., 1990; Fang and Hirsch, 1998; Journet *et al*., 2001) and homologues to *ENOD40* and *Ljnin* have been identified in various non-leguminous species (Schauser *et al*., 1999).

The effect of Ca^{2+} on GUS elicitation both in root (in combination with *M. loti* bacteria) and shoot tissue of *L. japonicus* T90 seedlings is consistent with the *gus* gene acting as a 'reporter' for regulation of the putative Ca^{2+}-binding protein (*LjCbp1*) downstream of the insertion site (Figure 4.5). The role of Ca^{2+} in regulating *gus* is unclear, particularly due to the conflicting effects of EGTA in different tissue types, but further examination of the expression profile in shoot tissue may provide additional clues.

The data also indicated that expression of *gus*, and therefore potentially *LjCbp1*, may be associated with meristematic activity. Webb *et al*. (2000) reported that GUS activity diminished in mature and senescing nodules which may be consistent with a role in meristematic growth. Previous investigations in soybean demonstrated that meristematic activity in nodules ceased 18 dpi. Soybean nodules developed more quickly than *L. japonicus* (Elaine Tuck, unpublished data) indicating that nodule meristems may persist for longer in the latter. However, the elicitation of GUS in non-meristematic tissue, such as cotyledons and hypocotyls, does not support this theory, nor does the fact that none of the 'classical' hormones appeared to stimulate expression. It is difficult to explain therefore how the response is implemented, although the involvement of Ca^{2+} and Ca^{2+}-regulated genes in meristematic activity has been reported and may suggest the presence of a pathway that operates alongside that of hormones. However, regulation may be dependent upon other signalling cascades, and it

could be that several, as yet unknown, factors are also involved in meristem development. Alternatively, expression may simply be defined by a developmental stage that is, as yet, unidentified.

The reduced elicitation of GUS in shoot tissue in the absence of added $CaCl_2$ but presence of EGTA is difficult to explain but nevertheless is consistent with the *gus* gene reporting an aspect of Ca^{2+} signalling. Co-ordination with chelators does not inactivate divalent cations but rather increases their solubility, thereby facilitating their involvement in chemical reactions (Graf *et al*., 1984). In the case of transition metals, for example iron ($Fe^{2+/3+}$) or copper ($Cu^{+/2+}$), these could include Fenton reactions ($F^{2+} + H_2O_2 \rightarrow {}^{\cdot}OH + OH^-$) leading to the production of highly reactive and damaging hydroxyl radicals. Therefore, one hypothesis is that the presence of EGTA stimulates a stress response in the plant, which subsequently elicits GUS. The presence of increasing concentrations of $CaCl_2$ will titrate out the EGTA and so reduce the stress response. However, there are no other data (for instance, a responsiveness of *gus* expression in T90 to pro-oxidants) to support this theory at present.

Ca^{2+} channel antagonist data suggested a nifedipine-sensitive but verapamil-insensitive mechanism is involved in the signalling upstream of *gus* expression. Since nifedipine has been reported to bind more effectively to depolarised cells, the effect may be due to interference with the cell depolarisation events known to be involved in early nodulation. Since nifedipine binds to L-type Ca^{2+} channels, these results provide some evidence for the presence of L-type channels in *L. japonicus*.

In addition to the positive elicitors of GUS, a number of hormones were found not to elicit GUS activity in T90. The involvement of all the 'classic' hormones in the nodulation process has been implicated repeatedly (discussed in Section 1.5.7) and suggests that *gus* expression should be affected by the exogenous application of such hormones. Present data suggest that either *gus* acts upstream of plant hormones, or that a pathway is involved in *gus* transcription that is parallel to hormonal stimulation. It is possible that *gus* expression is upregulated before the induction of changes in hormones but it seems likely that multiple pathways exist

in the nodulation process which allow for the expression of certain genes irrespective of the regulation of others, even though they are involved in the same overall process.

The nitric oxide donor sodium nitroprusside was also tested on T90 and found not to elicit GUS. As a point of note, the higher concentration of sodium nitroprusside (5mM) did not appear to have any deleterious effect on the plant material during the incubation time, in contrast to *Arabidopsis thaliana* in which such concentrations are fatal (Luis Mur, personal communication).

In summary, the basal level of expression of the *gus* gene in uninoculated tissues, as demonstrated in Chapter 3, is not visible in histochemically stained roots. However, GUS activity becomes visible within eight hours of inoculation with the rhizobial symbiont *M. loti* and within four hours with Nod factor derived from *M. loti* strain R7A. GUS activity was also elicited in response to chitin, an element that is in common with Nod factors and mycorrhiza fungi. GUS activity in T90 was not specific to compatible strains of nodulating bacteria, but did correspond to the degree in which each strain appeared to be effective in nodulating *L. japonicus*. Results suggest that GUS activity in T90 is affected by differences in Nod factor structure, that the presence of Nod factor itself elicits GUS in the early stages of nodulation, but that the presence of specific sugars, most effectively acetyl fucose, on the reducing end of the molecule contribute to sustained GUS activity and concomitantly to successful nodulation. The degree of GUS elicitation in roots inoculated with *M. loti* also correlated positively with increasing Ca^{2+} concentration and was negatively affected by the presence of 0.5mM EGTA and 1mM of the Ca^{2+} channel blocker nifedipine.

Investigations into the elicitation of GUS in T90 using factors likely to affect Ca^{2+} signalling provide some preliminary data that suggest *gus* expression is regulated by Ca^{2+} and may therefore reflect expression of downstream *LjCbp1*. However, *gus* regulation may require additional regulatory elements as Ca^{2+} alone was not sufficient to elicit GUS in T90 roots. The observation that the only biotic stimuli so far observed to elicit GUS in T90 are organisms that may share a common host-recognition and developmental pathway perhaps supports the hypothesis that a

subset of the genes required for AM symbiosis has been commandeered for nodulation (Duc *et al*., 1989; Gollotte *et al*., 1995; Kistner and Parniske, 2002). The mechanism by which nifedipine works suggest that GUS elicitation may relate to cell depolarisation events.

Chapter 5

5.0 Ethyl methane sulphonate mutagenesis of T90

5.1 Introduction

Spontaneous and induced mutations in plant genes provide a powerful and significant resource for scientific research. Investigations into the functions of wild-type genes are made possible through the observation of the phenotypic consequences of mutations in those genes. The use of mutagenic agents to elicit phenotypic variation in plants has been fundamentally important in the genetic dissection of plant phenomena and has been practised for more than 70 years (Vizir *et al*., 1996).

Since the early events in plant-microbe interactions are determined by the expression of what are often interaction-specific genes, much emphasis in research has been based on elucidating the genetic determinants of the interactions. Various mutagenic programmes, using a variety of inducing agents, have generated valuable resources of symbiotically-affected plant lines and have resulted in the detailed characterisation of several legume mutants (Wang *et al*., 1990; Imaizumi-Anraku *et al*., 1997; Szczyglowski *et al*., 1998; Bonfante *et al*., 2000; Imaizumi-Anraku *et al*., 2000; Senoo *et al*., 2000; Genre and Bonfante, 2002; Kawaguchi *et al*., 2002; Krusell *et al*., 2002; Limpens *et al.*, 2003; Madsen *et al*., 2003; Radutoiu, *et al*., 2003; Esseling *et al*., 2004). A summary of some key legume mutants that highlight different stages of impaired nodulation is presented in Table 5.1.

In order to detect mutant phenotypes, plant material must be highly inbred. The model legumes *L. japonicus* and *M. truncatula* provide ideal backgrounds for screening as both are autogamous. The genetic bases of several mutant phenotypes have been determined in both species, most of which were described in some detail in Chapter 1.

Table 5.1. Nodulation mutants affected in different stages of symbiosis.

Stage and mutant	Nod/ myc	Phenotype	Species	Nature of mutagen	Reference
Early Nodulation					
nfr1[1,2] and *nfr5*[1,2,3]	-/+	No *rh* response, no Ca^{2+}-spiking, no *NIN-GUS* or *LjCBP1-GUS* expression.	*L. japonicus*	Tn	Radutoiu *et al.*, 2003 Madsen *et al.*, 2003
syRKK[3,4] *noRK*[1,4] *sym19*	-/-	Balloon swelling *rh* tips. *It* penetrate as far as epidermal cells[5]. Ca^{2+} response unresolved[6].	*L. japonicus* *M. truncatula* *P. sativum*	Tn γ-ray EMS	Stracke *et al.*, 2002 Endre *et al.*, 2002 Schneider *et al.*, 1999
Dmi1 and *3*	-/-	Blocked between *has* and *hab*, *dmi1* blocked pre-Ca^{2+}-spiking, *dmi3* blocked post-Ca^{2+}.	*M. truncatula*	γ -ray	Catoira *et al.*, 2000
castor and *pollux*	-/-	Balloon swelling of *rh* tips. No *it*. *It* rarely penetrate roots.	*L. japonicus*	EMS	Bonfante *et al.*, 2000 and Imaizumi-Anraku *et al.*, 2004
Sym3	-/-	Some *rh* response.	*L. japonicus*	Tn	Parniske *et al.*, 2000
nin	-/+	*rh* responses but no *ccd* or *it*. Encodes a putative developmental regulator.	*L. japonicus*	Tn	Schauser *et al.*, 1999
Late Nodulation					
Har1[1,7]	-/+	Hypernodulating	*L. japonicus*	EMS	Krusell *et al.*, 2002
sickle	-/?	Ethylene-insensitive	*M. truncatula*		Penmetsa and Cook, 1997
sym72	-/-	Highly reduced AM colonisation	*L. japonicus*		Senoo *et al.*, 2000
alb1[8]	-/?	Fix$^-$, small, white nodules	*L. japonicus*	EMS	Imaizumi-Anraku *et al.*, 2000
te7	-/?	Fix$^-$, no bacteroids formed	*M. truncatula*		Bénaben *et al.*, 1995
rug4[1,9]	-/?	Fix$^-$, wrinkled seed	*P. sativum*		Craig *et al.*, 1999

Key: *ccd*, cortical cell division; EMS, ethyl methane sulfonate; *hab*, hair branching; *has*, hair swelling; *h*, hyphae; *it*, infection threads; *rh*, root hairs; Tn, transposon; Tn, transposon tagging; ?, not known; [1] gene cloned; [2] gene encodes LysM-type serine/threonine receptor kinase; [3] homologue of *Pssym10* (Madsen *et al.*, 2003); [4] encodes leucine-rich repeat receptor kinase; [5] phenotype described is in *L. japonicus*; [6] see Esseling *et al.*, (2004); [7] encodes serine/threonine receptor kinase; [8] also shows delayed nodulation; [9] encodes sucrose synthase.

The first nodulation gene to be cloned in *L. japonicus* was *Nin*, shown to be required for nodule inception (Schauser *et al*., 1999). The *Nin* locus was identified through transposon mutagenesis. An autonomous mobile element was inserted into the plant genome using T-DNA mediated genetic transformation. Several mutants were identified in the M_1 generation that appeared to be wild-type in the M_2 generation. Such revertants indicated that the transposon element had reactivated, permitting restoration of the wild-type phenotype. Transposon elements are bordered by inverted repeat regions which leave 'footprints' that can be subsequently isolated using the transposon sequence as a molecular probe. In this way the mutated locus in *nin* was 'tagged'**.** Plants expressing the *nin* phenotype appear to be impaired after initial Nod factor perception, but before the occurrence of extensive cortical cell division and also before the formation of infection threads. The features of the NIN protein indicate that it acts as a transcriptional regulator of genes required for nodule development (Schauser *et al*., 1999). The *Nin* gene may not be required for general plant development as mutants did not exhibit morphological changes in roots, shoots, leaves, flowers or seeds (Schauser *et al*., 1999).

In 2002, two receptor-like kinases were identified. The *har1* mutant (formerly *sym78*), for hypernodulation aberrant root, a putative serine/threonine receptor-kinase (Krusell *et al*., 2002), was isolated from a population of EMS-induced mutants (Szczyglowski *et al*., 1998) using map-based cloning techniques. Plants mutated in the *Har1* locus exhibit excessive nodule or lateral root growth and an extended nodulation zone (Krusell *et al*., 2002). Grafting experiments have demonstrated that the shoot genotype is responsible for negative regulation of nodule development and inhibition of root elongation and shoot growth, although transcripts of the *Har1* gene are found in various tissues, including roots (Nishimura *et al*., 2002).

SymRK encodes a leucine-rich repeat receptor-like kinase and was identified from a transposon-tagged line (Stracke *et al*., 2002). Unlike *Nin* and *Har1*, mutations in *SymRK* affect symbiotic establishment with both mycorrhiza and rhizobia. Identification of the *SymRK* locus defines an important stage in understanding the development of both symbioses, as it is the first and so far only gene to be

identified for this early developmental step that is common to both mycorrhiza and rhizobia. Attempted infection of *symRK* mutants with *M. loti* elicits exaggerated swelling of root hairs but no hair curling as seen in wild-type seedlings. AM fungal penetration is arrested in epidermal cells within which hyphae frequently exhibit exaggerated swelling and deformation (Stracke *et al*., 2002). An orthologue of *symRK*, *noRK* for nodulation receptor kinase (formerly *dmi2*), has also been cloned in *M. sativa*. Mutants with orthologous phenotypes have also been detected in *Melilotus alba, P. sativum* and *Vicia hirsuta* (Endre *et al*., 2002; Stracke *et al*., 2002).

Mutation in the *NoRK*/*SymRK* gene appears to prevent effective curling of root hairs, entrapment of nodulating bacteria and subsequent formation of infection threads (Esseling *et al*., 2004). Previously, Catoira *et al*. (2000) reported that root hair deformations were absent in *noRK* mutants. However, Esseling *et al*. (2004) demonstrated that root hairs from seedlings containing the *noRK* mutation were extremely touch-sensitive. This touch-sensitivity resulted in growth termination in root hairs, thereby preventing root hair deformation in response to the method of Nod factor application adopted by Catoira *et al*. (2000). Esseling *et al*. (2004) demonstrated that a more careful method of application of Nod factor elicited a wild-type root hair deformation response in *noRK* mutants, with the exception of the three dimensional, multi-faceted curling, mentioned above. Their method of Nod factor application involved allowing the seedlings recovery time between manipulations and the very gradual introduction (~800µl in ~1 minute) of medium containing Nod factor. Esseling *et al*. (2004) also postulated that the touch-sensitivity exhibited by *noRK* mutants may be due to the factor preventing the formation of the three-dimensional wild-type root hair curling, as touching of the root hair tip against the shank of the hair cell may be sufficient to induce growth termination.

More recently, the genes *nfr1* and *nfr5* (formerly *sym1* and *5*, respectively) were molecularly defined. These mutants were identified through transposon mutagenesis. As described in Chapter 1 (Section 1.5.4), *Nfr1* and *Nfr5* also encode receptor kinases of the serine/threonine, LysM-type (Madsen *et al*., 2003; Radutoiu *et al.,* 2003) and define a stage of the nodulation pathway that is not

shared with mycorrhization but is upstream of *SymRK/NoRK* (Figure 1.9). Both genes are required to be functional for plant recognition of rhizobial Nod factors (Radutoui *et al*., 2003; Madsen *et al*., 2003).

Two other recently cloned genes from *M. truncatula* were identified from the mutants *dmi1* and *dmi3*, originally identified from the same γ –ray mutagenised population as *noRK* (Catoira *et al*., 2000). The *Dmi1* gene appears highly conserved among angiosperms and encodes a protein with low similarity to ligand-gated cation channels and is required for Nod factor-induced Ca^{2+}-spiking (Ané, *et al*., 2004). *Dmi3* acts downstream of Nod factor-induced Ca^{2+}-spiking and encodes a protein with high sequence identity to Ca^{2+}/calmodulin–dependent protein kinases (Lévy *et al*., 2004; Mitra, *et al*., 2004). *Dmi3* may modify its activity in response to Ca^{2+} oscillations and function to decode and transduce the Ca^{2+}-spiking signal to downstream components (Mitra *et al*., 2004). Both genes are required for mycorrhizal colonisation as well as nodulation (Lévy *et al*., 2004; Mitra, *et al*., 2004).

Interestingly, the *Dmi3* gene was cloned simultaneously by two groups, using two different methods. The first method was a traditional approach of positional cloning (Lévy *et al*., 2004) and the second and faster method, a new approach based on the low-abundance of transcripts of mutated genes in mRNA (Mitra, *et al*., 2004).

In *L. japonicus* the *Castor* and *Pollux* genes were recently cloned (Imaizumi-Anraku *et al*., 2004). Several mutant alleles exist, generated through different mechanisms, including EMS. Mutations in these genes result in balloon-like swelling of root hairs and an absence of infection threads. Reponses to AM fungi are also affected and hyphae rarely penetrate root epidermal cells (Bonfante *et al*., 2000). Also in *L. japonicus*, *sym3* (Schauser *et al*., 1998) has been identified through transposon tagging. The phenotype associated with *sym3* is twisting of root hairs (Jens Stougaard, personal communication).

With the exception of the *har1* mutant, the above plant lines are all affected in the early stages of nodulation. Many other mutants have been identified in the later

stages of the rhizobial infection process and phenotypes include delayed nodulation or impaired N-fixation (Imaizumi-Anraku *et al*., 2000; Bénaben *et al*., 1995; Craig *et al*., 1999). Some of these mutants are listed in Table 5.1. These lines will not be detailed further, other than to state that these, too, provide further understanding into both the development and regulation of both rhizobial and mycorrhizal symbiosis. As is implied in Table 5.1, no nod^+/myc^- mutants have yet been identified, possibly because the genes required for nodulation are derived from those permitting mycorrhization (Section 1.4.1).

The T90 line, generated using T-DNA insertional mutagenesis, is the first report of a successful promoter-trapping approach to gene tagging in a legume. The reliability of early *gus* expression following challenge with a rhizobial symbiont in the T90 line made this an interesting candidate as a tool in a further screen for symbiotic mutants. As T90 exhibits GUS activity following both rhizobial and mycorrhizal inoculation it provides a distinctively clear and easily visualised marker for identifying changes and delays in rhizobial nodulation and mycorrhizal symbiotic colonisation, as well as the usual phenotype of failure to develop nodules or permit AMF colonisation. In addition, because GUS activity following rhizobial inoculation is visible within hours (see Chapter 4), GUS mutants can be identified within a short time period. T90 does not have a clear nodulation phenotype, but the staining pattern of GUS in this line appears to be linked to that of *LjCbp1*. It may therefore be involved in Ca^{2+} signalling in both symbioses, as has already been shown for *Dmi1* and *Dmi3* (Lévy *et al*., 2004; Mitra, *et al*., 2004).

In view of the potential usefulness of the T90 line, it was chosen for a mutagenesis programme using the chemical ethyl methane sulphonate (EMS). EMS is one of a number of chemical mutagens useful for generating plants that can be subsequently used to elucidate gene function. The mechanism of mutation is through the alkylation of DNA causing base pair transitions, most often GC to AT, due to the mispairing of O^6-alkyl-G with T (Vizir *et al*., 1996). EMS is therefore assumed to cause point mutations, although studies in *Drosophila* have shown that it may also produce *N*-alkylation of G and A, leading to depurination of DNA, resulting in subsequent chromosomal aberrations (Vizir *et al*., 1996). A range of mutant phenotypes have been generated in various plant species using EMS

mutagenesis. These EMS-generated mutants have been useful for investigations into processes including embryonic development, flowering, growth and anther and leaf development (Johnson *et al*., 1994; Peters, 1999; Sanders *et al*., 1999), as well as symbiosis (Duc and Messager, 1989; Borisov *et al*., 1993).

The aim of this work was to develop a dual screen for both rhizobial and mycorrhizal symbionts based on GUS activity in EMS-treated T90 seedlings. Since the half-life of GUS has been assessed in green tobacco plants to be three to four days (Weinmann *et al*., 1994) and the screen in T90 EMS-treated seedlings for each symbiont would be temporally separated, localised GUS staining in nodules, as described in Section 4.1.4, should be distinguishable from diffuse staining associated with mycorrhizal fungi, as described in Section 4.1.4. Absent or aberrant elicitation of the GUS enzyme following inoculation with either symbiont could thus be used to identify plants affected in either category at a locus upstream of the *gus* insertion. In this way, mutant lines potentially impaired in Ca^{2+} signalling during the early stages of root nodule formation and mycorrhization, could be identified.

EMS treatment of *L. japonicus* has been carried out by a number of groups (Wang *et al*., 1990; Imaizumi-Anraku *et al*., 1997; Szczyglowski *et al*., 1998; Bonfante *et al*., 2000; Imaizumi-Anraku *et al*., 2000; Senoo *et al*., 2000; Kawaguchi *et al*., 2002; Krusell *et al*., 2002) using different concentrations of mutagen. A comparison of results is therefore useful for greater understanding of the effects of mutagenesis. The following chapter details findings of a mutagenesis programme that was conducted in collaboration with the group of Dr Martin Parniske at the Sainsbury Laboratory, Norwich, using *L. japonicus* T90 line and presents three mutants impaired in GUS expression in the early stages of nodulation. Comparison will also be made to the published data of EMS-generated mutants.

5.2 Results and Discussion

5.2.1 Experimental design

Mutagenesis of approximately 1300 T90 seeds was carried out at the Sainsbury Laboratory, Norwich (as outlined in Section 2.7.1). EMS-treated T90 M_2 generation seed (709 lines) were screened at the Sainsbury Laboratory, Norwich. Seedlings were generated and inoculated with *M. loti* as described in Sections 2.7.6 and 2.7.7. Figure 5.1 shows EMS-treated T90 M_2 generation seeds germinating on Fåhraeus medium with 0.5% Gelrite® in a Petri dish. Approximately two weeks after sowing, seedlings were inoculated with *G. intraradices*, according to Section 2.7.9. Screening for GUS staining, nodulation and mycorrhization mutants was carried out in accordance with Sections 2.7.8 and 2.7.10, respectively. Mycorrhizal colonisation of EMS-treated lines was compared to interactions with non-mutagenised T90 plants.

M_1 generation EMS-treated T90 plants were not uniform in seed production, perhaps due to reduced fertility, and many lines were not available to screen in Norwich. Therefore, once all available M_2 generation lines (709) had been screened, M_1 generation plants that had not yet produced sufficient seed (n=30), plus 268 M_2 generation putative mutants (Table 5.2) were transferred to IGER, Aberystwyth, as described in Section 2.7.10.

A repeat screen, using seed from the same batches of M_2 generation putative mutants, was carried out at IGER, Aberystwyth, in accordance with Section 2.7.11. Whole seedlings, rather than 3mm root tips, from the 224 putative mutant lines identified in Norwich (figures in red, Table 5.2) were harvested in order to gain a better understanding as to whether there existed genuine change in GUS expression. Three putative mutants were chosen for further examination on the basis that they showed the most aberrant GUS staining. A summary of the screen of EMS-mutagenised plants, including the location of different stages, is presented in Figure 5.2.

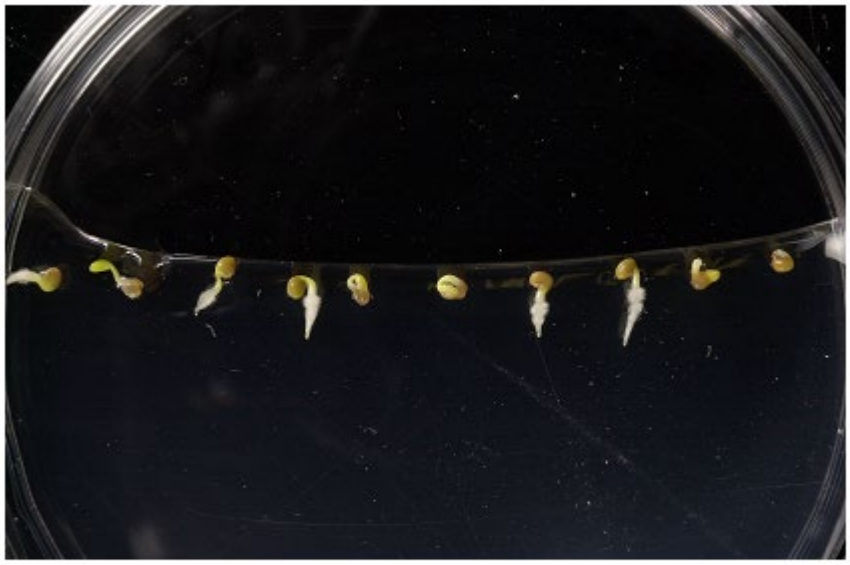

Figure 5.1. Petri dish (90mm) containing germinating M_2 seedlings of EMS-treated T90 seeds.

Table 5.2. Summary of T90 putative mutants in M_3 generation: initial screen at Sainsbury Laboratory.

Shoot phenotype	Number	Percentage of total[1]	Root phenotype	Number	Percentage of total[1]
Miniature	3	0.4	Nod$^-$	30	4.0
Dwarf	3	0.4	Fix$^-$	2	0.4
Gravitropic	1	0.1	Myc$^-$	17	2.4
Albino	2	0.3	Nod/Myc$^-$	1	0.1
Narrow-leaf	1	0.1	GUS$^{-/delayed}$	224	31.6
Crinkled leaf	1	0.1	Hypernodulator	11	1.6
Unifoliate	1	0.1			
Chlorotic	2	0.3			

[1] Total of 709 lines. Lines in red were transferred to IGER, Aberystwyth.

Figure 5.2. Outline of timing, location and procedure for EMS-treatment and screen in T90 line. Boxes with thick edges indicate end-points.

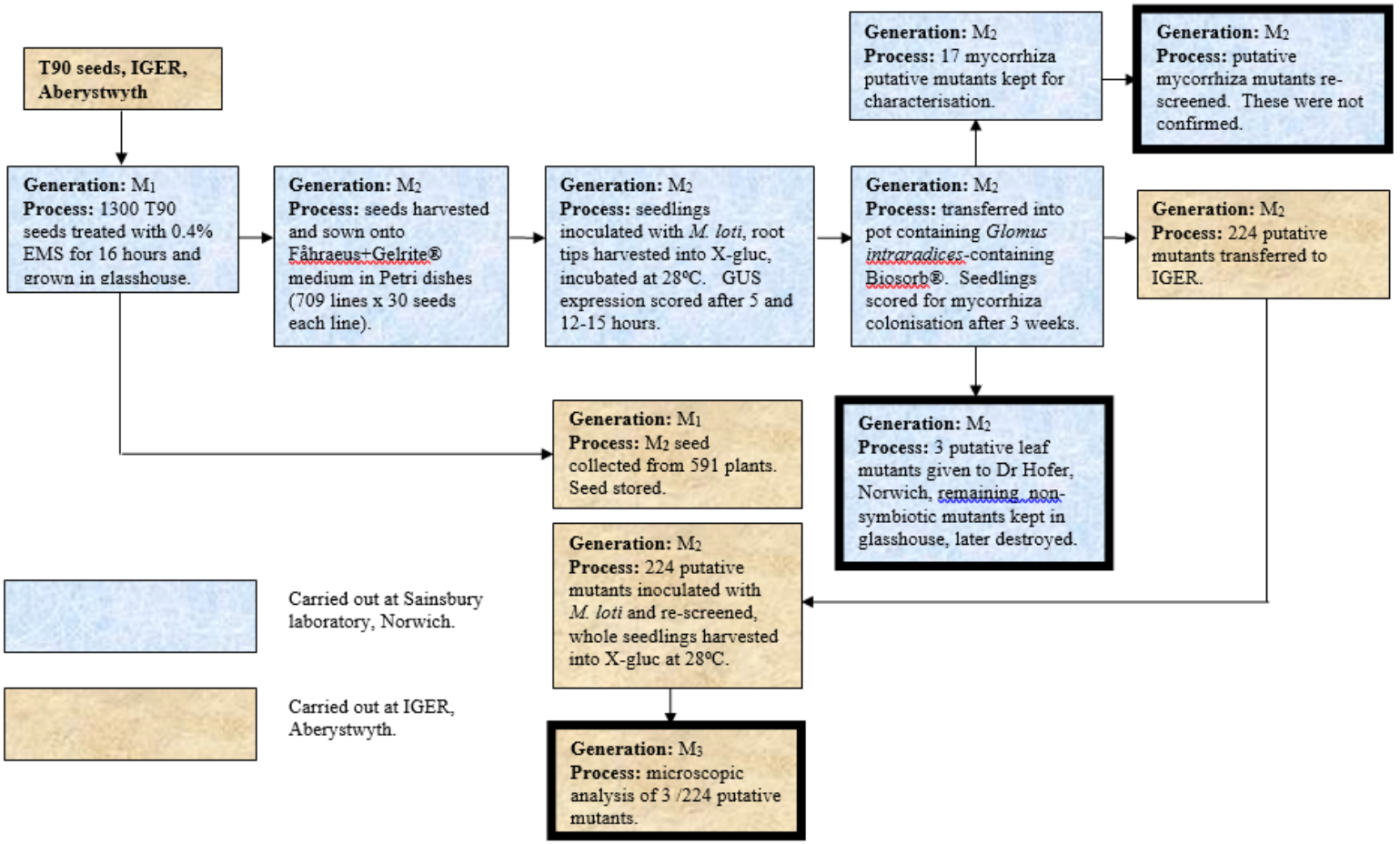

5.2.2 Identification of putative mutants

Mutagenesis of T90 seed resulted in the generation of a range of putative mutants in root nodulation symbiosis and root and leaf development. EMS treatment affected the percentage germination of seeds and fertility of plants. Out of 709 lines screened at the Sainsbury laboratory, 59 lines (8.3%) had lethal mutations or died before screening and 120 (17%) were infertile. In addition to the infertile lines, a range of seed production was also observed. In some cases only one or two seed were generated, compared to several grams in other lines. The earliest stages of the development of many seedlings were also affected, in 216 lines less than 50% seeds germinated. A summary of data from the initial investigations of mutagenic material carried out at the Sainsbury Laboratory, Norwich, U.K. is presented in Table 5.2.

The efficiency of the mutation process in the *L. japonicus* EMS-treated T90 screen is indicated in the M_2 generation by the presence of the albino phenotype at the frequency of 0.2%. This compares with figures in *A. thaliana* EMS mutagenesis experiments which range from 0.02 to 1.8 (Feldmann *et al*., 1994).

The GUS histochemical assay (Figure 5.3) revealed a potential 224 lines with aberrant staining. Other putative mutants were: 30 nod^-, 2 fix^- 17 myc^-, 1 nod^-/myc^- and 11 hypernodulating (nod^{++}) (Table 5.2). On rare occasions, GUS activity was observed in what appeared to be the vasculature of T90 control seedlings.

Three leaf development mutants were observed. These included an example of chimerism in line T0344, which showed two mutant phenotypes, a narrow-leaf and a dwarf plant (Figure 5.5 A and B, respectively). Two other shoot mutant phenotypes, a unifoliate leaf and a crinkled leaf are shown in Figure 5.5 C and D. The T90 control leaf phenotype is shown in Figure 5.4.

Subsequent examination of nine of the 30 putative nod^- lines (Table 5.2) at IGER identified that they were, in fact, nod^+. Line T0203 was verified as nod^- but died

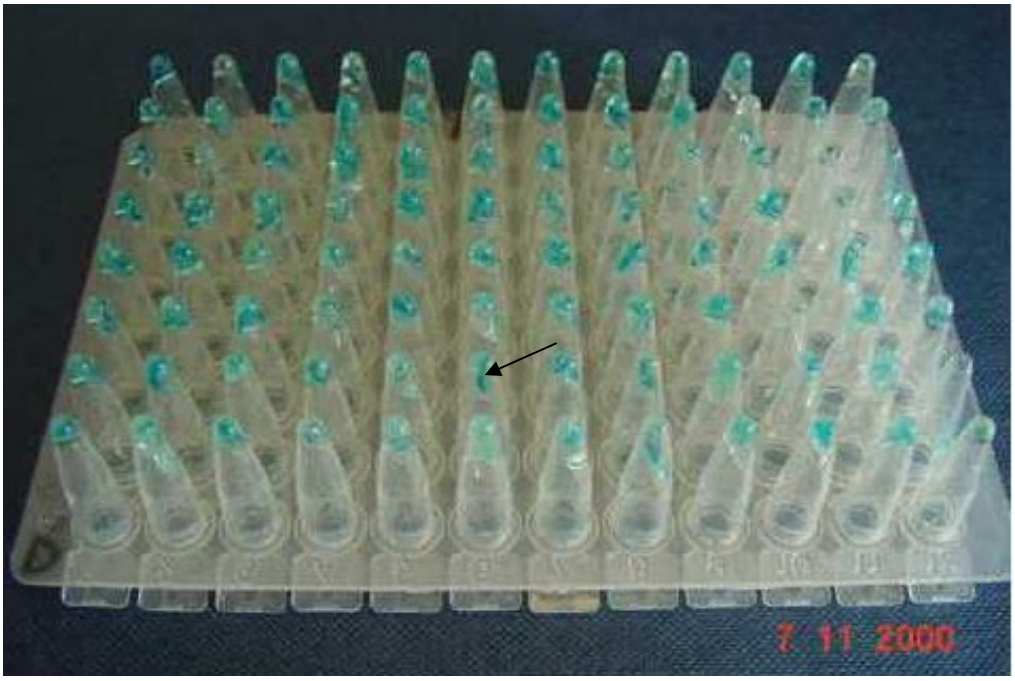

Figure 5.3. GUS stained root tips of 96 M_2 generation EMS-generated mutants of T90 in an upturned PCR plate. Arrow indicates histochemically-stained 3mm root tip.

Figure 5.4. T90 control showing two trifoliate leaves. Magnification x3.

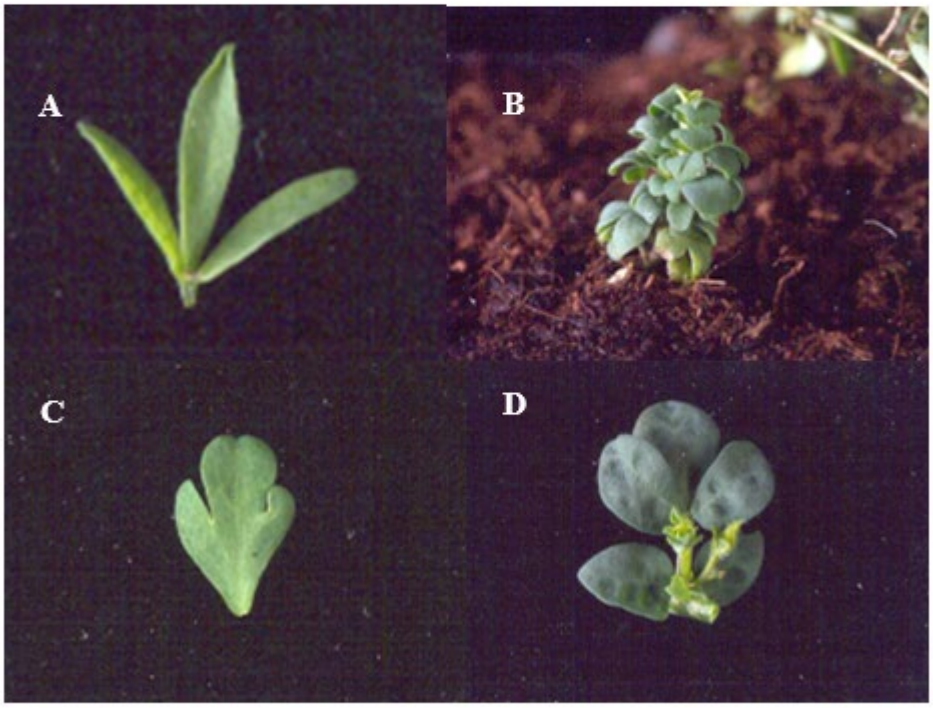

Figure 5.5. Shoot phenotypes identified during initial screen of M_2 EMS lines. A and B, chimeric line T0344 shows narrow-leaf trifoliate (A) and dwarf (B) mutant phenotypes; C, broad-leafed unifoliate in line T0360; D, crinkled leaf phenotype in line T0648. Magnifications: A, x4; B, x1; C, x4; D, x2.

before it was confirmed whether this line was also GUS$^-$. However, data from the first screen showed that all but one seedling stained positive for GUS, the seedling that stained negatively had an unhealthy root and so was not selected for further screening. Remaining M_2 seedlings from this line were lost to Sciarid fly.

One of the putative fix$^-$ plant phenotypes was later identified as fix$^+$.

Due to the screening process of inoculation with *M. loti* and subsequently *G. mosseae* it was sometimes unclear from histochemical staining whether GUS activity was induced by rhizobia or mycorrhiza. It appeared that nodulation was on-going, rather than a one-off event after initial inoculation with *M. loti*. However, traditional microscopic analysis, following staining with trypan blue, revealed seven lines with absent or few vesicles/arbuscules, five lines that had aberrant hyphal formation and two lines that elicited epidermal vesicles. Three lines remained uncharacterised. The traditional method was more time-consuming than simply screening for GUS activity, but the dual screen proved unsuccessful for the reason indicated. However, none of the 17 potential mycorrhiza mutants could later be confirmed.

Re-screening of the 224 GUS putative mutants at the histochemical level revealed 12 that had delayed or very faint expression, two with apparently absent expression and two with an otherwise aberrant expression pattern. Figure 5.6 shows T90 unmutagenised control seedlings exhibiting normal GUS activity compared with line T0468, a weak-staining T90 EMS mutant. Four other lines appeared to demonstrate excessive GUS elicitation. A summary of the various putative mutants is presented in Table 5.3.

Figure 5.6. T90 unmutagenised control line compared to GUS^{reduced} line T0468. A, T90; B, T0468. Magnification A and B x3.2.

Table 5.3. Summary of putative T90 mutants in M_1, M_2 and M_3 generations.

Phenotype	Line numbers	Total number
GUS activity		
GUS over-expressor	T0020, T0820, T0877.1, T1229.2	4
GUS weak stain	T0212, T0264[1], T0425.2, T0440, T0454[2], T0467, T0468, T0475, T0512, T0736, T0772, T0814[3], T0858, T0951	14
Otherwise aberrant GUS activity	T0958[6], T1067[4]	2
Nodulation		
Nod$^-$	T0203[5]	1
Hypernodulator	T0162[7], T0539, T0666, T0739b, T0768.1, T0790[7], T0811, T0865.1, T0869, T0872.2 and T0872.3, T1105[7], T1167, T1253[7]	13
Fix$^-$	T0825	1
Other		
Slow growth	T0076[7], T0765	2
Aberrant root	T0425.1	1

All lines are M_2 generation except where indicated. [1] M_3 generation, also showed aberrant GUS staining (Figure 5.9); [2] no nodules identified; [3] large nodules; [4] M_3 generation, GUS elicitation in vasculature (Figure 5.8 E and F); [5] Plant now dead, no remaining seed; [6] M_3 generation, isolated GUS activity and potential aberrant starch accumulation (Figure 5.8 A-D); [7] M_1 generation, not yet screened in M_2.

5.2.3 Further analyses of putative mutants, M_2 and M_3 generations

A summary of M_2 mutants is presented in Table 5.3. Of the original putative nod^- plants, 20 have not yet been confirmed as nod^- and are not included in these data.

Microscopic examination of three putative mutants, compared with T90 control (Figure 5.7), revealed interesting phenotypes. Line T0958.4 showed apparently normal GUS expression in one developing nodule (Figure 5.8 A), but isolated and fragmented expression in other nodules of the same plant (Figure 5.8 B). Another plant of this line (T0958.2) showed a similar phenotype (Figure 5.8 D). Line T0958.4 also appeared to have excessive accumulation of starch granules in the root tissue (Figure 5.8 C). Line T1067 is also pictured in Figure 5.8 (E and F). T1067 shows apparently normal expression in root nodules but GUS activity can also be observed clearly in the vasculature. This phenomenon was occasionally observed in T90 plants (data not shown) but was not of an equivalent intensity to that seen in T1067. Seedlings from line T0264 (Figure 5.9 A-E), which had previously appeared to be GUS^-, were found to have expression similar to that of T0958 in isolated pockets of epidermal tissue and at the periphery of a mature nodule (Figure 5.9 F-H). Expression was also identified in a single curling root hair cell (Figure 5.9 F).

A total of 13 putative hypernodulating mutants await confirmation of phenotype and subsequent characterisation. Four of these lines include M_2 plants that have not yet been tested for GUS activity at the M_3 stage.

In all, 20 M_2 lines were affected in GUS elicitation, 3 of which were confirmed in the M_3 generation, and 11 M_2 lines were affected in symbiosis, including one confirmed non-nodulation mutant. Four further M_1 lines appeared to show hypernodulation phenotypes.

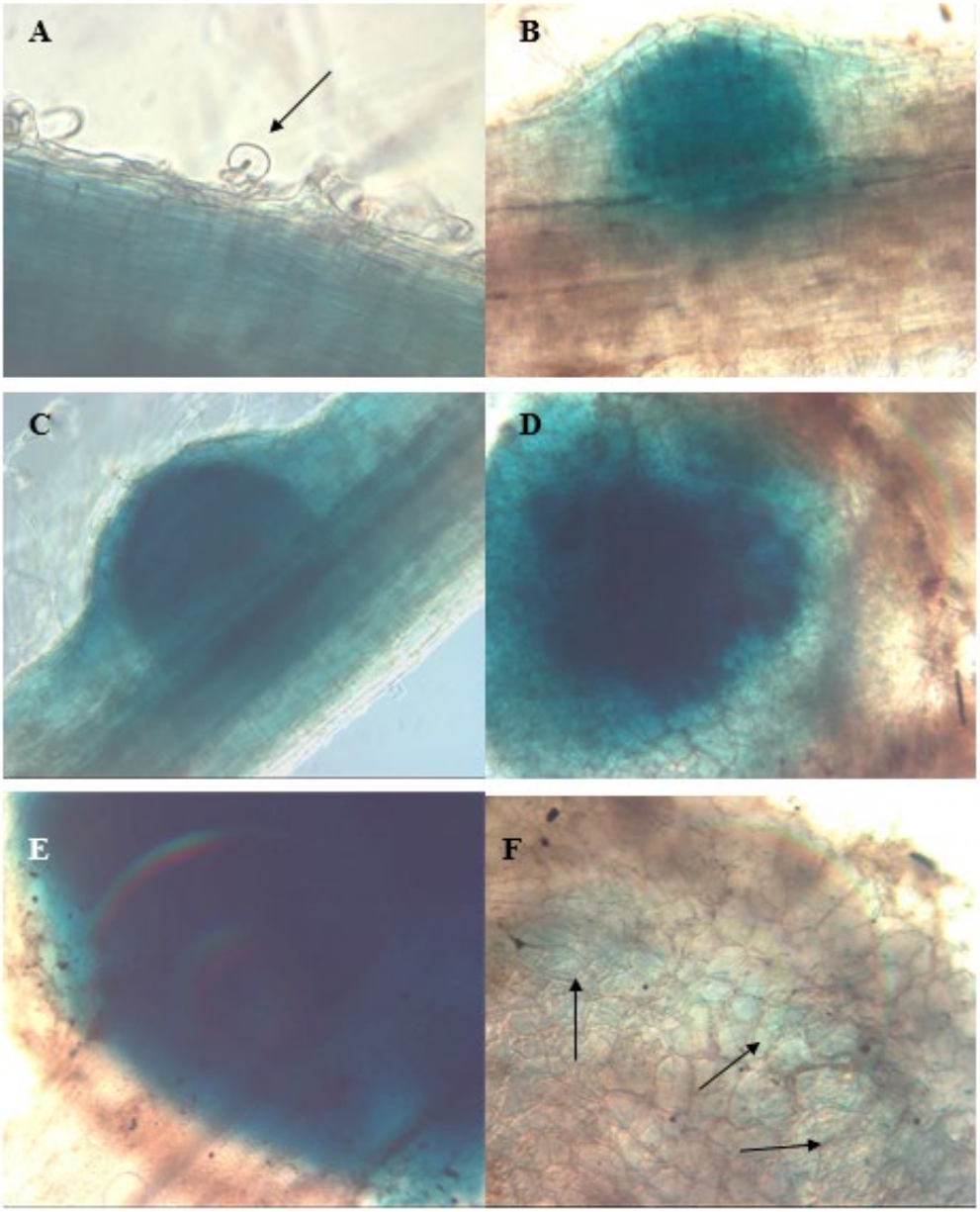

Figure 5.7. Progression of GUS activity in *Lotus japonicus* T90 line following inoculation with *M. loti* strain NZP2235. Root sections were taken from mature plants and show different stages of infection events. A, root hair curling (arrow) and GUS activity in root cortex; B-E, GUS activity in nodules of increasing maturity; F, GUS activity declining in senescing nodule (arrows). Magnifications: A, x80; B and C, x12.5; D x30; E and F x50.

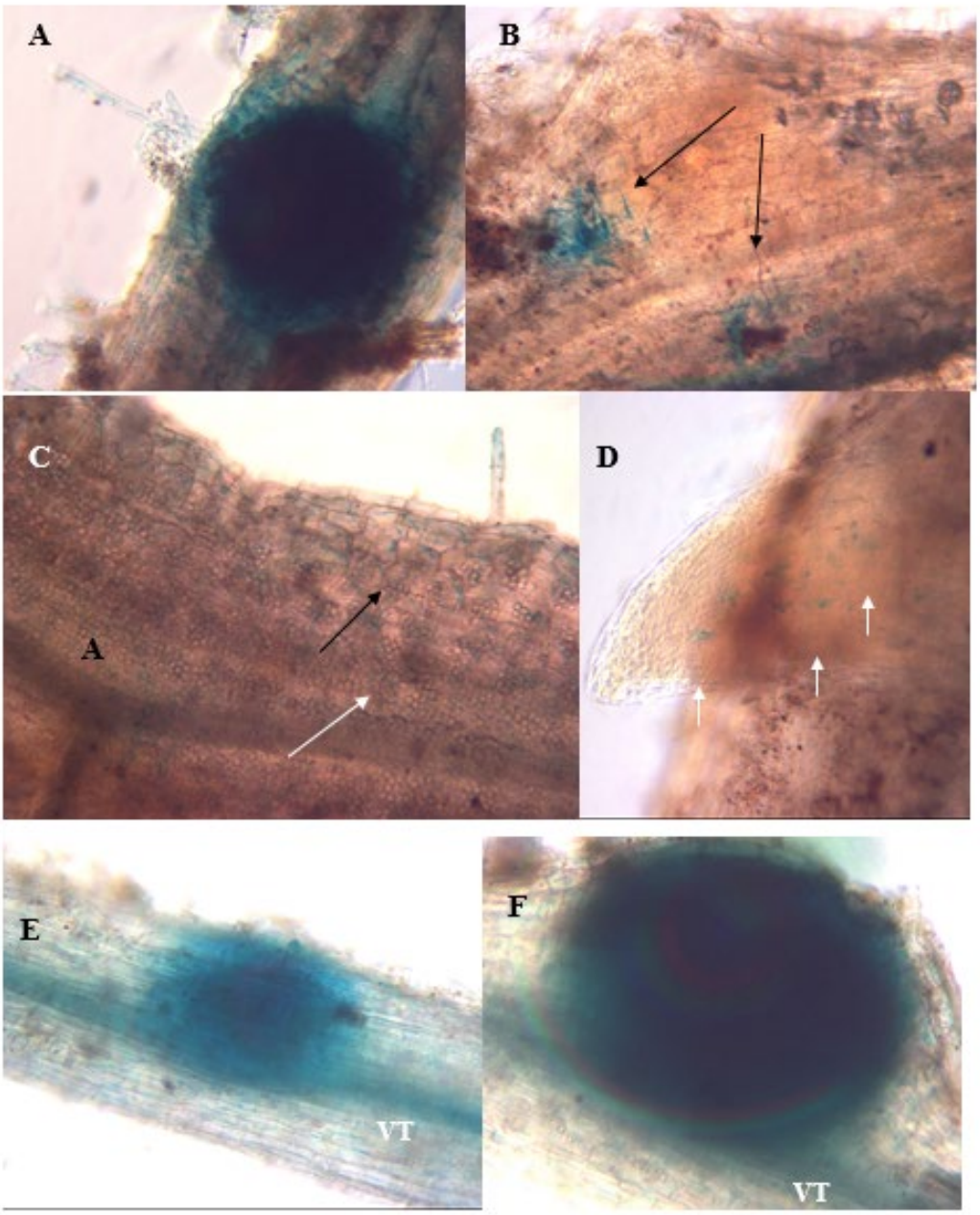

Figure 5.8. Root nodulation infection events and GUS activity in EMS mutant lines T0958 and T1067.2. A and B, two developing nodules in T0958.4 showing apparently normal activity in young nodule (A) and isolated and fragmented activity in older nodule (arrow) (B). C, Isolated patches of GUS activity (black arrow) and aberrant accumulation of starch granules (white arrow) in line T0958.4. D, developing lateral root in T0958.2 showing isolated patches of GUS activity (arrows). E and F, T1067.2 showing GUS activity in developing nodules and in vascular tissue (VT). Magnifications: A, B, E and F x20; C and D x40.

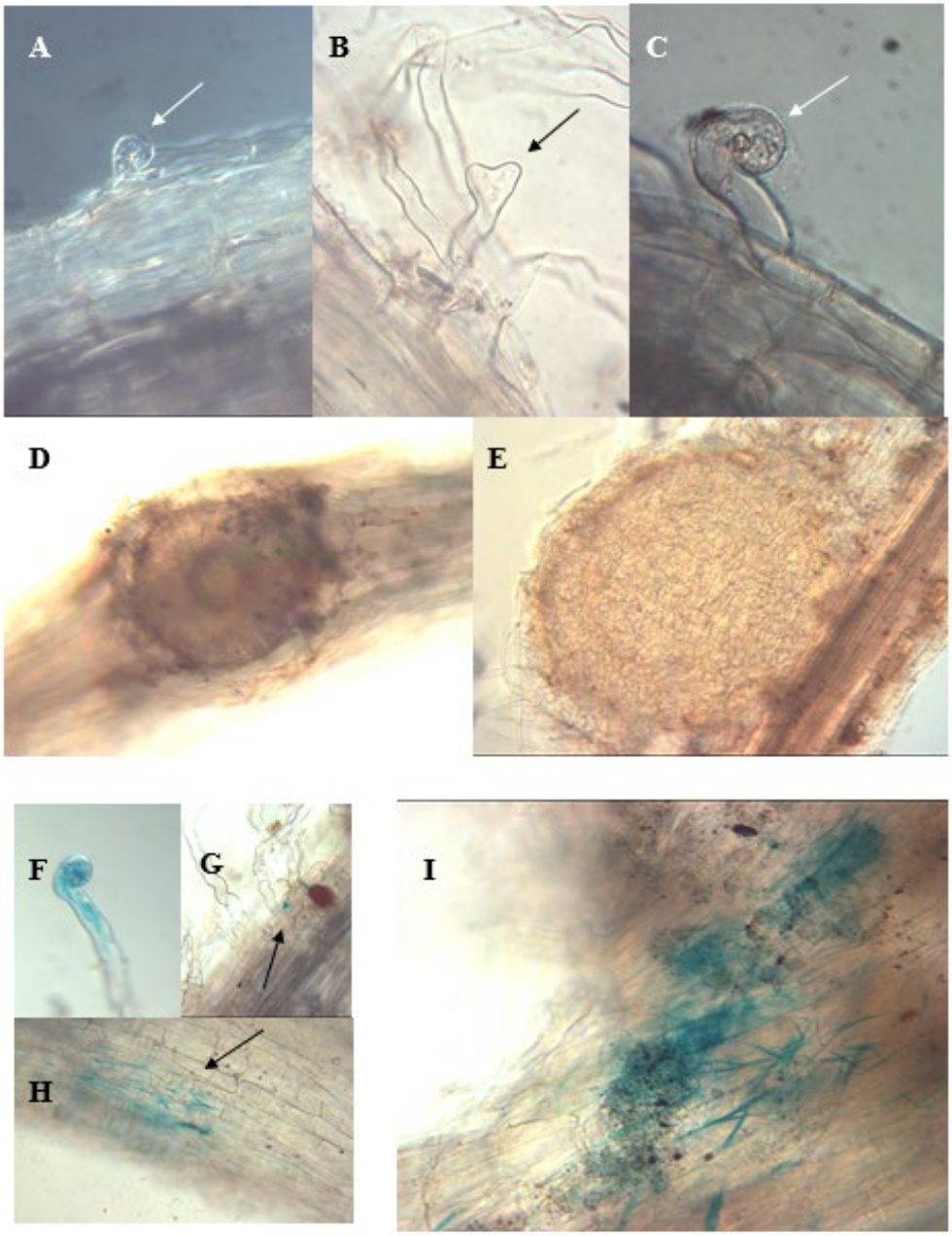

Figure 5.9. Root nodulation infection events in line T0264. A-E, Root hair deformations (arrows) (A-C) and young (D) and mature (E) nodules showing absence of GUS activity. F-I, Isolated GUS activity in curled root hair (F), epidermal cell (arrows) (G and H) and at basal edge of mature nodule (I). A&I, T0264.5; B, F&G, T0264.2; C, T0264.4; D&E, T0264.3 and H, T0264.1. Magnifications: A, B and F x200; C and I x250; D x12; E and H x20; G x150.

The non-nodulation/non-GUS putative mutants include slow growing lines T0076 and T0765, and line T0425 that has an aberrant root phenotype suggestive of agravitropism (data not shown). Other gravitropic mutants have been identified in *L. japonicus*, including the *astray* mutant (formerly *Ljsym77*, an EMS mutant) (Kawaguchi *et al*., 2002; Nishimura *et al*., 2002). The *astray* mutant also exhibits hypernodulation as well as a previously uncharacterised symbiotic phenotype, that of early initiation of nodule development (Nishimura *et al*., 2002). Five days after inoculation, Nishimura *et al*. (2002) observed four times as many nodules as wild-type plants. Two weeks after inoculation a ten percent greater nodulation zone was observed on mutant seedlings, with nodule primordia still being initiated on younger roots where wild-type seedlings were not (Nishimura *et al*., 2002). Plants with the *astray* mutation do not exhibit an abnormal response to ethylene or nitrogen compounds, both of which are involved in regulation of nodule development and insensitivity to which have been characteristics of previously characterised hypernodulating mutants (Heidstra *et al*., 1997; Penmetsa and Cook 1997). This mutant may prove highly informative in studies related to autoregulation in nodule development and characterisation of T90 EMS mutant T0425 may offer ways to expand this work further.

According to Feldmann *et al.* (1994), EMS is the most efficient amongst a range of chemical mutagens at inducing mutations and also has the least side effects in terms of lethality/sterility. Certainly the rate of mutation in this present study, as indicated by the occurrence of the albino phenotype (Section 5.2.2 and Table 5.2), was comparable with those in other EMS experiments. Webb *et al.* (*in press*) have recently tabulated results from several EMS programmes in *L. japonicus* that demonstrate, as in *Arabidopsis*, a variable frequency of the albino phenotype. In seeds treated with various concentrations of EMS over different exposure times the phenomenon occurred in 0.8 to 3.8% M_2 seedlings (Webb *et al*., *in press*). The lowest frequencies did not always correlate with the lowest concentrations/exposures. This indicates that some other factor may affect the mutation rate, although concentration and time of exposure are generally considered the major determinants (Vizir *et al*., 1996). The concentration and exposure used in this present study are comparable not only with other studies in *L. japonicus*, but also in other legumes, although ranges vary considerably from

0.4% and 16 hours (Imaizumi-Anraku *et al*., 1997) to 0.6% and 3 hours (Szczyglowski *et al*., 1998) to 1% and 6 hours (Duc and Messager, 1989).

Ultimately, the production of mutants is in itself the definitive measure of the success of mutagenesis and this screen has provided a number of interesting plant lines for further study. Several putative nod$^-$, GUS staining and hypernodulating mutants generated from the programme have not only provided material to help dissect the symbiotic signalling pathway but have also provided additional key information regarding *gus* expression in the T90 line.

The isolation of T90 mutants which fail to show GUS activity, yet demonstrate apparently normal nodule formation suggests that at least one signalling component upstream of T90 is not essential for symbiosis with *M. loti*. The EMS data also indicate that expression of the *gus* gene is not essential for normal nodulation. However, lines T0264 and T0958 have not yet been examined for any differences in infection progression, nodule number or N-fixation compared with T90 control plants. Although abolishment of *LjCbp1* expression has not been investigated in GUS$^-$ or GUS^{reduced} lines further investigations into *gus* regulation in these lines may provide evidence for the downstream function and importance of *LjCbp1* if, indeed, the regulation of the two genes is linked. Webb *et al.* (2000) observed that plants homozygous for the T-DNA insertion showed reduced expression of *LjCbp1* in homozygous material compared with Gifu wild-type but exhibited no apparent phenotype. These data could therefore support the suggestion that *LjCbp1* is not essential for nodulation. However, it has yet to be determined by sequencing whether any of the EMS-induced mutations have affected the T-DNA region and thereby directly knocked out the *gus* gene.

Based on phenotype, it is possible that mutations observed in T0264 and T0958 are allelic; complementation analyses must be performed for these and other mutant lines (see below). Mutagenised M_1 plants can be chimeric for heterozygous mutations that may be transmitted to the M_2, as was observed in mutated line T0344. Since any multiple mutations can influence the phenotypic expression of a mutation of interest and complicate its characterisation, the EMS-treated T90 plants will have to be repeatedly back-crossed to the original T90

control line. In such a way the mutant phenotype can be 'cleaned up' and thus reveal whether the phenotype is due to the effect of a single-gene mutation. According to Vizir *et al.* (1996), provided the mutation of interest and any contaminating mutation is unlinked (or linked but lie more than 50 centimorgans apart), six back crosses will give a 98% probability of separating the mutations. Intensive back crossing does not ensure the separation of closely linked mutations however and this must be borne in mind when observing any apparent pleiotropic effects.

On-going genetic analysis of mutant lines will require a thorough investigation of the mutant phenotype. This should include the detailed observation of infection events using genetically modified bacteria harbouring either the *hemAlacZ* or GFP construct (Quaedvlieg *et al*., 1998; Stuurman *et al*., 2000) as well as a comprehensive analysis of other physiological features such as flower, leaf and root morphology. Inheritance of the mutant phenotype(s) must then be analysed through subsequent generations and followed by allelism tests with known mutations showing a similar phenotype. Reciprocal crosses should also be conducted to check the possibility of the non-nuclear location of the mutation and segregation and co-segregation analyses should be carried out with various tester lines. Finally, map-based cloning will need to be performed to isolate and clone the mutant loci.

T90 has also functioned as a tool in providing crosses to existing early nod$^-$ mutants to further dissect the symbiotic pathway (Radutoiu, 2003; Judith Webb, unpublished data). Crosses with *Ljnin* resulted in what appeared to be accumulated GUS activity indicating that *gus* expression in T90 lies upstream of *Ljnin*, it also demonstrates the close association of GUS in T90 with the nodulation pathway, as a blockage of the pathway by the *Ljnin* mutation prevented the normal pattern of expression. Continued efforts in generating, characterising and mapping plant mutants such as those discussed here, combined with the sequencing projects presently under way for different legume species, will provide much deeper understanding of the genetic basis of symbiosis.

Chapter 6

6.0 Summary, conclusions and future work

The symbiosis between leguminous plants and root-nodulating rhizobia is an essential part of global agriculture and is fundamental to the sustainable farming practice essential for a growing population with limited resources. The importance of AM fungi to ecosystems, managed and otherwise, has also been highlighted, as has the need to maximise the potential afforded by both micro-symbionts.

Understanding the genetic control of symbiosis may be one of the major challenges of the 21st century, but the advent and application of a range of new techniques, approaches and materials is accelerating the pace of studies and aiding our understanding of plant-symbiont interactions.

The genetics of the rhizobial partner in root nodulation is now fairly well understood. The relatively small size of bacterial genomes has enabled many of the bacterial genomes involved in this symbiosis to be sequenced and characterised and their roles identified. Indeed, Broughton and Perret (1999) have postulated that a group of less than 400 genes permit gram-negative bacteria to be symbiotic. By contrast, significantly slower progress has been made in identifying those plant genes involved in either root-nodulating or mycorrhizal symbioses, and research into AM fungi is a relatively new and considerably more complicated area for fungal geneticists.

The identification of plant genes involved in the root nodulation symbiosis has been hampered by the complexity of host systems. The intricacies of signalling between symbionts and plants are still poorly understood. However, genetics in plants is progressing and the current focus on model legumes such as *L. japonicus* and *M. truncatula* permits comprehensive and large-scale studies on interactions between plants able to form symbioses with both rhizobia and AM fungi.

Efforts in recent years to establish model systems that avoid some of the complications of cultivated species have already proved worthwhile. The

development of appropriate model legumes and the initiation of sequencing projects of the genomes of both *L. japonicus* and *M. truncatula,* as well as completion of sequencing of their respective rhizobial symbionts, has advanced and accelerated symbiosis research. Transposon tagging, EMS mutagenesis and map-based cloning have already led to the isolation of four genes, *Nfr1 , Nfr5, Nin* and *Har1,* in *L. japonicus* that are required for successful interaction with root-nodulating bacteria (Krusell *et al*., 2002; Madsen *et al*., 2004; Radutoiu *et al*., 2004; Schauser *et al*., 1999) and three, *SymRK*, *Castor* and *Pollux* (Imaizumi-Anraku *et al*., 2004; Stracke *et al*., 2002), essential for both rhizobial and mycorrhizal symbioses. The orthologues of several of these genes have also been isolated in *M. truncatula* and *P. sativum* (Endre *et al*., 2002; Limpens *et al*., 2003) and plant mutants with orthologous phenotypes have been identified in *Melilotus alba, P. sativum* and *V. hirsuta* (Endre *et al*., 2002; Stracke *et al*., 2002).

Several other plant lines, occurring both naturally and also those generated through a range of mutagenic programmes, are in various stages of characterisation and cloning, aided by new reverse genetics technologies such as RNAi and TILLING (Bosher and Labouesse, 2000; Perry *et al*., 2003).

A complementary approach in T-DNA-mediated promoter-trapping in *L. japonicus* led to the identification of T90, a *gus*-tagged line showing expression of the transgene within three days of inoculation with the rhizobial symbiont *M. loti* (Webb *et al*. 2000) and also with the AM symbionts *G. mosseae* and *G. intraradices* (Parniske, personal communication).

This present work has set out to develop the work of Webb *et al*. (2000) by seeking to confirm their findings and ascertain a number of additional facts relating to the regulation and possible function of *LjCbp1*. In recognition of the potential of T90 as a tool in elucidating further aspects of the nodulating signalling pathway a mutagenesis screen was also carried out.

Webb *et al*., (2000) suggested that *LjCbp1* may be part of a family of similar genes in *L. japonicus* due to the banding pattern in their Southern analyses of the *LjCbp1* sequence probed with cDNA. The presence of, certainly CaM, isoforms in species

such as *Arabidopsis thaliana, Glycine max* and *Phaseolus vulgaris* endorses this likelihood. However, PCR amplification of *L. japonicus* DNA using *LjCbp1* primers from the coding sequence (Chapter 3) produced only a single band indicating that at least very closely related family members may not be present in *L. japonicus*. Furthermore, a thorough search of *L. japonicus* EST databases failed to reveal homologous genes that may mask gene redundancy in *L. japonicus*, although other *LjCbp*-like genes were identified (Section 3.2.1).

However, sequences exhibiting higher similarity were identified in other legumes, such as *G. max* and *Medicago truncatula*, as well as in non-legumes such as *Populus tremuloides* and *A. thaliana*. This may imply a particular role of *LjCbp1* in *L. japonicus* as the presence of what may be gene families in other species does not appear to be reflected in *L. japonicus*. It is difficult to postulate what these data mean with respect to the role of *LjCbp1*-like genes, but their presence in a wide range of organisms, not just plants, implies a conserved function. Since sequences with high similarity exist in non-legume species, it suggested that *LjCbp1* is not exclusively involved in symbiotic interactions. It is certainly not uncommon for sequences similar to those of genes involved in nodulation to be present in non-legumes. Several of the early nodulin genes, such as *ENOD*s *12* and *40* and *LjNin* have been reported to have homologues in non-leguminous species (Fang and Hirsch, 1998; Schauser *et al*., 1999; Scheres *et al*., 1990).

Determination of the transcriptional start site of the *LjCbp1* gene confirmed the full length mRNA sequence at 1004 bp, longer than that initially published (Webb *et al*., 2000) and encodes a protein of 230 amino acids and 24 KDa. This places the protein outside the CaM prototype described in Section 3.1.1 although it may still belong to the CaM-like group. No obvious function could be deduced by comparisons with similar proteins in other species as none of those closely related have yet been characterised. However, over 90 per cent identity was shared with predicted proteins in various legume and non-legume species, those that were classified were either designated Ca^{2+}-binding proteins, putative CaMs or CaM-like proteins. Preliminary investigations revealed that the protein product of *LjCbp1* underwent a mobility shift in the presence of Ca^{2+}, indicating that this protein does indeed bind Ca^{2+}.

An additional feature of LjCbp1 that was not previously determined because of the error in sequencing is the presence of a putative signal peptide at the N-terminus (Section 3.2.1 and Figure 3.8). This may indicate that LjCbp1 is targeted to an organelle, such as the endoplasmic reticulum or vacuole where Ca^{2+} is stored.

Molecular characterisation of the inserted *gus* reporter gene and *LjCbp1* revealed that both were present in non-inoculated roots and also in shoot tissues (Section 3.2.5). These again are new data. Parallel analysis of both genes revealed correlation in their expression profiles (Section 3.2.5.3) and also confirmed the results of Webb *et al*. (2000) that regulation of *LjCbp1* was impaired in T90 seedlings. This may suggest that a marked decrease or down regulation of *LjCbp1* does not inhibit nodulation.

LjCbp1 shows upregulation within six hours of inoculation with the root-nodulating *M. loti*. Although it was not confirmed that *gus* transcripts were similarly upregulated in this time frame, corresponding GUS activity was demonstrated through histochemistry within eight hours of rhizobial inoculation.

Characterisation of GUS elicitation in T90 included the analysis of a range of factors that may be expected to elicit reporter gene activity, if indeed this gene is associated with either symbiosis, or Ca^{2+}-signalling, or both. Factors eliciting GUS in T90 included Nod factor derived from *M. loti* and chitosan, a chitin-derivative. Data also indicated that the mechanism by which these factors regulate *gus* gene expression may be mediated by Ca^{2+}. Consistent with the T-DNA insertion lying within the putative promoter region of a Ca^{2+}-binding protein, activity of GUS in both shoot and in root tissue in the presence of *M. loti* was influenced by Ca^{2+} and was perturbed by a number of factors known to affect Ca^{2+} pathways (Section 4.2.4). These factors included the metal chelator EGTA and the Ca^{2+} channel antagonist nifedipine. By extension, this implicated Ca^{2+} in the regulation of *LjCbp1*.

This project has established a role for *gus* expression in T90 in reporting the regulation of a gene involved in Ca^{2+}-signalling during symbioses with root-

nodulating bacteria and AM fungi, as well as, perhaps, some undefined physiological stage of development. It must be noted, however, that the mechanisms governing the expression patterns of these genes may disassociate. GUS activity in T90 may be an artefact and not reflect the regulation of this locus as it would appear in wild-type *L. japonicus*, but the accumulated data in this thesis nevertheless support its usefulness as a reporter for both *LjCbp1* regulation and early signalling in root nodulation. In conclusion, GUS activity in T90 may not be directly reporting the expression of *LjCbp1*, but seems to be an indicator of some of the factors able to influence its expression. Such factors may have chitin, as an elicitor, in common (Chapter 4).

It should be mentioned that a potential resource not utilised in this project was that of fluorimetry (Section 4.1.2). In the first instance, where time-course experiments were being established, levels of GUS activity were not under investigation, but rather the localisation of staining. However, during later experiments set up to ascertain the effect of Ca^{2+} on GUS elicitation, the use of such an assay would likely have aided quantification of the low levels of activity observed in shoot tissue. However, because these were only preliminary investigations minimal amounts of tissue were used which did not permit the use of fluorimetry.

EMS mutagenesis of T90 established this line as a useful tool in screening for novel phenotypes in the early stages of nodulation. A number of putative nod^{-}, fix^{-} and nod^{++} mutants were identified, as well as several GUS staining mutants, two of which showed aberrant GUS activity that was either absent from nodules entirely or markedly reduced compared to T90 controls. These lines appeared to nodulate normally, however. These data and the fact that the range of different rhizobial strains tested on T90 (Section 4.2.3) all elicited some GUS activity in T90 may also suggest that this gene lies on a different pathway to that required for nodulation, since only four strains (including *M. loti*) were able to form nodules on *L. japonicus*.

The EMS mutants provide a further resource for symbiosis research and have contributed towards the characterisation of GUS::*LjCbp1*. Additional characterisation of these mutants through use of bacteria expressing the *hemAlacZ*

promoter and GFP constructs will help establish the role of these mutants in the elucidation of symbiosis signal transduction networks.

The accommodation of an organism within a plant and subsequent metabolic exchange requires diverse and complex responses on both sides. For instance, defence-related compounds from the plant and pathogenic-related compounds from the bacteria must be suppressed and controlled in order to provide a stable environment for the relationship between plant cells and rhizobia. In addition, physicochemical differences between plant cells housing bacteria and adjacent uninfected ones must also be maintained. In some cases this may require the prevention of bacterial invasion of cells adjacent to those already infected, in order to prevent hypernodulation and an excessive drain on the plant's resources, thus necessitating a suppression of defence responses in one cell and the stimulation of protective responses in another (Tajima *et al*., 2000). It is possible that GUS elicitation is in response to the suppression of plant defence responses, particularly since activity diminishes in senescing nodules (Webb *et al*., 2000). One hypothesis could therefore be that an encrypted Ca^{2+} message, sustained through a chitin-based stimulus, elicits prolonged *gus* expression and that the pattern of this expression is encoded by other determinants. These determinants could relate to Nod factor chemical decorations, lipopolysaccharide molecules and flavonoid compounds, in the case of rhizobia, and 'Myc' factors and fungal cell wall compounds, in the case of mycorrhiza. Therefore *LjCbp1* could function during this Ca^{2+} signalling. Chitin has recently been shown to induce Ca^{2+}-mediated defence responses in soybean cells (Zuppini *et al*., 2004). Therefore it seems likely that it could elicit plant responses that are involved in the suppression of these same defence mechanisms.

One of the earliest nodulation genes found to respond to inoculation with host-specific bacteria is *ENOD11*, identified in *M. truncatula* (Journet *et al*., 2001). A transgenic line expressing a *MtENOD11* promoter-GUS fusion (*pMtENOD11)* exhibits GUS activity within three to six hours after inoculation with the plant's rhizobial symbiont *Sinorhizobium meliloti* (Journet *et al*., 2001). Transcripts of this gene were also observed as early as three hpi in $polyA^+$ mRNA extracts (Journet *et al*., 2001). Expression of the gene appears to localise in developing

nodule structures, as well as on the root surface of infection sites either above developing nodules or where infections in root hairs have arrested (Journet *et al*., 2001). *MtENOD11* encodes a putative repetitive proline-rich protein (RPRP) and is similar, in both the reputed product it encodes and its spatiotemporal expression pattern, to *MtENOD12* (Journet *et al*., 2001; Journet *et al*., 1994; Pichon *et al*., 1992). Expression of both these genes diminishes in mature nodules and becomes restricted to the distal end of the nodule (Journet *et al*., 2001; Journet *et al*., 1994; Pichon *et al*., 1992), thus correlating with pre-infection and infection events throughout nodulation.

Activation of the *ENOD11* promoter occurs at a similar time point to the first detection of GUS in T90, and potentially therefore *LjCbp1*, after the addition of Nod factor. Taking into account the slower nodulation phenotype of *L. japonicus*, it seems that these two genes may be activated at very similar stages.

Therefore it seems that the expression pattern of *Cbp1* in *L. japonicus* may be temporally and spatially similar to both *ENOD11* and *12* in *M. truncatula* indicating that expression of these genes may be regulated by similar events or elements during rhizobial infection. The transcripts of *LjCbp1*, if represented by GUS, do not become restricted to the distal end of the nodule as with *ENOD*s *11* and *12*, but of course these are two different types of nodules, determinate versus indeterminate, and therefore likely to show variation at this developmental stage.

There are other similarities in expression between the expression of *ENOD*s *11* and *12* in *M. truncatula* and *gus*/*LjCbp1* in T90. Non-symbiotic GUS expression in the p*MtENOD11* line was found to be present in a number of aerial organs, including cotyledons and pulvini. Elicitation of GUS in T90 was identified in such tissues in a similarly non-symbiotic manner (Section 4.2.4), although the existence of genes involved in symbiosis but not exclusive to it is not new (Schauser *et al*., 1999), neither is the identification of a gene involved in symbiosis but not essential for it (Csanádi *et al*., 1994). However, other non-symbiotic expression of p*MtENOD11* was identified in tissues that did not correlate with that of GUS in T90, such as root apices, lateral root primordia, stomatal guard cells and in the outer layer of the endosperm during seed development (Journet *et al*., 2001). It

could be that elicitation of GUS in T90 in such tissues is in a very small number of cells and therefore not visible under normal circumstances. Perhaps a relationship exists in the regulation of the expression of these two genes that is most apparent during symbiosis, but not entirely exclusive to it. Interestingly, the expression from a *MtAnn1* promoter *gus* fusion was also identified in root tissues associated with lateral root development and in the subapical region of the root tip, both without inoculation (de Carvalho-Niebel *et al*., 2002). The elicitation of GUS in T90, and therefore it seems of *LjCbp1*, appears to show greater symbiotic specificity than *ENOD*s*11*, *12* and *MtAnn1*.

It could be argued that the upregulation observed in *LjCbp*1 expression is not great, however it is important to remember that even small degrees of fluctuation can lead to an amplification effect downstream. However, observations of the level of expression of *LjCbp1* in hairy root cultures showed a high level of expression without a correspondingly high level of GUS activity (Judith Webb, unpublished results). These data point to a dissociation of the upstream signalling mechanism for the two genes that maybe represents the effect of different, as yet unidentified, environmental factors. The region of promoter between the T-DNA insert and *LjCbp1* may become important under these particular conditions. If this is the case, the list of hormones, signalling-related, and other abiotic substances tested against GUS elicitation (Chapter 4), should also be tested against *LjCbp1*.

The observation of GUS activity within eight hours of inoculation with purified Nod factor places the gene early in the signalling pathway and on a par with *ENOD*s *11* and *12* in *Medicago* species. Crosses between *Ljsym4-2* and T90 do not express GUS (Parniske and Webb, personal communication), placing T90 *gus* downstream of this locus. This also lends support that this locus is connected with the symbiosis. Plans are underway to investigate whether Ca^{2+}-spiking in the T90 line is similar to that in wild-type plants (Webb, personal communication). It seems that regulation of the *gus* transgene in T90 lies between *Castor* and the *nin* gene (see Figure 1.9), since crosses between *Ljnin* and T90 are GUS positive after challenge with *M. loti* (Webb, personal communication). The existence of genes involved in symbiosis but not exclusive to it is not novel (Schauser *et al*., 1999), nor is the identification of a gene involved in symbiosis, but not essential for it

(Csanádi *et al*., 1994). However, the lack of a notable phenotype makes it more difficult to assign a function to *LjCbp1*. The identification or creation of mutants using reverse genetics techniques such as TILLING or RNAi, respectively, could clarify the importance of *LjCbp1* in early signal transduction.

The value of T90 in future work is perhaps as a tool. In addition to the tagged mutants available from the EMS screen, promoter analysis, particularly of the region upstream of the T-DNA insertion, since it is this region that appears to confer symbiosis specificity, will be of paramount importance and promises the potential of a region governing part of a symbiosis-specific locus of *L. japonicus*. The characterisation of this region will be facilitated by the upstream sequence available on TAC LjT15I02; an additional 12 Kb section preceding the T-DNA insertion is ready for construct analysis. This extensive region may be important for regulation as binding sites for transcriptional regulators have been identified as far as 10 Kb up or downstream of transcription start sites, as the compaction of DNA in chromatin means that, physically, regions may be quite close (Franklin Pugh, 2001). Furthermore, the importance of Ca^{2+} in the nodulation signal transduction pathway, not to mention in signal transduction generally, has been well established. The isolation of a promoter involved in Ca^{2+} signalling and potentially triggered by chitin, that is expressed in root cells during symbioses between *L. japonicus* and both rhizobia and mycorrhiza and in shoot tissues during what appears to be an as yet undefined developmental stage is highly significant. It provides potential for investigations into several broad areas of plant research including pollen tube growth, cell development and differentiation, and root hair growth.

The advent of tractable model legumes, combined with advances made in genomics, has fuelled interest in legume-symbiont research. It is worth bearing in mind, however, that *L. japonicus* and *M. truncatula* account for only a fraction of the overall diversity in legumes. We have been slow to recognise important traits in the past and if we concentrate too hard on a few species we may miss out on some of the important agronomic traits of the future (Doyle and Lucknow, 2003), for instance, those that will perform well in a climate with elevated temperature or with higher carbon dioxide levels. However, the application of the techniques of

transcriptomics, proteomics and metabolomics will provide a framework within which current and future knowledge will fit. Major and possibly unexpected benefits will accrue from our advanced understanding of the intricate association between plants and their symbionts. But comments made by Allen and Allen (1981) about the need for research in this area are truer and more pressing than ever today: the rich diversity of leguminous species is being destroyed in many cases and yet the need for such species is increasing. According to Nwokolo (1996), most people in the developing countries have seen an outrageous increase in local prices of food due to devaluation of the local currency in order to meet the International Monetary Fund conditions for restructuring loans, to spur foreign investments and to encourage exports. Nwokolo stated that the resulting resurgence of interest in and enhanced consumption of cowpeas, common beans, pigeon pea and other pulses is no temporary or seasonal resurgence because food shortages and high prices in Africa seem to be as endemic as malaria and mosquitoes, as common as drought and famine.

References

Allen, O. N. and Allen, E. K. (1981). The Leguminosae. A source book of characteristics, uses and nodulation. MacMillan Publishers Ltd, London, U.K.

Allen, G. J., Kwak, J. M., Chu, S. P., Llopis, J., Tsien, R.Y., Harper, J. F. and Schroeder, J. I. (1999). Cameleon calcium indicator reports cytoplasmic calcium dynamics in *Arabidopsis* guard cells. *Plant Journal* **19** (6), 735-747.

Altschul, S.F., Madden, T.L., Schäffer, A.A., Zhang, J., Zhang, Z., Miller, W. and Lipman, D.J. (1997). Gapped BLAST and PSI-BLAST: a new generation of protein database search programs. *Nucleic Acids Res*earch **25**, 3389-3402.

Ané, J. M., Kiss, G. B., Riely, B. K., Penmetsa, R. V., Oldroyd, G. E. D., Ayax, C., Lévy, J., Debellé, F., Baek, J. M., Kalo, P., Rpsenberg, C., Roe, B. A., Long, S. R., Dénarié, J. and Cook, D. R. (2004). *Medicago truncatula DMI1* required for bacterial and fungal symbiosis in legumes. *Science* **303** (5662), 1364-1367.

Aoki, T., Akashi, T. and Ayabe, S. (2000) Flavonoids of leguminous plants: structure, biological activity, and biosynthesis. *Journal of Plant Research* **113**, 475-488.

Arabidopsis-Genome-Initiative (2000). Analysis of the genome sequence of the flowering plant *Arabidopsis thaliana*. *Nature* **408**, 796-815.

Arambarri, A. M. (1999). Illustrated Catalogue of *Lotus* L. Seeds (Fabaceae). *In:* Trefoil: The Science and Technology of *Lotus*. P. R. Beuselinck, ed. American Society of Agronomy, Inc, Madison, Wisconsin, U.S.A.

Ardourel, M., Demont, N., Debellé, F., Maillet, F., de Billy, F., Promé, J.C., Dénarié, J. and Truchet, G. (1994). *Rhizobium meliloti* lipooligosaccharide nodulation factors: different structural requirements for bacterial entry into target root hair cells and induction of plant symbiotic developmental responses. *Plant Cell* **6,** 1357-1374.

Arnold DB. and Heintz, N. (1997). A calcium responsive element that regulates expression of two calcium-binding proteins in Purkinje cells. *Proceedings of the National Academy of Sciences of the United States of America* **94** (16), 8842-7.

Asaimizu, E., Kato, T., Sato, S., Nakamura, Y., Kaneko, T. and Tabata, S. (2003). Structural analysis of a *Lotus japonicus* genome. IV. Sequence features and mapping of seventy-three TAC clones which cover the 7.5 Mb regions of the genome. *DNA Research* **10**, 115-122.

Banba, M., Siddique, A. B. M., Kouchi, H., Izui, K. and Hata, S. (2001). *Lotus japonicus* forms early senescent root nodules with *Rhizobium etli*. *Molecular Plant-Microbe Interactions* **14**, 173-180.

Barker, D. G., Bianchi, S., Blondon, F., Dattée, Y., Duc, G., Essad, S., Flament, P., Gallusci, P., Génier, G., Guy, P., Muel, X., Tourneur, J., Dénarié, J. and Huguet, T. (1990). *Medicago truncatula*, a model plant for studying the molecular genetics of the *Rhizobium*-legume symbiosis. *Plant Molecular Biology Reporter* **8**, 40-49.

Bénaben, V., Duc, G., Léfèbvre, V. and Huguet, T. (1995). Te7, an inefficient symbiotic mutant of *Medicago truncatula* Gaertn cv Jemalong. *Plant Physiology* **107**, 53-62.

Bennett, M. D. and Leitch, I. J. (2004). Plant DNA C-values database (release 3.0, Dec. 2004) http://www.rbgkew.org.uk/cval/homepage.html.

Berridge, M. J., Bootman, M. D. and Lipp, P. (1998). Calcium - a life and death signal. *Nature* **395**, 645-648.

Bhatla, S. C., Kiessling, J. and Reski, R. (2002). Observation of polarity induction by cytochemical localization of phenylalkylamine-binding sites in regenerating protoplasts of the moss *Physcomitrella patens*. *Protoplasma* **219**, 99-105.

Blackburn, G. M. and Gait, M. J., eds. (1990). Nucleic acids in chemistry and biology. IRL Press, Oxford, U.K.

Bonfante, P., Genre, A., Faccio, A., Martini, I., Schauser, L., Stougaard, J., Webb, J. and Parniske, M. (2000). The *Lotus japonicus Ljsym4* gene is required for the successful symbiotic infection of root epidermal cells. *Molecular Plant-Microbe Interactions* **13**, 1109-1120.

Borget, M. (1992). Food legumes. Macmillan Press, London and Basingstoke, U.K.

Borisov, A. Y., Morzhina, E. V., Kulikova, O. A., Tchetkova, S. A., Lebsky, V. K. and Tikhonovich, I. A. (1993). New symbiotic mutants of pea (*Pisum sativum*) affecting either nodule development or symbiosome development. *Symbiosis* **14** (1-3), 297-313.

Bosher, J. M. and Labouesse, M. (2000). RNA interference: genetic wand and genetic watchdog. *Nature Cell Biology* **2**, E31-E36.

Braam, J., Sistrunk, M. L., Polisensky, D. H., Xu, W., Purugganan, M. M., Antosiewicz, D. M., Campbell, P. and Johnson, K. A. (1997). Plant responses to environmental stress: regulation and functions of the *Arabidopsis TCH* genes. *Planta* **203**, S35-S41.

Bras, C. P. (2003). The symbiosis between *Lotus japonicus* and rhizobia: function of nod factor structural variation. PhD thesis, Leiden university, Leiden, The Netherlands.

Broughton, W. J. and Perret, X. (1999). Genealogy of legume-*Rhizobium* symbioses. *Current Opinion in Plant Biology* **2**, 305-311.

Camas, A., Cárdenas, L., Quinto, C. and Lara, M. (2002). Expression of different calmodulin genes in bean (*Phaseolus vulgaris* L.): Role of nod factor on calmodulin gene regulation. *Molecular Plant-Microbe Interactions* **15**, 428-436.

Cárdenas, L., Dominguez, J., Quinto, C., López-lara, I. M., Lugtenberg, B. J. J., Spaink, H., Rademaker, G. J., Haverkamp, J. and Thomas-Oates, J. E. (1995). Isolation, chemical structures and biological activity of the lipo-chitin oligosaccharide nodulation signals from *Rhizobium etli*. *Plant Molecular Biology* **29**, 453-464.

Cárdenas, L., Holdaway-Clarke, T. L., Sanchez, F., Quinto, C., Feijo, J. A., Kunkel, J. G. and Hepler, P. K. (2000). Ion changes in legume root hairs responding to Nod factors. *Plant Physiol*ogy **123,** 443–452.

Catoira, R., Galera, C., de Billy, F., Penmetsa, R. V., Journet, E. P., Maillet, F., Rosenberg, C., Cook, D., Gough, C. and Denarie, J. (2000). Four genes of *Medicago truncatula* controlling components of a nod factor transduction pathway. *Plant Cell* **12**, 1647-1665.

Celio, M. R., Pauls, T. L. and Schwaller, B. (1996). Introduction to EF-hand calcium-binding proteins. *In:* Guidebook to the calcium-binding proteins. Oxford University Press, New York, U.S.A.

Chen, X. and Wu, R. (1997). Direct amplification of unknown genes and fragments by uneven polymerase chain reaction. *Gene* **185**, 195-199.

Chua, K. -Y., Pankhurst, C. E., MacDonald, P. E., Hopcroft, D. H., Jarvis, B. D. W. and Scott, D. B. (1985). Isolation and characterization of transposon Tn5-induced symbiotic mutants of *Rhizobium loti*. *Journal of Bacteriology* **162**, 335-343.

Cleveland, C. C., Townsend, A. R., Schimel, D. S., Fisher, H., Howarth, R. W., Hedin, L. O., Perakis, S.S., Latty, E.F., Von Fischer, J. C., Elseroad, A. and Wasson, M. F. (1999). Global patterns of terrestrial biological nitrogen (N_2) fixation in natural ecosystems. *Global Biogeochemical Cycles*, **13** (2), 623-645.

Clover, R. H., Kieber, J. and Signer, E. R. (1989). Lipopolysaccharide mutants of *Rhizobium meliloti* are not defective in symbiosis. *Journal of Bacteriology* **171**, 3961-3967.

Cook, D. R., VandenBosch, K., de Bruijn, F. J. and Huguet, T. (1997). Model legumes get the nod. *Plant Cell* **9**, 275-280.

Cooke, D. E. and Webb, K. J. (1997). Stability of CaMV 35S-*gus* gene expression in (Bird's foot trefoil) hairy root cultures under different growth conditions. *Plant Cell, Tissue and Organ Culture* **47**, 163-168.

Cordier, C., Gianinazzi, S. and Gianinazzi-Pearson, V. (1996). Colonisation patterns of root tissues by *Phytophthora nicotiane* var *parasitica* related to reduced disease resistance in mycorrhizal tomato. *Plant and Soil* **185** (2), 223-232.

Craig, J., Barratt, P., Tatge, H., Déjardin, A., Handley, L., Gardner, C. D., Barber, L., Wang, T., Hedley, C., Martin, C. and Smith, A. M. (1999). Mutations at the *rug4* locus alter the carbon and nitrogen metabolism of pea plants through an effect on sucrose synthase. *Plant Journal* **17**, 353-362.

Csanádi, G., Szécsi, J., Kaló, P., Kiss, P., Endre, G., Kondorosi, A., Kondorosi, E. and Kiss, G. B. (1994). *ENOD12*, an early nodulin gene, is not required for nodule formation and efficient nitrogen fixation in alfalfa. *Plant Cell* **6**, 201-213.

Cserzo, M., Wallin, E., Simon, I., von Heijne, G. and Elofsson, A. (1997). Prediction of transmembrane alpha-helices in prokaryotic membrane proteins: the Dense Alignment Surface method. *Protein Engineering* **10**, 673-676.

Cullimore, J. V., Ranjeva, R. and Bono, J. J. (2001). Perception of lipo-chitooligosaccharidic Nod factors in legumes. *Trends in Plant Science* **6**, 24-30.

de Carvalho-Niebel, F., Timmers, A. C. J., Chabaud, M., Defaux-Petras, A. and Barker, D. G. (2002). The Nod factor-elicited annexin *MtAnn1* is preferentially localised at the nuclear periphery in symbiotically activated root tissues of *Medicago truncatula*. *Plant Journal* **32**, 343-352.

de Jong, A. J., Cordewener, J., Lo Schiavo, F., Terzi, M., Vandekerckhove, J., Van Kammen, A. and De Vries, S. C. (1992). A carrot somatic embryo mutant is rescued by chitinase. *Plant Cell* **4**, 425-433.

Dénarié, J., Debellé, F. and Promé, J. C. (1996). Rhizobium lipo-chitooligosaccharide nodulation factors: Signaling molecules mediating recognition and morphogenesis. *Annual Review of Biochemistry* **65**, 503-535.

D'Haeze, W., Gao, M. S., De Rycke, R., Van Montagu, M., Engler, G. and Holsters, M. (1998). Roles for azorhizobial nod factors and surface polysaccharides in intercellular invasion and nodule penetration, respectively. *Molecular Plant-Microbe Interactions* **11**, 999-1008.

D'Haeze, W., De Rycke, R., Mathis, R., Goormachtig, S., Pagnotta, S., Verplancke, C., Capoen, W. and Holsters, M. (2003). Reactive oxygen species and ethylene play a positive role in lateral root base nodulation of a semiaquatic legume. *Proceedings of the National Academy of Sciences*, U.S.A. **100,** 11789–11794.

Downie, J. A. and Walker, S. A. (1999). Plant responses to nodulation factors. *Current Opinion in Plant Biology* **2** (6), 483-489.

Doyle, J. J. and Lucknow, M. A. (2003). The rest of the iceberg. Legume diversity and evolution in a phylogenetic context. *Plant Physiology* **131** (3), 900-910.

Duc, G. and Messager, A. (1989). Mutagenesis of pea (*Pisum sativum* L.) and the isolation of mutants for nodulation and nitrogen fixation. *Plant Science* **60**, 207-213.

Ehrhardt, D. W., Wais, R. and Long, S. R. (1996). Calcium spiking in plant root hairs responding to *Rhizobium* nodulation signals. *Cell* **85**, 673-681.

El Yahyaoui, F., Küster, H., Ben Amor, B., Hohnjec, H., Pühler, A., Becker, A., Gouzy, J., Vernié, T., Gough, C., Niebel, A., Godiard, L., Gamas, P. (2004). Expression profiling in *Medicago truncatula* identifies more than 750 genes differentially expressed during nodulation, including many potential regulators of the symbiotic program. *Plant Physiology* **136** (2), 3159-76.

Endre, G., Kereszt, A., Kevei, Z., Mihacea, S., Kalo, P. and Kiss, G. B. (2002). A receptor kinase gene regulating symbiotic nodule development. *Nature* **417**, 962-966.

Engstrom, E. M., Ehrhardt, D. W., Mitra, R. M. and Long, S. R. (2002). Pharmacological analysis of nod factor-induced calcium spiking in *Medicago truncatula*. Evidence for the requirement of type IIA calcium pumps and phosphoinositide signaling. *Plant Physiology* **128**, 1390-1401.

Esseling, J. J., Lhuissier, F. G. P. and Emonds, A. M. C. (2004). A nonsymbiotic root hair tip growth phenotype in *NORK*-mutated legumes: implications for nodulation factor-induced signalling and formation of a multifaceted root hair pocket for bacteria. *Plant Cell* **16** (4): 933-944.

Ewaza, T., Smith, S. E. and Smith, A. (2002). P metabolism and transport in AM fungi. *Plant and Soil* **244**, 221-230.

Fåhraeus, G. (1957). The infection of clover root hairs by nodule bacteria studied by a simple glass technique. *Journal of General Microbiology* **16**, 374-381.

Fang, Y. W. and Hirsch, A. M. (1998). Studying early nodulin gene *ENOD40* expression and induction by nodulation factor and cytokinin in transgenic alfalfa. *Plant Physiology* **116**, 53-68.

Farrar, K., Evans, I. M., Topping, J.F., Souter, M.A., Nielsen, J.E. and Lindsey K. (2003). EXORDIUM - a gene expressed in proliferating cells and

with a role in meristem function, identified by promoter trapping in *Arabidopsis*. *Plant Journal* **33** (1), 61-73.
Feldmann, K., Mamlberg, R. L. and Dean, C. (1994). Mutagenesis in *Arabidopsis*. *In: Arabidopsis*. Cold Spring Harbor Laboratory Press, U.S.A.
Felle, H. H., Kondorosi, E., Kondorosi, A. and Schultze, M. (1995). Nod Signal-Induced Plasma-Membrane Potential Changes in Alfalfa Root Hairs Are Differentially Sensitive to Structural Modifications of the Lipochitooligosaccharide. *Plant Journal* **7**, 939-947.
Felle, H. H., Kondorosi, E., Kondorosi, A. and Schultze, M. (1998). Elevation of the cytosolic free [Ca^{2+}] is indispensable for the transduction of the nod factor signal in alfalfa. *Plant Physiology* **121** (1), 273-279.
Felle, H. H., Kondorosi, E., Kondorosi, A. and Schultze, M. (1999). Nod factors modulate the concentration of cytosolic free calcium differently in growing and non-growing root hairs of *Medicago sativa* L. *Planta* **209** (2), 207-212.
Felsenstein, J. (1993). PHYLIP (Phylogenetic Inference Package) version 3.6., Distributed by the author. Department of Genetics, University of Washington, Seattle.
Finan, T. M. (2002). Evolving insights: symbiosis islands and horizontal gene transfer. *Journal of Bacteriology* **184** (11), 2855-2856.
Firmin, J. L., Wilson, K. E., Rossen, L. and Johnston, A. W. B. (1986). Flavonoid activation of nodulation genes in *Rhizobium* reversed by other compounds present in plants. *Nature* **324**, 90-92.
Fisher, R. F. and Long, S. R. (1992). *Rhizobium* - plant signal exchange. *Nature* **357**, 655-660.
Franklin Pugh, B. (2001). RNA polymerase II transcription machinery. *In:* Transcription Factors. J. Locker, ed. BIOS Scientific Publishers Ltd, Oxford, U.K.
Frühling, M., Roussel, H., Gianinazzi-Pearson, V., Pühler, A. and Perlick, A. M. (1997). The *Vicia faba* mycorrhizal fungus *Glomus fasciculatum*. *Molecular Plant-Microbe Interactions* **10** (1), 124-131.
Gagnon, H. and Ibrahim, R. K (1998). Aldonic acids: A novel family of nod gene inducers of *Mesorhizobium loti*, *Rhizobium lupini*, and *Sinorhizobium meliloti*. *Molecular Plant-Microbe Interactions* **11** (10), 988-998.
Galibert, F., Finan, T. M., Long, S. R., Puhler, A., Abola, P., Ampe, F., Barloy-Hubler, F., Barnett, M. J., Becker, A., Boistard, P., Bothe, G., Boutry, M., Bowser, L., Buhrmester, J., Cadieu, E., Capela, D., Chain, P., Cowie, A., Davis, R. W., Dreano, S., Federspiel, N. A., Fisher, R. F., Gloux, S., Godrie, T., Goffeau, A., Golding, B., Gouzy, J., Gurjal, M., Hernandez-Lucas, I., Hong, A., Huizar, L., Hyman, R. W., Jones, T., Kahn, D., Kahn, M. L., Kalman, S., Keating, D. H., Kiss, E., Komp, C., Lalaure, V., Masuy, D., Palm, C., Peck, M. C., Pohl, T. M., Portetelle, D., Purnelle, B., Ramsperger, U., Surzycki, R., Thebault, P., Vandenbol, M., Vorholter, F. J., Weidner, S., Wells, D. H., Wong, K., Yeh, K. C. and Batut, J. (2001). The composite genome of the legume symbiont *Sinorhizobium meliloti*. *Science* **293**, 668-672.

Galloway, J. N., Schlesinger, W. H., Levy, H., Michaels, A. and Schnoor, J. L. (1995). Nitrogen fixation: anthropogenic enhancement-environmental response. *Global Biogeochemical Cycles* **9**, 235-252

Gamas, P., Niebel, F. D. C., Lescure, N. and Cullimore, J. V. (1996). Use of a subtractive hybridization approach to identify new *Medicago truncatula* genes induced during root nodule development. *Molecular Plant-Microbe Interactions* **9**, 233-242.

García-Garrido, J. M. and Ocampo, J. A. (2002). Regulation of the plant defence response in arbuscular mycorrhizal symbiosis. *Journal of Experimental Botany* **53** (373), 1377-1386.

Gehring, C. A., Williams, D. A., Cody, S.H. and Parish, R. W. (1990). Phototropism and geotropism in maize coleoptiles are spatially correlated with increases in cytosolic free calcium. *Nature* **7** (345), 528-530.

Genomatix (1998). http://www.genomatix.de/. Genomatix Software GmbH.

Genre, A. and Bonfante, P. (2002). Epidermal cells of a symbiosis-defective mutant of *Lotus japonicus* show altered cytoskeleton organisation in the presence of a mycorrhizal fungus. *Protoplasma* **219**, 43-50.

Gianinazzi-Pearson, V. (1996). Plant cell responses to arbuscular mycorrhizal fungi: getting to the roots of the symbiosis. *The Plant Cell* **8**, 1871-1883.

Giller, K. E. and Wilson, K. J. (1991). Nitrogen fixation in tropical cropping systems, 1st Edition. CAB, Wallingford, U.K.

Goddijn, O. J. M., Lindsey, K., van der Lee, F. M., Klap, J. C. and Sijmons, P. C. (1993). Differential gene expression in nematode-induced feeding structures of transgenic plants harbouring promotergusA fusion constructs. *The Plant Journal* **4** (5), 863-873.

Gollotte, A., Gianinazzi-Pearson, V. and Gianinazzi, S. (1995). Immunodetection of infection thread glycoprotein and arabinogalactan protein in wild-type *Pisum sativum* (L) or an isogenic mycorrhiza-resistant mutant interacting with *Glomus mosseae*. *Symbiosis* **18**, 69-85.

Gonzalez-Ballester, D., de Montaigu, A., Higuera, J. J., Galvan, A. and Fernandez, E. (2005). Functional genomics of the regulation of the nitrate assimilation pathway in *Chlamydomonas*. *Plant Physiology* **137** (2), 522-533.

Goodsell, D. S. (2005). Molecule of the month. Website address: http://www.rcsb.org/pdb/molecules/pdb58_1.html

Graf, E., Mahoney, J. R., Bryant, R. G. and Eaton, J. W. (1984). Iron-catalyzed hydroxyl radical formation. Stringent requirement for free iron coordination site. *Journal of Biological Chemistry* **259**, 3620-4.

Gressent, F., Mantegazza, N., Cullimore, J. V., Driguez, H., Ranjeva, R. and Bono, J. J. (2002). High-affinity nod factor binding site from *Phaseolus vulgaris* cell suspension cultures. *Molecular Plant-Microbe Interactions* **15**, 834-839.

Haas, B.J., Volfovsky, N., Town, C. D., Troukhan, M., Alexandrov, N., Feldmann, K. A., Flavell, R. B., White, O. and Salzberg, S. L. (2002). Full-length messenger RNA sequences greatly improve genome annotation. *Genome Biology* **3** (6), 29.

Handberg, K. and Stougaard, J. (1992). *Lotus japonicus*, an Autogamous, Diploid Legume Species for Classical and Molecular-Genetics. *Plant Journal* **2**, 487-496.

Harris, J. M., Wais, R. and Long, S. R. (2003). *Rhizobium*-Induced Calcium Spiking in *Lotus japonicus*. *Molecular Plant-Microbe Interactions* **14**, 335-341.

Hartwig, U. A., Joseph, C. M. and Phillips, D. A. (1991). Flavonoids released from alfalfa seeds enhance growth rate of *Rhizobium meliloti*. *Plant Physiology* **95** (3), 797-803.

Haseloff, J. and Amos, B. (1995). GFP in plants. *Trends in Plant Genetics* **11** (8), 328-329.

Haseloff, J., Siemering, K., R., Prasher, D., C. and Hodge, S. (1997). Removal of a cryptic intron and subcellular localization of green fluorescent protein are required to mark transgenic *Arabidopsis* plants brightly. *Proceedings of the National Academy of Sciences of the United States of America* **94** (6), 2122–2127.

Hebe, G., Hager, A. and Salzer, P. (1999). Initial signalling processes induced by elicitors of ectomycorrhiza-forming fungi in spruce cells can also be triggered by G-protein-activating mastoparan and protein phosphatase-inhibiting cantharidin. *Planta* **207**, 418-425.

Heidstra, R., Geurts, R., Franssen, H., Spaink, H. P., Van Kammen, A. and Bisseling, T. (1994). Root Hair Deformation Activity of Nodulation Factors and Their Fate on *Vicia sativa*. *Plant Physiology* **105** (3), 787–797.

Heidstra, R., Nilsen, G., Martinez-Abarca, F., van Kammen, A. and Bisseling, T. (1997). Nod Factor-Induced Expression of Leghemoglobin to Study the Mechanism of NH_4NO_3 Inhibition on Root Hair Deformation. *Molecular Plant-Microbe Interactions* **10** (3), 215-220.

Higo, K., Ugawa, Y., Iwamoto, M. and Korenaga, T. (1999). Plant *cis*-acting regulatory DNA element (PLACE). *Nucleic Acids Research* **27**, 297-300.

Hirsch, A. M. (1992). Developmental biology of legume nodulation. *New Phytologist* **122**, 211-237.

Hirsch, A. M., Bhuvaneswari, T. V., Torrey, J. G. and Bisseling, T. (1989). Early nodulin genes are induced in alfalfa root outgrowths elicited by auxin transport inhibitors. *Proceedings of the National Academy of Sciences of the United States of America* **86**, 1244-1248.

Hirsch, A. M. and Fang, Y. W. (1994). Plant hormones and nodulation: what's the connection? *Plant Molecular Biology* **26**, 5-9.

Hoagland, D.R. and Arnon, H.I. (1938). Synthetic media for hydroponic culture. *California Experimental Agriculture Publication* **347,** 35-37.

Hughes, M. A. (1996). Plant Molecular Genetics. Dorset Press, Dorset, U.K..

Imaizumi-Anraku, H., Kawaguchi, M., Koiwa, H., Akao, S. and Syono, K. (1997). Two ineffective-nodulating mutants of *Lotus japonicus* - different phenotypes caused by the blockage of endocytotic bacterial release and nodule maturation. *Plant and Cell Physiology* **38**, 871-881.

Imaizumi-Anraku, H., Kouchi, H., Syono, K., Akao, S. and Kawaguchi, M. (2000). Analysis of *ENOD40* expression in alb1, a symbiotic mutant of *Lotus japonicus* that forms empty nodules with incompletely developed nodule vascular bundles. *Molecular and General Genetics* **264**, 402-410.

Imaizumi-Anraku, H., Takeda, N., Charpentier, M., Perry, J., Miwa, H., Umehara, Y., Kouchi, H., Murakami, Y., Mulder, L., Vickers, K., Pike, J., Downie, A., J., Wang, T., Sato, S., Asamizu, E., Tabata, S., Yoshikawa, M., Murooka, Y., Wu, G. J., Kawaguchi, M., Kawasaki, S.,

Parniske, M. and Hayashi, M. (2004). Plastid proteins crucial for symbiotic fungal and bacterial entry into plant roots. *Nature* **433**, 527-531.

Jakobek, J. L., Smith-Becker, J. A. and Lindgren, P. B. (1999). A bean cDNA expressed during a hypersensitive reaction encodes a putative calcium-binding protein. *Molecular Plant-Microbe Interactions* **12** (8), 712-719.

Jang, H. J., Pih, K. T., Kang, S. G., Lim, J. H., Jin, J. B., Piao, H. L. and Hwang, I. (1998). Molecular cloning of a novel Ca^{2+}-binding protein that is induced by NaCl stress. *Plant Molecular Biology* **37**, 839-847.

Jefferson, R. A., Kavanagh, T. A. and Bevan, M. W. (1987). Gus fusions - beta-glucuronidase as a sensitive and versatile gene fusion marker in higher-plants. *Embo Journal* **6**, 3901-3907.

Jenkinson, D. S. (2001). The impact of humans on the nitrogen cycle, with focus on temperate arable agriculture. *Plant Soil* **228** (1), 3-15.

Johnson, S., Liu, C. M. and Hedley, C. L. (1994). An analysis of seed development in *Pisum sativum*. The isolation of mutants defective in embryo development. *Journal of Experimental Botany* **45** (280), 1503-1511.

Journet, E. P., El-Gachtouli, N., Vernoud, V., de Billy, F., Pichon, M., Dedieu, A., Arnould, C., Morandi, D., Barker, D. G. and Gianinazzi-Pearson, V. (2001). *Medicago truncatula ENOD11*: A novel RPRP-encoding early nodulin gene expressed during mycorrhization in arbuscule-containing cells. *Molecular Plant-Microbe Interactions* **14**, 737-748.

Journet, E. P., Pichon, M., Dedieu, A., de Billy, F., Truchet, G. and Barker, D. G. (1994). *Rhizobium meliloti* Nod factors elicit cell-specific transcription of the *ENOD12* gene in transgenic alfalfa. *Plant Journal* **6**, 241-249.

Kaneko, T., Nakamura, Y., Sato, S., Asamizu, E., Kato, T., Sasamoto, S., Watanabe, A., Idesawa, K., Ishikawa, A., Kawashima, K., Kimura, T., Kishida, Y., Kiyokawa, C., Kohara, M., Matsumoto, M., Matsuno, A., Mochizuki, Y., Nakayama, S., Nakazaki, N., Shimpo, S., Sugimoto, M., Takeuchi, C., Yamada, M. and Tabata, S. (2000). Complete genome structure of the nitrogen-fixing symbiotic bacterium *Mesorhizobium loti*. *DNA Research* **7**, 331-8.

Kapulnik, Y. and Douds, D. J. (2000). *In:* Arbuscular Mycorrhizas: Physiology and Function. Y. Kapulnik and D. Douds, eds., pp. 1. Kluwer Academic Publishers, Dordrecht, Holland.

Kawaguchi, M., Imaizumi-Anraku, H., Koiwa, H., Niwa, S., Ikuta, A., Syono, K. and Akao, S. (2002). Root, root hair, and symbiotic mutants of the model legume *Lotus japonicus*. *Molecular Plant-Microbe Interactions* **15**, 17-26.

Kenton, P., Mur, L. A. J. and Draper, J. (1999). A requirement for calcium and protein phosphatase in the jasmonate-induced increase in tobacco leaf acid phosphatase specific activity. *Journal of Experimental Botany* **50**, 1331-1341.

Kertbundit, S., De Greve, H., Deboeck, F., Van Montagu, M. and Hernalsteens, J. (1991). *In vivo* random β-glucuronidase gene fusions in *Arabidopsis thaliana*. *Proceedings of the National Academy of Sciences of the United States of America* **88,** 5212-5216.

Kimball, J. W. (2005). Second messengers. Website address: http://users.rcn.com/jkimball.ma.ultranet/BiologyPages/S/Second_messengers.html.

Kirkbride, J. H. (1999). *Lotus* systematics and distribution. *In:* Trefoil: the science and technology of *Lotus*. P. R. Beuselinck, ed. American Society of Agronomy, Inc, Madison, Wisconsin, U.S.A.

Kistner, C. and Parniske, M. (2002). Evolution of signal transduction in intracellular symbiosis. *Trends in Plant Science* **7**, 511-518.

Knight, H. and Knight, M. R. (2001). Abiotic stress signalling pathways: specificity and cross-talk. *Trends in Plant Science* **6**, 262-267.

Koizumi, N., Mizuguchi, H., Kondoh, M., Fujii, M., Hayakawa, T. and Watanabe, Y. (2004). Efficient gene transfer into human trophoblast cells with adenovirus vector containing chimeric type 5 and 35 fiber protein. *Biological and Pharmaceutical Bulletin* **27** (12), 2046-2048.

Koncz, C., Martini, N., Mayerhofer, R., Koncz-Kalman, Z. and Körber, H. (1989). High-frequency T-DNA mediated gene tagging in plants. *Proceedings of the National Academy of Sciences of the United States of America* **86**, 8467-71.

Kosuta, S., Chabaud, M., Lougnon, G., Gough, C., Dénarié, J., Barker, D. G. and Bécard, G. (2003). A diffusible factor from arbuscular mycorrhizal fungi induces symbiosis-specific *MtENOD11* expression in roots of *Medicago truncatula*. *Plant Physiology* **131**, 952-962.

Krusell, L., Madsen, L. H., Sato, S., Aubert, G., Genua, A., Szczyglowski, K., Duc, G., Kaneko, T., Tabata, S., de Bruijn, F., Pajuelo, E., Sandal, N. and Stougaard, J. (2002). Shoot control of root development and nodulation is mediated by a receptor-like kinase. *Nature* **420**, 422-426.

La Rue, T. A. and Weedon, N. F. (1994). The symbiosis genes of the host. *Proceedings of the 1st European Nitrogen Fixation Conference*, 147-151.

Langdon, T., Seago, C., Mende, M., Leggett, M., Thomas, H., Forster, J. W., Thomas, H., Jones, N. and Jenkins, G. (2000). Retrotransposon Evolution in Diverse Plant Genomics. *Genetics* **156**, 313-325.

Lee, J. Y. and Harmon, A. C. (1995). Characterization of soybean calmodulin-like domain protein- kinase (CDPK) isoforms expressed in *Escherichia coli*. *Plant Physiology* **108**, 141-141.

Legocki, A. B., Karlowski, W. M., Podkowinski, J., Sikorski, M. and Stepkowski, T. (1997). Advances in molecular characterization of the yellow lupin *Bradyrhizobium* sp. (*Lupinus*) symbiotic model. *In:* Biological fixation of nitrogen for ecology and sustainable agriculture. A. Legocki, H. Bothe and A. Puhler, eds., pp. 263-266. Springer, Berlin, Germany.

Legue, V., Blancaflor, E., Wymer, C., Perbal, G., Fantin, D. and Gilroy, S. (1997). Cytoplasmic free Ca^{2+} in *Arabidopsis* roots changes in response to touch but not gravity. *Plant Physiology* **114** (13), 789-800.

Lerouge, P., Roche, P., Faucher, C., Maillet, F., Truchet, G., Promé, J. C. and Dénarié, J. (1990). Symbiotic host-specificity of *Rhizobium meliloti* is determined by a sulfated and acylated glucosamine oligosaccharide signal. *Nature* **344**, 781-784.

Lescot, M., Déhais, G. T., Marchal, K., Moreau, Y., Van de Peer, Y., Rouzé, P. and Rombauts, S. (2002). PlantCARE, a database of plant *cis*-acting

regulatory elements and a portal to tools for *in silico* analysis of promoter sequences. *Nucleic Acids Research* **30**, 325-327.

Leung, J., Merlot, S. and Giraudat, J. (1997). The *Arabidopsis* ABSCISIC ACID-INSENSITIVE2 (ABI2) and ABI1 genes encode homologous protein phosphatases 2C involved in abscisic acid signal transduction. *Plant Cell* **9** (5), 759-771.

Lévy, J., Bres, C., Geurts, R., Chalhoub, B., Kulikova, O., Duc, G., Journet, E. P., Ané, J. M., Lauber, E., Bisseling, T., Débarié, J., Rosenberg, C. and Debellé, F. (2004). A Putative Ca^{2+} and Calmodulin-Dependant Protein Kinase Required for Bacterial and Fungal Symbioses. *Science* **303** (5662), 1361-1364.

Liao, B. R., Gawienowski, M. C. and Zielinski, R. E. (1996). Differential stimulation of NAD kinase and binding of peptide substrates by wild-type and mutant plant calmodulin isoforms. *Archives of Biochemistry and Biophysics* **327**, 53-60.

Limpens, E., Franken, C., Smit, P., Willemse, J., Bisseling, T. and Geurts, R. (2003). LysM domain receptor kinases regulating rhizobial Nod factor-induced infection. *Science*, **302**, 630-633.

Lindsey, K. and Topping, J. F. (1996). T-DNA-mediated Insertional Mutagenesis. *In*: Plant gene isolation: principles and practice. G. D. Foster and D. Twell, eds., pp. 215-245. John Wiley & Sons Ltd., Chichester, U.K.

Lindsey, K. and Wei, W. (1993). Tissue culture, transformation, and transient gene expression in Arabidopsis. *In: Arabidopsis*. A practical approach. Z. A. Wilson, ed. Oxford University Press, Oxford. U.K.

Lindsey, K., Wei, W., Clarke, M. C., McArdle, H. F., Rooke, L. M. and Topping, J. F. (1993). Tagging genomic sequences that direct transgene expression by activation of a promoter trap in plants. *Transgenic Research* **2**, 33-47.

López-Lara, I. M., Vandenberg, J. D. J., Thomas-Oates, J. E., Glushka, J., Lugtenberg, B. J. J. and Spaink, H. P. (1995). Structural Identification of the Lipo-Chitin Oligosaccharide Nodulation Signals of *Rhizobium loti*. *Molecular Microbiology* **15**, 627-638.

Madsen, E. B., Madsen, L. H., Radutoiu, S., Olbryt, M., Rakwalska, M., Szczyglowski, K., Sato, S., Kaneko, T., Tabata, S., Sandal, N. and Stougaard, J. (2003). A receptor kinase gene of the LysM type is involved in legume perception of rhizobial signals. *Nature* **425**, 637-640.

Martínez-Abarca, F., Herrera-Cervera, J.A., Bueno, P., Sanjuan, J., Bisseling, T. and Olivares, J. (1998). Involvement of salicylic acid in the establishment of the *Rhizobium meliloti*–alfalfa symbiosis. *Molecular Plant–Microbe Interactions* **11,** 153–155.

Mathesius, U., Schlaman, H. R. M., Spaink, H. P., Sautter, C., Rolfe, B. G. and Djordjevic, M. A. (1998). Auxin transport inhibition precedes root nodule formation in white clover roots and is regulated by flavonoids and derivatives of chitin oligosaccharides. *Plant Journal* **14**, 23-34.

Mathesius, U., Weinman, J. J., Rolfe, B. G. and Djordjevic, M. A. (2000). Rhizobia can induce nodules in white clover by "hijacking" mature cortical cells activated during lateral root development. *Molecular Plant-Microbe Interactions* **13**, 170-182.

Méndez, R. and Wells, D. (2002). Location, location, location: translational control in developmental and neurobiology. *Trends in Plant Science* **12**, 407-409.

Minami, E., Kouchi, H., Cohn, J. R., Ogawa, T. and Stacey, G. (1996). Expression of the early nodulin, *ENOD40*, in soybean roots in response to various lipo-chitin signal molecules. *Plant Journal* **10**, 23-32.

Mitra, R. M., Gleason, C. A., Edwards, A., Hadfield, J., Downie, J. A., Oldroyd, G. E. D. and Long, S. R. (2004). A Ca^{2+}/calmodulin-dependent protein kinase required for symbiotic nodule development: Gene identification by transcript-based cloning. *Proceedings of the National Academy of Sciences of the United States of America* **101** (13), 4701-4705.

Muller, J., Wiemken, A. and Boller, T. (2001). Redifferentiation of bacteria isolated from *Lotus japonicus* root nodules colonized by Rhizobium sp NGR234. *Journal of Experimental Botany* **52**, 2181-2186.

Murphy, A., Peer, W. A. and Taiz, L. (2000). Regulation of auxin transport by aminopeptidases and endogenous flavonoids. *Planta* **211**, 315-324.

Nakamura, Y. and Tabata, S. (2001). Towards a Unified Genome Database of Nitrogen Fixation and Photosynthesis Organisms. *Genome Informatics* **12**, 498-499.

Neill, S., Desikan, R. and Hancock, J. (2002). Hydrogen peroxide signalling. *Current Opinion in Plant Biology* **5**, 388–395.

Niebel, F. D., Lescure, N., Cullimore, J. V. and Gamas, P. (1998). The *Medicago truncatula MtAnn1* gene encoding an annexin is induced by nod factors and during the symbiotic interaction with *Rhizobium meliloti*. *Molecular Plant-Microbe Interactions* **11**, 504-513.

Niehaus, K., Kapp, D. and Puhler, A. (1993). Plant defense and delayed infection of alfalfa pseudonodules induced by an exopolysaccharide (EPS-I)-deficient *Rhizobium meliloti* Mutant. *Planta* **190**, 415-425.

Niehaus, K., Lagares, A. and Puhler, A. (1998). A *Sinorhizobium meliloti* lipopolysaccharide mutant induces effective nodules on the host plant *Medicago sativa* (Alfalfa) but fails to establish a symbiosis with *Medicago truncatula*. *Molecular Plant-Microbe Interactions* **11**, 906-914.

Nielsen, H., Engelbrecht, J., Brunak, S. and von Heijne, G. (1997). Identification of prokaryotic and eukaryotic signal peptides and prediction of their cleavage sites. *Protein Engineering* **10**, 1-6.

Nishimura, R., Hayashi, M., Wu, G-J., Kouchi, H., Imaizumi-Anraku, H. and Murakami, Y., Kawasaki, S., Akao, S., Ohmori, M., Nagasawa, M., Harada, K., and Kawaguchi. (2002). HAR1 mediates systemic regulation of symbiotic organ development. *Nature* **420,** 426–429.

Nukui, N., Ezura, H., Yuhashi, K. I., Yasuta, T. and Minamisawa, K. (2000). Effects of ethylene precursor and inhibitors for ethylene biosynthesis and perception on nodulation in *Lotus japonicus* and *Macroptilium atropurpureum*. *Plant and Cell Physiology* **41**, 893-897.

Nwokolo, E. (1996). The need to increase consumption of pulses in the developing world. *In:* Food and feed from legumes and oilseeds. E. Nwokolo and J. Smartt, eds., pp. 419. Chapman and Hall, London. U.K.

Oldroyd, G. E. D. (2001). Dissecting symbiosis: developments in Nod factor signal transduction. *Annals of Botany* **87**, 709-718.

Oldroyd, G. E. D. and Downie, J. A. (2004). Calcium, kinases and nodulation signalling in legmes. *Nature Reviews Molecular Cell Biology* **5** (11), 566-576.

Oldroyd, G. E. D., Engstrom, E. M. and Long, S. R. (2001). Ethylene inhibits the Nod factor signal transduction pathway of *Medicago truncatula*. *Plant Cell* **13**, 1835-1849.

Orozco-Cárdenas, M. L. and Ryan, C. A. (2002). Nitric oxide negatively modulates wound signaling in tomato plants. *Plant Physiology* **130,** 487-493.

Ovtsyna, A. O., Schultze, M., Tikhonovich, I. A., Spaink, H. P., Kondorosi, E., Kondorosi, A. and Staehelin, C. (2000). Nod factors of *Rhizobium leguminosarum* bv. *viciae* and their fucosylated derivatives stimulate a nod factor cleaving activity in pea roots and are hydrolyzed *in vitro* by plant chitinases at different rates. *Molecular Plant-Microbe Interactions* **13**, 799-807.

Papdopoulos, Y. A. and Kelman, W. M. (1999). Traditional Breeding of *Lotus* Species. *In:* Trefoil: the science and technology of *Lotus*. P. R. Beuselinck, ed. American Society of Agronomy, Inc, Madison, Wisconsin, U.S.A.

Parniske, M. (2004). Molecular genetics of the arbuscular mycorrhizal symbiosis. *Current Opinion in Plant Biology* **7**, 414-421.

Parniske, M., Coomber, S., Kistner, C., Mulder, L., Pitzsche, A., Stougaard, J., Szczyglowski, K., Webb, K. J. and Stracke, S. (2000). Plant Genetics of Symbiosis. *In:* Molecular genetics of model legumes. Impact for legume biology and breeding. M. Parniske and N. Ellis, eds. Keely Print, Norwich, U.K.

Parniske, M., Schmidt, P. E., Kosch, K. and Müller, P. (1994). Plant defense responses of host plants with determinate nodules induced by EPS-defective EXO-b mutants of *Bradyrhizobium japonicum*. *Molecular Plant-Microbe Interactions* **7**, 631-638.

Payne, R., ed. (2000). "The Guide to Genstat, Part 2: Statistics." VSN International, Oxford, U.K.

Penmetsa, R. V. and Cook, D. R. (1997). A legume ethylene-insensitive mutant hyperinfected by its rhizobial symbiont. *Science* **275**, 527-530.

Perret, X., Staehelin, C. and Broughton, W. J. (2000). Molecular basis of symbiotic promiscuity. *Microbiology and Molecular Biology Reviews* **64** (1), 180-201.

Perry, J. A., Wang, T. L., Welham, T. J., Gardner, S., Pike, J. M., Yoshida, S. and Parniske, M. (2003). A TILLING reverse genetics tool and a web-accessible collection of mutants of the legume *Lotus japonicus*. *Plant Physiology* **131**, 866-871.

Peters, A. D. (1999). The effects of pathogen infection and mutation on life history characteristics in *Arabidopsis thaliana*. *Journal of Evolutionary Biology* **12** (3), 460-470.

Peters, N. K., Frost, J. W. and Long, S. R. (1986). A plant flavone, luteolin, induces expression of *Rhizobium meliloti* nodulation genes. *Science* **233**, 977-980.

Phillips, J. M. and Hayman, D. S. (1970). Improved procedures for clearing roots and staining parasitic and vesicular-arbuscular mycorrhizal fungi for

rapid assessment of infection. *Transactions of the the British Mycological Society* **55**, 158-161.
Pichon, M., Journet, E. P., Dedieu, A., de Billy, F., Truchet, G. and Barker, D. G. (1992). *Rhizobium meliloti* elicits transient expression of the early nodulin gene-*ENOD12* in the differentiating root epidermis of transgenic alfalfa. *Plant Cell* **4**, 1199-1211.
Pidwerny, M. (2005). The nitrogen cycle. http://www.physicalgeography.net/fundamentals/9s.html.
Piepho, R. W. (2003). Pharmacology of the calcium channel blockers. Vol. 2003, pp. http://www.emory.edu/WHSC/MED/CME/CCB/pharm.html.
Piñeros, M. and Tester, M. (1997). Calcium channels in higher plant cells: selectivity, regulation and pharmacology. *Journal of Experimental Botany* **48**, 551-577.
Pingret, J. L., Journet, E. P. and Barker, D. G. (1998). Rhizobium Nod factor signaling: Evidence for a G protein- mediated transduction mechanism. *Plant Cell* **10**, 659-671.
Postgate, J. (1982). The fundamentals of nitrogen fixation. University of Cambridge Press, Cambridge, U.K.
Postgate, J. (1992). Bacterial evolution and the nitrogen-fixing plant. *Philosophical Transactions of the Royal Society B*, **338,** 409-416.
Price, N. P. J., Rélic, B., Talmont, E., Lewin, A., Promé, D., Pueppke, S. G., Maillet, F., Dénarié, J., Promé, J. C. and Broughton, W. J. (1992). Broad-Host-Range Rhizobium Species Strain NGR234 Secretes a Family of Carbamoylated, and Fucosylated, Nodulation Signals That Are O-Acetylated or Sulfated. *Molecular Microbiology* **6**, 3575-3584.
Puppo, A., Groten, K., Bastian, F., Carzaniga, R., Soussi, S., Mercedes Lucas, M., Rosario de Felipe, M., Harrison, J., Vanacker, H., and Foyer, C. H. (2005). Legume nodule senescence: roles for redox and hormone signalling in the orchestration of the natural aging process. *New Phytologist* **165**, 683-701.
Quaedvlieg, N. E. M., Schlaman, H. R. M., Admiraal, P. C., Wijting, S. E., Stougaard, J. and Spaink, H. P. (1998). Fusions between green fluorescent protein and beta- glucuronidase as sensitive and vital bifunctional reporters in plants. *Plant Molecular Biology* **38**, 861-873.
Radutoiu, S., Madsen, L. H., Madsen, E. B., Felle, H. H., Umehara, Y., Grønlund, M., Sato, S., Nakamura, Y., Tabata, S., Sandal, N. and Stougaard, J. (2003). Plant recognition of symbiotic bacteria requires two LysM receptor-like kinases. *Nature* **425**, 585-592.
Randall, P. J. and Bouma, D. (1973). Zinc deficiency, carbonic anhydrase, and photosynthesis in leaves of spinach. *Plant Physiology* **52**, 229-232.
Reddy, A. S. N. (2001) Calcium: silver bullet in signalling. *Plant Science* **160** (3), 381-404.
Remy, W., Taylor, T. N., Hass, H. and Kerp, H. (1994). Four hundred million year old vesicular arbuscular mycorrhizae. *Proceedings of the National Academy of Sciences of the United States of America* **91,** 11841-11843.
Resendez, E., Ting, J., Kim, K. S., Wooden, S. K. and Lee, A. S. (1986). Calcium ionophore A23187 as a regulator of gene expression in mammalian cells. *Journal of Cell Biology* **103**, 2145-2152.

Roberts, D. M. and Harmon, A. C. (1992). Calcium-modulated proteins - targets of intracellular calcium signals in higher plants. *Annual Review of Plant Physiology and Plant Molecular Biology* **43**, 375-414.

Roche, P., Debellé, F., Maillet, F., Lerouge, P., Faucher, C., Truchet, G., Dénarié, J. and Promé, J. C. (1991). Molecular basis of symbiotic host specificity in *Rhizobium meliloti* - *Nodh* and *Nodpq* genes encode the sulfation of lipo-oligosaccharide signals. *Cell* **67**, 1131-1143.

Rottingen, J. A. and Iversen, J. G. (2000). Ruled by waves? Intracellular and intercellular calcium signalling. *Acta Physiologica Scandinavica* **169**, 203-219.

Ryle, G. J. A., Powell, C. E. and Gordon, A. J. (1978). The effect of source of nitrogen on the growth of Fiskeby soyabean: The carbon economy of whole plants. *Annals of Botany* **42**, 637-648.

Salzman, R. A., Fujita, T., Zhu-Salzman, K., Hasegawa, P. M. and Bressan, R. A. (1999). An improved RNA isolation method for plant tissues containing high levels of phenolic compounds or carbohydrates. *Plant Molecular Biology Reporter* **17**, 11-17.

Sanders, D., Pelloux, J., Brownlee, C. and Harper, J. F. (2002). Calcium at the crossroads of signaling. *Plant Cell* **14**, S401-S417.

Sanders, P. M., Bui, A.Q., Weterings, K., McIntire, K.N., Hsu, Y.C., Lee, P.Y., Truong, M.T., Beals, T.P. and Goldberg, R.B. (1999). Anther developmental defects in *Arabidopsis thaliana* male-sterile mutants. *Sexual Plant Reproduction* **11** (6), 297-322.

Santi, C., Svistoonoff, S., Constans, L., Auguy, F., Duhoux, E., Bogusz, D. and Franche1, C. (2003). Choosing a reporter for gene expression studies in transgenic actinorhizal plants of the Casuarinaceae family. *Plant and Soil* **254**, 229–237.

Santos, R., Herouart, D., Puppo, A. and Touati, D. (2000). Critical protective role of bacterial superoxide dismutase in rhizobium-legume symbiosis. *Molecular Microbiology* **38**, 750–759.

Sato, S., Kaneko, T., Nakamura, Y., Asamizu, E., Kato, T. and Tabata, S. (2001). Structural analysis of a *Lotus japonicus* genome. I. Sequence features and mapping of fifty-six TAC clones which cover the 5.4 Mb regions of the genome. *DNA Research* **8,** 311-318.

Schafleitner, R. and Wilhelm, E. (2002). Isolation of wound inducible genes from *Castanea sativa* stems and expression analysis in the bark tissue. *Plant Physiology and Biochemistry* **40** (3), 235-245.

Schauser, L., Handberg, K., Sandal, N., Stiller, J., Thykjaer, T., Pajuelo, E., Nielsen, A. and Stougaard, J. (1998). Symbiotic mutants deficient in nodule establishment identified after T-DNA transformation of *Lotus japonicus*. *Molecular and General Genetics* **259**, 414-423.

Schauser, L., Roussis, A., Stiller, J. and Stougaard, J. (1999). A plant regulator controlling development of symbiotic root nodules. *Nature* **402**, 191-195.

Scheres, B., Van De Wiel, C., Zalensky, A., Horvath, B., Spaink, H., Van Eck, H., Zwartkruis, F., Wolters, A. M., Gloudemans, T., Vankammen, A. and Bisseling, T. (1990). The *ENOD12* Gene-product is involved in the infection process during the pea *Rhizobium* interaction. *Cell* **60**, 281-294.

Schlaman, H., Gisel, A., Quaedvlieg, N., Bloemberg, G., Lugtenberg, B., Kijne, J., Potrykus, I., Spaink, H. and Sautter, C. (1997). Chitin oligosaccharides

can induce cortical cell division in roots of *Vicia sativa* when delivered by ballistic microtargeting. *Development* **124**, 4887-4895.
Schlaman, H. R. M., Okker, R. J. H. and Lugtenberg, B. J. J. (1992). Regulation of Nodulation Gene-Expression by NodD in Rhizobia. *Journal of Bacteriology* **174**, 5177-5182.
Scholte, M., D'Erfurth, I., Ripa, S., Mondy, S., Jean, V., Durand, P., Breda, C., Trinh, T.H., Rodriguez-Llorente, I., Kondorosi, E., Schultze, M., Kondorosi, A. and Ratet, P. (2002). T-DNA tagging in the model legume *Medicago truncatula* allows efficient gene discovery. *Molecular Breeding* **10**, 203-215.
Schweiger, P. F. and Jakobsen, I. (1999). The role of mycorrhizas in plant P nutrition, fungal uptake kinetics and genotype variation. *In:* Plant Nutrition - Molcular Biology and Genetics. G. and A. Jensen, eds., pp277-289. Kluwer Academic Publishers, Dordrecht, Holland.
Scott, D. B., Young, C. A., Collins-Emerson, J. M., Terzaghi, E. A., Rockman, E. S., Lewis, P. E. and Pankhurst, C. E. (1996). Novel and complex chromosomal arrangement of *Rhizobium loti* nodulation genes. *Molecular Plant-Microbe Interactions* **9**, 187-197.
Senoo, K., Solaiman, M. Z., Kawaguchi, M., Imaizumi-Anraku, H., Akao, S., Tanaka, A. and Obata, H. (2000). Isolation of two different phenotypes of mycorrhizal mutants in the model legume plant *Lotus japonicus* after EMS-treatment. *Plant and Cell Physiology* **41**, 726-732.
Shahmuradov, I. A., Gammerman, A. J., Hancock, J. M., Bramley, P. M. and Solovyev, V. V. (2003). PlantProm: a database of plant promoter sequences. *Nucleic Acids Research* **31**, 114-117.
Sharma, P. K., Kundu, B. S. and Dogra, R. C. (1993). Molecular mechanism of host-specificity in legume-*Rhizobium* symbiosis. *Biotechnology Advances* **11**, 741-779.
Shattock (2003). A brief guide to T-type calcium channels. pp. http://www.kcl.ac.uk/depsta/biomedical/pharmacology/jm324_5/T%20channel%20notes%20-%20Dr%Shattock.pdf.
Shaw, S.L. and Long, S.R. (2003). Nod factor inhibition of reactive oxygen efflux in a host legume. *Plant Physiology* **132**, 2196–2204.
Smartt, J. (1990). Grain Legumes: Evolution and genetic resources. Cambridge University Press, Cambridge.
Smith, S. E. and Read, D. J. (1997). Mycorrhizal Symbiosis. Academic Press Limited, London, U.K.
Snedden, W. A. and Fromm, H. (1998). Calmodulin, calmodulin-related proteins and plant responses to the environment. *Trends in Plant Science* **3**, 299-304.
Soltis, D.E., Soltis, P. S., Morgan, D. R., Swensen, S. M., Mullin, B. C., Dowd, J. M. and Martin, P. G. (1995). Chloroplast gene sequence data suggest a single origin of the predisposition for symbiotic nitrogen-fixation in Angiosperms. *Proceedings of the National Academy of Sciences of the United States of America* **92** (7), 2647-2651.
Spaink, H. P. (1992). Rhizobial lipo-oligosaccharides - answers and questions. *Plant Molecular Biology* **20**, 977-986.
Spaink, H. P., Sheeley, D. M., Van Brussel, A. A. N., Glushka, J., York, W. S., Tak, T., Geiger, O., Kennedy, E. P., Reinhold, V. N. and Lugtenberg, B. J. J. (1991). A novel highly unsaturated fatty-acid moiety of lipo-

oligosaccharide signals determines host specificity of *Rhizobium*. *Nature* **354**, 125-130.

Spaink, H. P., Wijfjes, A. H. M., Van Vliet, T. B., Kijne, J. W. and Lugtenberg, B. J. J. (1993). Rhizobial lipo-oligosaccharide signals and their role in plant morphogenesis - are analogous lipophilic chitin derivatives produced by the plant. *Australian Journal of Plant Physiology* **20**, 381-392.

Sprent, J.I. (1979). The biology of nitrogen fixing organisms. McGraw-Hill, N.Y., U.S.A.

Sprent, J. I. (2001). *In:* Nodulation in legumes. Royal Botanic Gardens, Kew, U.K.

Sprent, J. I. and Sprent, P. (1990). Nitrogen fixing organisms: pure and applied aspects. Cambridge University Press, Cambridge, U.K.

Staehelin, C., Muller, J., Mellor, R. B., Wiemken, A. and Boller, T. (1992). Chitinase and peroxidase in effective (Fix^+) and ineffective (Fix^-) soybean nodules. *Planta* **187**, 295-300.

Staehelin, C., Schultze, M., Kondorosi, E., Mellor, R. B., Boller, T. and Kondorosi, A. (1994). Structural modifications in *Rhizobium meliloti* Nod factors influence their stability against hydrolysis by root chitinases. *Plant Journal* **5**, 319-330.

Stougaard, J. (2001). Genetics and genomics of root symbiosis. *Current Opinion in Plant Biology* **4**, 328-335.

Stracke, S., Kistner, C., Yoshida, S., Mulder, L., Sato, S., Kaneko, T., Tabata, S., Sandal, N., Stougaard, J., Szczyglowski, K. and Parniske, M. (2002). A plant receptor-like kinase required for both bacterial and fungal symbiosis. *Nature* **417**, 959-962.

Strynadka, N. C. J. and James, M. N. G. (1989). Crystal structures of the helix-loop-helix calcium-binding proteins. *Annual Review of Biochemistry* **58**, 951-998.

Stuurman, N., Bras, C. P., Schlaman, H. R. M., Wijfjes, A. H. M., Bloemberg, G. and Spaink, H. (2000). Use of green fluorescent protein color variants expressed on stable broad-host range vectors to visualize rhizobia interacting with plants. *Molecular Plant-Microbe Interactions* **13**, 1163-1169.

Sumner, L. W., Mendes, P. and Dixon, R. A. (2003) Plant metabolomics: large-scale phytochemistry in the functional genomics era. *Phytochemistry* **62**, 817-836.

Szczyglowski, K., Shaw, R. S., Wopereis, J., Copeland, S., Hamburger, D., Kasiborski, B., Dazzo, F. B. and de Bruijn, F. J. (1998). Nodule organogenesis and symbiotic mutants of the model legume *Lotus japonicus*. *Molecular Plant-Microbe Interactions* **11**, 684-697.

Tajima, S., Takane, K., Nomura, M. and Kouchi, H. (2000). Symbiotic nitrogen fixation at the late stage of nodule formation in *Lotus japonicus* and other legume plants. *Journal of Plant Research* **113**, 467-473.

Takahashi, Y., Ogra, Y. and Suzuki, K.T. (2004). Synchronized generation of reactive oxygen species with the cell cycle. *Life Sciences* **75**, 301–311.

Timmers, A. C. J., Soupene, E., Auriac, M. C., de Billy, F., Vasse, J., Boistard, P. and Truchet, G. (2000). Saprophytic intracellular rhizobia in alfalfa nodules. *Molecular Plant-Microbe Interactions* **13**, 1204-1213.

Topping, J. F., Wei, W. and Lindsey, K. (1991). Functional tagging of regulatory elements in the plant genome. *Development* **112**, 1009-1019.

Torres, M. A., Onouchi, H., Hamada, S., Machida, C., Hammond-Kosack, K. E. and Jones, J. D. G. (1998). Six *Arabidopsis thaliana* homologues of the human respiratory burst oxidase (gp91(phox)). *Plant Journal* **14** (3), 365-370.

Truchet, G., Barker, D. G., Camut, S., de Billy, F., Vasse, J. and Huguet, T. (1989). Alfalfa nodulation in the absence of *Rhizobium*. *Molecular and General Genetics* **219**, 65-68.

Truchet, G., Roche, P., Lerouge, P., Vasse, J., Camut, S., de Billy, F., Promé, D. and Dénarié, J. (1991). Sulphated lipo-oligosaccharide signals of *Rhizobium meliloti* elicit root nodule organogenesis in alfalfa. *Nature* **351**, 670-673.

Tsyganov, V. E., Voroshilova, V. A., Herrera-Cervera, J. A., Sanjuan-Pinilla, J. M., Borisov, A. Y., Tikhonovich, I. A., Priefer, U. B., Olivares, J. and Sanjuan, J. (2003). Developmental downregulation of rhizobial genes as a function of symbiosome differentiation in symbiotic root nodules of *Pisum sativum*. *New Phytologist* **159**, 521-530.

Urtz, B. E. and Elkan, G. H. (1996). Genetic diversity among Bradyrhizobium isolates that effectively nodulate peanut (*Arachis hypogaea*). *Canadian Journal of Microbiology* **42**, 1121-1130.

van Brussel, A. A. N., Zaat, S. A. J., Cremers, H., Wijfeelman, C. A., Pees, E., Tak, T. and Lugtenberg, B. J. J. (1986). Role of plant root exudate and Sym plasmid-localized nodulation genes in the synthesis by *Rhizobium leguminosarum* of Tsr factor, which causes thick and short roots on common vetch. *Journal of Bacteriology* **165**, 517-522.

van der Holst, P. P. G., Schlaman, H. R. M. and Spaink, H. P. (2001). Proteins involved in the production and perception of oligosaccharides in relation to plant and animal development. *Current Opinion in Structural Biology* **11**, 608-616.

van Rhijn, P., Fang, Y., Galili, S., Shaul, O., Atzmon, N., Wininger, S., Eshed, Y., Lum, M., Li, Y., To, V., Fujishige, N., Kapulnik, Y. and Hirsch, A. M. (1997). Expression of early nodulin genes in alfalfa mycorrhizae indicates that signal trasnduction pathways used in forming arbuscular mycorrhizae and *Rhizobium*-induced nodules may be conserved. *Proceedings of the National Academy of Sciences of the United States of America* **94** (10), 5467-5472.

van Workum, W. A. T., van Slageren, S., van Brussel, A. A. N. and Kijne, J. W. (1998). Role of exopolysaccharides of *Rhizobium leguminosarum* bv. *viciae* as host plant-specific molecules required for infection thread formation during nodulation of *Vicia sativa*. *Molecular Plant-Microbe Interactions* **11**, 1233-1241.

Vijn, I., Christiansen, H., Lauridsen, P., Kardailsky, I., Quandt, H. J., Broer, I., Drenth, J., Jensen, E. O., Vankammen, A. and Bisseling, T. (1995). A 200 bp region of the pea *ENOD12* promoter is sufficient for nodule-specific and Nod factor-induced expression. *Plant Molecular Biology* **28**, 1103-1110.

Vizir, I., Thorlby, G. and Mulligan, B. (1996). Classical mutagenesis and genetic analysis. *In:* Plant gene isolation: principles and practice. G. D. Foster

and D. Twell, eds., pp. 215-245. John Wiley & Sons Ltd., Chichester, U.K.

Walker, S. A. and Downie, J. A. (2000). Entry of *Rhizobium leguminosarum* bv. *viciae* into root hairs requires minimal nod factor specificity, but subsequent infection thread growth requires *nodO* or *nodE*. *Molecular Plant-Microbe Interactions* **13**, 754-762.

Walker, S.A., Viprey, V. and Downie, J. A. (2000). Dissection of nodulation signaling using pea mutants defective for calcium-spiking induced by Nod-factors and chitin oligomers. *Proceedings of the National Academy of Sciences of the United States of America* **97** (24), 13413-13418.

Wang, T. L., Hadavizideh, A., Harwood, A., Welham, T. J., Harwood, W. A., Faulks, R. and Hedley, C. L. (1990). An analysis of seed development in *Pisum sativum* XIII. The chemical induction of storage product mutants. *Plant Breeding* **105**, 311-320.

Watson, B., Asirvatham, V., Wang, L. and Sumner, L. W. (2003). Mapping the proteome of *Medicago truncatula*. *Plant Physiology* **131**, 1104-1123.

Webb, K. J., Gibbs, M. J., Mizen, S., Skøt, L. and Gatehouse, J. A. (1996). Genetic transformation of *Lotus corniculatus* with *Agrobacterium tumefaciens* and the analysis of the inheritance of transgenes in the T_1 generation. *Transgenic Research* **5**, 303-312.

Webb, K. J., Robbins, M. P., Wang, T. L., Parniske, M. and Marquez, A. J. (*in press*). Mutagenesis in *Lotus japonicus*. *In: Lotus* handbook. Kluwer Academic Publishers, Dordrecht, Holland.

Webb, K. J., Skøt, L., Nicholson, M. N., Jorgensen, B. and Mizen, S. (2000). *Mesorhizobium loti* increases root-specific expression of a calcium-binding protein homologue identified by promoter tagging in *Lotus japonicus*. *Molecular Plant-Microbe Interactions* **13**, 606-616.

Wegel, E., Schauser, L., Sandal, N., Stougaard, J. and Parniske, M. (1998). Mycorrhiza mutants of *Lotus japonicus* define genetically independent steps during symbiotic infection. *Molecular Plant-Microbe Interactions* **11**, 933-936.

Weinmann, P., Gossen, M., Hillen, W., Bujard, H. and Gatz, C. (1994). A chimeric transactivator allows tetracycline-responsive gene expression in whole plants. *Plant Journal* **5**, 559-569.

White, P. J. and Broadley, M. R. (2003). Calcium in plants. *Annals of Botany.* **92** (4), 487-511.

Yang, G. P., Debelle, F., Savagnac, A., Ferro, M., Schiltz, O., Maillet, F., Promé, D., Treilhou, M., Vialas, C., Lindstrom, K. and Promé, J. C. (1999). Structure of the *Mesorhizobium huakuii* and *Rhizobium galegae* Nod factors: a cluster of phylogenetically related legumes are nodulated by rhizobia producing Nod factors with alpha, beta-unsaturated N-acyl substitutions. *Molecular Microbiology* **34**, 227-237.

Yokota, E., Muto, S. and Shimmen, T. (1999). Inhibitory regulation of higher-plant myosin by Ca^{2+} ions. *Plant Physiology* **119** (1), 231-239.

Zielinski, R. E. (1998). Calmodulin and calmodulin-binding proteins in plants. *Annual Review of Plant Physiology and Plant Molecular Biology* **49**, 697-725.

Zucchi, R. and Ronca-Testoni, S. (1997). The Sarcoplasmic Reticulum Ca^{2+} Channel/Ryanodine Receptor: Modulation by Endogenous Effectors, Drugs and Disease States. *Pharmacological Review* **49**, 1-52.

Zuppini, A., Baldan, B., Millioni, R., Favaron, F., Navazio, L. and Mariani, P. (2004). Chitosan induces Ca^{2+}-mediated programmed cell death in soybean. *New Phytologist* **161**(2), 557-568.